Characterization and Quantification of Traffic Load Spectra in Texas Overweight Corridors and Energy Sector Zones: Final Report

TECHNICAL REPORT STANDARD TITLE PAGE

1. Report No. FHWA/TX-19/0-6965-1	2. Government Accession No.	3. Recipient's Catalog No.
4. Title and Subtitle Characterization and Quantification of Traffic Load Spectra in Texas Overweight Corridors and Energy Sector Zones: Final Report		**5. Report Date** August 2019; Published November 2019
		6. Performing Organization Code
7. Author(s) Reza S. Ashtiani, Ali Morovatdar, Carlos Licon, Cesar Tirado, Jaime Gonzales, and Sergio Rocha		**8. Performing Organization Report No.** TX 0-6965-01
9. Performing Organization Name and Address Center for Transportation Infrastructure Systems The University of Texas at El Paso El Paso, Texas 79968-0516		**10. Work Unit No.**
		11. Contract or Grant No. Project No. 0-6965
12. Sponsoring Agency Name and Address Texas Department of Transportation Research and Technology Implementation Division P.O. Box 5080 Austin, Texas 78763-5080		**13. Type of Report and Period Covered** Technical Report Sept. 1, 2017 – Aug. 31, 2019
		14. Sponsoring Agency Code

15. Supplementary Notes

Project performed in cooperation with Texas Department of Transportation and the Federal Highway Administration.

16. Abstract

Energy-related activities such as natural gas and crude oil production in Texas have created large volumes of overweight (OW) truck operations, resulting in expedited deterioration and premature failure of transportation infrastructures. This project's primary goal was to develop a database of the site-specific axle load spectra for energy corridors in South Texas. The secondary goal was to establish a mechanistic framework, based on the axle load spectra, to quantify the pavement damages associated with the OW truck operations. The primary step for the mechanistic quantification of the damages imparted on pavement facilities was accurate characterization of the traffic operations in energy developing zones. Therefore, our research team deployed portable weight-in-motion devices in summer 2018 and winter 2019 to ten representative sites in the Eagle Ford Shale region. The results were synthesized to compile the axle load spectra database. Subsequently, the research team developed a novel framework for the quantification of the pavement damages associated with OW truck operations in the field. A series of non-destructive tests were conducted in the field to develop a database of pavement layers characteristics. Using the site-specific information regarding the traffic loading data and pavement material properties, this study developed new sets of damage equivalency factors, specifically tailored towards the unique features of the network. The proposed mechanistic approach revealed that the modified damage factors were substantially higher compared to the traditional industry-standard axle load factors. Further investigation of the contribution of the climatic factors and pavement profiles underscored the significance of these components for accurate assessment of the damage equivalency factors. In a separate effort, our research team established a framework for mechanistic evaluation of the reduction of the expected service life of pavements due to changes in the traffic characteristics post energy-developing era. Numerical simulations, cross validated by field design and maintenance plans, indicated that the majority of the studied sections sustained substantial loss of service life due to changes in traffic patterns. The reduction of the service life was appreciably higher for less robust pavement sections, such as FM roads, compared to the SH and US highways. Ultimately, the research team developed a web-based module for the visualization of the findings of the project and further use by districts across the state.

17. Key Words Portable WIM Devices, Overweight Trucks, Axle Load Spectra, Nondestructive Testing, Pavement Damage Quantification, Finite Element Method, TxME, OS, OW	18. Distribution Statement No restrictions. This document is available to the public through the National Technical service, 5285 Port Royal Road, Springfield, Virginia 22161, www.ntis.gov		
19. Security Classif. (of this report) Unclassified	20. Security Classif. (of this page) Unclassified	21. No. of Pages 192	22. Price

Characterization and Quantification of Traffic Load Spectra in Texas Overweight Corridors and Energy Sector Zones: Final Report

By:

Reza S. Ashtiani, Ph.D., P.E.
Ali Morovatdar, MSCE
Carlos Licon Jr., BSCE
Cesar Tirado, Ph.D.
Jaime Gonzales, BSCS
Sergio Rocha, BSEE

Project 0-6965

DISCLAIMERS

The contents of this report reflect the view of the authors who are responsible for the facts and the accuracy of the data presented herein. The contents do not necessarily reflect the official views or policies of the Texas Department of Transportation or the Federal Highway Administration. This report does not constitute a standard, a specification or a regulation.

The material contained in this report is experimental in nature and is published for informational purposes only. Any discrepancies with official views or policies of the Texas Department of Transportation or the Federal Highway Administration should be discussed with the appropriate Austin Division prior to implementation of the procedures or results.

NOT INTENDED FOR CONSTRUCTION, BIDDING, OR PERMIT PURPOSES

Reza S. Ashtiani, Ph.D., P.E.
Ali Morovatdar, MSCE
Carlos Licon Jr., BSCE
Cesar Tirado, Ph.D.
Jaime Gonzales, BSCS
Sergio Rocha, BSEE

Acknowledgements

Executive Summary

In recent years, Texas has experienced significant increase in the energy-related activities such as natural gas and crude oil productions. Despite many positive economic impacts, these energy development activities have created large volumes of Over Weight (OW) truck traffic operations in the network which adversely affected the longevity of transportation infrastructure systems such as pavements and bridges. A prime example of that is the unprecedented energy production activities in highly active oils fields such as Permian Basin and the Eagle Ford Shale region in the past decade. Due to the sudden explosion of drilling activities, the local government agencies and TxDOT were not able to ramp up their pavement preservation and maintenance efforts to meet the unexpected demand. Lack of funding resources coupled with unclear guidelines are among the many elements that contribute to the delay of the pavement maintenance and repair in several counties across the state. The quantification of the energy development impacts and taxing loading conditions on the highway network is the prelude to adopting proper rehabilitation strategies to meet the future growth of traffic in overload corridors. This can effectively protect the taxpayers' resources spent on transportation systems each year. Consequently, there is a pressing need to accurately quantify the damages imparted by the Over-Size/Over-Weight (OS/OW) truck operations in the affected networks.

The primary goal of the project was to develop a database of the site-specific axle load spectra for overload corridors in South Texas energy developing areas. The secondary goal of the project was to establish a mechanistic framework, based on the axle load spectra, to quantify the pavement damages associated with the OW truck operations in overload corridors of East and Southeast Texas.

To achieve the project objectives, initially, the research team developed and distributed a survey questionnaire among the TxDOT Districts in order to document the extent, severity, and location of severely distressed sites affected by OS/OW vehicles. The outcome of this survey resulted in identifying the roads and highways that were potential candidates to deploy Weigh-In-Motion (WIM) units. Based on our discussion with project advisors, the main emphasis was on Districts located in the Eagle Ford Shale Region. The final sites were selected based on extensive communications with TxDOT personnel, project advisors, proximity to the oil refineries, neighboring oil and gas wells, and number of wells in the vicinity of the energy developing areas.

The project team deployed portable WIM devices in summer of 2018 and winter of 2019 in ten representative sites. The results were instrumental for the development of axle load spectra to satisfy the primary objective of the project. The data collection was conducted for at least 14 days per site for both the summer and winter seasons to characterize the seasonal variations of the truck

traffic in the overload network. The researchers further post-processed the axle load spectra information to identify the extent to which the representative pavement sections accommodate super-heavy loads in the studies network. The results showed an alarming number of overweight vehicles, significantly above the Texas permissible limits, in the network. Based on the analysis of the portable WIM data, on average Farm-to-Market roads were found to be subjected to approximately 64% overweight vehicles. The average overweight truck percentages for State Highways and US Highways were 36% and 45%, respectively. In addition, Gross Vehicle Weights (GVW) in excess of 250,000 lb. for FM roads, and approximately 364,000 lb. were recorded for state highways.

In combination with the field traffic characterization, the research team conducted a series of nondestructive tests such as Ground Penetrating Radar (GPR) and Falling Weight Deflectometer (FWD) on representative pavement sections to develop a database of the pavement layers characteristics. Post-processed data such pavement profile and back-calculated layer modulus were instrumental for further development of modified damage equivalency factors and the remaining life analysis of the representative pavement sections in this study. To fulfill the secondary objective of the project, the research team developed a mechanistic framework for the quantification of the pavement damages associated with overweight truck operations in the region. The proposed approach allows for the calculation of the damage factors tailored towards the specific characteristics of vehicles operating in the network with consideration of environmental conditions and unique features of the transportation systems. Subsequently, the traffic loading characteristics with back-calculated layer properties, directly derived from field data collection efforts, were used as input in a 3D finite element system to calculate critical input parameters in the modified Equivalent Axle Load Factors (EALF) models.

The modified damage factors were further contrasted with traditional industry-standard EALF values as part of task #5 in this project. The developed mechanistic approach confirmed that the modified EALF values were substantially higher than traditional industry-standard axle load factors currently employed by the pavement design industry. Such underestimation of the axle load factors can potentially jeopardize the pavement design and rehabilitation plans in the overload corridors of energy developing areas in Texas.

Another noteworthy finding of this project pertains to the relevance of the type of pavement facility and the modified damage factors. It was revealed that overlooking the influence of the type of roadway facility in damage quantification can potentially incur systematic errors for accurate assessment of the service life of the pavements in overload corridors. Therefore, it deems necessary to cluster similar highways, in terms of functionality and structural layer profile, to realistically represent the damages imparted by OW truck operations. Based on the proposed mechanistic

EALFs, specifically developed in this project, FM roadways with less robust pavement profile, had the highest damage factors, compared to SH and US highways.

The research team also deployed FWD testing in the summer and winter months to investigate the influence of environmental factors on the pavement stiffness properties and the damage equivalency factors. The modified damage factors were found to be sensitive to the time of the year and seasonal variations of the pavement stiffness properties. The post-processed results showed that the EALF values derived from the numerical simulations with summer-based layer modulus were significantly higher than the winter-based damage factors. This is primarily attributed to the viscoelastic behavior of the asphalt layers and the variations of stiffness properties of granular layers due freeze-thaw effects or changes in the saturation state of the unbound granular layers due moisture infiltration or evapotranspiration during the service life of pavements. Therefore incremental assessment of the damages, rather than single value average damage factor, better represent the detrimental influence of overload vehicles in highway networks.

In a separate effort, the research team developed a mechanistic framework for the assessment of the reduction of the expected service life of pavements due to changes in the traffic characteristics post energy developing era. The research team developed a novel algorithm to retrace and backtrack the traffic distributions at the onset of energy developing activities for each specific pavement section in this study. The results were further juxtaposed to repair and preservation plans to account for possible pavement rehabilitation measures during the period of study.

The numerical simulations using TexasME for ten representative pavement sections revealed the impact of the overload truck traffic operations on the loss of serviceability transportation facilities in the overload corridors. The reduction of service life were more pronounced for FM roads, with less robust structural capacity compared to SH and US highways. This is primarily due to the fact that these roadways with a thin surface and base layers were not designed or intended to carry such heavy loads. The analysis also indicated that the majority of studied FM roads either closely approaching their expected service life or exceeded the distress limits set forth by TxDOT.

The results of the study were further summarized in a web-based module. The web-based module allows for graphical visualization of site-specific information, such as EALF values with consideration of the unique features sites, traffic distributions, axle load spectra, vehicle classifications, seasonal variations of truck traffic, and the results for the remaining life analysis of representative pavement sections in this study. This module also incorporates provisions to export the axle load spectra for further analysis by TxDOT engineers and the pavement design industry in Texas.

TABLE OF CONTENTS

LIST OF FIGURES

LIST OF TABLES

1. Introduction

1.1 Background

The energy production activities in South Texas significantly contributes to the economy of the impacted counties and the state as a whole for many years to come. It provides employment for thousands of Texans, especially in economically disadvantaged areas in the region. Additionally, since the beginning of the drilling operations in the region, the influx of workforce and severance taxes has resulted in the generation of unprecedented tax revenue for many local government agencies in Texas energy sector zones. Despite many positive economic impacts, the development of energy resources has adversely impacted the transportation infrastructure systems such as pavements and bridges. Since the beginning of energy activities in the region, damaged local and county roads have been a major source of inconvenience for the local residents.

The quantification of the energy development impacts and taxing loading conditions on transportation facilities in the energy development areas is the prelude to develop uniform compensation strategies to offset the costs incurred to the users of the transportation systems in the affected network. Currently the lack of a uniform and practical structure resulted in widespread and even contradicting approaches. Consequently, there is a pressing need to accurately quantify the damages imparted by the Over-Size Over-Weight (OS/OW) truck operations to protect the taxpayers' investment in the transportation system.

The primary step for the mechanistic quantification of the damages imparted on pavement facilities pertains to accurate characterization of the traffic operations in energy developing zones. Currently, TxDOT adopted the Axle Load Spectra (ALS) concept as one of the means to traffic characterization in the TxME pavement design system. In this approach the performance of the pavement sections is tied to the hourly, weekly, monthly and seasonal distributions of different classes of vehicles in the network. This will allow for the determination of incremental damage imparted by a specific class of truck at a specific timeframe on a pavement section. Additionally, the axle load spectra characterization is an integral component for the calculation of the cumulative damage during service life of pavements. Therefore, it deems necessary to develop databases of traffic operations as a function of time for different types of pavement facilities to accurately assess the pavement performance, calculate reduction in service life due to overload truck operations, and to adopt proper rehabilitation strategies to meet the future growth of traffic in affected corridors.

1.2 Project Objectives

The main goal of the project was to develop traffic axle load spectra database by deployment of the portable Weight in Motion (WIM) devices in energy developing areas of South Texas. Using

the developed axle load spectra database, the secondary goal of the project was to establish a mechanistic framework for pavement damage quantification associated with the specific characteristics of overweight vehicles operating in the network.

1.3 Research Tasks

To address the research objectives of this project, ten Tasks were identified and incorporated in this study. Figure 1.1 provides a summary of the tasks, and their corresponding technical objectives. To optimize the project deliverables considering the time and funding constraints, a two-year comprehensive study was conducted during fiscal year (FY) 2018 and FY 2019.

Project Initiation

> **Task 0 – Value of Research**
> **Activity Highlight:** Determine Project's Value of Research

> **Task 1 – Review of the Literature**
> **Activity Highlight:** Document the current methodologies for the characterization of the traffic for the design and performance evaluation of the pavement structures.

Data Collection and Analysis

> **Task 2 – Survey TxDOT Districts**
> **Activity Highlight:** Document and gather knowledge from districts affected by overload truck traffic to identify severity of damage and identify impacted sites due to energy development activities.

> **Task 3 – Development of the Axle Load Spectra Database**
> **Activity Highlight:** Development of a comprehensive database of vehicle types and frequencies of trucks active in the network.

> **Task 4 – Survey of the Candidate Sites for In-Depth Evaluation**
> **Activity Highlight:** Utilization of the nondestructive testing equipment such as FWD and GPR in combination with visual survey of the network for the assessment of pavement conditions.

Numerical Analysis

> **Task 5 – Development of a Mechanistic Damage Equivalency Factor**
> **Activity Highlight:** Development of a novel approach to quantify the damages imparted on pavements by energy related activities in the region.

> **Task 6 – Remaining Life Analysis of Pavement Sections**
> **Activity Highlight:** Determination of the serviceability loss of the pavements and expected new service life due to energy development operations in selected sites in the overload corridors.

Online Module

> **Task 7 – Web-Based Tool for Highway Network Assessment**
> **Activity Highlight:** Develop a web-based tool for visual representation of truck traffic patterns and imparted damages on the pavement systems in energy developing areas.

Project Closeout

> **Task 8 – Technology Transfer and Training**
> **Activity Highlight:** Develop a training document to be delivered to TxDOT personnel.

> **Task 9 – Documentation of Results**
> **Activity Highlight:** Comprehensive documentation of the surveyed data, developed databases, post processed data, and best practice recommendations.

Figure 1.1. Work Plan Overview.

1.4 Report Contents and Organization

The general organization of this report is provided in this section. Subsequent to the introductory chapter detailing the project objectives and the envisioned tasks to meet the objective of the project, the following information was presented in succinct yet detailed manner in this report:

- Chapter 2: literature review
- Chapter 3: analysis of the survey of TxDOT's Districts conducted prior to the field trials
- Chapter 4: deployment of the portable WIM devices, calibration procedure and algorithms, and the development of axle load spectra for ten representative sites.
- Chapter 5: field testing and evaluation of the pavement sections
- Chapter 6: development of new site-specific axle load equivalency factors considering the environmental factors and type of transportation facility.
- Chapter 7: analysis of the remaining life of pavement sections in the overweight corridors.
- Chapter 8: development of a web-based module for visualization of the findings of the project.
- Chapter 9: conclusions, summary of the report and list of major findings, and recommendations.

Additionally, the following two appendices complement this report:

- Appendix A summarizes the information pertaining to the field visual inspections conducted on the representative sites in the field.
- Appendix B includes the information associated with the pavement type and layer thicknesses for all ten selected overload corridors, extracted from the PMIS database for further validation purposes.

2. Literature Review

2.1 Texas Energy Sector and Impact on State Highway Network

2.1.1 Economic Impact

Advances in technology, particularly in crude oil extraction, natural gas production, wind energy farms, and other pertinent industries have yielded exponential growth in energy development. The development of these energy resources in the energy sector zones substantially contributes to the economy of the state as well as individual sectors. In Texas, it predominantly influences economically disadvantaged areas where it provides employment for thousands of Texans. In addition, such economic activities provide several forms of tax revenue due to the generation of sales taxes, hotel taxes, and severance taxes. Figure 2.1 shows the different shale plays across the continental United States and more importantly across Texas, where it is observed that most of the state lies in regions with basins and active shale plays.

Figure 2.1. United States Oil and Gas Shale Regions (from U.S. Energy Information Administration, Drilling Productivity Report, 2011).

Energy development activities in the Eagle Ford Region alone have grown from 581 barrels per day in 2008, to over 1.1 million barrels per day as of June 2014, and over 4 billion cubic feet per day of natural gas (Turnstall et al., 2014). In the Permian Basin, the total crude oil production is estimated to be over 1.4 million barrels a day (Ewing et al., 2014). Figures 2.2 and 2.3 illustrate the oil and natural gas production and the new-wells for oil and natural gas production per rig in

the Eagle Ford Shale Region, respectively. Moreover, Figures 2.4 and 2.5 show the oil and natural gas production and the new-wells for oil and natural gas production per rig in the Permian Basin up to November 2017.
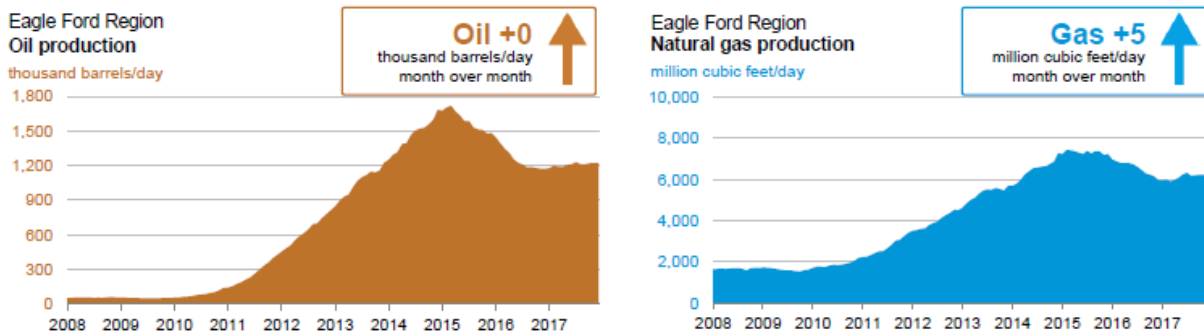
Figure 2.2. Oil and Natural Gas Production for the Eagle Ford Region (from U.S. Energy Information Administration, Drilling Productivity Report, 2017).
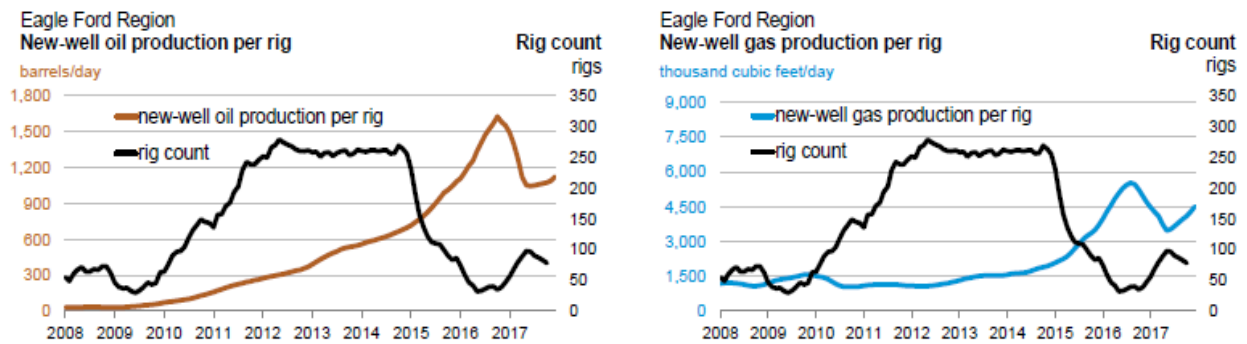
Figure 2.3 .New-well Oil and Natural Gas Production for the Eagle Ford Region (from U.S. Energy Information Administration, Drilling Productivity Report, 2017).
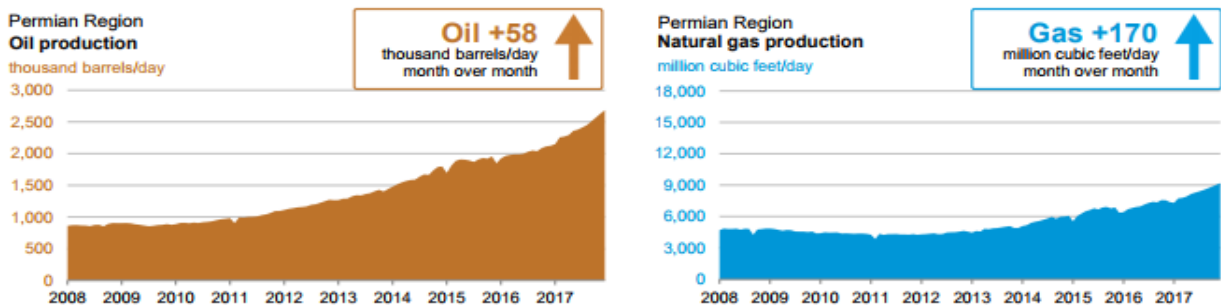
Figure 2.4. Oil and Natural Gas Production for the Permian Basin (from U.S. Energy Information Administration, Drilling Productivity Report, 2017).
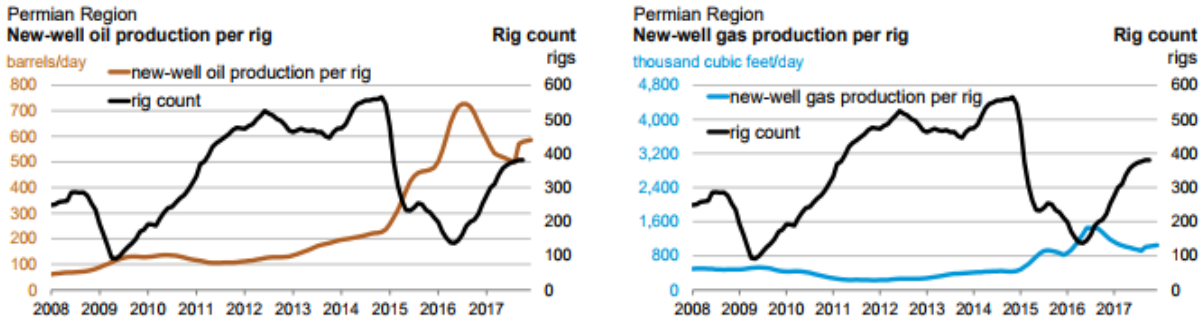
Figure 2.5. New-Well Oil and Natural Gas Production for the Permian Basin (from U.S. Energy Information Administration, Drilling Productivity Report, 2017).

The contributions of these energy development areas are excessively intriguing that several studies have been conducted to assess their socio-economic impacts in affected Districts. A 2014 study conducted by the Rawls College of Business at Texas Tech University examined the economic impact of oil and gas industry in the Permian Basin (Ewing et al.,2014). The report indicated that in 2013, the Texas Portion of the Permian Basin's oil and gas industry supported over 444,000 jobs, generated $113.6 billion in economic output and contributed with over $71.1 billion to the gross product of the state (Ewing et al., 2014). The detailed results of this study is tabulated in Table 2.1. Technological improvements such as horizontal drilling and hydraulic fracturing have led to drastic increases in productivity. The Permian Basin has seen such productivity increases that it now has the greatest rig count of any basin or region in the world (Ewing et al., 2014).

Table 2.1. Economic Impact of the Permian Basin in 2013, in Millions of USD (after Ewing et al., 2014)

Impact Type	Employment	Labor Income	Total Value Added	Output
Direct Effect	0.19	15,706.91	40,086.45	77,880.00
Indirect Effect	0.13	6,238.98	11,405.09	21,103.16
Induced Effect	0.12	4,297.03	8,724.07	14,646.35
Total Effect	0.44	26,242.09	60,215.61	113,629.51

Note: Labor income, total value added and output are measured in current USD.

In another study conducted by the Center of Community and Business Research (CCBR) at The University of Texas at San Antonio, the authors concluded that the Eagle Ford Shale is the largest single oil and gas development in the world based on capital expenditures (Turnstall et al., 2013). CCBR focused their study on the impacts of the 15 most active energy producing counties and their 6 neighboring counties. This study concluded that the economic impact in 2013 for the 21 county-area amounted to 155,000 jobs and $87 billion in total economic output (Turnstall et al., 2014). Total impacts for Eagle Ford Shale are summarized in Table 2.2. The Eagle Ford Shale paid nearly $5.6 billion in salaries and benefits to workers and provided over $2.2 billion for local and state governments (Turnstall et al., 2014). Additionally, the CCBR also made moderate predictions

for the year 2023 in the 15-county area and the greater 21-county area that presented staggering revenue figures (Table 2.3). The 21-county area was estimated to employ 196,660 people, provide over $4 billion for local and state governments, and generate over $137 billion in economic output (Turnstall et al., 2014).

Table 2.2. Total Impacts for Eagle Ford Shale 21-County Area in 2013 (after Turnstall et al., 2014)

	Economic impact	Direct	Indirect	Induced	Total
Core 15-county area	Output	$61,470,280,412	$7,941,100,117	$2,418,234,050	**$71,829,614,579**
	Employment, full-time	42,607	52,333	19,375	**114,315**
	Payroll	$2,027,428,721	$1,539,076,337	$584,718,872	$4,151,223,930
	Gross regional product	$30,448,269,805	$4,333,962,004	$1,542,827,867	$36,325,059,676
	Local government revenues				$2,025,968,804
	State revenue, including severance taxes				$2,028,406,113
Core and neighboring 21-county area	Output	$70,725,115,021	$12,896,817,708	$4,135,496,654	**$87,757,429,382**
	Employment, full-time	51,652	71,648	31,684	**154,984**
	Payroll	$2,707,017,870	$2,036,271,899	$896,394,413	$5,639,684,182
	Gross regional product	$32,992,259,490	$7,199,851,186	$2,640,560,616	$42,832,671,293
	Local government revenues				$2,218,877,342
	State revenue, including severance taxes				$2,214,664,000

Table 2.3. Total Impacts for Eagle Ford Shale 21-County Area in 2023 (Turnstall et al., 2014)

	Economic Impact	Direct	Indirect	Induced	Total
Core 15-county area	Output	$90,168,212,826	$10,893,464,660	$5,332,379,266	**$106,394,056,752**
	Employment, full-time	36,785	71,309	42,699	**150,793**
	Payroll	$6,311,816,751	$2,035,342,931	$1,289,319,720	$9,636,479,402
	Gross regional product	$52,608,595,765	$5,805,086,021	$3,402,243,230	$61,815,925,016
	Local government revenues				$3,741,688,868
	State revenue, including severance taxes				$3,774,006,283
Core and neighboring 21-county area	Output	$110,576,454,317	$19,636,284	$7,488,598,501	**$137,428,984,102**
	Employment, full-time	38,767	99,786	58,107	**196,660**
	Payroll	$6,718,204,896	$3,432,856,335	$1,927,647,160	$12,078,708,391
	Gross regional product	$57,330,415,830	$10,686,840,880	$4,777,170,284	$72,794,426,994
	Local government revenues				$4,073,239,614
	State revenue, including severance taxes				$4,098,369,070

2.1.2 Impact on Texas Infrastructure

Despite many positive economic impacts and benefits that energy companies generate; the development of these energy resources has significantly affected the state and local transportation infrastructure. This is more pronounced during oil and gas fracking operations where there is a large volume of truck traffic in a short timeframe associated with the transportation of fresh water, chemicals, and sand to the sites as well as the transportation of the wastewater from the sites (Bierling, et al., 2014). It is estimated that the volume of truck traffic to bring one gas well into production is equivalent to eight million cars and an additional two million cars per year to maintain one gas well (TxDOT, 2016).

In addition to the substantial truck traffic operations, the transportation of heavy construction equipment and drilling rig components has also contributed to damages that local and county roads experience. These local and county roads were not designed or built to accommodate such high volumes of truck traffic or heavy loads. Therefore, even a few passages such as exceeding loading conditions can result in substantial damage and reduced service life of transportation facilities in the region. Moreover, these roads lack appropriate width to accommodate wider vehicles, thus increased truck traffic quickly deteriorates shoulders which in turn, contributes to the accelerated damage of the pavements and causes safety concerns for the travelling public (Bierling, et al., 2014). Damaged roads and bridges are also a major source of inconvenience for energy companies, local residents, school buses, and emergency vehicles. In the last five years of the state's ongoing drilling and fracking boom, Texas has become one of the deadliest states in total traffic fatalities, with over 3,120 fatalities in 2015 (Olsen, 2014). Table 2.4 provides information on motor vehicle crash deaths per state and highlights Texas as the state with the most fatal crashes, deaths, and deaths per 100 million vehicle miles travelled.

Table 2.4. Motor Vehicle Crash Deaths per State in 2015 (after Insurance Institute for Highway Safety, 2016)

State	Population	Vehicle miles traveled (millions)	Fatal crashes	Deaths	Deaths per 100,000 population	Deaths per 100 million vehicle miles travel
Alabama	4,858,979	67,257	783	849	17.5	1.26
Alaska	738,432	5,045	60	65	8.8	1.29
Arizona	6,828,065	65,045	810	893	13.1	1.37
Arkansas	2,978,204	34,897	472	531	17.8	1.52
California	39,144,818	335,539	2,925	3,176	8.1	0.95
Colorado	5,456,574	50,437	506	546	10.0	1.08
Connecticut	3,590,886	31,592	253	266	7.4	0.84
Delaware	945,934	9,931	122	126	13.3	1.27
D.C.	672,228	3,557	23	23	3.4	0.65
Florida	20,271,272	206,982	2,699	2,939	14.5	1.42
Georgia	10,214,860	118,107	1,327	1,430	14.0	1.21
Hawaii	1,431,603	10,301	86	94	6.6	0.91
Idaho	1,654,930	16,662	198	216	13.1	1.30
Illinois	12,859,995	105,223	914	998	7.8	0.95
Indiana	6,619,680	78,819	756	821	12.4	1.04
Iowa	3,123,899	33,161	282	320	10.2	0.96
Kansas	2,911,641	31,379	322	355	12.2	1.13
Kentucky	4,425,092	48,675	694	761	17.2	1.56
Louisiana	4,670,724	48,180	674	726	15.5	1.51
Maine	1,329,328	14,629	144	156	11.7	1.07
Maryland	6,006,401	57,516	472	513	8.5	0.89
Massachusetts	6,794,422	59,257	291	306	4.5	0.52
Michigan	9,922,576	97,843	893	963	9.7	0.98
Minnesota	5,489,594	57,395	375	411	7.5	0.72
Mississippi	2,992,333	39,890	604	677	22.6	1.7
Missouri	6,083,672	71,918	802	869	14.3	1.21
Montana	1,032,949	12,345	204	224	21.7	1.81
Nebraska	1,896,190	20,101	218	246	13	1.22
Nevada	2,890,845	25,925	296	325	11.2	1.25
New Hampshire	1,330,608	13,094	103	114	8.6	0.87
New Jersey	8,958,013	75,393	522	562	6.3	0.75
New Mexico	2,085,109	27,435	269	298	14.3	1.09
New York	19,795,791	127,230	1,046	1,121	5.7	0.88
North Carolina	10,042,802	111,879	1,275	1,379	13.7	1.23
North Dakota	756,968	10,036	111	131	17.3	1.31
Ohio	11,613,423	113,673	1,029	1,110	9.6	0.98
Oklahoma	3,911,338	47,713	588	643	16.4	1.35
Oregon	4,028,977	35,999	412	447	11.1	1.24
Pennsylvania	12,802,503	100,945	1,102	1,200	9.4	1.19
Rhode Island	1,056,298	7,833	41	45	4.3	0.57
South Carolina	4,896,146	51,726	909	977	20.0	1.89
South Dakota	858,469	9,324	115	133	15.5	1.43
Tennessee	6,600,299	76,670	884	958	14.5	1.25
Texas	27,469,114	258,122	3,124	3,516	12.8	1.36
Utah	2,995,919	29,604	256	276	9.2	0.93
Vermont	626,042	7,314	50	57	9.1	0.78
Virginia	8,382,993	82,625	711	753	9.0	0.91
Washington	7,170,351	59,653	516	568	7.9	0.95
West Virginia	1,844,128	19,827	246	268	14.5	1.35
Wisconsin	5,771,337	62,073	523	566	9.8	0.91
Wyoming	586,107	9,597	128	145	24.7	1.51
U.S total	321,418,821	3,095,373	32,166	35,092	10.9	1.13

There is no exact way to correlate deaths to energy development activities. However, the counties that experienced the largest increase in accidents were in the Permian Basin and the Eagle Ford Shale, as shown in Figure 2.6. In 2013, there were 3,430 traffic reported accidents in the energy development areas that resulted in serious injuries or fatalities. The 26-county in energy development areas that stretches from Laredo to Huntsville accounted for 236 of fatalities of the total reported accidents (TxDOT, 2014).
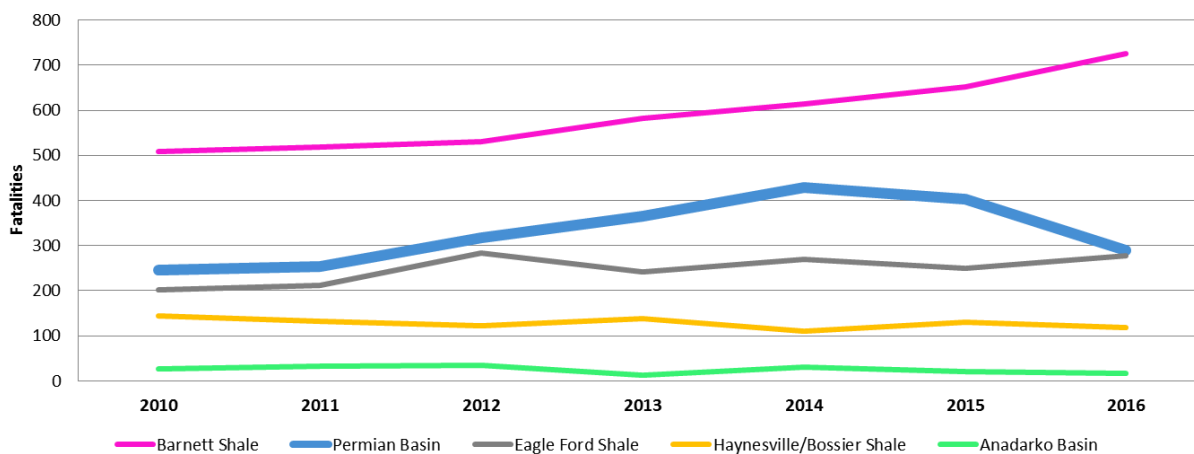
Figure 2.6. Safety Statistics in the Texas Energy Sectors in 2010 through 2016 (from TxDOT, Permian Road Safety Coalition Safety Forum, 2017).

2.1.3 Strategies to Address Energy Development Impacts

Several state DOTs have implemented various policies and programs to help address the impacts of energy developments. For instance, they have posted weight limits, created bonds and maintenance agreements. In addition to establishing active industry engagement and implementing provisional capital improvement programs (Bierling, et al., 2014). Several DOTs have also established a policy to reduce the allowable weight of roads and bridges to 10 tons or less per vehicle to preserve the service life of their transportation infrastructure. States such as Pennsylvania and West Virginia have created bond policies and road use agreements with the energy development users that places financial and roadway maintenance responsibility on them (Bierling, et al., 2014). One Pennsylvania DOT official reported that the energy development industries in their states have covered "tens to hundreds of millions of dollars" in roadway maintenance and upgrades.

Pennsylvania has also created highly active industry engagement programs such as the Governor's Marcellus Shale Advisory Commission and has enforced regular meetings with the Marcellus Shale Coalition. These meetings are regarded as highly effective because they allow Pennsylvania

DOT officials to work alongside the industry to address roadway needs. The lack of such programs in most states leads to limited communication with energy companies, difficulties solving problems and poor planning of future developments. TxDOT has initiated this strategy by conducting workshops with energy sector stakeholders. Additionally, increases in transportation funding allow DOTs to create capital improvement programs that enhance the serviceability of roadway infrastructures in energy development areas. TxDOT has created capital improvement programs to target the energy development sectors with the House and Senate appropriations such as the HB 1025, 83R, 2015 - $225 million and the SB 1747, 83R, 2015 - $225 million (TxDOT, 2016).

In 2016, TxDOT created the Energy Sector Corridor Improvement program to strengthen pavements and provide safety enhancements on important roads. The program identified road projects by prioritizing corridors with high frequencies of injury or fatal crashes, segments that cross multiple Districts, and segments that connect energy sector activity. TxDOT then identified and categorized these corridors into two priorities; Priority 1 and Priority 2. The Energy Sector Corridor Improvement program proposed the corridor improvement estimates as displayed in Table 2.5. The results indicate that the largest dollar amount for the rehabilitation of pavements is associated with the Eagle Ford Shale ($596 million) and the Permian Basin ($676 million) (TxDOT, 2016). The total funding needs for Priority 1 corridors amounted to $1.8 Billion in projects, while an additional $1.25 Billion in projects was identified for Priority 2 corridors, as shown in Tables 2.5 and 2.6, respectively. The energy sector corridor improvements are allocated to the strengthening of 1,125 miles of pavement; adding 50 miles of shoulders, 20 miles of lanes and constructing 521 miles of passing lanes in Super-2 Corridors (TxDOT, 2016).

Table 2.5. Energy Sector Corridor Improvement Estimates (Reproduced from TxDOT, Transportation Planning and Programming Division)

Energy Play Energy Play	Priority 1 Corridor Estimate
Eagle Ford Shale	$596M
Permian Basin	$676M
Barnett Shale	$271M
Anadarko Basin	$97M
Haynesville-Bossier	$179M
Total	**$1.8 Billion**

Table 2.6. Energy Sector Corridor Improvement Miles (Reproduced from TxDOT, Transportation Planning and Programming Division)

Energy Sector Corridor Improvements Energy Sector Corridor Improvements	
Strengthening/ Reinforcing Pavement Structure	1,125 miles
Adding Shoulders to Protect Pavement Edges	50 miles
Adding/Widening lanes for Safety	20 miles
Constructing Passing Lanes on Super 2 Corridor	521 miles
Total Miles to Improve	**1,716 miles**

There is no doubt that energy development sectors have a positive economic impact on the local and state economies, and this impact is expected to continue for more than a decade. However, the damages that heavy truck volumes impart on the transportation's infrastructure are severe and cannot be neglected, Figure 2.7 illustrates a map of the major energy developing areas throughout Texas. It is estimated that between 12,000 to 24,000 oil and gas wells were permitted each year in Texas for the last decade (Railroad Commission of Texas, 2013). The truck traffic associated with each good development and production is estimated to range from 1,000 to 4,000 loaded trucks per well.

The total loaded trucks traveling to and from wells represents a significant amount of loaded truck volume that local and county roads were not designed to accommodate. As a result of the increased truck traffic, these roads quickly deteriorate and require substantial maintenance and reparations. In addition, maintenance costs on severely damaged Farm to Market roads has increased significantly from $500 - $1,500 per mile prior to oil and gas developments to $35,000 -$45,000 post-development (Epps and Newcomb, 2016). Local governments are expected to spend around $200 million per year for maintenance and rehabilitation. While at the state level, it is anticipated that TxDOT will invest $500 million per year for safety, maintenance and capacity need on the energy sector oil and gas impacted roadways (Epps and Newcomb, 2016). The authors also concluded that taking precautionary measures to address roadway conditions is a more cost-effective approach to protect the transportation infrastructure facilities.
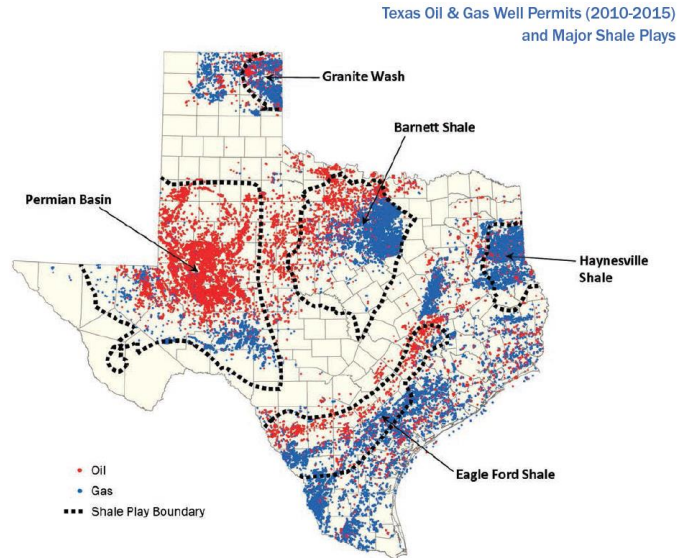
Figure 2.7. Texas Oil and Gas Well Permits from 2010 to 2015 (from TxDOT, 2016).

2.1.4 Importance of this Study

TxDOT is currently seeking a methodology to assess the energy development impacts on the transportation infrastructure in energy development regions. The lack of a uniform and practical structure for dealing with the impacts of the energy development has resulted in unclear and even contradicting approaches. Given this situation, it is imperative to properly characterize the traffic distributions in the region to properly assess the damages imparted by heavy truck operations in the affected network. According to the Center for Community and Business Research (CCBR), it is estimated that roadways currently require $2 billion in total maintenance per year, $1 billion for damage to state highways and $1 billion for damages to local and county roads (Turnstall et al., 2013). However, many counties do not have the funding to address these damaged roads. Rebuilding a paved road can cost local agencies more than $1 million amounting to the total annual maintenance and construction budget that most of these departments can afford to allocate (TxDOT, 2016). Damaged roads also affect the energy development industry in the forms of equipment damage and lower operating speeds due to poor road conditions amounting to $1.5 to 3.5 billion (Epps et al., 2013).

2.2 Traffic Characterization

2.2.1 FHWA Vehicle Classification

The Federal Highway Administration (FHWA) classifies vehicular traffic into 13 vehicle classifications beginning with motorcycles in Class 1 through trucks with seven or more axles in

Class 13. The most prevalent commercial truck configuration is the five-axle tractor-semitrailer that belongs to Class 9. Figure 2.8 illustrates the FHWA Vehicle Classification Chart, while the

Figure 2.8 FHWA 13 Vehicle Classification Chart (from the Federal Highway Administration, 2014).

2.2.2 Texas's Current Axle and Weight Limits

Table 2.7 lists the maximum GVW limits, axle loads limits, and truck size limits that are allowed on Texas Highway without a permit. The Texas Transportation Code Chapter 621: "General provisions relating to vehicle size and weight" sets Texas's current Truck Size and Weight (TS&W) regulation. Table 2.8 provides the maximum legal weight as a function of a number of

axles and distance any group of two or more consecutive axles. The maximum legal weights can be calculated using equation 2.1 as:

$$W = 500 \cdot \left[\frac{L \cdot N}{N-1} + 12 \cdot N + 36 \right],$$
(2.1)

where W is the maximum overall Gross Vehicle Weight (GVW) of the group, L is the distance in feet between the axles of the group that are the farthest apart, and N is the number of axles in the group.

Table 2.7. Texas Permissible Truck Size and Weight Limits (after TxDOT)

Item/ Description	Limits	Illustrations
Weight		
Gross Vehicle Weight	80,000 lb.	
Steering (Front) Axle	12,000 lb.	
Tandem Axle Group	34,000 lb.	
Tridem Axle Group	42,000 lb.	
Quad Axle Group	50,000 lb.	
Size		
Width	8.5 ft (8 ft 6 inches)	
Height	14.0 ft (14 ft 0 inches)	
Length		
Single-Motor Vehicle	45.0 ft (45 ft 0 inches)	
Truck-Tractor	Unlimited	
Semitrailer or two vehicle combination	59.0 ft (59 ft 0 inches)	
Two- or three-vehicle combination	65.0 ft (65 ft 0 inches)	

16

Table 2.8. Texas Current Texas Permissible Weight Table (after TxDOT and TxDMV)

Distance in Feet	Axles					
	2	3	4	5	6	7
4	34,000					
5	34,000					
6	34,000					
7	34,000					
8	34,000	34,000				
8+	38,000	42,000				
9	39,000	42,500				
10	40,000	43,500				
11		44,500				
12		45,000	50,000			
13		45,000	50,500			
14		46,500	51,500			
15		47,500	52,000			
16		48,000	52,500	58,000		
17		48,500	53,500	58,500		
18		49,900	54,000	59,000		
19		51,400	54,500	60,000		
20		52,800	55,500	60,500	66,000	
21		54,000	56,000	61,000	66,500	
22		54,000	56,500	61,500	67,000	
23		54,000	57,500	62,500	68,000	
24		54,000	58,700*	63,000	68,500	74,000
25		54,500	59,650*	63,500	69,000	74,500
26		55,500	60,600*	64,000	69,500	75,000
27		56,000	61,550*	65,000	70,000	75,500
28		57,000	62,500*	65,500	71,000	76,500
29		57,500	63,450*	66,000	71,500	77,000
30		58,500	64,000*	66,500	72,000	77,500
31		59,000	65,350*	67,500	72,500	78,000
32		60,000	66,300*	68,000	73,000	78,500
33			67,250*	68,500	74,000	79,000
34			68,200*	69,000	74,500	80,000
35			69,150*	70,000	75,000	
36			70,100*	70,500	75,500	
37			71,050*	71,000	76,000	
38			72,000*	72,000*	77,000	
39			72,000*	72,500	77,500	
40			72,000*	73,000	78,000	
41			72,000*	73,500	78,500	
42			72,000*	74,000	79,000	
43			72000*	75,000	80,000	
44			72000*	75,500		
45			72,000	76,000		
46			72,500	76,500		
47			73,500	77,500		
48			74,000	78,000		
49			74,500	78,500		
50			75,500	79,000		
51			76,000	80,000		

*These figures were carried forward from Article 6701d-11, Section 5(a)(4) when Senate Bill 89 of the 64th Texas Legislature amended it on December 16, 1974. The amendment provided that axle configurations and weights that were lawful as of that date would continue to be legal under the increased weight limits.

*These figures apply only to an axle spacing greater than 8 feet but less than 9 feet.

2.3 Traffic Characterization and Pavement Design Approaches

2.3.1 AASHTO 1993 Pavement Design Guide

AASHTO's Guide for Design of Pavement Structures has been extensively used as a reference for the design of new and rehabilitated highways pavements. AASHTO's Guide was established based on empirical design approaches obtained from the AASHTO Road Test. The primary motivation for this design approach was to establish a uniform framework for the design and rehabilitation of rigid and flexible pavements (AASHTO, 1993). However, there are several drawbacks associated with the AASHTO's pavement design guide. The first problem that pavement designers and other professionals face is that accepted procedures rely on experimental information that was developed 50 to 60 years ago from field measurements in the late 1950s and early 1960s. Additionally, the Road Test was limited to one location, Ottawa in Illinois, with single subgrade type, specific climatic condition, and approximately 1.2 million load repetitions The relationships that were established from the AASHTO Road Test are more relevant to similar design parameters, vehicle characteristics, and climatic conditions. For instance, the data used to develop the actual AASHTO Guide equations were based on traffic loadings of approximately 1.2 million 18-kip ESALs. In contrast, pavements today are designed to carry loadings beyond 100 million 18-kip ESALs during their design life (Hallin et al., 2007). Consequently, designs based on projections that are beyond the dataset tend to be significantly inaccurate and untrustworthy. Additionally, limited material inputs into the design procedure of flexible pavements did not allow for new changes and improvements of materials. Listed below are some of the limitations associated with the nature of the AASHTO Road Test as follows (Highway Research Board, 1962).

1. The experiments were not inclusive of all the materials as they only tested materials and road soils related to that specific site.
2. The test site experienced environmental conditions not representative of conditions in all regions. The experiments were conducted at one specific site with unique environmental condition that are not representative of diverse climate of the US.
3. Relationships were extrapolated to longer design periods (15-30 years) using limited 2-year field test data.
4. Limited type of trucks used for trafficking the test sections.
5. The current construction equipment and techniques are vastly different from 1960s.

The traffic characterization in the AASHTO's Guide for Design of Pavement Structures relied on the Equivalent Single Axle Loads (ESAL's) concept. An ESAL is the number and weight of all axle loads from vehicles expressed as 18,000-lbs or 18kips, the reference axle load is an 18-Kip load carried by a single axle with dual tires (TxDOT, 2005). This concept was developed to establish a damage relationship for comparing the effects of axles carrying different weight. The

design of ESALs is a traffic load summary statistic that represents a mixed stream of traffic with different axle configurations and axle loads estimated over an analysis period of a pavement and converted to an equivalent number of 18-Kip single axle loads (TxDOT, 2005). The procedure for calculating design ESALs are summarized in Table 2.9.

Table 2.7 Formulation for Determining ESALs.

Formulation	Equation	Variables
ESALs	$$\sum ESALs = T_f TGDL(365)Y$$	T_f = truck factor T = percentage of trucks in average daily traffic (ADT) G = growth factor D = directional distribution factor L = lane distribution factor Y = design period in years
Truck factor T_f	$$T_f = \left(\sum_{i=1}^{m} p_i F_i \right) A$$	p_i = percentage of total repetitions F_i = equivalent axle load factor for the ith load group A = average number of axles per truck m = number of axle groups
Growth factor G	$$G = \frac{(1+g)^n - 1}{g}$$	g = annual growth rate n = analysis period in years

The primary concern with ESALs is not the actual load of the axle, but more importantly, the damage inflicted to the pavement caused by the wheel load. The traffic characterization using the ESAL concept is incapable to capture the seasonal variations in damage imparted by different load groups. In addition, the original axle load equivalency factors developed in this procedure are greatly influenced by factors such as material properties, surface thickness, distress type, failure type, and by the pavement type.

2.3.2 Mechanistic-Empirical Pavement Design Guide

The National Cooperative Highway Research Program (NCHRP) under Project 1-37A was established to improve the pavement design procedure. This updated Mechanistic-Empirical Pavement Design Guide (MEPDG) was based on an extensive assessment of previous research, practices, literature, and available databases relevant to pavement design. The MEPDG provided a uniform basis for the design of flexible, rigid, and composite pavements. This hierarchical design methodology incorporated comprehensive traffic, climatic, and material properties of layers for reliable analysis and design of pavements. To aid in the implementation of the new design procedure the NCHRP created supporting software along with training documents. The following

section provides detailed explanation regarding the use of axle load spectra for the characterization of the traffic information in the MEPDG.

2.3.3 Axle Load Spectra

The axle load spectra or axle load distribution factors are the percentage of the total axle applications within each load interval for single, tandem, tridem, and quad axle configurations (Jiang et al, 2008). The axle load spectra approach was a major departure from the traditional ESAL quantification. According to Jiang et al. (2008), using the axle load spectra to represent vehicle loads as the traffic input in the TxME software will enable users to: analyze the impacts of different traffic loads on pavements, analyze the effects of different materials and impacts of seasons, perform forensic analysis of pavement conditions, and to provide an optimal pavement structure design. The load intervals for each axle configuration are defined as: single axles (3,000 lb to 40,000 lb at 1.000-lb intervals), tandem axles (6,000 lb to 80,000 lb at 2,000-lb intervals), and tridem and quad axles (12,000 lb to 102,000 lb at 3,000-lb interval) (NCHRP 2004). Examples and tables of the axle load spectra are showed in Chapter 4 of this report.

Prozzi et al. (2005) conducted a study to assess the implications associated with the new axle load spectra methodology in the MEPDG guide. The research team conducted a sensitivity analysis and pavement evaluation from traffic data provided by TxDOT's Transportation Planning and Programming Division (TPP). In addition, researchers developed a methodology for specifying the accuracy of WIM equipment based on the effect that it has on pavement performance. The authors concluded that the use of continuous distribution functions is more advantageous than the proposed discrete axle load spectra. Analysis of traffic growth rate and growth factors were also conducted, and tables were prepared for the selection of both of these factors. The authors claimed the use of traffic growth rate and growth factors allow pavement designers to select values based on the anticipated design reliability. The authors also highlighted the issues associated with non-uniform distribution of the WIM stations across Texas highways. Ultimately, the researchers reported the following outcomes and recommendations for their study:

1. Significant benefits could result from collecting WIM data at 12-week intervals that would allow capturing weekly, monthly, and seasonal variations.
2. Traffic loading data should be pre-processed and only four axle configurations should be used for pavement design (steering axles, single axles with dual wheels, tandem and tridem axles).
3. To increase accessibility of WIM data, TPP's should consider a complementary system of temporary WIM stations that operate across Texas environments, and facilities that are under-represented by the network of permanent WIM stations.
4. Traffic volume seasonality and growth are best forecasted by models that jointly capture

both aspects simultaneously.

5. A plan should be developed to collect the following data for supporting the ME Guide: differentiation between single axles with single wheels and single axles with dual wheels, distribution of tire inflation pressures, and distribution of vehicle speed.

Turochy et al. (2005, 2015) conducted a study to examine the differences among national-level traffic inputs developed from the MEPDG, and state-level traffic inputs developed from Alabama Department of Transportation (ALDOT) WIM sites from site-specific traffic data. Researchers divided the entire traffic input range considered in the MEPDG into 13 groups and evaluated the effects of the three levels of data independently for each group. In addition, an unbiased quality control procedure was developed and applied to the ALDOT WIM data to produce traffic inputs at levels 1, 2, and 3. The researchers also determined the sensitivity of the pavement thickness required for the flexible and rigid pavement to different levels of traffic data in Alabama. Furthermore, they provided axle load recommendations for future use by ALDOT for both rigid and flexible pavements.

Xiao and Wu (2016) conducted a study that presents a systematic index approach to relate the truckload spectra directly to pavement performance and characterizes traffic loadings for volume, load, and damage. This study investigated the following four summary indices: cumulative truck volume (CTV), cumulative truckload (CTL), equivalent single axle load (ESAL), and relative pavement performance impact (RPPI) (Xiao, 2016). According to Xiao, numerical evaluation analysis of 30 axle load spectra, 18 vehicle class distributions, 2 truck configurations, and 2 pavement types were conducted to illustrate how the summary indices could be used. Results suggested that the systematic indices used in the study had a clear correlation with pavement performance. In addition, the results can aid engineers by allowing them to compare different load spectra and allowing them to understand the relationship between pavement performance and traffic for any specific design at any desired time (Xiao, 2016).

Prozzi et al. (2017) reviewed the work previously done under TxDOT Project 0-6736, Rider 36 Oversize/Overweight (OS/OW) Vehicle Fees Study, and extended the work to evaluate the effects of different axle configurations on pavements and bridges. According to the researchers, an increase in the current GVW and axle load limits would yield reduced fuel consumption, reduced CO_2 emissions, and reduced truck congestion. The authors proposed an increase in current GVW and axle load limits in Texas and indicated that it would not result in increased infrastructure consumption. In contrast, they suggested using innovative axle configurations that would allow trucks to carry heavier loads with no additional pavement consumption. Furthermore, the researchers developed guidelines for infrastructure friendly vehicle configurations based on different factors such as axle type, load per axle, and the distance between axles. In addition, a

cost recovery method that adequately funds repairs to roads used by the overweight vehicles was also developed.

Walubita et al. (2019) aimed to generate statewide site specific traffic data that served as input for ME pavement design purposes. In this study the authors also proposed to explore the use portable WIM units and pneumatic tube classifiers to serve as commentary data to the permanent WIM stations in Texas. The study included 39 permanent WIM stations, 11 portable WIM stations, and 15 pneumatic tube stations from which the authors used clustering analysis to group the WIM data and estimate future ME traffic data. In addition, the authors created excel macros to analyze the traffic data and an access database to report all the gather data. Other prominent studies related to the advancements in characterizing axle load spectra are summarized in Table 2.10.

Table 2.8 Previous Studies for Characterizing Axle Load Spectra

Authors	Objective	Key Findings
Buchanan (2004)	The objective of this study was to assist the Mississippi Department of Transportation in developing traffic inputs and the axle load spectra for the new MEPDG guide.	Buchanan examined the WIM data that consisted of weight and axle distributions then determined the base annual axle load spectra for single, tandem, tridem, and quantum axle configurations for the Mississippi long-term pavement performance (LTPP) sites. The axle load spectra data that was developed helped them with the implementation of the new MEPDG.
Mohammad et al. (2005)	The primary objective of this study was to develop the axle load spectra for the state of Washington using axle load data collected from permanent WIM stations located throughout the state. The secondary objective was to compare the values from the developed load spectra to historical ESALs data.	Researchers were able to develop the axle load spectra that is compatible with the requirements of the MEPDG for the state of Washington. They concluded that for single axle configuration the values they obtained were fairly similar to the default values of the MEPDG and the MnROAD results. While in tandem and tridem axles the values they produce were more conservative than the default values.
Turochy et al. (2005)	The objectives of this study were to develop accurate truck factors for use in pavement design and to develop new statistical models for axle load distributions.	Researchers evaluated the effects of variation in axle load spectra on pavement design requirements from different locations using the 1993 AASHTO pavement design guide and the MEPDG guide. A statistical model of axle load distribution was also created using data from WIM sites. The authors also reported that the developed single axle models explained 98.6% of the total variation in the data while the developed tandem axle models explained 96.2% of the total variation
Hajek et al. (2005)	This study followed the results of Phase 1 by the authors to develop a methodology for estimating axle load spectra. The objective of Phase 2 was to apply the methodology developed in Phase 1 for 500 LTPP sites to obtain annual axle load spectra.	Researchers evaluated the overall quality of traffic data for 980 (LTPP) sites and the projection of the axle loads for all LTPP sites with satisfactory traffic data. Moreover, axle load projections were developed for 558 LTPP traffic sites from all available data up to 1998 that had adequate traffic monitoring data in the IMS database.
Prozzi and Hong (2006)	The objective of this study was to assess the implications associated with the new axle load spectra methodology in the MEPDG guide. The authors also considered the evaluation of current equipment and methodology for data collection and evaluation of the structural design of pavements.	The research team conducted sensitivity analysis and pavement evaluation from traffic data provided by TxDOT's Transportation Planning and Programming Division (TPP). In addition, researchers developed a methodology for specifying the accuracy of WIM equipment based on the effect that it has on pavement performance. It was determined that the use of continuous distribution functions is more advantageous than the proposed discrete axle load spectra.

Table 2.8 Previous Studies for Characterizing Axle Load Spectra (cont.)

Authors	Objective	Key Findings
Haider and Harichandran (2007)	The objective of this study was to develop a methodology for modeling the axle load spectra based on axle loads from truck weight and volume data.	This study concluded that using truck weights and proportions on a highway can be used to determine the axle load spectra for the different axle configurations. Truck weights can be estimated for existing data or they can be easily measured if adequate models are developed from local truck traffic characteristics.
Swan et al. (2008)	The objective of this study was to obtain the best default values for traffic input parameters required by the MEPDG.	This study used periodic commercial traffic surveys to obtain the best default values for traffic input parameters required by the MEPDG. Researchers developed default input parameters in terms of axle load spectra for two Ontario regions and compared them to the default values of the traffic input parameters required by the MEPDG. In addition, researchers also found the axle load spectra for Ontario has a smaller number of heavily overloaded axles, and peaks between loaded and unloaded axles are more distinct.
Jian et al. (2008)	The objective of this study was to provide traffic data input parameters required by the MEPDG using truck traffic information collected from WIM stations.	Researchers collaborated with the Indiana Department of Transportation (INDOT) to obtain truck traffic information from the traffic data collected by WIM stations. The truck traffic spectra and other traffic inputs were created for INDOT to implement in the MEPDG guide. Additionally, AADT data was used to analyze the spatial distributions of traffic volumes in Indiana.
Ishak et al. (2008)	The objective of this study was to address the traffic data needs of LADOTD for the implementation of the MEPDG.	Researchers conducted this study to address the traffic data needs associated with the implementation of the MEPDG. They also developed the axle load spectra from axle weight data obtained from 2003 to 2006 from portable WIM stations and proposed recommendations to LA DOTD for the collection of traffic data.
Sayyady et al. (2011)	The objective of this study was to create regional average truck axle load distribution factors (ALDFs) using WIM data collected from North Carolina roadways using multidimensional clustering.	According to the researchers, the multidimensional clustering analysis developed representative clusters showing that ALDFs clusters have unique characteristics for primary roads, secondary roads, collectors, and local roads. In addition, this study's contributions are creating a multidimensional clustering analysis that is guided and supports MEPDG damage-based analysis, ALDF clusters that characterize specific traffic patterns in North Carolina, and an easy to use decision tree to help pavement designers to select ALDF input parameters.

Table 2.8 Previous Studies for Characterizing Axle Load Spectra (cont.)

Authors	Objective	Key Findings
Turochy et al. (2015)	The objective of this study was to examine the differences among national-level traffic inputs developed from the MEPDG, state-level traffic inputs developed from ALDOT WIM sites, and from site-specific traffic data.	Researchers divided the entire traffic input range considered in the MEPDG into 13 groups and evaluated the effects of the three levels of data independently for each group. The sensitivity of the pavement thickness required for flexible and rigid pavement of different levels of traffic data in Alabama was also developed. Ultimately, the authors provided axle load recommendations for future use by ALDOT for both rigid and flexible pavements.
Xiao and Wu (2016)	The objective of this study was to explore different approaches that provide meaningful data of the load spectra, and that relate pavement performance to traffic loading.	This study presents a systematic index approach that relates the truckload spectra directly to pavement performance and characterizes traffic loadings for volume, load, and damage. According to the authors, numerical evaluation analysis of 30 axle load spectra, 18 vehicle class distributions, 2 truck configurations, and 2 pavement types were conducted to explore the feasibility of using the summary indices. Results suggested that the systematic indices used in the study had a clear correlation with pavement performance.
Prozzi et al. (2017)	The objective of this research was to develop a methodology to quantify relative consumption of different axle loads and vehicle configuration on the transportation infrastructure.	Evaluated the effects of different axle configurations on pavements and bridges. An increase in the current GVW and axle load limits would allow reduced fuel consumption, reduced CO_2 emissions, and reduced truck congestion. A cost recovery method that can potentially fund the road repairs was proposed.
Walubita et al. (2019)	The primary objective of this research was to generate statewide traffic data for ME pavement design using clustering analysis. In addition, the authors sought to explore the use of other methods of obtain WIM traffic data and volume counts.	Using clustering analysis from 39 permanent WIM stations, 11 portable WIM stations, and 15 pneumatic stations across Texas the authors were able to generate future ME traffic data estimates. The authors also reported the portable WIM to be a cost effective method of collecting WIM data with a 92.5% reliable if properly installed and calibrated.

2.3.4 Hierarchical Traffic Input for MEPDG

The axle load spectra data for all axles single, tandem, and tridem is a required input in the MEPDG, however, it is recognized that some state highway agencies and smaller municipalities may not have the resources needed to collect detailed traffic data over time (NCHRP, 1999). Therefore, a hierarchical approach was adopted for developing the traffic inputs of new and rehabilitated pavement design to facilitate the use of the guide. This approach allows highway

agencies to maximize the reliability of pavement design due to the accuracy and variability of available data. The hierarchical approach for traffic was divided into the following four levels (NCHRP, 1999).

Level 1 Inputs – Site/Project Specific Vehicle Classification and Axle Weight Data

Level 1 requires the collection and analysis of site/project-specific traffic data for the design and evaluation of high-volume highways. The traffic data collected at the site includes Automated Vehicle Classifier (AVC) data such as daily, weekly, monthly, seasonal, and annual number of specific class of vehicles, traveling over the roadway, as well as the weight measurements by WIM systems (NCHRP,1999). Level 1 is regarded as the most accurate that provides the greatest reliability due to the use of actual axle weights and vehicle classification recorder at or near the project site.

Level 2 Inputs – Site-Specific Vehicle Classification and Regional Axle Weight Data

Level 2 uses traffic data from regional or state axle weight for similar projects and roadways to develop the axle load spectra for each different type of vehicle.

Level 3 Inputs – Regional Vehicle Classification and Axle Weight Data

Level 3 does not require site/project specific AVC and WIM data other than average annual daily traffic (AADT) and truck percentage information. Level 3 uses regional and statewide vehicle classification and axle weight data to develop the axle load spectra from similar highways.

2.3.5 Texas Mechanistic-Empirical (Tx-ME) Pavement Design System

Under TxDOT Research Project 0-6622, a study was performed to establish models, testsand design procedures to mechanistically design and analyze pavements with considerations of materials and climatic condition of Texas (Hu et al., 2014). This resulted in the development of the Texas Mechanistic-Empirical Flexible Pavement Design System (TxME). This system allows TxDOT pavement designers to take advantage of the recent approaches for materials characterization and performance assessment of flexible pavements. In addition to the mechanistic-empirical models and performance-based material characterization, TxME allows the incorporation of traffic load spectrum. It also includes a reliable approach to incorporate materials variability for design purposes. The TxME has two levels of traffic inputs. Level 1 requires the user to enter the traffic load spectrum, while Level 2 pertains to the use of traditional ESALs. Figure 2.9(a) shows the pavement input structure and parameters pertaining to the axle load spectra. Figure 2.9(b) shows the input window for entering the axle load distribution (in terms of the percentage of truck traffic) per vehicle class, axle group, and weight. This information can be

imported and exported as comma-separated values files. Table 2.11 summarizes the traffic input for each design level in the TxME.
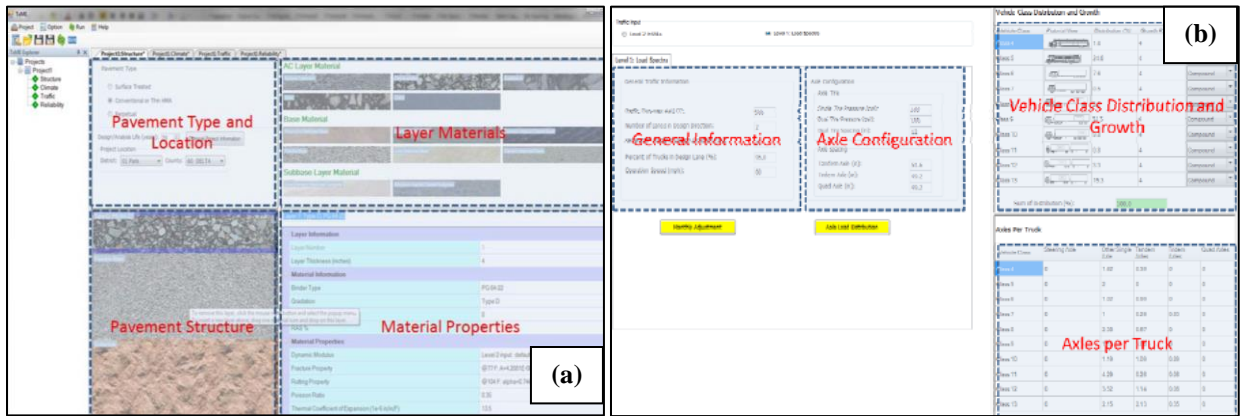
Figure 2.9 (a)TxME Pavement Structure and (b) TxME Traffic Input Data

Table 2.9. Traffic Inputs for TxME

Level of Traffic Inputs	Approach	Inputs
Level 1	Traffic load spectrum	*General traffic information:* - Average annual daily truck traffic (AADTT), two-way - Number of lanes in design section - Percentage of trucks in design direction, % - Percentage of trucks in design lane, % - Operational speed (mph) *Axle configuration:* - Tire pressure (for single and dual tires), in psi - Dual tire spacing (in.) *Axle spacing:* - Tandem axle (in.) - Tridem axle (in.) - Quad axle (in.) *Vehicle class distribution and growth for each class (Class 4 – 13):* - Vehicle class distribution, % - Growth rate, % *Axle numbers for each vehicle class (Class 4 – 13):* - Steering Axle (single axle, single tire) - Other Single Axle (single axle, dual tires) - Tandem Axle - Tridem Axle - Quad Axles *Traffic monthly adjustments factors per class (Class 4 – 13)* *Axle load distribution per class, season (month), and weight* - Axle factors, %
Level 2	Traffic ESALs	- 20-year ESAL (one lane and one direction), in millions - Average daily truck traffic at the beginning - Average daily truck traffic the end of 20-yr. period - Tire pressure - Operation speed (mph)

2.4 Weigh-In-Motion (WIM) Systems

The primary purposes of weigh-in-motion (WIM) systems are (1) to record truck weights or axle loads for road analysis, (2) to screen trucks as a part of commercial vehicle weight enforcement operation and (3) to use weight information to calculate tolls on toll roads, bridges or tunnels. For research purposes, the collected data can be used for planning of roadways, road repairs, and maintenance, and to reduce traffic and its consequences (traffic congestion, accidents, etc.). A typical WIM system consists of four components: a processor and data storage unit, vehicle classification system, user communication unit, and relevant weight sensors. WIM technology allows measuring the dynamic tire forces of a moving vehicle to estimate the corresponding tire loads of the static vehicle.

WIM devices are commonly categorized based on their portability by three categories: permanent, semi-permanent, and portable systems. Permanent WIMs collect and analyze data exclusively at a single, fixed location. Semi-permanent systems have sensors built into the pavement but their data acquisition system can be disconnected and used at a different instrumented location. Portable devices can be moved as a whole for use at different locations. Weigh-in-motion systems can be categorized based on use and speed as described in Table 2.12 There are several factors that contribute to the accurate measurement of the traffic information using WIM devices.

Table 2.10. Classification of WIM Technology Based on Speed

WIM Category	Characteristics
High Speed Weigh-in-Motion (HS-WIM)	Data collection performed under normal traffic speed. No disturbance of traffic flow. Accuracy =15%. Overloaded vehicles diverted to the checkpoint.
Low-Speed Weigh-in-Motion (LW-WIM)	Speed restriction to minimize dynamic effects.
Bridge Weigh-in-Motion (B-WIM)	Use existing bridge to weigh vehicles via measurement of the structural response of the bridge while vehicle crossing.

2.4.1 Permanent WIM Stations

Permanent Weigh-In-Motion (WIM) stations are typically used for collecting accurate weight data and traffic volume. Axle load sensors are embedded in the pavement perpendicular to the direction of the traffic flow. Installation of WIM sensors in permanent WIM stations are divided into two groups from the installation method point of view (Burnos and Rys, 2017):

- Sensors installed in a small cut in the pavement at a depth of 1 to 4 in. (2 to 10 cm). In this case, the sensor does not have direct contact with the vehicle wheel and the axle load is transmitted to the sensor by the pavement and installation grout (which is used to fill up

the groove). Polymer and piezo-ceramic sensors are mounted using this installation method.

- Sensors installed in the pavement, flush with the pavement surface. In this case, the sensor has direct contact with the vehicle tire. Bending plate, quartz, and capacitive sensors are mounted using this installation method.

Figure 2.10 illustrates different types of sensors and their corresponding installation method for instrumenting permanent and semi-permanent WIM stations.
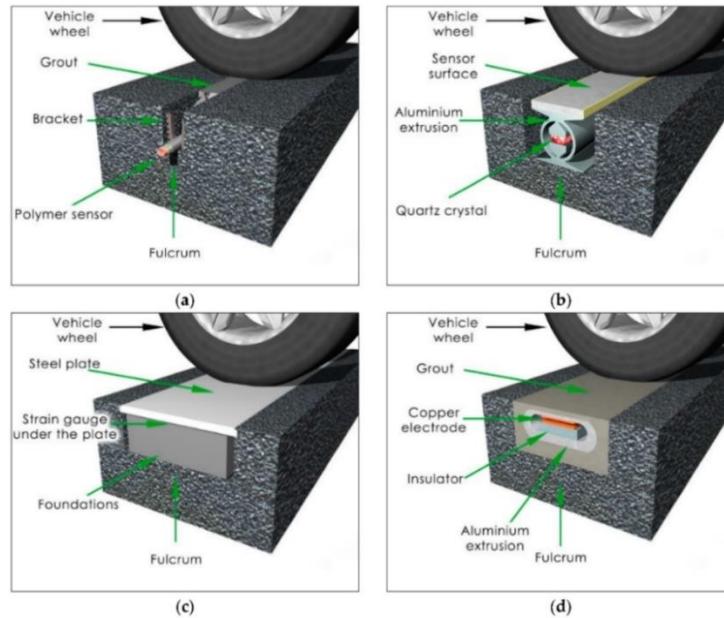
Figure 2.10. Mounting of (a) polymer sensor below the pavement surface, and (b) quartz sensor, (c) bending plate and (d) capacitive sensor installed on the level of the pavement surface (after Burnos and Rys, 2017).

As the fulcrum for the sensor is the pavement regardless of the mounting method, Burnos and Rys (2017) evaluated the effect of pavement properties on the WIM system. The researchers assumed that the pavement, by itself, is an integral part of the weighing system; as the structural integrity of the pavement and the installation grout influence the weight measurements.

Despite the comprehensive data that can be extracted from the stationary WIM stations, the upfront installation funds and prohibitive maintenance costs are major challenges of such systems. According to Refai et al. (2014), permanent WIM installation could cost more than $200,000 per site, while static weight stations cost could exceed $800,000 per site. Figure 2.11 shows the active permanent WIM stations across Texas.
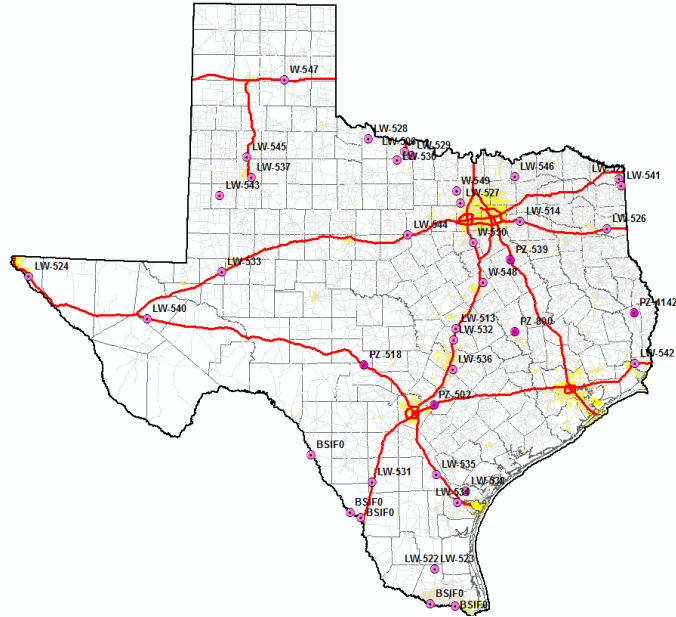
Figure 2.11. TxDOT WIM Stations (from TxDOT Truck Traffic and Loads).

2.4.2 Virtual WIM (V-WIM) stations

This system is the combination of WIM technology and Automatic Vehicle Identification (AVI) systems with a camera and Optical Character Recognition (OCR) software (Walubita et al., 2014). Similar to permanent WIM stations, the instrumentation of V-WIM stations involves axle load sensors embedded in the pavement perpendicular to the traffic flow direction. The technology for measuring axle loads is identical to the permanent WIM stations. According to Walubita et al. (2014), there are typically two setup options associated with this system as shown in Figure 2.12 (1) the system is connected with a digital warning signpost that instructs vehicles in violation to exit the highway, and (2) the system wirelessly transmits the data to an enforcement agency/agent.
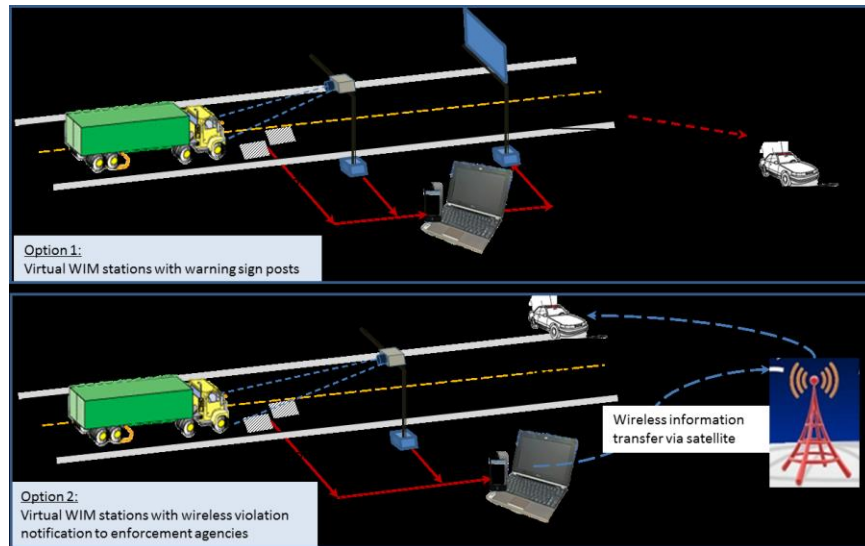
Figure 2.12. V-WIM System Installation (after Walubita et al., 2015).

2.4.3 Bridge Weigh-in-motion (BWIM)

Currently, bridge weigh-in-motion (B-WIM) systems can be divided in two different types. The first type of B-WIM systems are strain sensors coupled with separate axle-detecting sensors. These axle detecting sensors are a crucial part of the B-WIM system because they are designed to detect the presence of axles to calculate the vehicle speed, axle spacing, and classification. The second type of B-WIM system only uses strain gauge sensors that are mounted on bridge decks to detect axles and weight measurements (Al-Qadi et al.,2016). These systems could be nondestructively implemented in bridge decks by attaching a series of strain sensors beneath the bridge to record the bridge responses. The B-WIM system considers the full bridge as a weighing mechanism which can provide accurate results in terms of the axle weight, GVW, and classification of the vehicles passing over the bridges. In recent years, B-WIM systems have been deployed in several research projects to characterize the traffic loading information attributed to the site-specific conditions of the bridges (Lydon et al., 2016). Thus, the two major components that are essential for B-WIM systems are the algorithms used and the instrumentation techniques. Figure 2.13 illustrates the typical B-WIM system installed beneath the bridge deck and the strain peaks that would be detected.
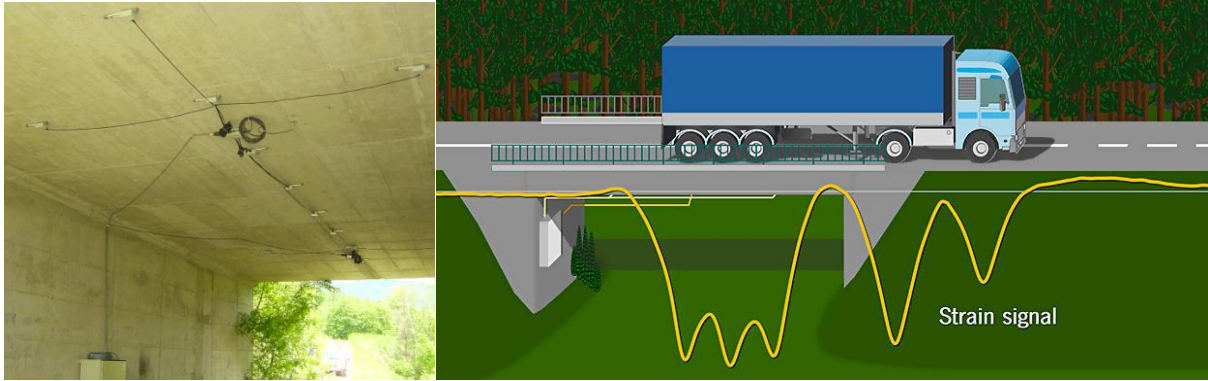
Figure 2.13. Typical B-WIM System Using Only Strain Sensors (from Labarrere, n.d.)

2.4.4 Portable Scales

Traditionally, portable scales have been used for the enforcement of load limits. These scales as shown in Figure 2.14 are designed for weighing either the wheel group or each axle to ensure the measurements comply with the regulations. Additionally, such portable scales are an integral part of the calibration process of portable and semi-portable WIM devices.

Figure 2.14. Figure PT300™ Static Wheel Load Scales (from Intercomp, n.d.)

2.4.5 Portable Weigh-in-Motion

Portable WIM systems as shown in Figure 2.15, are often preferred over the traditional permanent WIM stations due to the convenience, and the flexibility that they provided for the characterization of the traffic information. The lower cost associated with the temporary installation and maintenance of portable WIM systems has made them a viable option for the traffic data collection. There are several challenges for the use of portable WIM devices in the field. The most noteworthy anomaly is associated with the pavement roughness. The reliability of the collected data is greatly influenced by the vibrations generated due to the slope variance, surface cracks, rut depths, and patches on the pavement surface. Moreover, the WIM systems mounted above the surface also results in an additional dynamic motion. Such noises can potentially compromise the reliability of the static weight estimations based on dynamic measurements (Sridhar, 2008). Additionally, the flexible nature of the tire results in the adsorption horizontal force, which further adversely impact the accuracy of the results. Nonetheless, lower operating costs and ease of use makes the portable WIM systems a useful means for the collection of traffic information. Table 2.13 and 2.14 presents a comparison of different portable WIM systems.

Figure 2.15. (a) Low-Speed Portable WIM and (b) High-Speed Portable WIM. (from Intercomp n.d.)

Table 2.11. Summary of Low-Speed Portable Weigh-in-motion (LS-WIM) Systems using Portable Scales (from Walubita et al, 2015)

Category	Digiweigh DWP-80K	Intercomp LS-630	IRD DAW 300	Massload
Technological concept	Portable WIM using weighing plates	Portable WIM using weighing plates with wireless weighing technology	Portable WIM using weighing plates with Bluetooth® wireless technology	Portable WIM with ultraslim heavy-duty wheel load scales
Weight limit (dynamic)	40,000 lb per pad	44,000 lb per axle	44,000 lb per axle	40,000 lb per pad
Overload capacity	100% overload protection	150% overload protection	No information available	125% full scale safe, 150% full scale ultimate
Accuracy and reliability	Highly accurate (±3%)	Highly accurate (2 to 3%)	Highly accurate (±3%)	Highly accurate (±3% GVW at < 3 mph, ±5% GVW at 10 mph)
Speed	Low speed (< 5 mph)	Low speed (< 3 mph)	Low speed (< 6 mph)	Low speed (< 10 mph)
Ease of installation, simplicity of operation and user-friendliness	Easy setup. Simple and automatic. Operator presence required	Easy setup (< 15 min.). Simple and automatic. Operator presence required.	More complicated. Operator presence required.	Easy setup (1 < hour). Operator presence required.
Maintenance and sustainability	Easy maintenance	Easy maintenance	No information available	Easy maintenance
Cost	$6,400 and $3,500, respectively	$25,500	Ramp installation (Bluetooth) $37,841. Pit installation (wired) $25,073	$19,117
Data source	Vendor/supplier	Vendor/supplier	Vendor/supplier	Vendor/supplier

Table 2.12. Summary of High-Speed Portable Weigh-in-motion (HS-WIM) Systems using Strip Sensors (from Walubita et al, 2015)

Category	TRS Portable WIM	ECM Portable WIM	Intercomp
Technological concept	Portable WIM with piezo-electric sensors	Portable WIM with piezo-electric sensors	Portable WIM with wireless weighing technology
Accuracy and reliability	Fairly accurate (±15%)	Fairly accurate (±10 to 15%)	Highly accurate (2 to 3%)
Simplicity of operation and user-friendliness	Simple and automatic. Data collection for vehicle speeds ≥ 20 mph	Simple and automatic. Data collection at regular highway speed	Low speed (< 3 mph)
Ease of installation	Very easy (< 2 hours)	Fairly easy	Very easy (< 15 minutes)
Maintenance and sustainability	Requires calibration at every site	No information available	Easy maintenance
Cost	$11,911	$25,000	$25,500
Data source	Vendor/supplier	Vendor/supplier	Vendor/supplier

2.5 Sensor Technologies in WIM Systems

2.5.1 Strain Gauge Bending Plates

The bending plate device is used for traffic monitoring applications, overload detection, and data collection. It is a scale that is composed of two steel platforms that typically measured 2 ft by 6 ft and cover a 12-ft lane (Mohammad et al., 2005). These bending plates shown in Figure 2.16 use strain gages that measure tire load-induced strains that are analyzed to determine the tire load (Mohammad et al. 2005). Based on the manufacturer's information, such bending plates can weigh vehicles traveling between 5 km/h to 200 km/h and have a typical lifespan of more than 10 years.

Figure 2.16. IRD-Pad Bending Plate System (from International Road Dynamics Inc., n.d).

2.5.2 Hydraulic Load Cell

These type of certified load cells shown in Figure 2.17 are essentially large scales primarily used by truckers for self-weighting. They are one of the most accurate systems for collecting weight data however, they cannot record dynamic weight, are very expensive, require high maintenance cost, and have to be overhauled every 5 to 6 years.

Figure 2.17. Hydraulic Load Cells (from Cardinal Scales. n.d.)

2.5.3 Piezoelectric Sensors

Typical piezoelectric sensors consist of a copper strand that is surrounded by piezoelectric material and that is usually covered by a copper sheath or other material. Piezoelectric sensors measure the deformation induced by tire loads on the pavement and convert it to a charge that is equivalent to the deformation. These piezoelectric sensors shown in Figure 2.18 can be affixed to the pavement surface with conveyor belts, high strength tape, or metal fixtures. However, it is more common to embed them in the pavement by making a small groove on the surface, 1 to 2 in deep by 1 to 2 in wide, and cover them with resin (Mohammad et al., 2005). The installation procedures usually take less than a day however, once installed the piezoelectric sensors are left permanently in the pavement. In addition, these piezo sensors are able to record vehicles travelling at normal highway speeds.
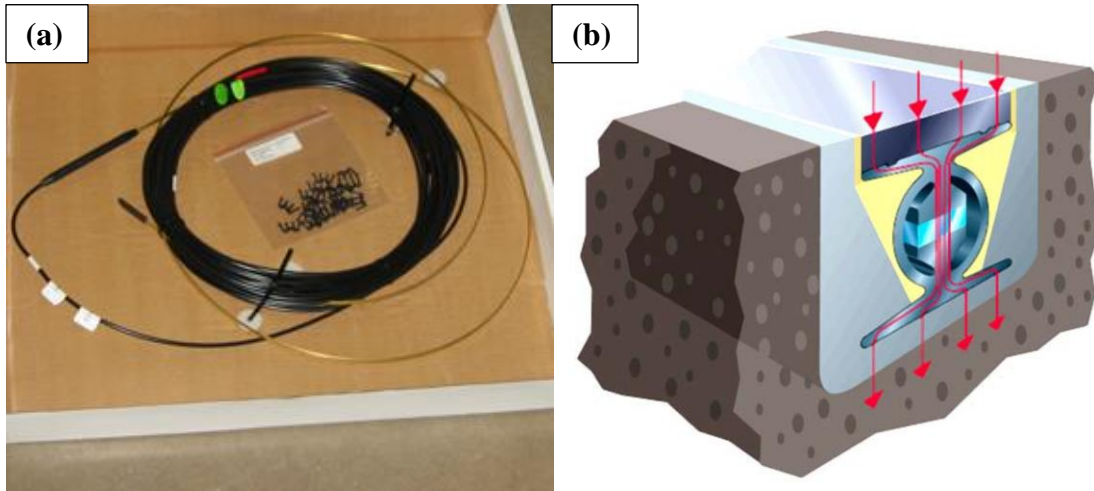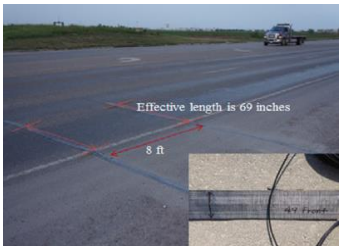
Figure 2.18. (a) RoadTrax BL Piezoelectric and (b) Kistler Lineas WIM Sensor. (from International Road Dynamics, n.d.)

Three separate studies conducted by different institutions using similar piezoelectric technologies are presented in Table 2.15 The researchers developed proprietary WIM systems using off-the-shelf components and stand-alone commercial WIM controllers. Thus, these studies propose a potential alternative to extremely expensive and labor-intensive installation of permanent WIM stations for the collection of traffic volume and weight data.

Table 2.13. Selected Research on WIM System by DOTs across the Nation

Researchers	Equipment	Components Used		Brief Description of the Study	Challenges of the Study
Faruk et al. (2016)	Effective length is 69 inches 8 ft	**WIM Controller**	TRS Portable WIM	The WIM system was deployed on an overweight corridor in Pharr District and provided reliable traffic data particularly for the first 7-days. The WIM system collected volume, vehicle classification, and weight distributions. Results showed that roughly 6.35% of trucks traveling in the Eastbound direction were overloaded (GVW >80kips). Sensors could be calibrated with a widely available TxDOT dump truck (Class6) and static scales.	Utilized pocket tape enclosures to affix the piezoelectric sensor to the pavement resulted in damages to the sensor, loss of operational functionalities, and accuracy. Sensors experience displacement due to continuous traffic loading, high temperatures, and housing tapes. In addition, reliability and accuracy of the collected data became questionable after 7 days, therefore seasonal data collection cannot be obtained using this WIM system.
		Sensor	Piezoelectric Roadtrax BL Sensor		
		Setup	Pocket Tape Enclosures		
		Lane Coverage	One Wheel Path (Right)		
		Sensor Length	6-feet		
Refai et al. (2014)		**WIM Controller**	IRD iSINC Lite	The portable WIM system was developed based on off-the-shelf components, commercially available WIM controllers, a solar powered unit with a total cost of $20,000. The portable WIM data was compared to permanent WIM data and the results indicated high correlation for both systems. In addition, the results showed that portable WIM system maintains data quality for short intervals and provides an alternative to permanent systems at about 10 percent of the cost.	Improper installation led to vibration of the sensor that resulted in the WIM controller over counting or misdetection of vehicles. In addition, using the default calibration factors for the sensors led to inaccurate vehicle classification and substantial weight error. Therefore, the portable WIM system should be calibrated at each site and every time the system is moved.
		Sensor	Piezoelectric Roadtrax BL Sensor		
		Setup	Galvanized Metal Sheets		
		Lane Coverage	One Wheel Path (Right)		
		Sensor Length	12-feet		
		Additional Monitor	REECE device		
Kwon (2012)		**WIM Controller**	Custom-Built WIM system	The data obtained from the developed WIM system was tested with data from a permanent WIM station with 97% agreement. According to the study, axle spacing and speed were almost identical with only .5% different, GVW was about 4% different, and vehicle classification was only 1.5% different. Based on the author's report, the results present an accurate account of traffic information.	The main challenge of this study was associated with the limitations of battery life for the data acquisition system. The battery for the system only lasted about 25 hours therefore, it requires daily visits from operators to exchange the battery. The weigh-pads also degraded after use causing wrinkles to form in the conveyer belt and to create errors during data collection.
		Sensor	Piezoelectric Roadtrax BL Sensor		
		Setup	Heavy Duty Conveyer Belt Pad		
		Lane Coverage	Full Lane		
		Sensor Length	12-feet		

3. Survey of TxDOT's Districts

3.1 Introduction

With assistance from the project advisory panel, the research team developed a survey questionnaire to document Districts affected by energy development operations. The main objective of this task was to document the extent, severity, and location of severely distressed sites primarily affected by oversize/overweight (OS/OW) vehicles. Additionally, the research team gathered information on OS/OW permits issued by the Department of Motor Vehicles (DMV).

Survey responses were received from the following 17 Districts: Dallas, Houston, Paris, Pharr, San Angelo, Bryan, Fort Worth, Corpus Christi, Laredo, Austin, Odessa, Tyler, Abilene, El Paso, San Antonio, Yoakum, and Beaumont as noted in Figure 3.1. Furthermore, the research team was particularly interested in the survey responses from the following Districts in the overload corridors of south Texas with emphasis on the Eagle Ford Shale region: 1) Laredo, 2) San Antonio, 3) Corpus Christi, 4) Yoakum, 5) Austin, 6) Bryan, and 7) Pharr District. This chapter summarizes all responses to the online survey and highlights the responses from Districts with overweight corridors and in the Eagle Ford Shale region. The collected information will be instrumental for selection of sites for deployment of the WIM devices and nondestructive field testing of representative pavements sections.
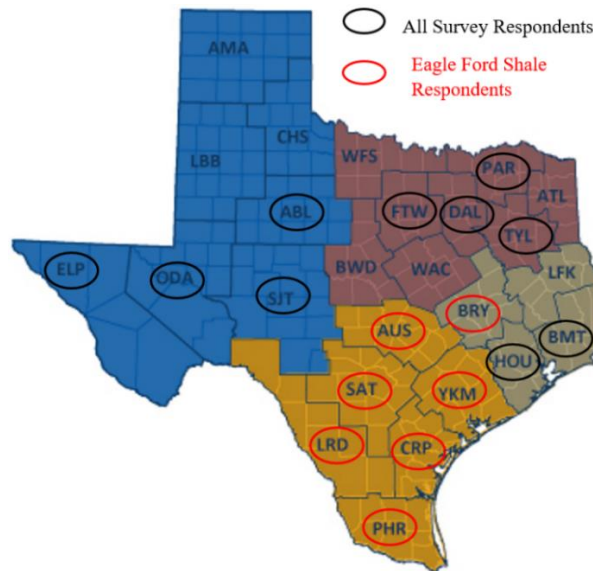
Figure 3.1. TxDOT Districts Respondent to Survey Questionnaire

3.2 Existing OS/OW PERMIT information

In recent years the utilization of oversize and overweight (OS/OW) vehicles has become more common due to higher industry demands. The use of (OS/OW) vehicles has several benefits such as reduction of traffic congestion, reduced fuel consumption, and lower CO_2 emissions as a result of fewer vehicles traveling in the highway systems. Despite the potential benefits of using (OS/OW) vehicles, heavier vehicles detrimentally impact the transportation infrastructure by accelerating pavement damage and causing premature failure (Batioja-Alvarez et al., 2018). These deteriorated highway systems require state agencies to spend millions in reconstruction, repair and maintenance as previously outlined in this chapter.

The recovery of the nation's economy coupled with the recent energy boom has led to significant increases in OS/OW permits issued by the DMV. Table 3.1 illustrates the number of Super Heavy Single-Trip permits for the movement of non-divisible loads or loads that exceed 254,300 lb in total gross weight issued between fiscal year 2004 and 2017. Since the initiative of tracking this permit, the number of issued permits doubled from the previous year until 2007. Then, the permits reach an all-time high in 2008 and 2009 with 1,238 and 1,525 issued permits, respectively; followed by several years of fewer issued permits and spiking up again in 2014 through 2016 – corresponding to the most recent boom in the oil and gas industry.

Table 3.1. Super Heavy Permits Issued by the TxDMV (from N. Edington, personal communication, February 12, 2018).

Fiscal Year	Super Heavy Permits Issued	Fiscal Year	Super Heavy Permits Issued
FY 2004	107	FY 2011	579
FY 2005	208	FY 2012	676
FY 2006	415	FY 2013	740
FY 2007	821	FY 2014	1,066
FY 2008	1,238	FY 2015	1,493
FY 2009	1,525	FY 2016	1,170
FY 2010	700	FY 2017	770

Figure 3.2, illustrates the annual volume of OS/OW permits issued between 1995 and 2017. Though the plot can be characterized by a fluctuating trend of increases and decreases in issued permits. The general trend of the plot shows that the issue of permits has been gradually increasing over the years. There are three noticeable peaks within each rise and fall of annual permits issued in 1998, 2008, and 2014. Expectedly, these years coincide with sharp increase in oil prices.
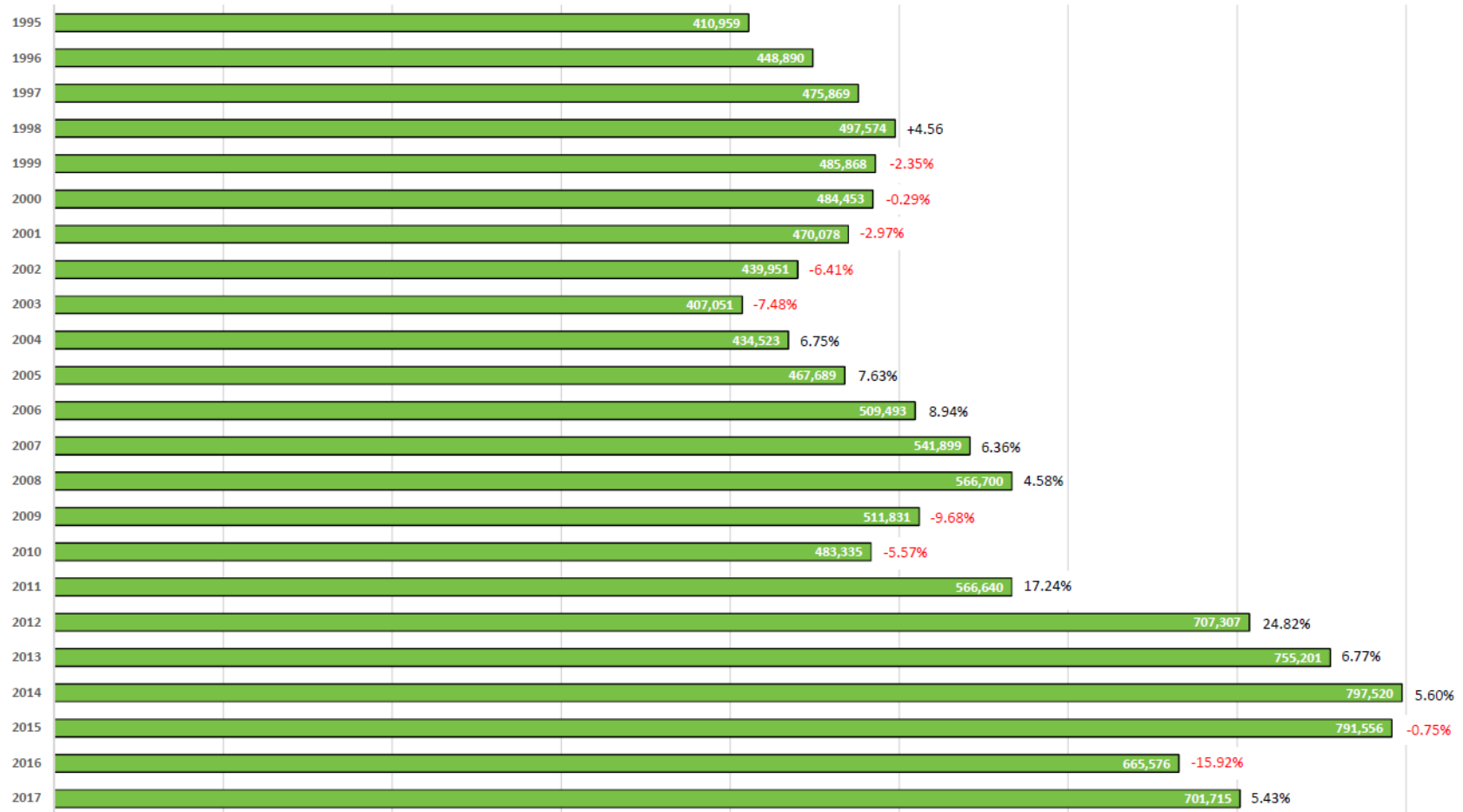
Figure 3.2. Annual Volume (1995-2017) of Oversize/Overweight (OS/OW) Permits Issued (from N. Edington, personal communication, February 12, 2018).

*Data compiled from the Texas Permitting and Routing Optimization System (TxPROS) by fiscal year and does not include Temporary Registration

Figure 3.3 shows the periods where peaks in price for the 42-gallon barrel of the West Texas Intermediate crude oil occur coincide with the years with peaks in OS/OW permits issuance by TxDMV.

Figure 3.3. West Texas Intermediate (WTI) Crude Oil History Chart (from Macrotrends, 2018).

Additionally, Table 3.2 illustrates the number of OS/OW permits issued for the oil and gas industry compared to the total permits. As evidenced in this table, the energy industry is responsible for slightly more than 1/3 of the total issued permits. In 2014 alone, the oil and gas industry accounted for nearly half of all issued permits. Therefore, it can be safely assumed that the annual volume of issued OS/OW permits is closely intertwined with the oil price per barrel and the energy development companies.

Table 3.2. Corresponding Percentage of Permits Issued to Gas and Oil Industry (from N. Edington, personal communication, February 12, 2018).

Fiscal Year	Gas and Oil Industry Percentage of Corresponding Permits
FY 2012	37%
FY 2013	43%
FY 2014	44%
FY 2015	41%
FY 2016	32%
FY 2017	37%

3.3 Survey Results

3.3.1 Are the Transportation Infrastructure Facilities in Your District Adversely Affected by Overweight Vehicles Due to Energy Development Activities?

From all the 17 Districts that responded to the survey questionnaire, 94.1% indicated that their transportation infrastructure has been adversely affected by overweight vehicles due to energy development activities, as shown in Figure 3.4. The Dallas District was the only District that did not report being severely affected by overweight vehicles. As expected, all respondents in the south Texas corridors and Eagle Ford Shale answered in the affirmative.
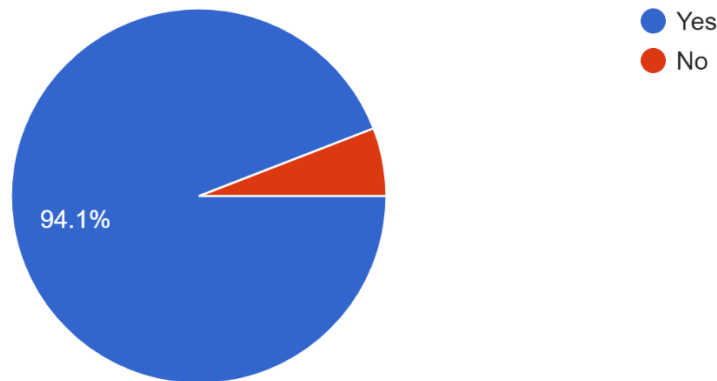
Figure 3.4. Percentage Districts Affected by Energy Development Operations.

3.3.2 The Severity of the Damages Imparted by Overweight Vehicles Associated with Energy Development Activities

Figure 3.5 illustrates the responses to the severity of the damages imparted by overweight vehicles in each District, ranked from minimal (1) to severe (10). Dallas District once again was the only District that did not rank the severity of the damages as high. All other respondents ranked the severity at a minimum of 5 or higher. Corpus Christi, Bryan, Abilene, Beaumont, and Tyler Districts all ranked the severity at 7. While El Paso, Houston, Laredo, Yoakum, and San Antonio District ranked the severity at 8. The Districts with the highest ranked severity were San Angelo, Austin, and Odessa Districts at 9, 9, and 10, respectively. The results clearly indicate that the severity of the damages is more pronounced in Districts with active energy development operations.
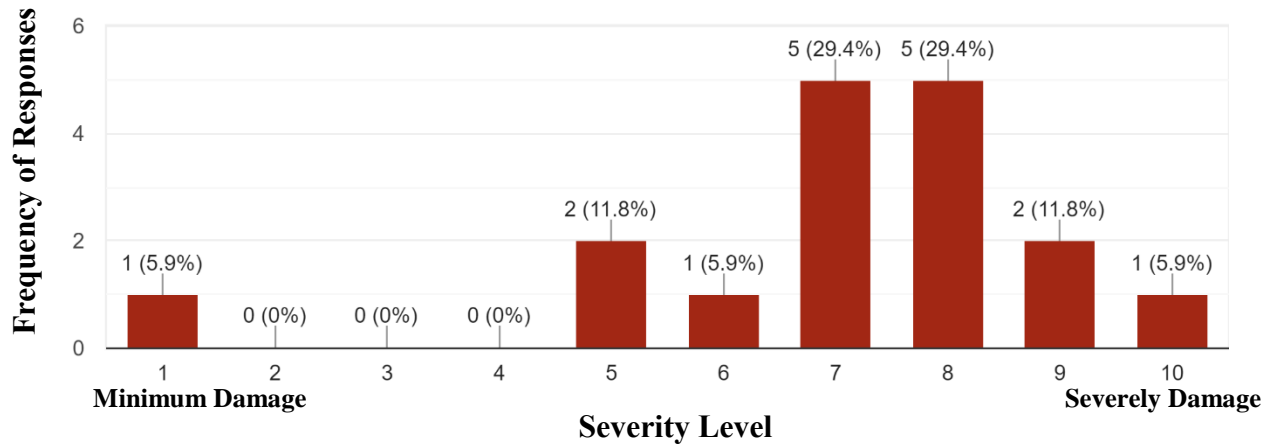
Figure 3.5. Severity of the Damages Imparted by Energy Development Operations

3.3.3 Typical Pavement Distresses/Damages Due to Energy Production Activities in TxDOT's Districts

One of the main objectives of the survey was to identify the typical pavement distresses and damages that the Districts experience. As shown in Figure 3.6, the most prevalent type of distresses among all the Districts are rutting (82.4%), potholes (82.4%), and fatigue cracking (76.5%). Other common distresses indicated by the respondents are slippage cracks (58.8%), edge cracks (58.8%), raveling (52.9%), and longitudinal/traverse cracking (52.9%). Tyler District indicated that the destruction of the seal coat and pavement at the entrance of well sites is also a notable distress that was not listed in our questionnaire. More importantly, for districts strictly in the Eagle Ford Shale region the top pavement distresses were rutting and pot holes, as indicated in Figure 3.7. Based on the Districts responses, the results indicate that most of the distresses and damages caused by energy development operations are inflicted on flexible pavements. Figure 3.7 also illustrates that the damages associated with rigid pavements are not a significant issue with the Districts in the Eagle Ford Shale. This could be attributed to few lane miles of rigid pavements as compared to the flexible pavement sections in the south Texas corridors. This conclusion is in agreement with the information provided in section 3.11 of this chapter.
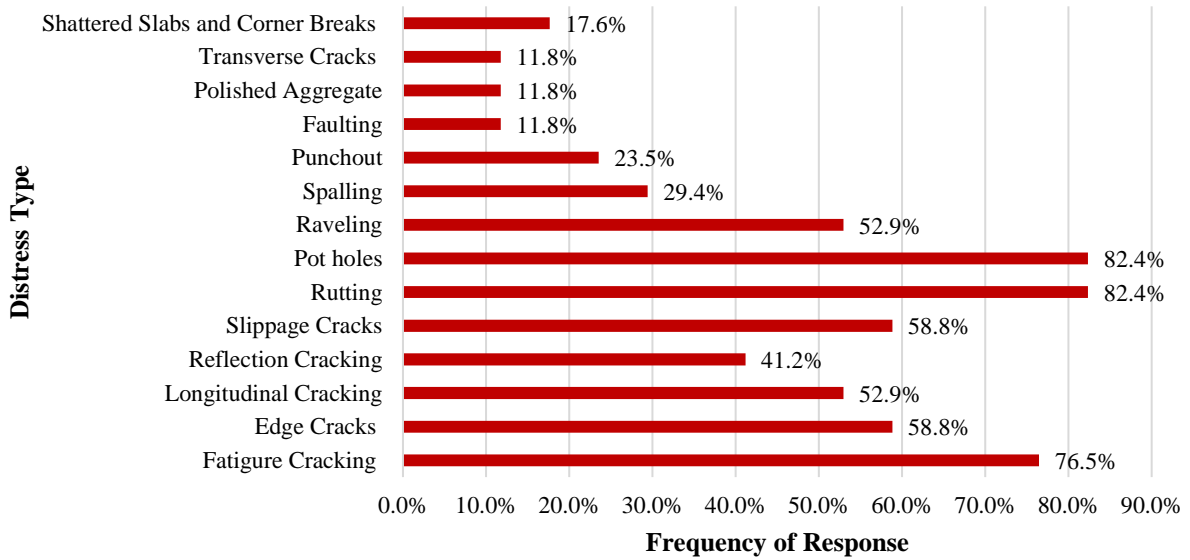
Figure 3.6. Typical Pavement Distresses and Damages Among All Responding Districts
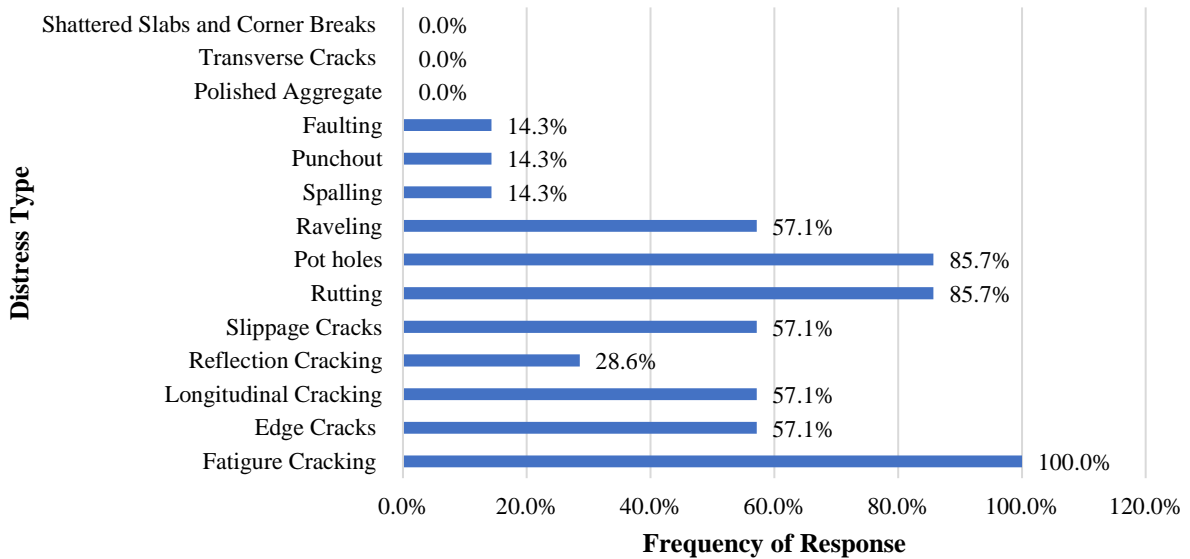
Figure 3.7. Typical Pavement Distresses and Damages Among Districts in the Eagle Ford Shale Region

3.3.4 Availability of active Weigh-In-Motion (WIM) Station in Each District

The majority of the Districts indicated that they do not have available active weigh-in-motion station in their District, as shown in Figure 3.8. However, Dallas, Paris, Pharr, Fort Worth, Corpus Christi, Laredo, and Odessa Districts indicated that they do have operational WIM stations.
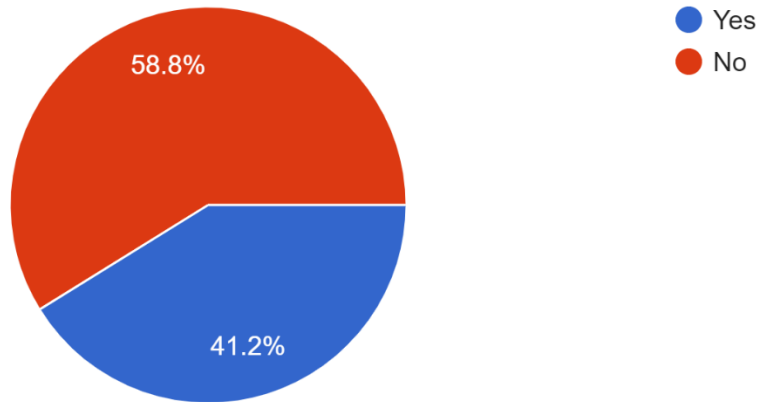
Figure 3.8. Availability of Operational Weigh-In-Motion (WIM) Stations in All TxDOT Districts

3.3.5 The Frequency of Over-Size/Over-Weight (OS/OW) Truck Traffic Experienced in Districts Highway Network

Figure 3.9 summarizes the District responses to question pertaining to the frequency of OS/OW truck traffic experienced in each District. El Paso, Abilene, and the Bryan Districts were the only Districts to rank the frequency of OS/OW truck traffic as relatively low. On a scale of 1 to 10, the majority of the respondents ranked the frequency of OS/OW traffic at 8 or higher in their Districts. The highest ranked frequencies were indicated by Tyler, Austin, Beaumont, Yoakum, and Odessa Districts, which are Districts in active energy development zones.
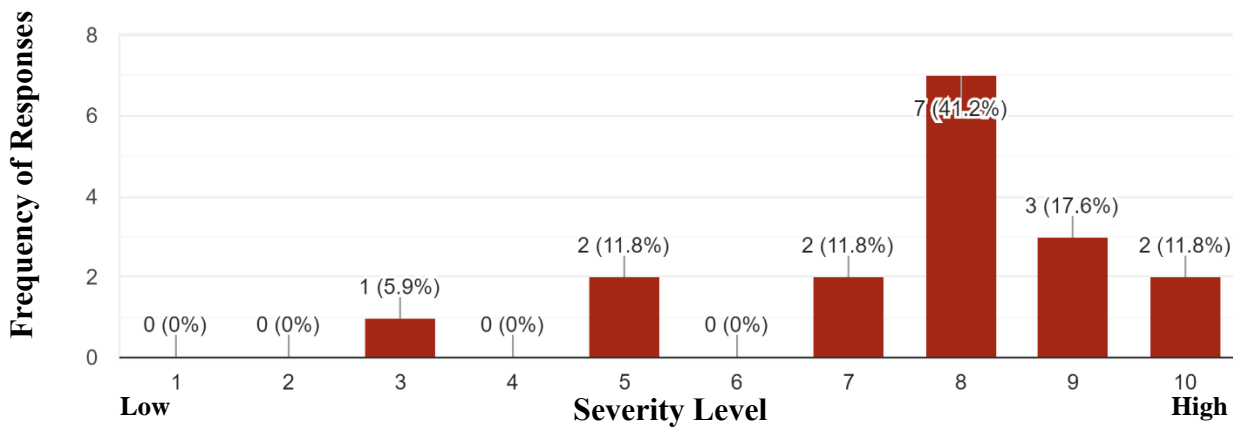
Figure 3.9. Frequency of Over-Size/Over-Weight (OS/OW) Truck Traffic Experienced

3.3.6 Growth Patterns for the Over-Size/Over-Weight (OS/OW) Truck Traffic in Districts

According to the observations of the different Districts throughout the state, nearly all the respondents indicated an increasing pattern in the frequency of the OS/OW truck traffic in their Districts. None of the Districts indicated that the traffic pattern has been similar to the pre-energy development era in Texas. Yoakum District indicated that the frequency of OS/OW has stayed the same in recent years, post energy boom. Corpus Christi District was the only District to indicate that the traffic operations of OS/OW trucks has been declining in recent years, results are illustrated in Figure 3.10.
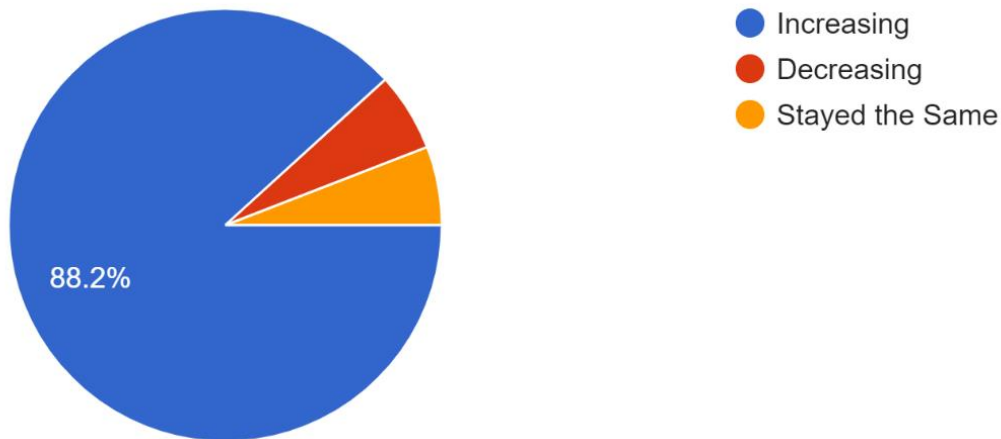
Figure 3.10. Growth Trends of Over-Size/Over-Weight (OS/OW) Truck Traffic

3.3.7 Highways with High Volume of OS/OW Truck Traffic and Severely Distressed Roads

One of the objectives of the survey was to gather information on OS/OW corridors and information on the location of the severely damaged highways and roadways in the energy development areas with emphasis on the Eagle Ford Shale region. This information will be crucial for the selection of sites for the deployment of WIM devices and non-destructive testing of representative sites. Table 3.3 illustrates the highways indicated by each District with high volume of OS/OW truck traffic. Table 3.4 illustrates specific Interstates, US Highways, State Highways, and Farm to Market roads listed by the TxDOT personnel as severely damaged. Predictably, some of the OS/OW corridors listed in Table 3.3 are the same ones that are severely damaged by the truck traffic operations, and are cross-listed in Table 3.4.

Table 3.3. Roadways with High Volume of OS/OW Truck Traffic.

No.	District	Response
1	Dallas	No Response
2	Houston	I-10, SH3, SH 146, SH 225, SH 332, SL 8, SS 330, FM 2004
3	Paris	IH30, US75, US69, SH37, US271, SH121, US377, SH19/24, SH11, SH154
4	Pharr	UP0281, US0281, IH0002, FM1016, SH0004, FM0511, SH0048
5	San Angelo	With the exception of Real and Edwards Counties most any road in the District could be subject to OS/OW
6	Bryan	IH 45, SH 6
7	Fort Worth	US281 SH59 FM730 SH114 IH20 SH171 FM51 SH199 US67 FM2481 SH108 FM8 FM219 IH30 IH820W US377 FM1187
8	Corpus Christi	US281 and US77
9	Laredo	US 83, FM133, FM 468, SH 97, FM 469
10	Austin	All US/IH routes
11	Odessa	All of Them
12	Tyler	Gregg & Rusk Counties-SH 149, US 259, US 80, LP 281, US 79, SH 43, IH 20
13	Abilene	No Response
14	El Paso	RM 652, FM 3541, FM 2185, US 62
15	San Antonio	SH 97, SH 72, SH 16, SH 85, FM 99, FM 2924, US 87, FM 140, FM 791, FM 1344, FM 541, FM 1582, FM 624
16	Yoakum	US 90a, US 77, US 183, SH35, FM 1593, US 59
17	Beaumont	US 90, SH 146, SH 321, SH 105, IH 10, US 59
* Districts highlighted in grey are within the Eagle Ford Shale Region		

Table 3.4. Severely Distressed Roadways that Need Maintenance and Reparations

No.	District	Response
1	Dallas	No Response
2	Houston	US59
3	Paris	No Response
4	Pharr	FM1847, FM1732, FM0803, UP0281, US0281, IH0002, FM1016, SH0004, FM0511, SH0048, FM0507, SS0206, FM1425, SH0107, SS0115, FM0681, SH0285
5	San Angelo	SH 137, RM 33, SH 163, US 277, US 83, FM 765, US 190, US 87
6	Bryan	Various FM roadways
7	Fort Worth	SH114 US281 FM2190 FM1191 FM4 FM51 IH20 FM8 FM2491 FM219 FM 1187 RM2871
8	Corpus Christi	Most distress occurred in Karnes/Live Oak: SH 72, FM 99, SH 239, SH 123, SH 80, etc. but most have been repaired beginning 2012
9	Laredo	FM 469, US 83
10	Austin	SH 142 In Caldwell County , SH 21 in Lee County, FM 20 in Bastrop County, US 77 in Lee County
11	Odessa	Most of Them
12	Tyler	SH 149, US 259, US 79, US 80, FM 2275, FM 840, US 84, FM 2658 and FM 3231
13	Abilene	No Response
14	El Paso	RM 652, FM 3541
15	San Antonio	FM 99, FM 2924, SH 85, SH 72, FM 624, FM 1099, SH 173
16	Yoakum	FM 1593, SH 35, US 183, SH 111, FM 2656, FM 238, SH 119, FM 2542
17	Beaumont	The roadways mentioned in question 9 have all had some needed repairs over time. None of them have significant issues at the moment due to planning and identifying projects that have helped to preserve the pavement (overlays, sealcoats, etc.)

* Districts highlighted in grey are within the Eagle Ford Shale Region

3.3.8 The Impact of Energy Development Activities on the Transportation Infrastructure Network, State Highways (SH), and Farm to Market (FM) Roads

Based on the survey results, all respondents in the Eagle Ford Shale ranked the severity of energy development operations at a minimum of 5 or greater. Yoakum, Laredo, San Antonio, and Austin Districts indicated that their transportation infrastructure has been severely impacted by the energy developments in the transportation network, as shown by Figure 3.11. The energy development impact on the Districts' state highways (SH) shown in Figure 3.12, was also significant. However,

all the Districts in the Eagle Ford Shale indicated that the energy development operations are more pronounced in their Farm to Market (FM) system as evidenced in Figure 3.13. The results clearly show that the existing pavement structures along the (FM) roads and some (SH) are the not sufficient to sustain the truck traffic operations by energy developing companies.
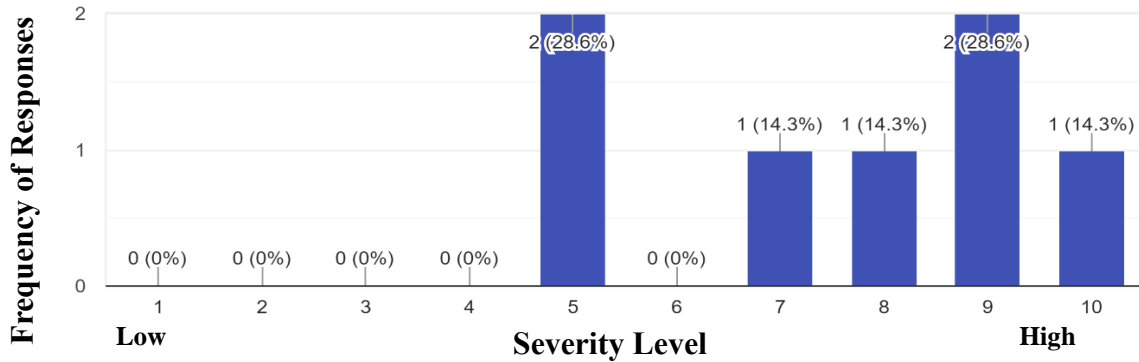
Figure 3.11. Energy Development Impact on the Transportation Infrastructure in the Eagle Ford Shale Region
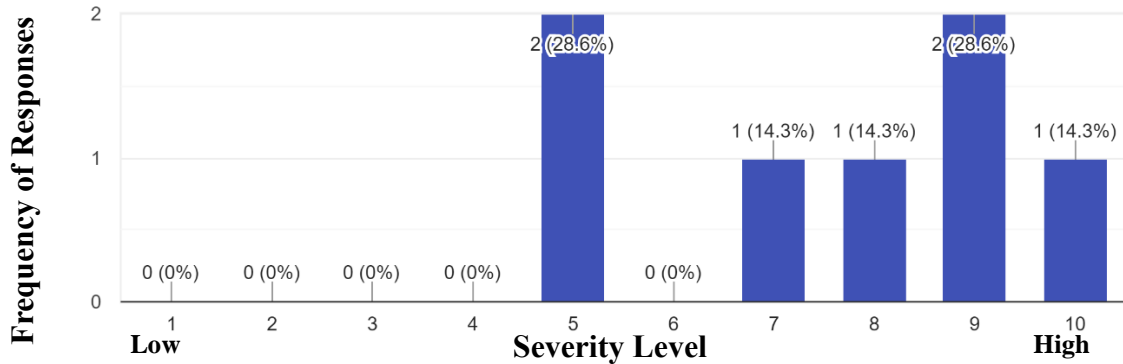
Figure 3.12. Energy Development Impact on State Highways (SH) in the Eagle Ford Shale Region
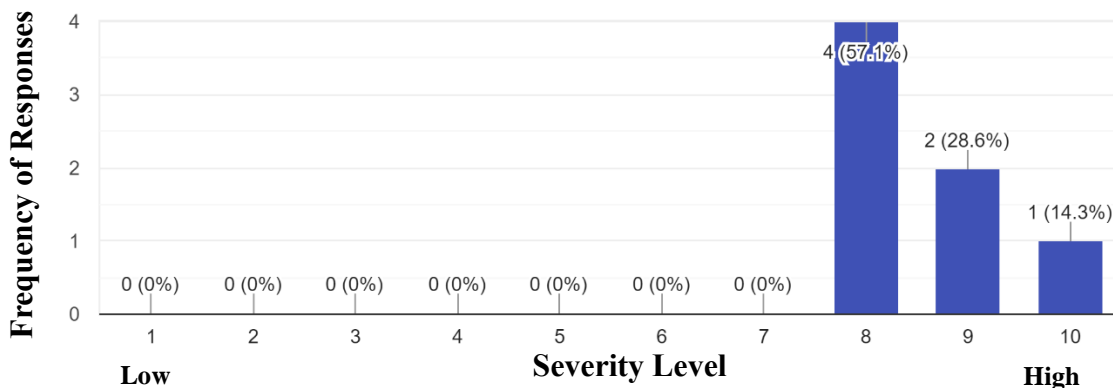
Figure 3.13 Energy Development Impact on Farm to Market (FM) roads in the Eagle Ford Shale Region

51

3.3.9 Typical Pavement Sections

According to the survey results, the most common pavement type for Districts in the Eagle Ford Shale region is the asphalt pavement with intermediate thickness (2-1/2" to 5-1/2"), followed by a tie between thick asphaltic concrete pavement (greater than 5-1/2"), and thin surfaced flexible base pavement (less than 2-1/2"). The results suggest that flexible pavements are the most prevalent pavement sections in the Eagle Ford Shale region. Bryan, Austin, and San Antonio Districts were the only respondents to report presence of rigid pavements specifically, continuously reinforced concrete pavement (CRCP), as shown in Figure 3.14.
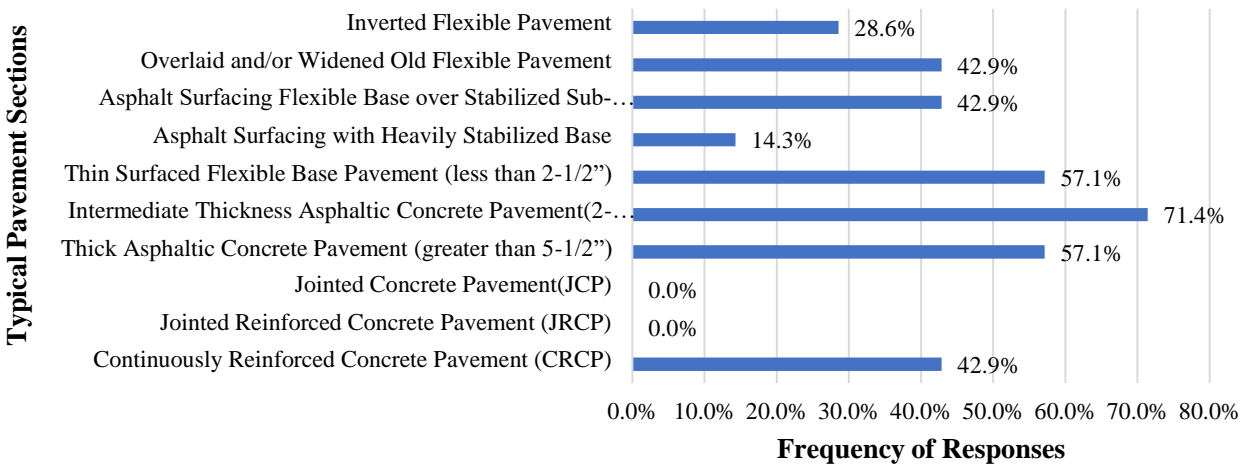
Figure 3.14. Typical Pavement Sections in the Eagle Ford Shale Region

3.4 Summary of the Major Points

- The oil and gas industry accounts for more than 1/3 of the total OS/OW permits issued in any given year.
- From the Districts that responded to the survey questionnaire, 94% indicated that their transportation infrastructure has been adversely affected by overweight vehicles due to energy development activities.
- The most prevalent type of distresses among all the Districts occur on flexible pavement, they are as follows: rutting (82.4%), potholes (82.4%), and fatigue cracking (76.5%).
- Energy development activities in the Eagle Ford Shale impacted Farm to Market (FM) roads the most adversely

4. Development of The Axle Load Spectra

4.1 Introduction

The main objective of this section is to outline the rationale for the site selection, the instrumentation efforts to collect the WIM data, and the development the axle load spectra database for representative sites in the energy development areas and overweight corridors of South Texas. In order to develop the axle load spectra, the research team collected the necessary traffic information by deploying portable weigh-in-motion (WIM) devices to ten selected roadways. Utilizing the portable WIM devices, the research team collected information pertaining to the Gross Vehicle Weight (GVW), axle weights, vehicle classification, axle configuration, traffic volume, and vehicle speed. Additionally, the research team focused on identifying the truck traffic, its distribution in the highway network, and the detrimental effect of overload traffic on the transportation infrastructure. Figure 4.1 illustrates a map of the locations of the ten selected sites throughout the different Districts in the Eagle Ford Shale region.
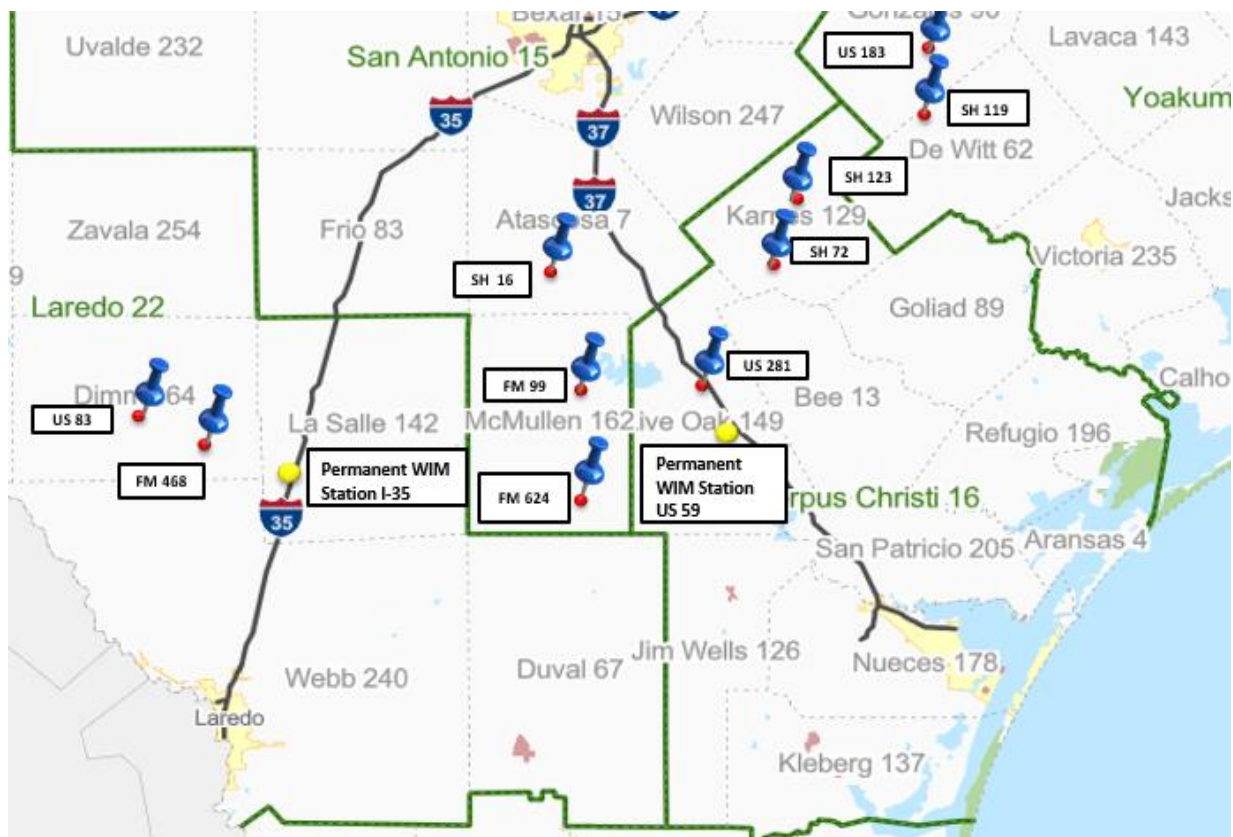
Figure 4.1. Selected Sites for Deployment of WIM Devices

4.2 Representative sites in the Eagle Ford Shale Network

The representative sites in the Eagle Ford Shale Region were selected based on the survey results after extensive communication with TxDOT personnel in Districts affected by energy developing activities. The research team focused on prioritizing roadways that were severely distressed and that accommodate high volume of Over Size/Over Weight (OS/OW) truck traffic in known energy developing areas and TxDOT priority corridors. In addition, the research team incorporated information such as: 1) proximity to the oil refineries, 2) neighboring oil and gas wells, 3) number of wells in the vicinity of the energy operations areas, 4) distress and conditions scores in the PMIS database, 5) current and upcoming construction/rehabilitation plans for roads in the affected highway network, and 6) previous research conducted. The study considered U.S. Highways, State Highways (SH), and Farm to Market (FM) roads to quantify the traffic operations and to further assess the detrimental effect of high volume/heavy truck traffic on the network. Major Interstate highways such as, I-35 and I-37 are better suited for truck traffic operations related to energy developments, and some even have operational WIM stations; therefore, these highways were not prioritized in this study. Table 4.1 shows the selected roadways accompanied by the rationale behind the selection of the roadway.

Table 4.1. Representative Roadways in Eagle Ford Shale Network

	District	County	Road Way	Online Survey		TxDOT Priority Corridor	Project Information	Well County Maps	Nearby Refineries & Oil/Gas Companies	PMIS Scores	Literature
1	LRD	La Salle /Dimmit	US 83	Listed as distressed road in network	Serves high volume of OS/OW traffic	TxDOT identified as priority corridor in Eagle Ford Shale Region.	1.Construction Scheduled 2. Finalizing for Construction 3. Projects Under Development	Numerous oil/gas wells in surrounding area as of 2015	1. Basic Energy Services 2. Chesapeake Energy 3. Stallion Oilfield 4.Eastern Oil Well Services 5.Sunbelt Oil& Gas Rentals	Low Distress and Condition Scores in PMIS database	N/A
2	LRD	La Salle	FM 469/ FM 468	Listed as distressed road in network	Serves high volume of OS/OW traffic	N/A	1.Construction Scheduled 2. Finalizing for Construction 3. Projects Under Development	Numerous oil/gas wells in surrounding area as of 2015	1. Chesapeake Energy on (FM 468) 2.All American Plains 3. NuStar 4. Patterson 239 5.Eog Resources 6.Noble Energy 7.NOVNational Oilwell Varco	Low Distress and Condition Scores in PMIS database	Referenced in Tech Memo TM-14-03. FM 468 in Cotulla in La Salle County. Experienced premature distress due to high volume& heavy traffic. Pavement was repaired by removing the existing surface treatment and placing 3" HMA layer.
3	SAT/ LRD	McMullen /La Salle	FM 624	Listed as distressed road in network	Serves high volume of OS/OW traffic	N/A	1.Construction Scheduled 2. Finalizing for Construction 3. Projects Under Development	Numerous oil/gas wells in surrounding area as of 2015	1. All American Plains 2. Storey Ranch	Low Distress and Condition Scores in PMIS database	Referenced in Tech Memo TM-15-01. Between SH 16 and La Salle County Line. Experienced premature distress due to high volume & heavy traffic. Used FWD, GPR, DCP, to assess the road conditions.
4	SAT/ CRP	McMullen Live Oak/ Karnes	FM 99	Listed as distressed road in network	Serves high volume of OS/OW traffic	N/A	1.Construction Scheduled 2. Finalizing for Construction 3. Projects Under Development	Numerous gas wells in surrounding area as of 2015	1.Coy City 1H on FM 99 2. Buckeye McMullen	Low Distress and Condition Scores in PMIS database	Referenced in Tech Memo TM-14-01. Construction project limits were from US 281A to the McMullen Co.Line. Researchers tested foam asphalt stabilization for 1-mile section
5	SAT/ LRD	Atascosa / McMullen	SH 16	Listed as distressed road in network	Serves high volume of OS/OW traffic	TxDOT identified as priority corridor in Eagle Ford Shale Region.	1.Construction Scheduled 2. Finalizing for Construction 3. Projects Under Development	Numerous oil/gas wells in surrounding area as of 2015	1. ETS Oilfield Services 2. Aery 1-1	Low Distress and Condition Score in PMIS database	N/A

Table 4.1 (cont.) – Representative Roadways in Eagle Ford Shale Network

	District	County	Road Way	*Online Survey		**TxDOT Priority Corridor	***Project Information	†Well County Maps	††Nearby Refineries & Oil/Gas Companies	†††PMIS Scores	‡Literature
6	CRP	Karnes	US 181/ SH123	Listed as distressed road in network	Serves high volume of OS/OW traffic	TxDOT identified as priority corridor in Eagle Ford Shale Region.	1.Construction Scheduled 2. Finalizing for Construction 3.Projects Under Development	Numerous gas wells in surrounding area as of 2015	1. Total Safety	Low Distress and Condition Score in PMIS database	N/A
7	CRP/ YKM/ SAT	Live Oak/ Karnes	SH72	Listed as distressed road in network	Serves high volume of OS/OW traffic	TxDOT identified as priority corridor in Eagle Ford Shale Region.	1.Construction Scheduled 2. Finalizing for Construction 3. Projects Under Development 4. Long Term Planning	Numerous oil wells in surrounding area as of 2015	1. Energy Transfer Plant (On FM626) 2. South Sugarloaf 3. Buckeye McMullen 4. Aery1-1	Low Distress and Condition Scores in PMIS database	Referenced in Tech Memo TM-14-06. Construction project limits were from SH 239 to FM 792 in Karnes County. Investigation was performed to establish the cause of premature distress, and recommendations were provided.
8	CRP	Karnes	US 281	Listed as distressed road in network	Serves high volume of OS/OW traffic	TxDOT identified as priority corridor in Eagle Ford Shale Region.	1.Construction Scheduled 2. Finalizing for Construction 3. Projects Under Development	Numerous gas wells in surrounding area as of 2015	1. Valero Three Rivers Refinery 2. Kinder Morgan Texas Pipeline	Low Distress and Condition Score in PMIS database	Site used by Walubita and Wenting in a case study to analyze traffic data by deploying a portable WIM system. Between Reference Marker 620 - 622
9	YKM/ CRP	Gonzales	US 183	Listed as distressed road in network	Serves high volume of OS/OW traffic	TxDOT identified as priority corridor in Eagle Ford Shale Region.	1.Construction Scheduled 2. Finalizing for Construction	Numerous oil wells in surrounding area as of 2015	1. Noble Royalties Inc. 2. Original Art in Oil	Low Distress and Condition Scores in PMIS database	N/A
10	YKM	De Witt	SH 119	Listed as distressed road in network	Serves high volume of OS/OW traffic	N/A	1.Construction Scheduled 2. Finalizing for Construction 3. Projects Under Development	Numerous gas wells in surrounding area as of 2015	1. Pipeline Construction	Low Distress and Condition Score in PMIS database	N/A

* Online survey questionnaire was answered by District Engineers and Maintenance Supervisors.

**Identified Priority Corridors where obtained from the PowerPoint presentation "Energy Sector Workshop" (2016) by Randy C. Hopmann.

***Construction project information was obtained for each roadway from TxDOT Project Tracker.

†Well County maps where used from TxDOT provided documents. Referenced in Implementation Report IR-16-01 "Well County Maps"

†† Google Maps used to Identify Refineries, Oil, Gas, and other Energy related companies

†††Distress Scores and Condition Scores for each roadway where obtained from the PMIS Database for years up to 2010.

‡ Information obtained from the extensive literature that was reviewed.

4.3 Weigh-In-Motion (WIM) Data Collection

4.3.1 Weight-In-Motion Equipment

For the primary data collection equipment, the research team selected the portable traffic recording system (TRS) unit from International Road Dynamics (IRD) to be in compliance with previous research efforts conducted by TxDOT. The TRS unit consists of a controller, piezo input box, piezo-electric sensors, and their protective cover, as seen in Figure 4.2. The TRS unit is the main data logger that records the traffic information from the sensors placed on the road. The type of sensors used in this study were the Roadtrax BL Class I piezoelectric sensors which were installed on the road using a specialized pocket tape. This tape is used to affix the sensors to the pavement surface and allows the sensors to be easily removed and reused at another site if still serviceable.

Table 4.2 shows the equipment details and layout of the sensors. The equipment utilized was the most advantageous in this study due to its cost-effectiveness, minimum installation time, and portable convenience. In contrast, permanent WIM stations typically have higher installation cost and maintenance requirements that makes them financially challenging to operate in a continuous manner. Furthermore, they require extensive installation efforts due to the small trenches that must be cut in the pavement to permanently place the sensors, inductive loops, or weight pads on the roads. The pavement damage on one hand and the traffic control requirements as well as the user delays are other disadvantages of such systems. Additionally, there are favorable scholarly publications by researchers in other states, such as Faruk et al. (2016) and Lubinda et al. (2019), regarding the reliability of the acquired traffic distribution and classification data using the portable TRS WIM units.

Figure 4.2. Field Equipment from Left to Right: TRS Controller, Piezo Input Box, 4in. Pocket Tape, Piezo-electric Sensors, Splice Protective Cover

Table 4.2. Portable WIM Equipment Details

WIM Equipment Used in Data Collection	
Data Logger	Portable TRS WIM Controller
Type of Sensor	Piezoelectric Roadtrax BL sensor
Sensor Placement	Pocket Tape Enclosure
Lane Coverage	One Wheel Path
Sensor Length	8-ft
Sensor Layout	2 Piezoelectric Sensors
Additional Devices Used	No Inductive Loops or Road Tubes were used

4.3.2 Field Installation

The field installation consisted of two piezoelectric sensors inserted into specialized 4 in. pocket tapes that are adhered to the pavement surface. The tapes with the inserted sensors are placed a predetermined distance, in our case 8 ft apart from one another, and connected to the main data acquisition system as shown in Figure 4.3. The sensors are installed to essentially just register one-wheel path; nonetheless, they nearly extend the entire length of the lane to account for wheel wander. The WIM unit automatically converts the data for 1-wheel path and translates it into the total axle weights and GVW by using an internal subroutine. For highways with multiple lanes in one direction, the piezo-sensors were installed in the outside lane of all highways, where the majority of the truck traffic travels. Moreover, during summer installations the research team had no problem installing the sensors because of the high temperature of the pavement surface. However, for winter installation the research team had to heat up the tapes and the roads surface with a heat torch to allow proper adherence between the tape-pavement interfaces, as show in Figure 4.4.
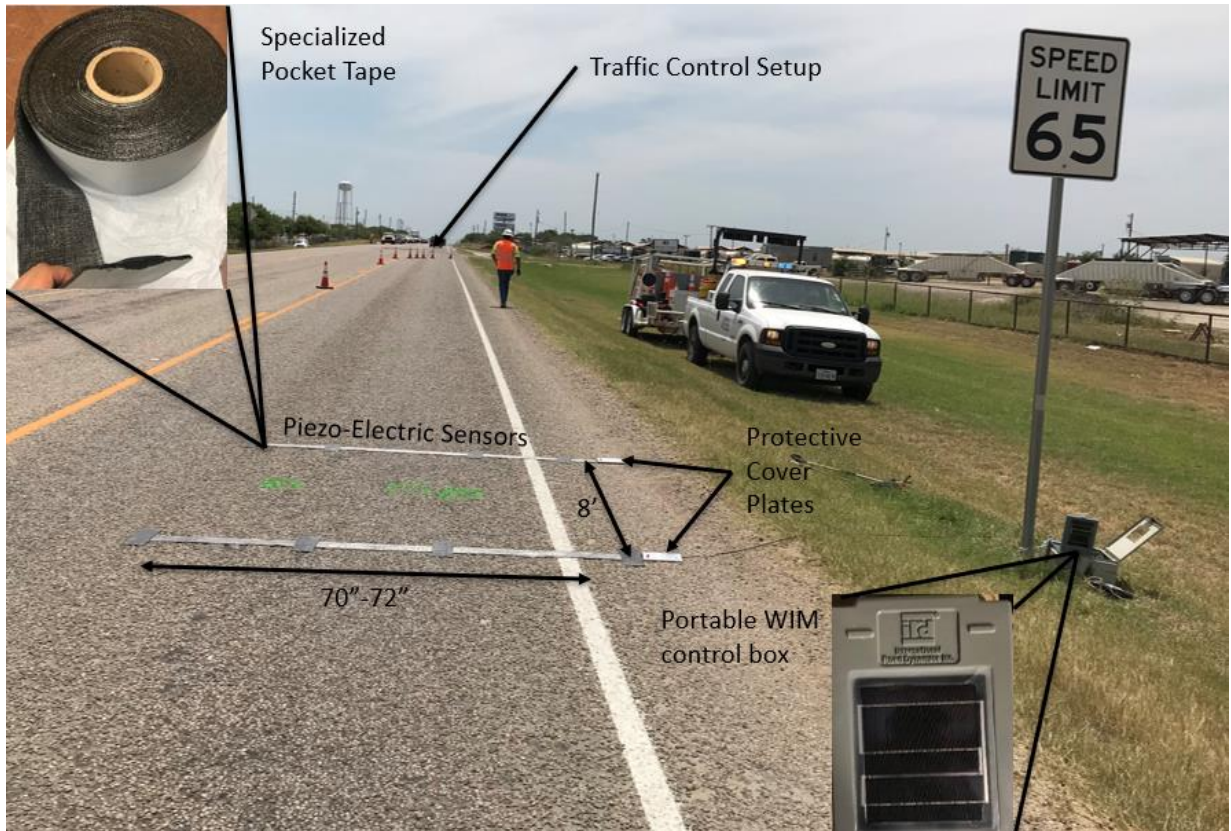
Figure 4.3. Typical Portable WIM Equipment Setup

Figure 4.4. Portable WIM Field Installation in the Winter Time

4.3.3 WIM Field Calibration

The research team successfully developed an effective method to properly calibrate the piezoelectric sensors to obtain accurate and reliable weigh-in-motion readings. Figure 4.5 shows a flow chart of the calibration process. This process was implemented at the time of installation and removal of the WIM devices. Calibration of the WIM systems were conducted at every test site before and after the collection period to optimize the accuracy and reliability of the WIM data. For this purpose, Class 6 trucks were selected as calibration vehicles due to their accessibility across all TxDOT Districts. Whereas Class 9 trucks were also selected due to their high frequency in the highway network. Therefore, both Class 6 and Class 9 trucks were used in the calibration procedure. Initially, the gross vehicle weights (GVW) and axle weights of these reference vehicles were measured using portable static axle scales and recorded as illustrated in Figure 4.6. The static weight of a fully loaded Class 6 dump truck typically ranged between 40 to 55 kips, and the loaded Class 9 truck typically ranged between 70 to 88 kips. The recorded static weights were then used as the target weight during the system calibration. The calibration runs were then conducted using with both reference vehicles while changing the vehicle speeds as shown in Figure 4.7. Finally, a calibration factor was then applied to the data until the target weight was within an acceptable tolerance. In addition to the pre-calibration procedures performed, the research team also conducted post-calibration on the piezo-sensors to ensure sensor functionality and WIM data quality.

1. *Using static scales, weigh the axles and GVW of the reference Class 6 and Class 9 trucks.*

2. *Drive the reference vehicles over the installed sensors.*

3. *Vehicle passes are conducted at different speeds. Usually a minimum of 5 passes at 3 speeds (+/-15 mph) the Speed Limit.*

4. *Adjust the calibration factors until the recorded dynamic weight matches the static weight.*

5. *Continue adjusting the Calibration Factor until the recorded weights are within an acceptable tolerance.*

Figure 4.5. Calibration Process Implemented

Figure 4.6. Static Axle Weight Measurements: (a)Class 6 Dump Truck (b) Class 9 Water Truck (c) Class 9 Belly Dump (d) Static Axle Weight Using Portable Scales.

Figure 4.7. Portable WIM Calibration Runs (a) Class 9 Belly Dump (b) Class 9 Water Truck (c) Class 6 Dump Truck

4.3.3 Sensor Life

The reliability and quality of the traffic data collection is paramount to the accuracy of the predicted damages in the proposed framework. Several factors contribute to the accuracy and reliability of the WIM data collections such as pavement condition, surface distresses, surface temperature, environmental conditions, and the field calibration procedure. However, based on the research team's experience in this project the operational service life of the piezo-sensors greatly influence the quality of the WIM-achieved traffic data. One way to assess the performance of the sensors is by analyzing the deterioration of the calibration factors over the operational life of the installed piezo-electric sensors in the field. Figure 4.8 shows the variation of the calibration factors for several sites in San Antonio, Laredo, Corpus Christi, and Yoakum Districts. The results pertaining to the sensors installed for over 50 days in the State Highway 123-80 in Corpus Christi (CRP-123-80) provides valuable insights on the longevity and service life of the piezo-electric sensors in overweight corridors of Eagle Ford Shale region.
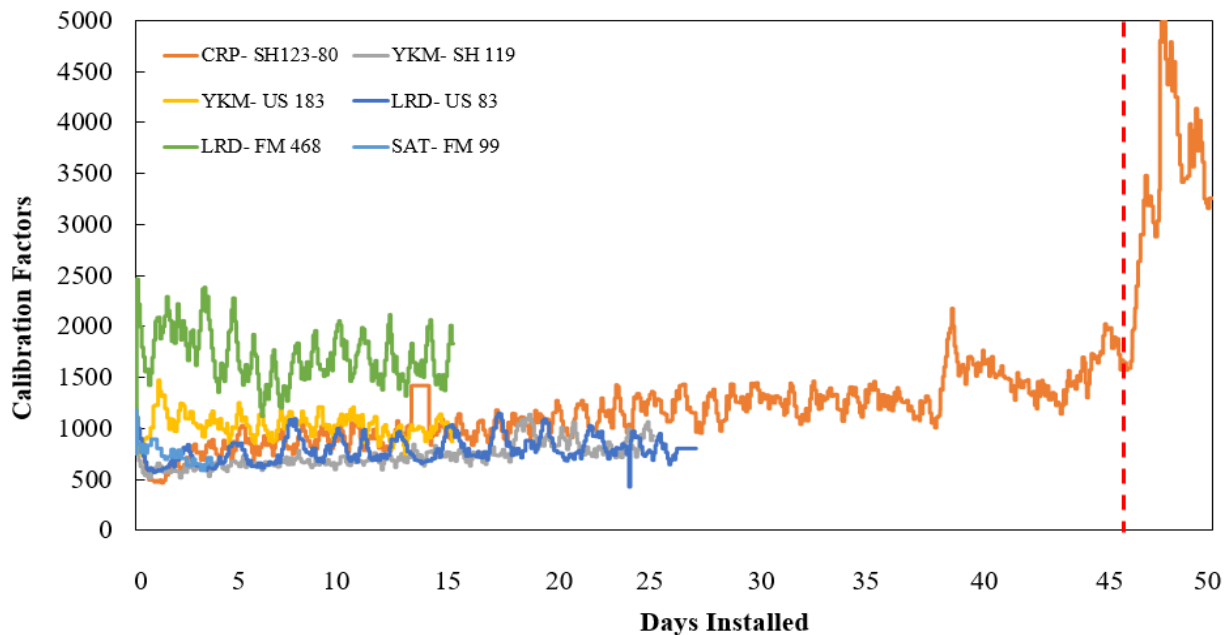
Figure 4.8. Site-Specific Calibration Factors.

4.4 Axle Load Spectra

The developed axle load spectra database was the compilation of portable WIM data collected at ten sites strategically distributed throughout the Eagle Ford Shale Region. The data collection was conducted in two-time intervals, summer and winter, to capture the effect of seasonal traffic variations, as well as the effect of environmental conditions on the damage quantification.

Moreover, the WIM units were left in the field continuously collecting data for a two-week time period per site. After sensor installation and data collection, the raw traffic data were compiled and analyzed to produce the following traffic information and traffic inputs listed in Table 4.3.

Table 4.3. Collected Traffic Data Using Portable WIM

Traffic Volume	Weight	Others
Average Daily Traffic (ADT)	Gross Vehicle Weights (GVW)	Vehicle Speed
Average Daily Truck Traffic (ADTT)	Axle Weights (Steering, Tandem, Tridem, Quad)	Speeding Vehicles
Percent Truck	Weight Distribution V.S Time	Axle Spacing
Vehicle Class Distribution	Overweight Vehicles	Wheelbase
Truck Class Distribution	Overweight Axles	Time
Hourly Distributions	Average Ten Daily Heaviest Wheel Loads (ATHWLD)	Date
Daily Distributions		

To develop the axle load spectra database the research team first extracted the raw traffic data from the TRS units and applied post-calibration factors. Then the data was processed and classified by axle type (Steering, Single, Tandem, Tridem, Quad) and load intervals and then formatted as axle load distribution (ALD) input files to be compatible with the TxME and AASHTOWare software. Table 4.4 shows a sample ALD distribution for tandem axles in US 281 of the Corpus Christi District. This information not only serves for ME pavement design purposes but also aids in traffic characterization, highway planning data, overweight/oversize documentation, and pavement damage quantification. Figure 4.9 provides the stepwise flow charts for the traffic characterization in the representative test sites. The collected information was established to create a unique comprehensive traffic database for US highways, State highways, and Farm to Market roads of energy developing areas in the Eagle Ford Shale Region.

Table 4.4. Sample Tandem Axle Distribution for TxME Traffic Inputs

Season		January	January	January	January	January	January	January	January	January	January
Veh. Class		4	5	6	7	8	9	10	11	12	13
	Total	100	100	100	100	100	100	100	100	100	100
	6000	4.12	0.00	0.92	0.00	3.96	0.17	0.00	0.00	0.00	0.00
	8000	7.06	0.00	3.68	0.00	5.95	0.91	0.00	0.00	0.00	4.17
	10000	7.65	0.00	8.88	0.00	8.29	2.65	0.00	0.00	0.00	0.00
	12000	5.88	0.00	7.20	0.00	10.45	4.26	0.00	0.00	7.29	12.50
	14000	3.53	0.00	11.18	0.00	9.55	4.99	2.30	0.00	8.33	4.17
	16000	1.76	0.00	7.50	0.00	7.93	5.74	1.15	0.00	7.29	12.50
	18000	1.18	0.00	6.74	0.00	6.49	5.74	5.75	0.00	6.25	4.17
	20000	4.71	0.00	7.04	0.00	9.19	6.02	4.60	0.00	17.71	8.33
	22000	5.29	0.00	7.20	0.00	9.01	6.24	4.60	0.00	14.58	0.00
	24000	9.41	0.00	5.97	0.00	4.68	7.46	8.05	0.00	10.42	4.17
	26000	10.00	0.00	5.97	0.00	5.59	8.85	14.94	0.00	11.46	4.17
	28000	7.06	0.00	8.12	0.00	4.68	9.19	14.94	0.00	9.38	4.17
	30000	12.94	0.00	3.83	0.00	3.60	7.71	6.90	0.00	2.08	4.17
	32000	6.47	0.00	4.59	0.00	2.34	6.37	11.49	0.00	1.04	0.00
	34000	5.88	0.00	2.30	0.00	1.98	5.29	9.20	0.00	1.04	8.33
	36000	2.94	0.00	2.14	0.00	2.16	4.71	2.30	0.00	1.04	0.00
	38000	0.59	0.00	1.99	0.00	0.54	3.52	1.15	0.00	2.08	4.17
	40000	0.59	0.00	1.38	0.00	1.26	3.16	3.45	0.00	0.00	8.33
	42000	1.76	0.00	0.77	0.00	0.90	2.51	2.30	0.00	0.00	8.33
	44000	0.59	0.00	0.77	0.00	0.18	1.84	4.60	0.00	0.00	4.17
	46000	0.00	0.00	0.61	0.00	0.54	1.24	0.00	0.00	0.00	0.00
	48000	0.00	0.00	0.31	0.00	0.18	0.69	1.15	0.00	0.00	0.00
	50000	0.00	0.00	0.00	0.00	0.18	0.34	1.15	0.00	0.00	0.00
	52000	0.59	0.00	0.15	0.00	0.36	0.22	0.00	0.00	0.00	0.00
	54000	0.00	0.00	0.15	0.00	0.00	0.12	0.00	0.00	0.00	4.17
	56000	0.00	0.00	0.31	0.00	0.00	0.03	0.00	0.00	0.00	0.00
	58000	0.00	0.00	0.15	0.00	0.00	0.01	0.00	0.00	0.00	0.00
	60000	0.00	0.00	0.15	0.00	0.00	0.02	0.00	0.00	0.00	0.00
	62000	0.00	0.00	0.00	0.00	0.00	0.00	0.00	0.00	0.00	0.00
	64000	0.00	0.00	0.00	0.00	0.00	0.00	0.00	0.00	0.00	0.00
	66000	0.00	0.00	0.00	0.00	0.00	0.00	0.00	0.00	0.00	0.00
	68000	0.00	0.00	0.00	0.00	0.00	0.00	0.00	0.00	0.00	0.00
	70000	0.00	0.00	0.00	0.00	0.00	0.00	0.00	0.00	0.00	0.00
	72000	0.00	0.00	0.00	0.00	0.00	0.00	0.00	0.00	0.00	0.00
	74000	0.00	0.00	0.00	0.00	0.00	0.00	0.00	0.00	0.00	0.00
	76000	0.00	0.00	0.00	0.00	0.00	0.00	0.00	0.00	0.00	0.00
	78000	0.00	0.00	0.00	0.00	0.00	0.00	0.00	0.00	0.00	0.00
	80000	0.00	0.00	0.00	0.00	0.00	0.00	0.00	0.00	0.00	0.00
	82000	0.00	0.00	0.00	0.00	0.00	0.00	0.00	0.00	0.00	0.00

The leftmost column is labeled "Axle Weights" (rotated, spanning the weight rows).
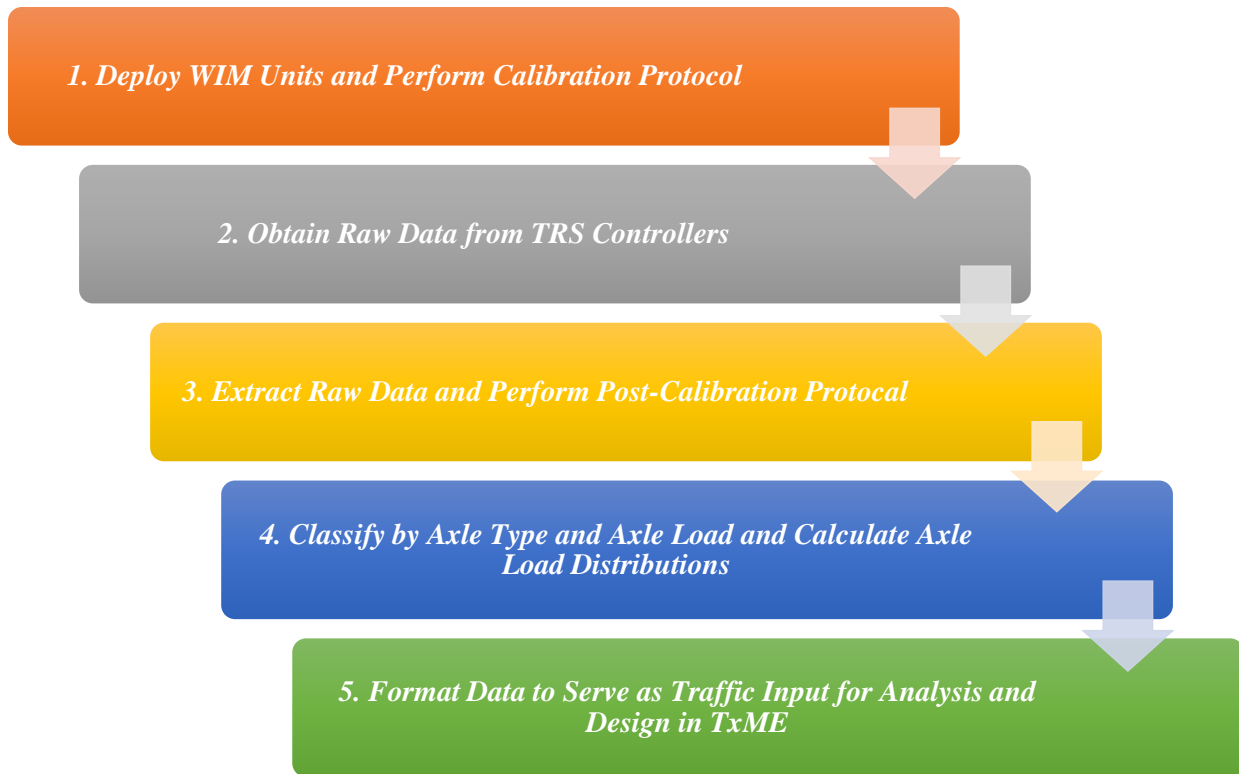
Figure 4.9. Portable WIM Data Processing Flowchart

4.4.1 Truck Class Distribution

The vehicle class distribution function was one of the most essential pieces of traffic information collected by the portable WIM units. This information is a direct input to the Texas Mechanistic pavement design software (TxME), and has a significant influence on the final result. From the collected traffic data, the most prevalent truck classes identified in all ten highways were Class 5 and Class 9 trucks as circled in Figure 4.10 Class 5 trucks have a steering axle and rear axle with dual tires, they are typically associated as small delivery trucks such Penske and U-Haul trucks. While Class 9 trucks have a single steering axle and two tandem axles in the back. The types of Class 9 trucks can range significant as they can be used to transport finished goods, oil, gasoline, equipment and much more.
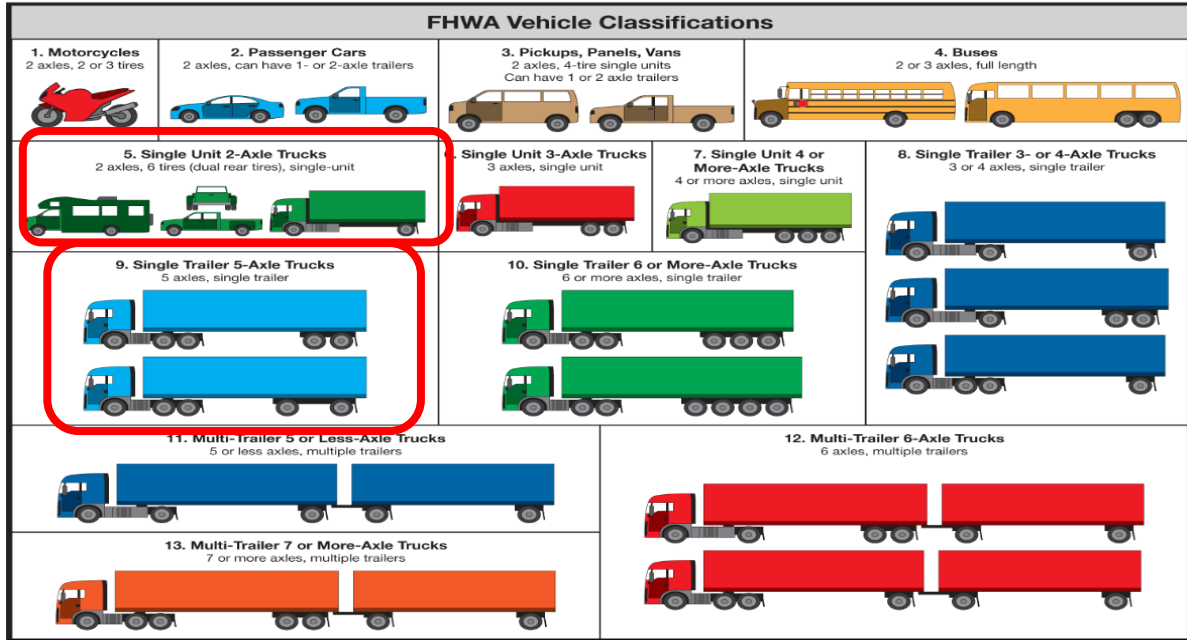
Figure 4.10. FHWA Vehicle Classifications

Figure 4.11 illustrates the truck class distributions comparisons versus percent trucks for all the different highway types (FM, SH, US). In all different highway structures Class 9 was the most common truck followed by Class 5. Farm-to-Market (FM) roads generally tend to have a higher number of Class 5 delivery trucks compared to the state highways (SH) and US highways. In contrast US highways had the highest Class 9 and fewest Class 5 trucks. Moreover, Figure 4.12 illustrates the truck class distributions among all the portable WIM sites in the Eagle Ford. These results are in agreement with the trends found in the literature.
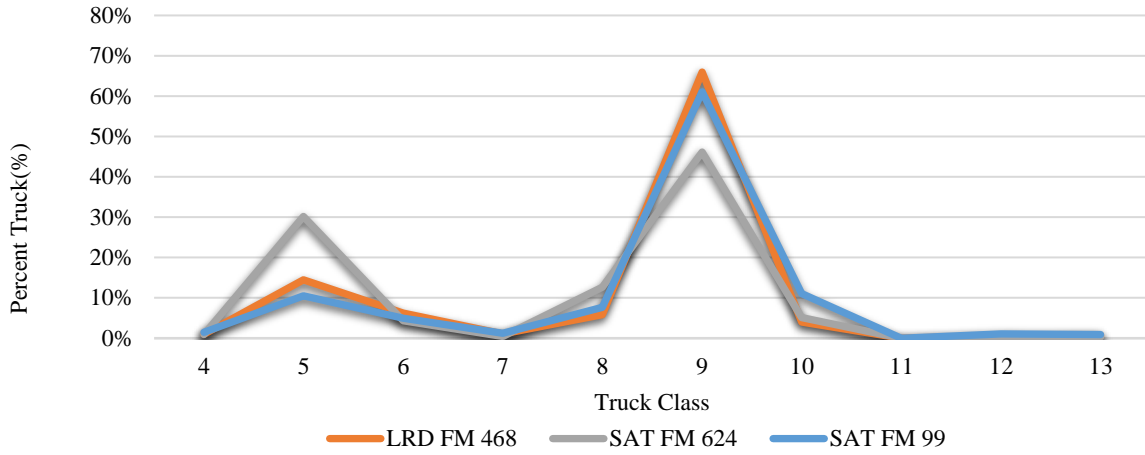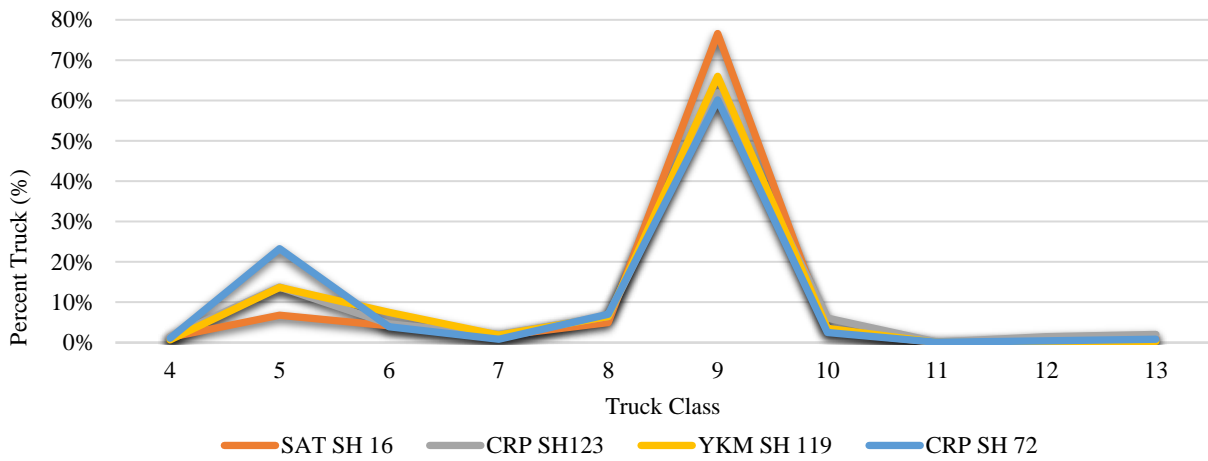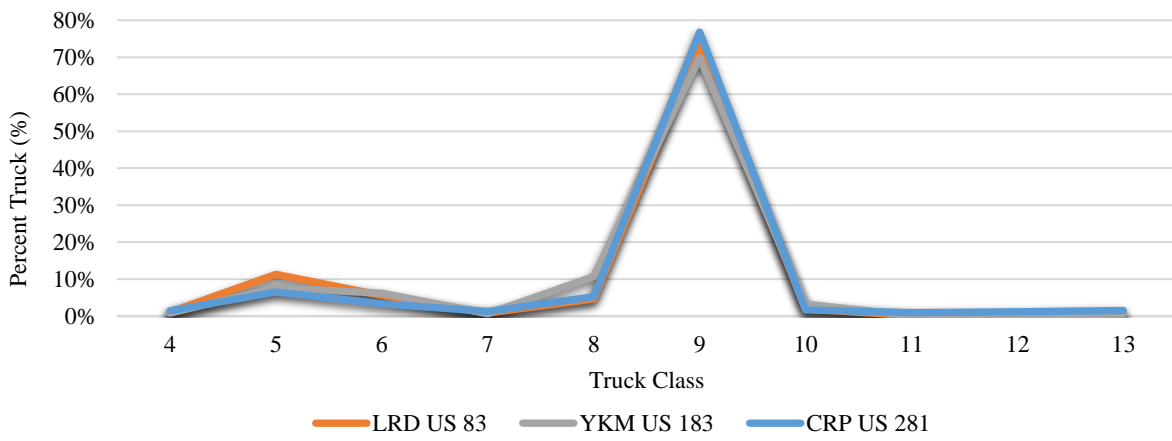
Figure 4.11. Truck Class Distributions: (a) FM Highways (b) SH Highways (c) US Highways in the Eagle Ford Shale

67
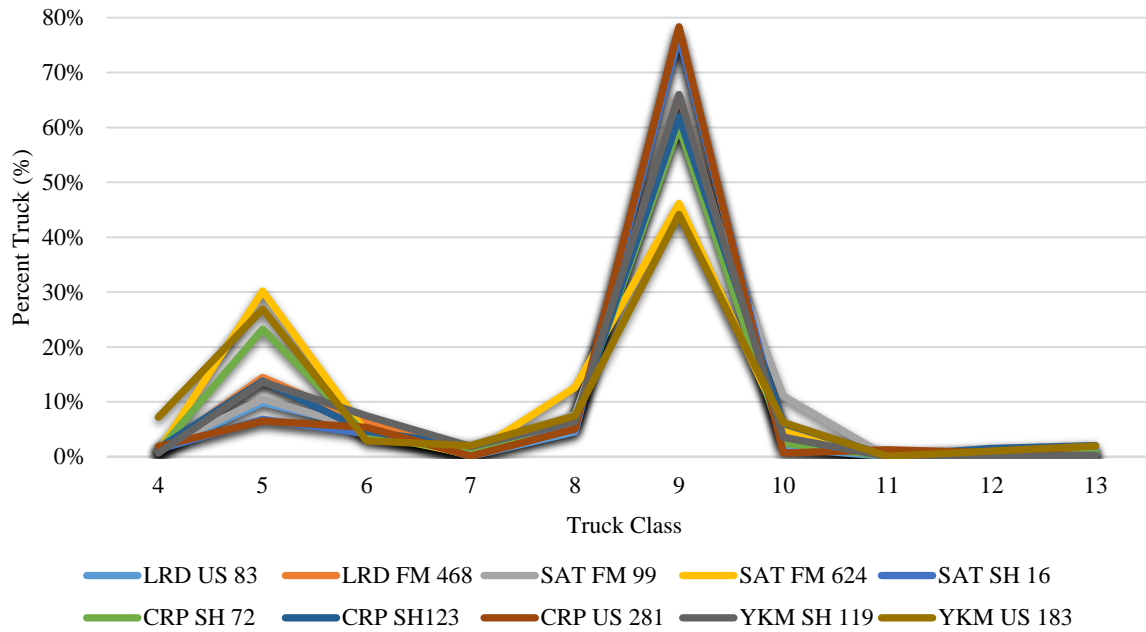
Figure 4.12. Truck Class Distributions of All Portable WIM Sites in the Eagle Ford Shale

4.4.2 Truck Misclassifications

Portable WIM units are characteristically very reliable at collecting and classifying vehicular traffic. Figure 4.13 illustrates the typical error classifications associated with each type of truck class. As illustrated, these misclassifications errors tend to be very low. The classes of trucks with the highest error percentage are Class 4 and Class 7. Class 4 is a predominant characterized by buses, and therefore, new bus configurations could be the source of that error. While Class 7 trucks are typically characterized by dump trucks with multiple rear axles that can be deployed when needed; they often have a lift axle that could mislead the algorithm the WIM unit uses. Other sources of errors can also be attributed to pavement surface imperfections, traffic driving over the sensor splice, damaged sensors, or unconventional truck configurations. Figure 4.14 illustrates the truck class distribution of US 83 in the Laredo District. This plot shows the truck class distribution of the summer and winter collection period and the differences are almost imperceptible. Despite two different data collection times, the portable WIM unit classified the incoming traffic appropriately.
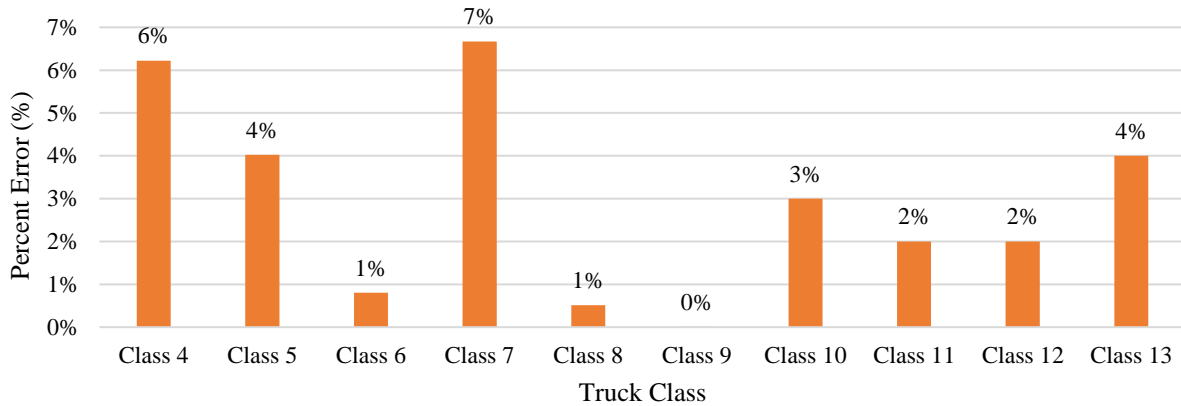
Figure 4.13. Truck Class Distributions Misclassification Error
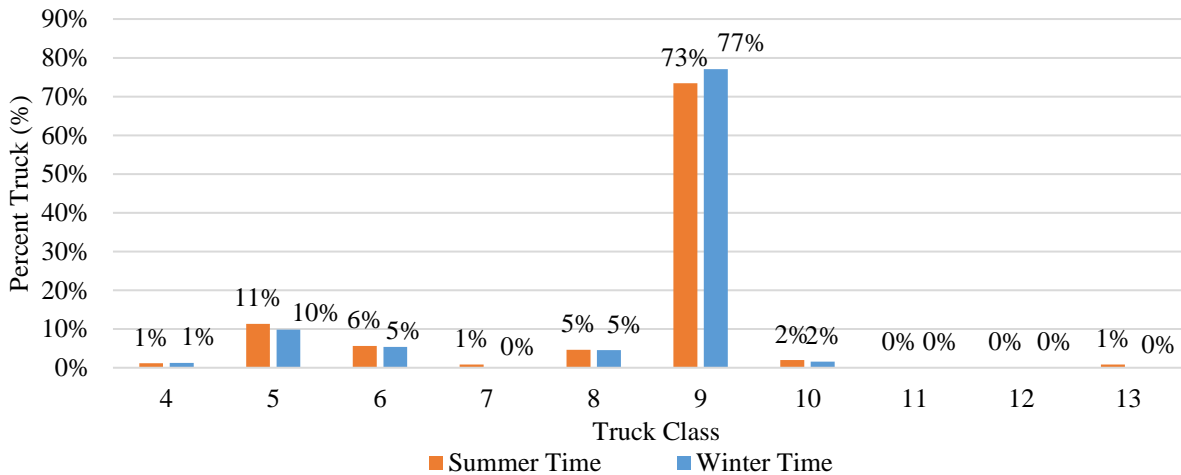
Figure 4.14. Seasonal Variation of Truck Class Distributions

4.4.3 Data Validation-Steering Axle Analysis

Contracting institutions and state agencies primarily favor and used portable WIM devices due to their minimal traffic interruption, cost effectiveness, and ease of operation in remote areas compared to stationary WIM stations. Validating WIM data can be cumbersome at times because researchers often don't have the means to justify the weight readings; thus, the reliability of the data becomes questionable. However, there are a few metrics that can give an indication of the accuracy and reliability of the WIM data being collected, such as using the steering axle weight of typical Class 9 trucks. According to truck manufacturers, typical steering axle weights of Class 9 trucks range between 8,000 to 12,000 lbs. The steering axle weight that was used as the reference axle weight during calibration of the portable WIM units was 10,500 lbs. Figure 4.15 illustrates the typical steering axle weight of Class 9 trucks in SH 16 of the San Antonio Districts. As shown

69

in the figure the bulk majority of the weight distributions fall within the expected 8,000 to 12,000 lbs range. As a matter of fact, 93% of the weight distributions fell in this range and 36% of weight distributions fell in the 10,500 lb interval. This proved that the WIM units are collecting accurate WIM data that is suitable for the development of the axle load spectra.
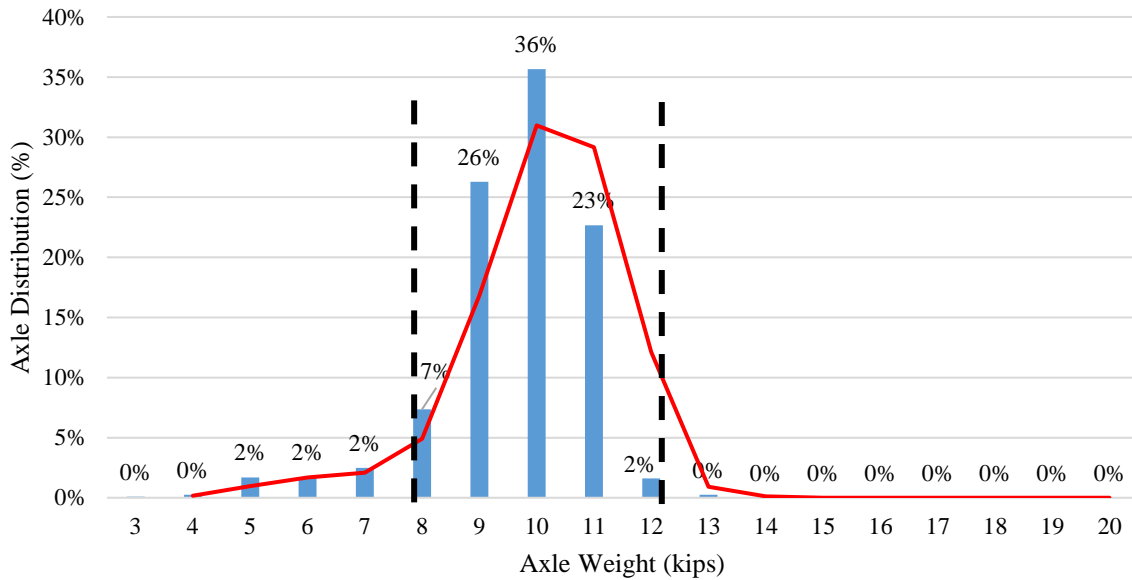
Figure 4.15. Steering Axle Weight Distribution of Class 9 Trucks in SH 16

Figure 4.16 and Figure 4.17 similarly illustrate steering axle plots of other WIM sites with one major distinction. The plot of Figure 4.16 was selected to show that the steering axle weight was still within the expected range however, the most common axle weight (37%) was in the lower spectrum at 9,000 lb. The researchers attributed the lower steering axle weights to the low GVW distributions collected at this site. In contrast, Figure 4.17(a) illustrates the steering axle weight of FM 468 in the Laredo District. This figure shows the steering axle weights in the higher spectrum with the most common axle weight (23%) at the 12,000 lb interval. The reason behind these results is attributed to the WIM data collected at FM 468, which contained some of the heaviest GVW distributions in the entire Eagle Ford Shale Region. Reference plots for the GVW Distributions for SH 119 and FM 468 are illustrated in Figure 4.17(b) and Figure 17(c).
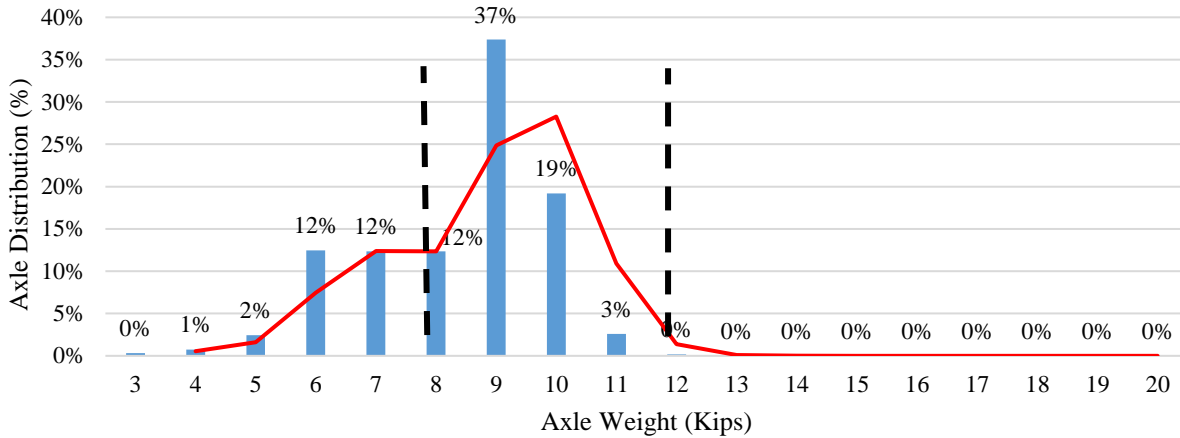
Figure 4.16. Steering Axle Weight Distribution of Class 9 Trucks in SH 119

(a)
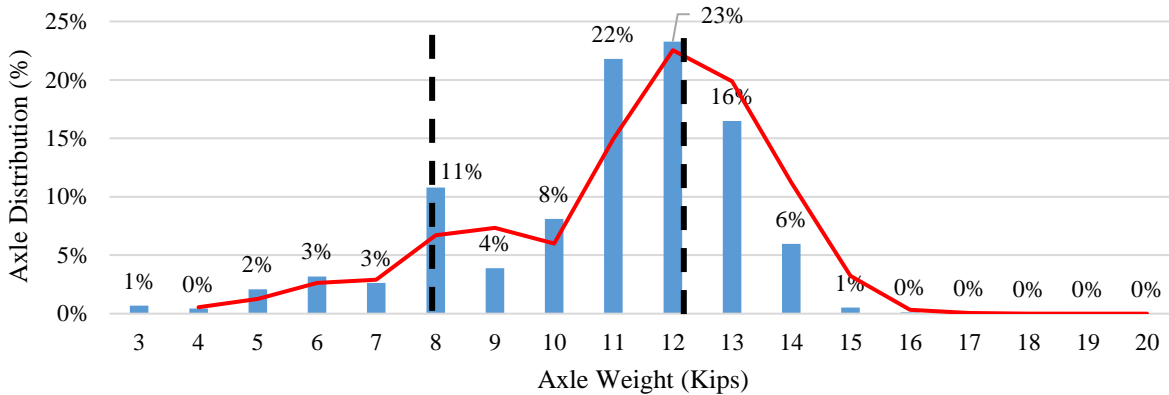
(b) SH 119 Class 9 GVW Distribution
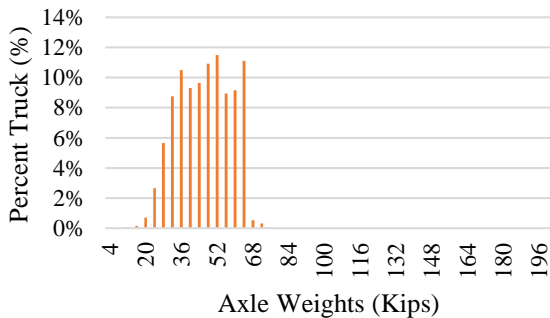
(c) FM 468 Class 9 GVW Distribution
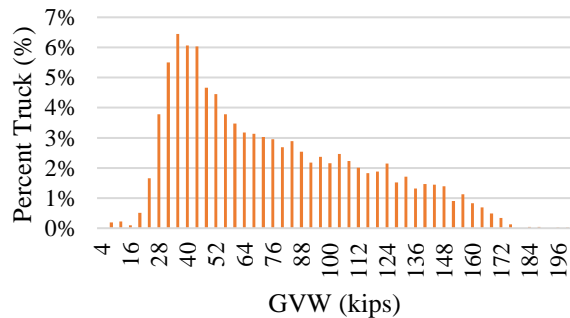
Figure 4.17. (a) Steering Axle Weight Distribution of Class 9 Trucks in FM 468 (b) Reference GVW Distribution SH 119 (C) Reference GVW Distribution FM 468

Figure 4.18 illustrates the average steering axle weight of Class 9 trucks for all portable WIM sites collected in the Eagle Ford Shale. A small spread of steering axle weights can be seen in the plot which can be attributed to a number of different reasons. Nonetheless, the vast majority of the steering axle weights are within the desired range. In addition, Figure 4.19 illustrates plots of all the steering axle weights collected for SH 16 and US 183 highways with their respective typical Coefficient of Variance (COV). These plots show a COV less than 15%, which is congruent with the error percentage ±15% indicated by the equipment manufacturer. Similar trends are true for the rest of the WIM test sites.
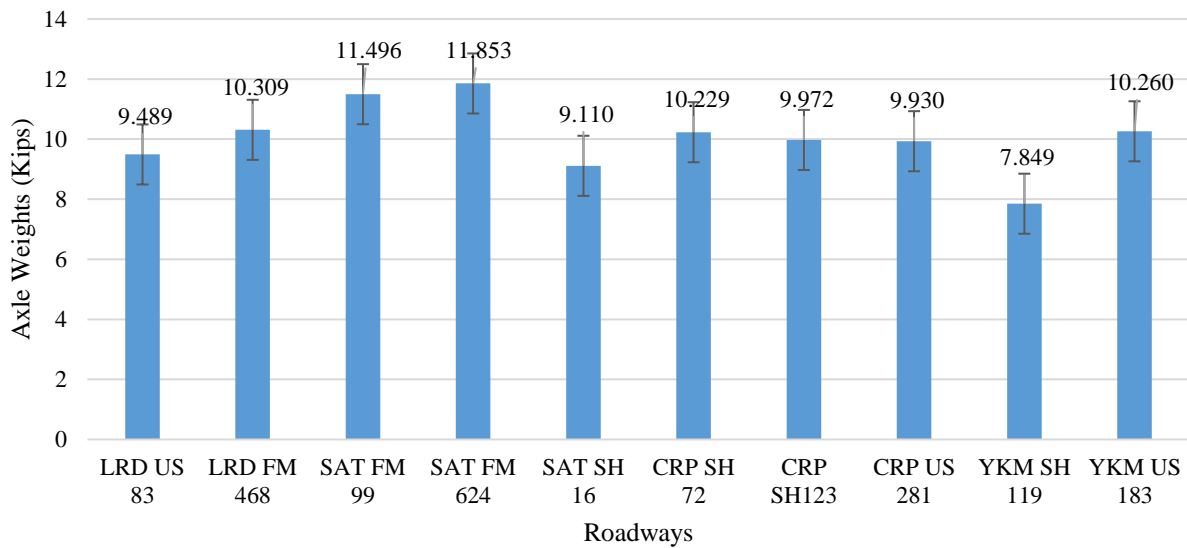
Figure 4.18. Steering Axle Weight Distributions of Class 9 Trucks in All Sites
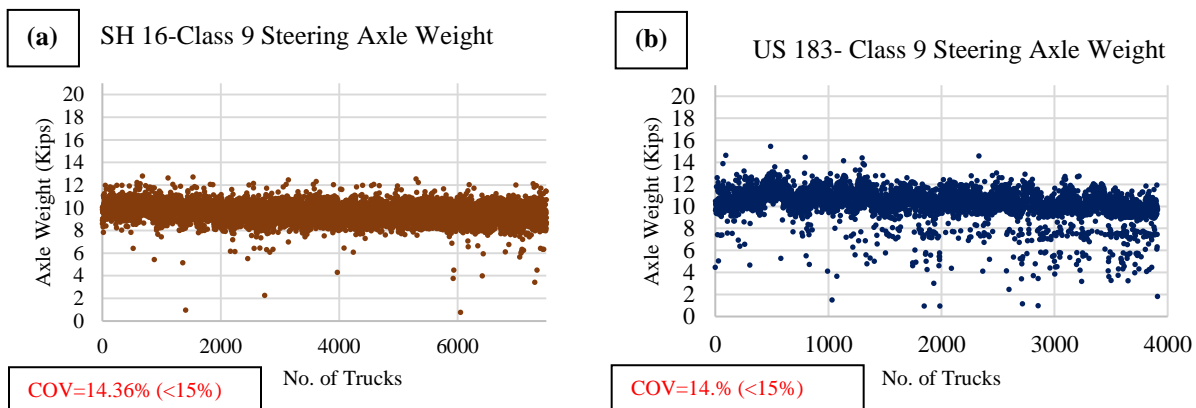
Figure 4.19. a) Class 9 Steering Axle Weight Coefficient of Variance (COV) for SH 119 (b) Class 9 Steering Axle Weight Coefficient of Variance (COV) for US 183

4.4.4 Gross Vehicle Weight (GVW) Analysis

Two types of GVW distributions were primarily observed throughout all the WIM sites. The first type of distribution is illustrated by Figure 4.20, which shows the gross vehicle weight distributions with respect to truck percentage for all classes of trucks in US 281 of the Corpus Christi District. This plot can be characterized by a bimodal distribution that is attributed to unloaded trucks in the 20,000 lb. to 44,000 lb. range and loaded trucks in the 76,000 lb. to 100,000 lb. range. These GVWs coincide with historical WIM data throughout Texas and the current LTPP data. However, it is important to note that the GVW distributions are shifted past the 80,000 lb. weight limit due to the large number of overloaded trucks this highway supports. Another metric that is often employed is the minimal gross vehicle weight analysis, in this check little to no trucks should be present at the 10,000 lb. or less weight interval. Figure 4.26 shows only 4% of the data in that range. Nonetheless, truck percentages in these range are acceptable because it is known that Class 5 trucks tend to be light vehicles that peak at that the 10,000 lb.-12,000 lb. weight interval.
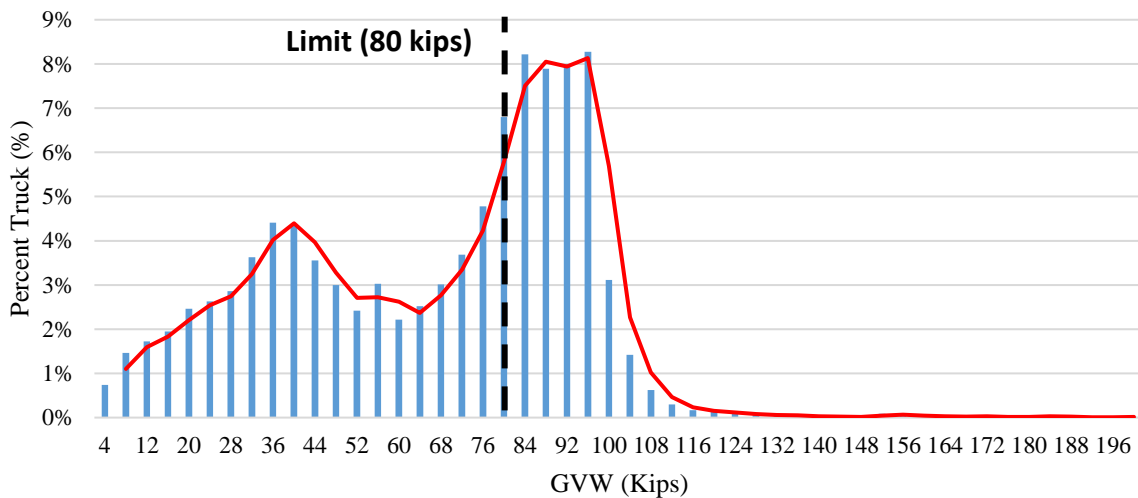
Figure 4.20. GVW Distributions of All Trucks in US 281

Furthermore, the second type of GVW distribution that was observed was located in areas with heavy traffic operations and overweight traffic. Usually, the bimodal distribution is significantly less pronounced as illustrate by Figure 4.21. Where a small peak is visible at the 12,000 lb. interval; due to the high number of Class 5 trucks. While a second peak is visible at the 36,000 lb. interval that is linked unloaded trucks. Despite the weight distributions peaking at a lower weight range, the plot also shows the GVW distribution extending all the way to the 180,000 lb. weight interval. The typical trucks that are the most prevalent in the energy development highway network can be seen in Figure 4.22.
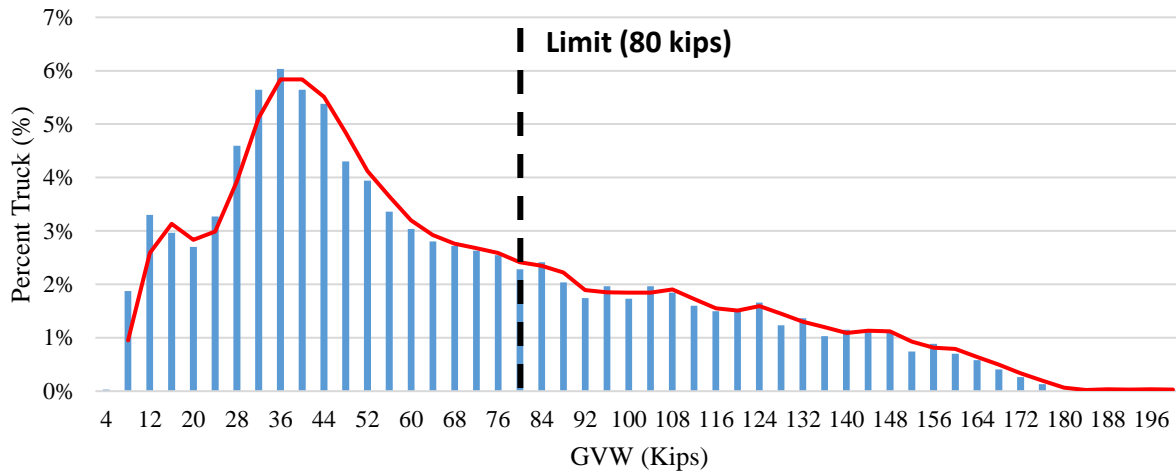
Figure 4.21. GVW Weight Distributions of All Trucks in FM 468

Figure 4.22. Class 9 Oil Tanker and Class 9 Sand Box Truck

4.4.5 Overweight (OW) Axle Analysis

One of the primary objectives of this study was to capture GVW and axle weight distributions of heavy vehicles operating in the overloaded corridors and energy sector zones of South Texas. In the process, the researchers captured very interesting results that are quite surprising. Eight out of the ten selected highways experienced a significantly high number overweight truck traffic (10%<). The Districts with the heaviest truck traffic operations were the Corpus Christi District and the Laredo District. However, despite having numerous oil/gas wells in the surrounding areas, pipeline construction, and equipment movement the highways in the Yoakum District were not as significantly affected. Figure 4.23 illustrates the overweight (OW) truck distributions of US 281 for both the summer and the winter time. The plot shows an overweight distribution of 17% in the winter time and an astounding 45% overweight distribution in the summer time. That is nearly half of all trucks travelling on this highway were overweight, this is a significant number of OW trucks that detrimentally impacts the pavement structure especially in the summer when the stiffness

properties of the asphalt layer are the weakest. The reason for the heavy truck traffic operations is due to a nearly oil refinery in Three Rivers, Texas and due to the transportation of heavy equipment as illustrated in Figure 4.24.
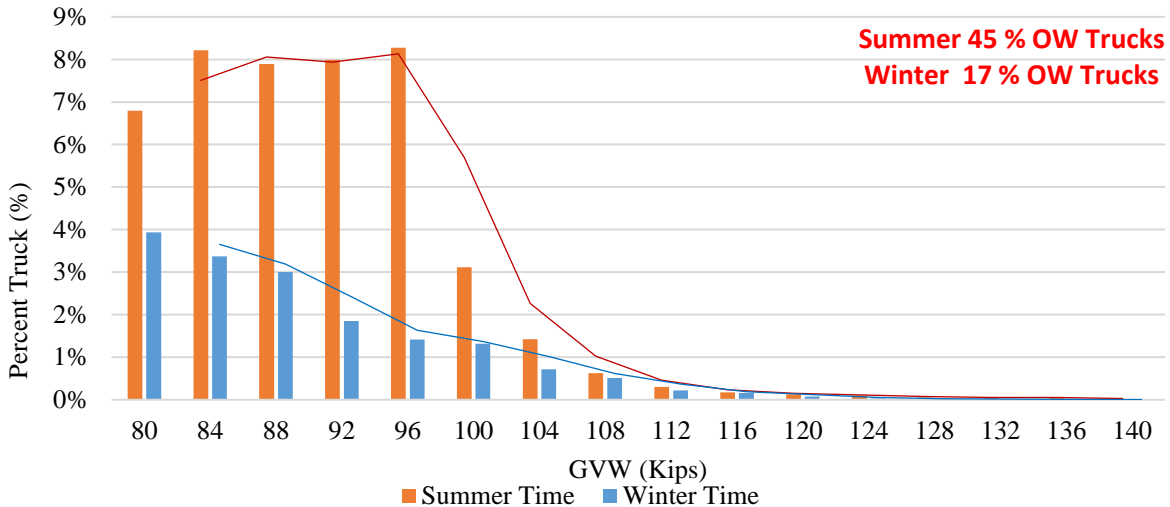
Figure 4.23. GVW Weight Distributions of All Trucks in FM 468

Figure 4.24. Heavy Traffic Operations in US 281 near Three Rivers Texas.

Meanwhile, Figure 4.25 also illustrates the OW truck distributions for FM 468 for both summer and winter time. Similarly, this plot also shows a smaller OW truck distribution for the winter at 12% compared to a 32% distribution for the summer time. The main distinction is that the summer distributions extend all the way to the 180,000 lb weight interval which is alarming for any roads, specially FM roads that are not designed to sustain such heavy truck weights. FM 468 also had some of the heaviest truck traffic in terms of GVW. The portable WIM unit deployed at this site captured trucks weighting in excess of 250,000 lb. Evidently, this site was the most damaged and

75

distressed site showing multiple distress types such as rutting, fatigue cracking, flushing, and pot holes among others.
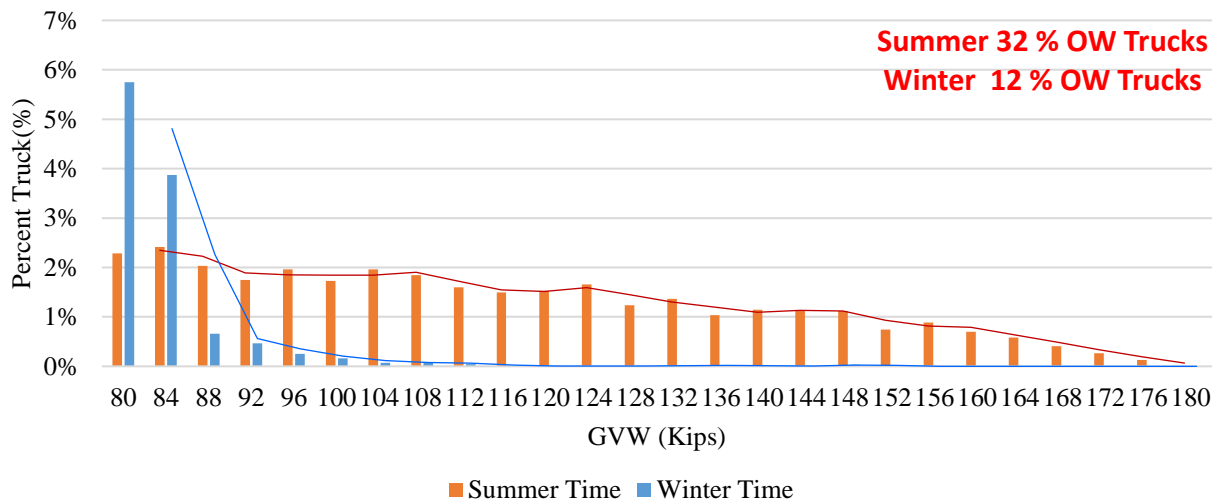
Figure 4.25. GVW Weight Distributions of All Trucks in FM 468

FM 99 is a small load zoned road with a weight limit set at 58,420lbs however, as shown in Figure 4.26 that limit does not prevent the oil and gas industry from driving over this road. Figure 4.27 illustrates the OW vehicle distributions plot of FM 99 in the San Antonio District for both the summer and winter collection time. The portable WIM unit deployed at this site captured data that characterized the overweight truck distributions as high as 56% for the summer time. While in the winter time as much as 63% of the truck traffic was overweight. These are incredibly high percentages of overweight truck traffic that detrimentally impact the pavement structures and bridges, the impacts of these heavy truck traffic operations are discussion in future sections.

Figure 4.26. Oversize/Overweight Loads travelling on FM 99 of the San Antonio District.
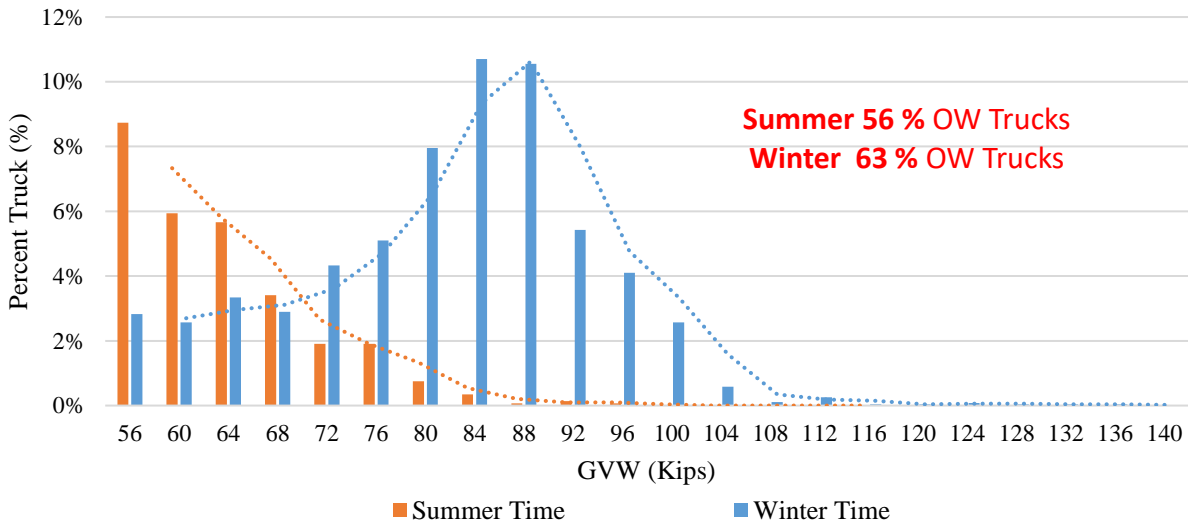
Figure 4.27. OW Weight Distributions of All Trucks in FM 99

Figure 4.28 illustrates OW truck distributions in SH 123/ BU 181 of the Corpus Christi District for both the summer and the winter time. The portable WIM data collected looked very consisted for both time intervals, characterizing the OW distribution for the winter time at 35% while the summer truck distribution at 36%. That is nearly a third of all truck traffic in this highway being overweight at any given season. In addition, GVW in excess of 360,000lbs have been recorded in this highway during the summer time. To verify the validity of the collected information the

research team contacted the local TxDOT office and it was confirmed that they had issues permits for trucks weighting in excess of 300,000lbs. In terms of damage quantification, a single passage of this load can be enough to impart significant damage to the pavement structure, culverts, and nearby bridges.
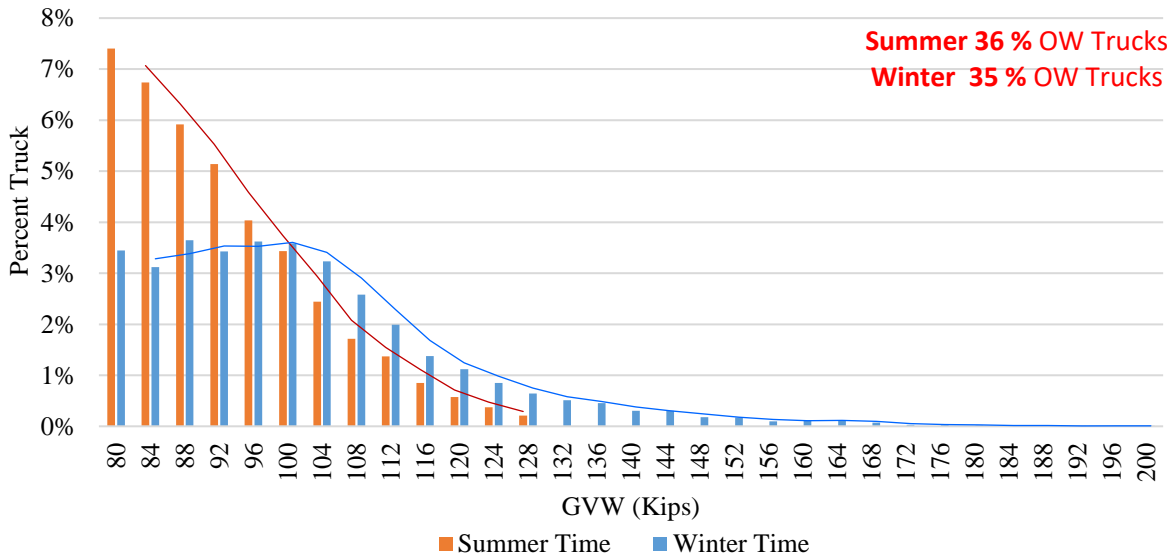
Figure 4.28. GVW Weight Distributions of All Trucks in SH 123/ BU181

Figure 4.29 illustrates the OW truck distributions among all FM, SH, and US highways in the Eagle Ford Shale. The trend that can be observed is that generally the OW truck distributions are highest in the summer time with the exception of US 83 and FM 99. This trend can be attributed for a number of different reasons however; the researchers link this trend to the seasonal variation of crude oil price per barrel. The price of oil generally tends to be more expensive in the summer time therefore energy companies are more enticed to produce more barrels of oil since they have a higher return on their investment. As a result, there are more wells being drilled that generate a plethora of truck traffic even for just one drilling site. In addition, the results show that Farm-to-Market roads can have overweight distributions up to 64%, state highways (SH) of up to 36%, and US highways up to 45% for highways in the surrounding network.
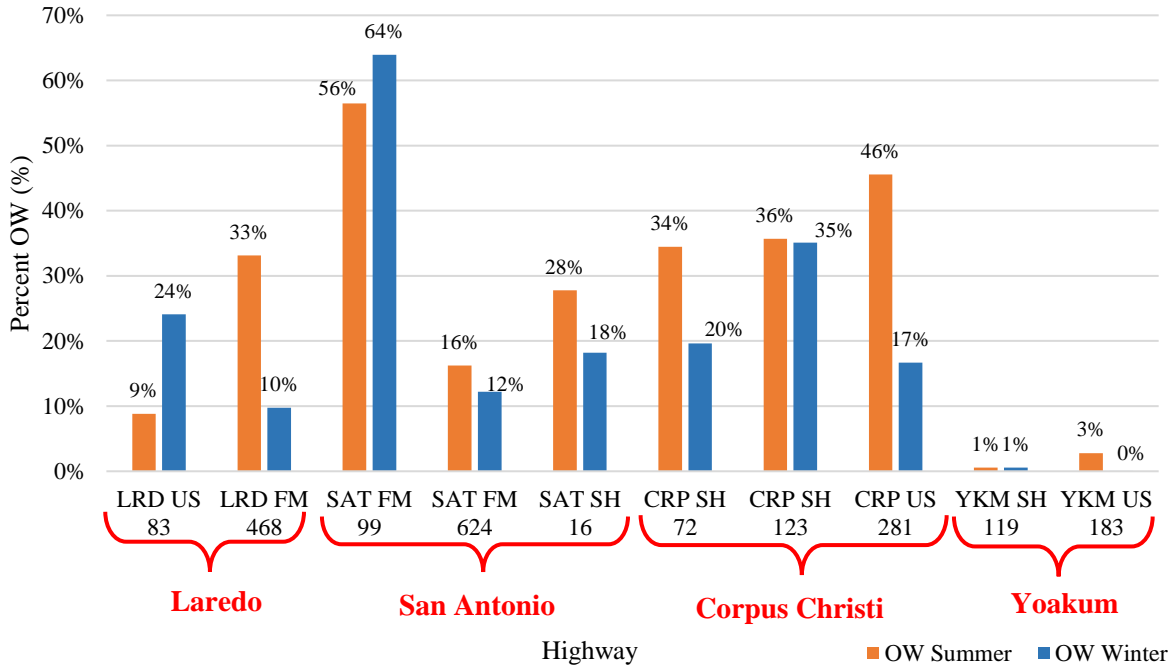
Figure 4.29. Seasonal Variation of OW Truck Traffic for All Ten Test Sites

4.4.6 Other Axle Analysis

Tandem axles typically follow similar weight distributions to that of Class 9 GVW trucks. This information coincides, since Class 9 trucks are the most common truck in almost any highway network, and it is composed of two tandem axles. In most highways, tandem axles are also typically characterized by a bimodal distribution that is attributed the unloaded and loaded tandem axles. Figure 4.30 illustrates this bimodal distribution of unloaded tandem axles in the range of 14,00lbs to 26,000lbs, while the loaded tandem axles in the 32,000lbs to 42,000lbs range for SH 72. Figure 4.31 illustrates the tridem axle weight distributions for SH 16 which show the distributions substantially shifted to the loaded and overloaded side. In addition, for heavy loaded highways such as the one illustrated in Figure 4.32, the quad axle distributions increase and then peaks in the 70,000lbs range, essentially showing significantly overloaded quad axles (79%).
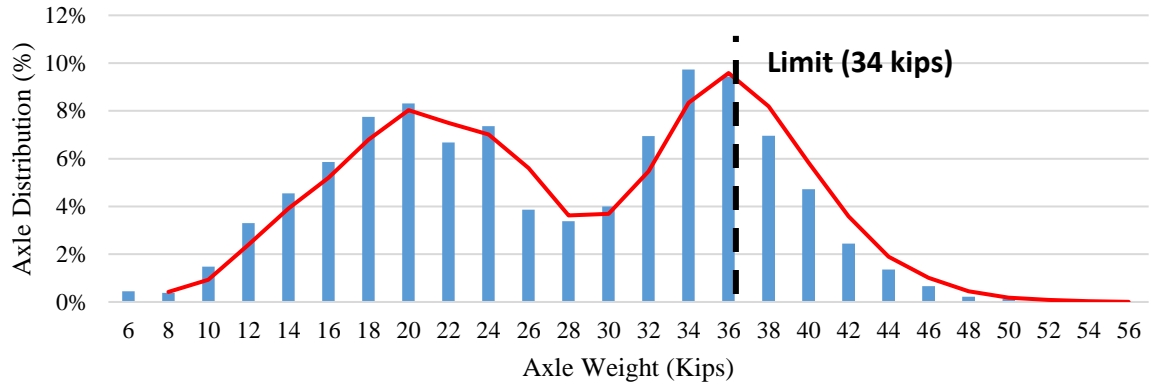
Figure 4.30. Tandem Axle Weight Distributions for All Trucks in SH 72
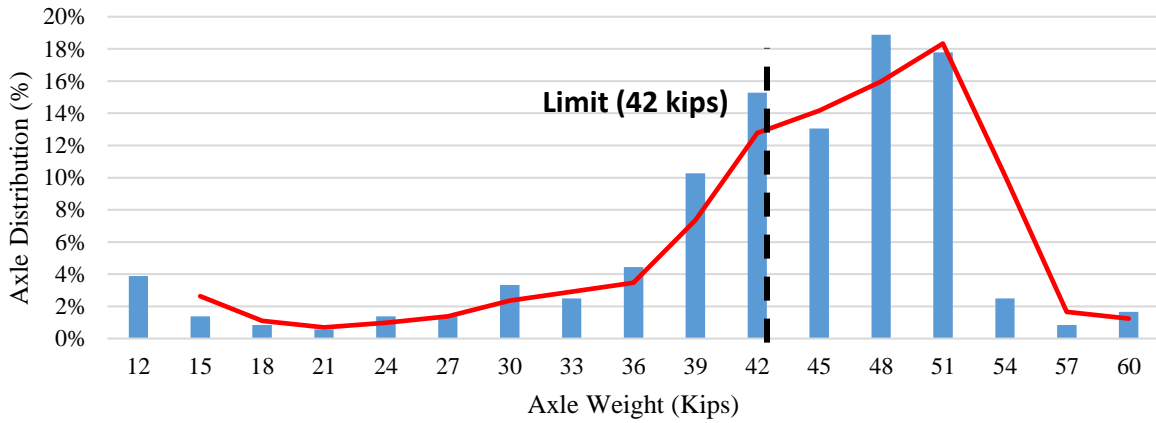
Figure 4.31. Tridem Axle Weight Distributions for All Trucks in SH 16
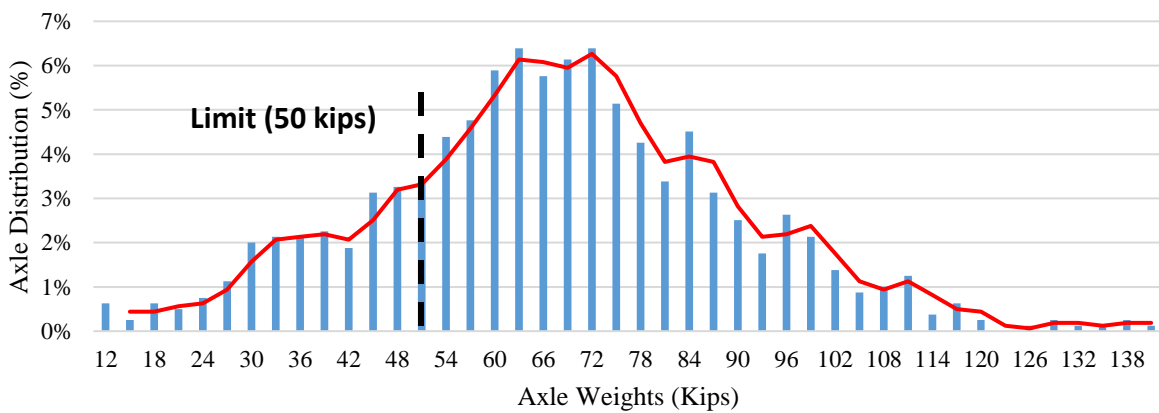
Figure 4.32. Quad Axle Weight Distributions for All Trucks in SH 123 / BU 181

4.4.7 Limitations and Drawbacks of Study

The major limitations and drawbacks of this study as listed below:

- Monthly adjustment factors were not able to be derived from WIM data collected.
- Since the data collection was only conducted in two time periods, summer and winter, for a length of two weeks, the researcher made the assumption that the time period measured gives an accurate measurement of weights for the entire year.
- The time interval in which the data was collected could have underestimated or overestimated the current traffic and vehicle loads.
- Since the big energy boom in the Eagle Ford Shale already occurred in the 2008-2012 era, the WIM data collected did not contained the heaviest GVW distributions the highway could have experienced.

4.4.8 Summary of the Major Points

- The Portable WIM provides is a simple and inexpensive method to collect specific weigh-in-motion data in rural locations and produce reliable and accurate results.
- The Portable WIM units collected satisfactory data that is suitable for the development of the axle load spectra for energy developing areas in the Eagle Ford Shale.
- The heaviest traffic operations were located in the Laredo, Corpus Christi, and San Antonio Districts with overweight distributions up to 33%, 46%, and 64% respectively.
- GVW greater than 360,000lbs were recorded in certain highways of the Eagle Ford Shale.
- FM Highways carried significantly heavy overweight traffic from the energy industry and they are the most adversely affected highways because of their overall thin pavement structure that was not designed to sustain such heavy loads.
- GVW distributions fluctuate significantly according to seasonal variations and the price of oil.

5. In-Depth Evaluation of the Pavement Condition

5.1 Introduction

This chapter documents the results of pavement condition surveys conducted at ten selected sites in the Eagle Ford Shale network. In addition, forensic studies using Non-Destructive Testing (NDT) were implemented to determine the pavement structure and layer properties. For this purpose, Falling Weight Deflectometer (FWD) and Ground Penetrating Radar (GPR) were deployed to the field for the determination of the layer profile and back-calculation of layer moduli in the surveyed network. The collected information will be utilized for damage quantification purposes as well as for remaining life analyses of the representative pavement sections.

5.2 Pavement Condition Evaluation

Proper evaluation of the pavement conditions is of primary concern to accurately quantify the pavement damages imparted by overweight truck traffic. The pavement condition is essentially interconnected with the functional and structural performance properties during the service life of the pavement sections. In order to properly assess the pavement condition, it is necessary to identify the type and the severity of the distress-related damages and the pavement layer configurations besides the layer stiffness properties. To achieve this objective, the research team conducted visual inspection surveys, GPR, and FWD tests in the ten pavement sections located in the San Antonio, Corpus Christi, Yoakum, and Laredo District. Table 5.1 indicates the selected roadways, the roadbed type, the data collection lane, the reference markers, and their exact GPS location.

Table 5.1. Location of Selected Roadways in Eagle Ford Shale Network

District	County	Roadway	Road Bed	Lane	TRM	GPS Coordinate
Laredo	Dimmit	**US 83** (SB Lane)	Single	K1	638	(28.504907, -99.838659)
Laredo	La Salle	**FM 468** (WB Lane)	Single	K6	440	(28.531170, -99.398022)
San Antonio	McMullen	**FM 624** (WB Lane)	Single	K6	500	(28.125868, -98.525511)
San Antonio	McMullen	**FM 99** (SB Lane)	Single	K1	588	(28.465600, -98.440487)
San Antonio	Atascosa	**SH 16** (SB Lane)	Single	K1	642	(28.784422, -98.540370)
Corpus Christi	Live Oak	**US 281** (NB Lane)	Multiple	L1	622	(28.452511, -98.183444)
Corpus Christi	Karnes	**SH 72** (WB Lane)	Single	K1	536	(28.739827, -97.940206)
Corpus Christi	Karnes	**BU 181/SH 123** (SB Lane)	Single	K1	552	(28.878125, -97.893333)
Yoakum	Gonzales	**US 183** (SB Lane)	Single	K6	580	(29.459768, -97.435360)
Yoakum	Dewitt	**SH 119** (WB Lane)	Single	K1	544	(29.036632, -97.572325)

5.3 Visual Inspection of Selected Sites in the Eagle Ford Shale

Visual inspection surveys were performed for all ten of the selected highways in the Eagle Ford Shale network listed previously in Table 5.1. The visual inspections of pavement sections were conducted under lane closure by examining 100 ft. before and 100 ft. after the portable WIM station. The research team documented and reported the different distress types present in each of the inspected sections per TxDOT's 2018 PMIS Pavement Rater's Manual. In addition, Figure 5.1 shows an illustration of the visual inspection plan the research team incorporated.
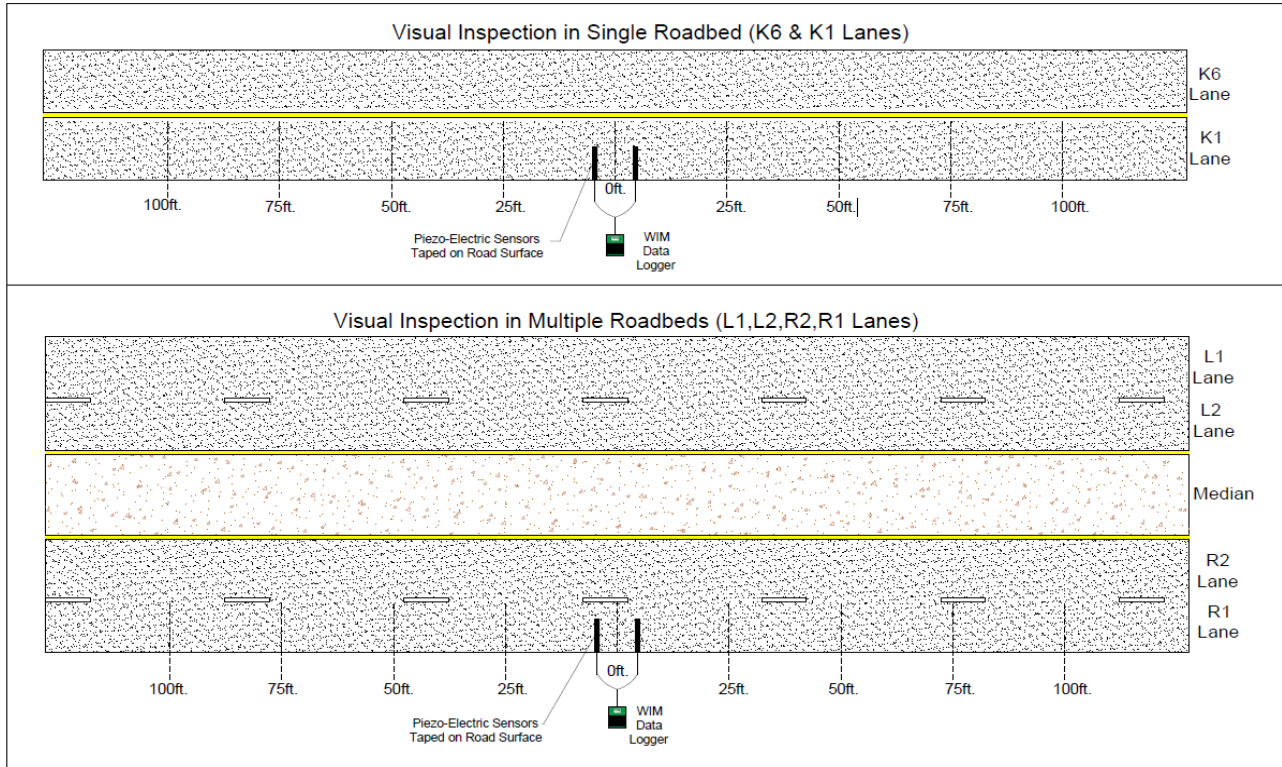
Figure 5.1. Visual Inspection Survey Illustration.

Table 5.2 lists a summary of the different pavement distresses associated with each of the inspected highways. As indicated in Table 2, rutting and flushing are the predominant pavement distresses related to highways in the Eagle Ford Shale. However, these distresses are expected as these highways service high volumes of heavily loaded truck traffic and overweight vehicles related to the oil-gas industry and heavy equipment transportation. Moreover, it was also found that the severe rutting and flushing were more pronounced in FM and SH roads because in addition to the heavy traffic, these highways also have less robust structural layers due to their nature of initial design. The safety of such pavement sections during wet seasons can become a concern as segments with severe rutting coupled with flushing can become extremely slippery due to accumulation of rainwater in the wheel path. Detailed information pertaining to the visual inspection conducted on the selected sites are provided in Appendix A.

84

Table 5.2. Pavement Distresses in Representative Roadways in Eagle Ford Shale Network

	District	Laredo		San Antonio			Corpus Christi			Yoakum	
	County	La Salle	Dimmit	Atascosa	McMullen	McMullen	Live Oak	Karnes	Karnes	Dewitt	Gonzales
	Roadway	FM 468	US 83	SH 16	FM 99	FM 624	US 281	SH 72	SH 123/ BU 181	SH 119	US 183
Pavement Distresses	Rutting	X	X	X	X	X	X	X	X		X
	Patching	X			X						
	Block Cracking	X									
	Alligator Cracking	X	X		X		X				
	Longitudinal Cracking						X				X
	Transverse Cracking										
	Raveling		X	X					X		
	Flushing	X	X	X	X	X	X	X	X		X
	Failures										
	Potholes	X			X						

5.4 Non-Destructive Testing

Non-destructive testing of the pavement section is the main procedure of determining the pavement structural characteristics. In recent years vast variety of nondestructive testing methods have been developed, which can provide critical information pertaining to the pavement structure. The UTEP research team deployed GPR and FWD devices as the non-destructive testing methods for further pavement condition evaluation.

5.4.1 Ground Penetrating Radar (GPR)

The research team conducted GPR testing on the selected pavement sections (Table 5.1) in overload corridors of the Eagle Ford Shale region. An air-coupled GPR unit equipped with a 2 GHz antenna was deployed in this study to properly evaluate the pavement layer configuration. The GPR system also consists of the data acquisition system and Distance Measuring Instrument (DMI), as shown in Figure 5.2. This air-coupled GPR is normally operated at highway speed and does not require traffic control, which is extremely important in the studied areas where lane closures are difficult and can potentially pose a safety issue for the travelling public.
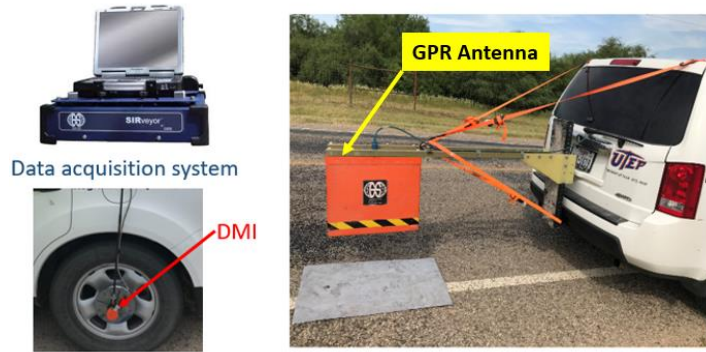
Figure 5.2. GPR Testing in Laredo District.

Using RADAN computer software, the research team analyzed and interpreted the GPR collected data associated with the 10 selected roadways in the Eagle Ford Shale Districts. It should be noted that the research team conducted GPR surveys two times in each roadway under similar conditions in order to ensure the accuracy of the collected data. Therefore, the reported pavement layer thicknesses are based on the average values between the two operated tests. Additionally, in order to properly assess the pavement layer thicknesses on one hand, and acquire comprehensive information regarding the type and material of the layers on the other, it deems necessary to validate the GPR testing data by comparing the collected results with other available TxDOT databases and interviews with District engineers.

- *Validation of the GPR Data Collected in the Network*

The research team conducted data mining from available databases (i.e. PMIS, intranet resources), pavement design plans, and communication with TxDOT personnel to confirm the pavement profiles of the studied sections.

To further explain this process, the GPR measurements from SH 72 are used as an example of measurements where post-processing required further verification. Figure 5.3 shows the GPR collected data for the specified location. Analysis of the GPR image showed a shallow interface corresponding to a 1.5 in. overlay on top of an HMA layer with a thickness that varies between 4 in. to 6 in., with an average of 5.1 in. However, from such image, the base-subgrade interface was not discernible. To verify the available and complement the missing information, the research team proceeded to contact the Districts to request pavement design plans and conducted an extensive search within the available databases.
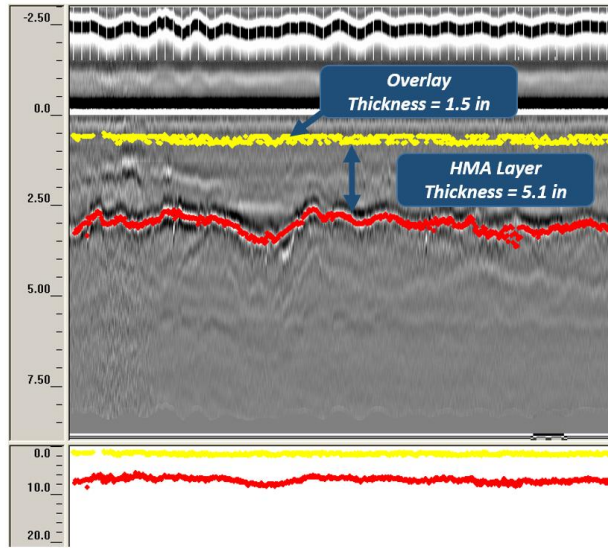
Figure 5.3. GPR Data from SH 72, Corpus Christi.

- *Pavement Design Plans*

    For the described case, the research team thoroughly reviewed the pavement design plans, corresponding to Reference Marker 536 of SH 72, located in Karnes County. Figure 5.4 shows the proposed design plans and specifications as of November 2017. From the design plans, State Highway 72 was designed to have a 1.5 in. asphalt overlay, 5 in. of HMA, 16 in. of 1% cement treated base (CTB) constructed over 8 in. of 3% cement treated subgrade (CTS). Thus, the overlay and HMA layer thicknesses obtained from post-processed GPR data were found to be in good agreement with the pavement design. In this case, the design plan further supplemented the base thickness missing from the GPR measurements.
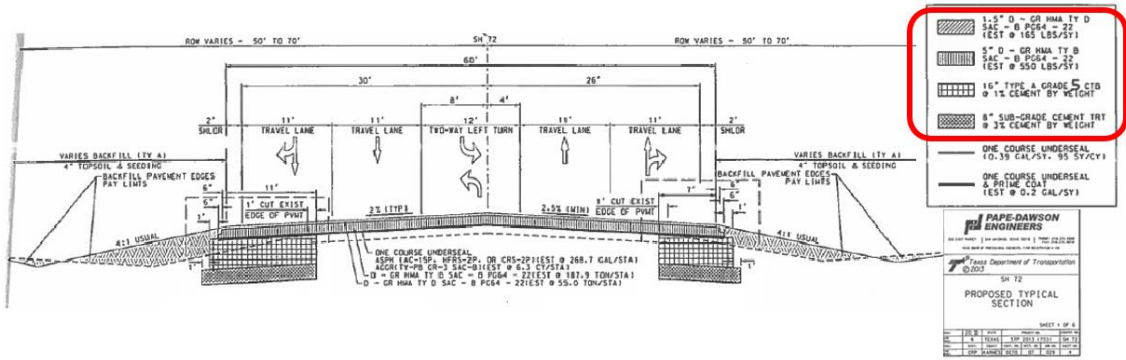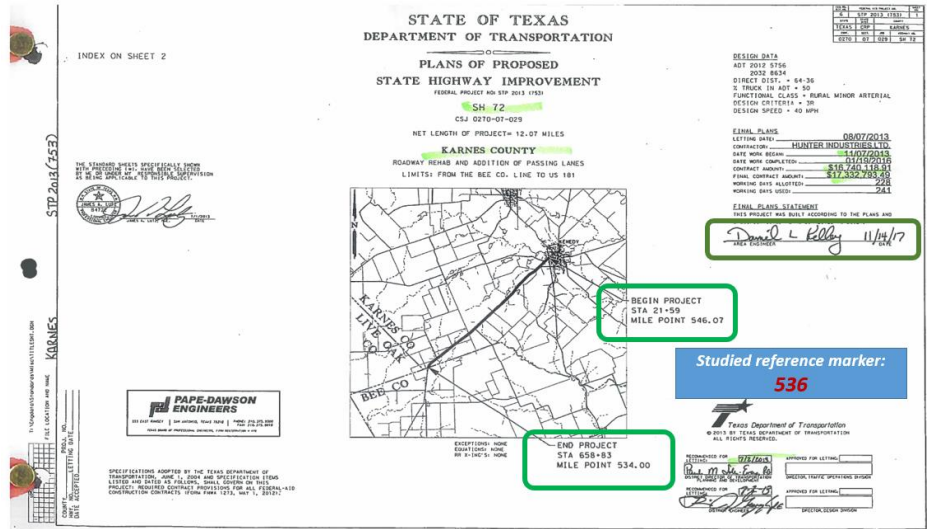
Figure 5.4. Pavement Design Plan for SH 72 in Karnes County (Corpus Christi).

- *PMIS Database*

  The research team also consulted the PMIS database to verify and cross-validate the pavement profile information. For the case used as example, the PMIS data records associated to SH 72, RM 536, in Corpus Christi District are shown in Figure 5.5. The PMIS records indicate that such section corresponds to Pavement Type 5. According to the PMIS Rater's Manual (TxDOT, 2016), Pavement Type 5 is defined as a pavement with medium thickness of AC, i.e. 2.5 - 5.5 in. This was found to be in line with our obtained GPR results. Appendix B also provides the information extracted from the PMIS database for all ten selected overload corridors.

Figure 5.5. PMIS Information associated with the Pavement Type of SH 72 in Corpus Christi (from PMIS Database, 2010).

- *TxDOT's Personnel Interview*

  The research team also communicated with TxDOT's District personnel to verify and/or supplement layer configuration information. For the case explained here, a shallow layer as seen by the GPR could be attributed either to an overlay or to the presence of moisture underneath the pavement surface. Communicating with TxDOT's maintenance supervisor confirmed the presence of an asphalt overlay in the SH 72 pavement structure.

- *TxDOT's Intranet Resources*

  TxDOT provided us access to a number of Intranet resources, which were considered as integral components to tackle the project tasks. For this reason, the research team comprehensively reviewed the available TxDOT intranet resources to gather information pertaining to the pavement structures. For the case described in this section, it was found in Technical Memorandum 14-06 (Sebesta, 2014) that a section along SH 72 in Karnes County was redesigned in 2014 to address the severe distresses it experienced due to the energy development traffic. The previous pavement structure consisted of 3.5 in. of HMA over 10.5 in. of a lightly cement stabilized base over a moderate to high PI clay subgrade. The severe pavement failure on this section of SH 72 was primarily attributed to disintegration of the upper part of the existing treated base by the heavy energy related truck traffic. The tech memo recommended SH 72 a 5 in. (at least) HMA surface layer in combination with a cement stabilized base layer. Moreover, Research Report RR-16-02 (Gurganus, 2016), recommended the use of an 8-in. base layer in Corpus Christi District. This information is in agreement with the GPR data obtained by the research team on SH 72.

Ultimately, Table 5.3 indicates the pavement layer thicknesses obtained from GPR results and validated by available information and databases.

Table 5.3. Pavement Layer Configurations attributed to the Representative Roadways in Eagle Ford Shale Region

District	County	Roadway	TRM	Information	Pavement Type	PMIS Definition	TxDOT's Personnel Interview	TxDOT's Intranet Resources	Overlay	AC	Base
				Roadway Information		Pavement Design Plans	PMIS Database		GPR Results (in)		
Laredo	Dimmit	US 83 (SB Lane)	Near 638	1.5 in. Overlay	10	Surface Treatment Pavement	-	-	1.5	4.8	6.2
Laredo	La Salle	FM 468 (WB Lane)	440	2.5 in. HMA, 6 in. Base	10	Surface Treatment Pavement	-	3 in. HMA	-	2.1	9.8
San Antonio	McMullen	FM 624 (WB Lane)	500	7.5 in. Base layer	6	Thin Asphaltic Concrete (Under 2.5")	GPR results are verified	6 in. Base layer	-	1.3	8.9
San Antonio	McMullen	FM 99 (SB Lane)	588	-	10	Surface Treatment Pavement	GPR results are verified	6 in. Base layer	-	1.5	8.3
San Antonio	Atascosa	SH 16 (SB Lane)	642	-	10	Surface Treatment Pavement	GPR results are verified	-	-	3.5	7.4
Corpus Christi	Live Oak	US 281 (NB Lane)	622	2 in. Overlay 4-6 in. HMA 18 in. Base	5	Medium Thickness AC (2.5"-5.5")	-	At least 8 in. of Base layer	1.5	5.5	18
Corpus Christi	Karnes	SH 72 (WB Lane)	536	1.5 in Overlay 5 in. HMA 16 in. CTB 8 in. Subgrade Cement Treated	5	Medium Thickness AC (2.5"-5.5")	This roadway has Overlay	At least 5 in. of AC, Cement Treated Base (CTB)	1.5	5.1	16[a] +8[b]
Corpus Christi	Karnes	SH 123 (SB Lane)	Near 552	5.5 in. HMA 15 in. Base	5	Medium Thickness AC (2.5"-5.5")		At least 8 in. of Base layer	-	5.5	15
Yoakum	Gonzales	US 183 (SB Lane)	Near 580	6 in. HMA 8 in. Base	5	Medium Thickness AC (2.5"-5.5")	-	At least 6 in. of Base layer	-	5.5	8
Yoakum	Dewitt	SH 119 (EB Lane)	Near 544	4 in. HMA 12 in. Base	5	Medium Thickness AC (2.5"-5.5")	-	At least 6 in. of Base layer	-	3.5	10.5

[a]Cement Treated Base (CTB) layer

[b]Cement Treated Subgrade

The pavement layer thicknesses and configurations obtained from GPR were further incorporated to back-calculation layer moduli from FWD data. Following section provides the information pertaining to the FWD testing results.

5.4.2 Falling Weight Deflectometer (FWD)

The research team collected FWD data associated with the studied pavement sections to identify the layers moduli. Figure 6 shows the FWD testing device used for the NDT testing of the representative sites. Seven deflection sensors (geophones) were used to measure the deflection bowl caused by the impulse load, as shown in the Figure 5.6 (c) and (d). The deflections obtained from the seven geophones were input into a back-calculation program to determine the layer moduli of the pavement structure.
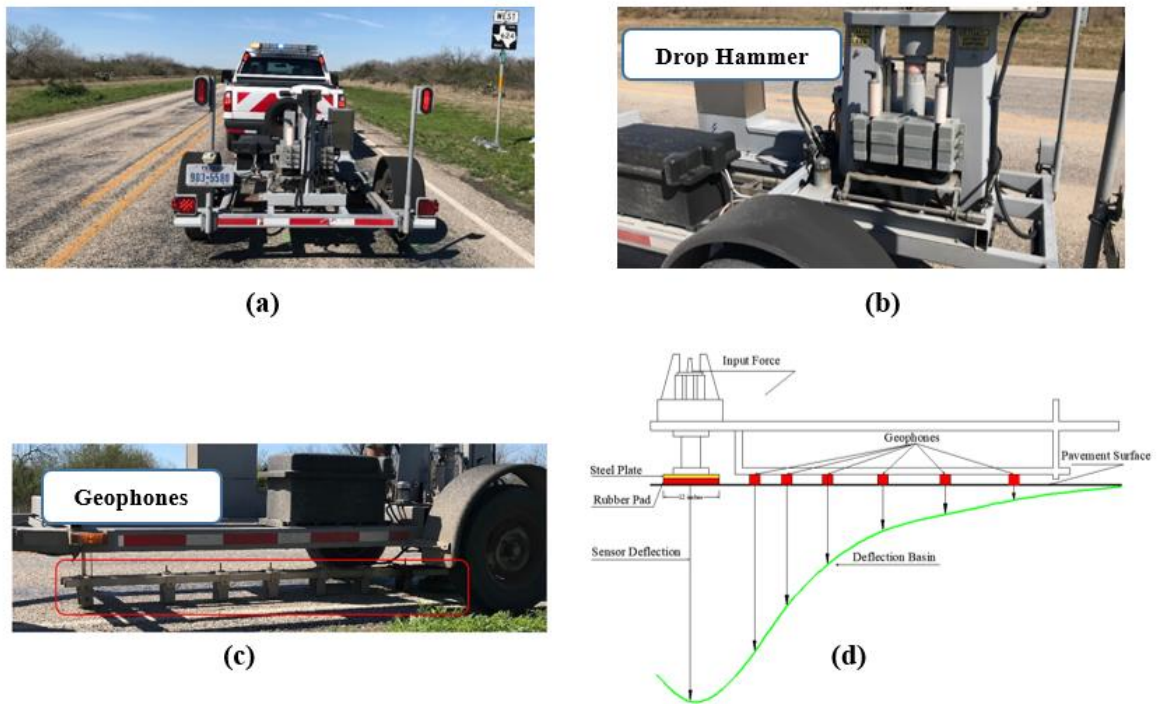
Figure 5.6. (a) TxDOT's Falling Weight Deflectometer (b) Drop Hammer (c) Geophones, (d) Deflection Basins obtained from the Seven Geophones.

Figure 5.7 shows the FWD setup that the research team arranged for data collection. Essentially, it was 3 drops per 3 test spots (at a 25' distance) in the right wheel path to consider the load-induced damage on back-calculated material properties. Same testing pattern followed in between both wheel-paths to mitigate the effect of possible systematic errors incurred in the back-calculation procedure. A variable load level scheme ranging from 6,000 lb. to 12,000 lb. imparted through a 12 in. diameter spring loaded plate on pavement surfaces.
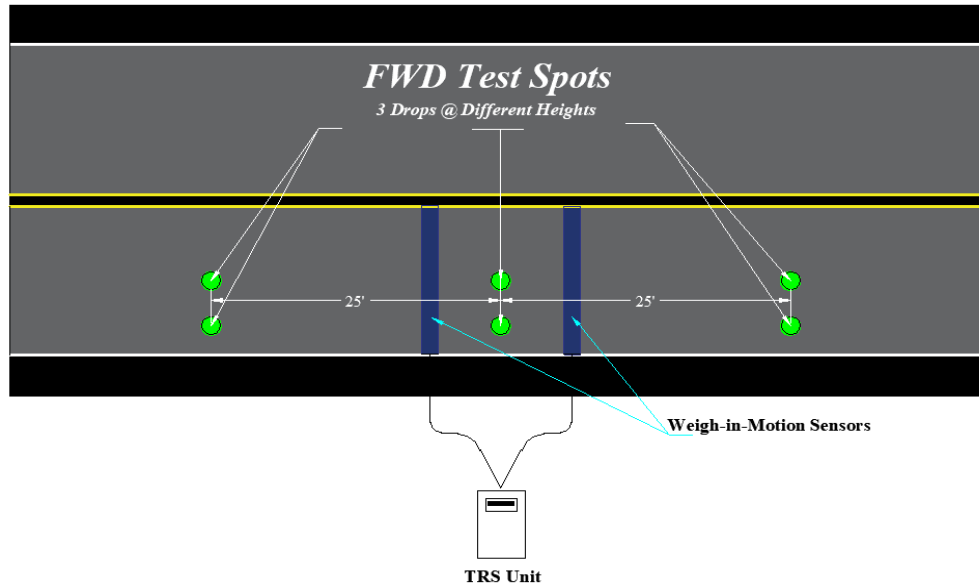
Figure 5.7. FWD Testing Setup.

To back-calculate modulus, an iterative scheme is used to calculate theoretical deflections by varying the material properties until an acceptable match of measured deflection is obtained. This is achieved using MODULUS 7 program.

It should be noted that the accuracy of the back-calculated layer modulus are highly linked with three main input parameters as follows:

- *Pavement Layer Thicknesses:* Accurate assessment of the layer thicknesses attributed to the multi-layer pavement systems is of outmost importance for the proper determination of the back-calculated layer modulus. This information was incorporated in the software as the initial step of the back-calculation procedure.
- *Seed Modulus:* The results of the iterative back-calculation procedure heavily depends on the initial seed value provided by the user. This makes the back-calculation process complex, since the programs cannot think for the user, and the process of arriving at a rational moduli value requires engineering judgment and comprehensive evaluation of all available data (Mehta, et al., 2003). In practice, engineers and researchers select seed values considering the particular region, pavement design, material type, and climatic condition.
- *Depth to Bedrock and Subgrade Modulus:* Under TxDOT Research Project 0-1175 (Chang, et al., 1992), the researchers investigated the importance of depth to bedrock in the accuracy of the FWD back-calculation procedure. The study attested that the value of depth to bedrock can significantly influence on the back-calculated layer modulus values. It was also found that a small error in the estimation of the subgrade elastic modulus would

lead to large errors in the back-calculated elastic moduli of other pavement layers, as the subgrade can contribute up to 60% of the surface deflection under the center of the applied load.

The FWD measurements from FM 624 roadway, are used as an example to explain the back-calculation procedure. Figure 5.8 shows the deflection basins diagram attributed to FM 624 roadway (for different loads) obtained from the seven FWD geophones.
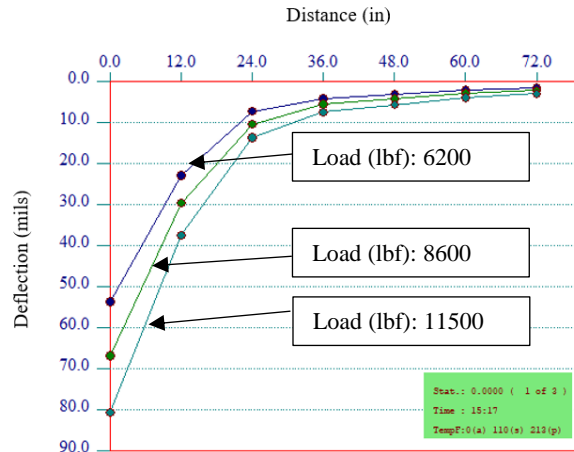
Figure 5.8. Deflection Basins from FM 624, San Antonio.

Figure 5.9 (a) illustrates the back-calculation program environment used to analyze the FWD deflection data. The GPR post-processed results were incorporated to the program, which considered as the main input parameters. Analysis of the GPR data indicates that the Farm to Market 624 is consisted of 1.3 in. of seal coat as the surface layer and 8.9 in. of granular base layer. Subsequently, using engineering judgment considering the roadway type, visual inspection of the sites, and reviewing the quoted typical range of moduli in the literature, the research team defined the seed modulus range in the program, as shown in Figure 5.9 (a). Furthermore, the depth to bedrock was automatically calculated by the program. Ultimately, running the software, the back-calculated layers modulus were obtained and a summary report was provided. Figure 5.9 (b) shows the snap shot of FM 624 back-calculation output results.

(a)


```
-----------------------------------------------------------------------------------------------------------------------
                                      TTI   MODULUS   ANALYSIS   SYSTEM   (SUMMARY REPORT)                 (Version 7.0)
-----------------------------------------------------------------------------------------------------------------------
  District:                                                              MODULI RANGE(psi)
  County  :                                      Thickness(in)        Minimum        Maximum      Poisson Ratio Values
  Highway/Road:                        Pavement:      1.31            300,000        400,000       H1: v = 0.35
                                       Base:          8.96             20,000         40,000       H2: v = 0.35
                                       Subbase:       0.00                                         H3: v = 0.00
                                       Subgrade:     49.48(by DB)                     10,000       H4: v = 0.40
-----------------------------------------------------------------------------------------------------------------------
             Load    Measured Deflection (mils):               Calculated Moduli values (ksi):      Absolute Dpth to
  Station    (lbs)    W1     W2     W3     W4     W5     W6     W7   SURF(E1)  BASE(E2)  SUBB(E3)  SUBG(E4) ERR/Sens Bedrock
-----------------------------------------------------------------------------------------------------------------------
  1204.000  11,655  78.06  38.55  10.05   5.95   5.45   4.72   3.68   400.0     20.0      0.0      5.8    36.68   62.2 *
  1228.000  11,436  96.92  47.24  16.25   7.35   6.09   3.99   2.95   300.0     20.0      0.0      6.3    32.67   61.5 *
  1254.000  11,809  89.30  45.68  13.93   8.07   6.18   4.60   3.19   375.7     20.0      0.0      6.1    32.18   56.0 *
-----------------------------------------------------------------------------------------------------------------------
  Mean:             88.09  43.82  13.41   7.12   5.91   4.44   3.27   358.6     20.0      0.0      6.0    33.84   59.8
  Std. Dev:          9.49   4.63   3.13   1.08   0.40   0.39   0.37    52.2      0.0      0.0      0.8     2.47    2.8
  Var Coeff(%):     10.77  10.57  23.36  15.13   6.74   8.82  11.37    14.5      0.0      0.0     20.2     7.31    4.8
-----------------------------------------------------------------------------------------------------------------------
```

(b)

Figure 5.9. Back-calculation Layer Moduli for FM 624 in San Antonio (a) Modulus Program Input, (b) Back-calculation Results.

Based on the results, it was found that the 8.9 in. granular base layer in FM 624 is relatively weak as all of the stiffness modulus values for this layer hit the lower allowed threshold of 20 ksi in the back-calculation procedure. It was also found that the FM 624 consisted of subgrade layer with low structural capacity (6 ksi) and surface layer with 358 ksi.

It should be noted that in order to properly evaluate the effect of seasonal variation and the climatic conditions on pavement stiffness properties, the research team conducted FWD test in both summer and winter seasons for selected corridors in the network and the obtained results are presented in the following section.

5.4.3 Seasonal Climate Variation Effect on Modulus Value

Temperature and moisture content are the prominent factors that affect the stiffness and strength properties of multi-layer pavement systems. Considering the fact that the HMA is viscoelastic in nature, its strength is greatly dependent on the temperature. Additionally, for granular base and subgrade layers the stiffness properties are highly connected with the moisture condition. Figure

5.10 illustrates the effect of moisture on soil particles. The change in stiffness is related to the state of moisture tension in unsaturated soils, also known as soil suction (Chandra et al., 1989). Soil suction is made up of two components:

1. Osmotic suction due to dissolved contaminants in the pore water, and
2. Matric suction due to the attraction between water soil particles.

The latter component is a negative pressure that exists in the soil water as a result of capillary tension. Soil suction is a measure of the soil's affinity for water and indicates the intensity with which it will attract water. The drier the soil, the greater the soil suction (Chen, 1988) and the stiffer the material owing to the greater capillary tension holding the soil particles together.
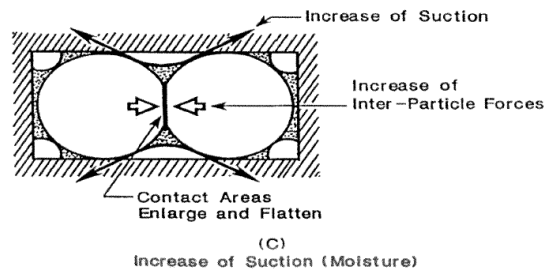
Figure 5.10. Effect of Moisture on Soil Particles.

Figure 5.11 illustrates the annual average temperature in San Antonio located in the Eagle Ford Shale region. As evidenced in this plot, the average temperature in summer season is 38% more than in winter. Moreover, as shown in Figure 5.12, average monthly precipitation, which is connected with potential moisture ingress in pavement layers, in summer season is approximately 138% higher than the winter season. Due to the significant differences in precipitation patterns and temperature regimens in summer and winter seasons, the materials properties are also appreciably different. For this reason, the research team devised a plan to perform FWD testing in both summer and winter times to capture the variation of the damage factors in different seasons of the year.
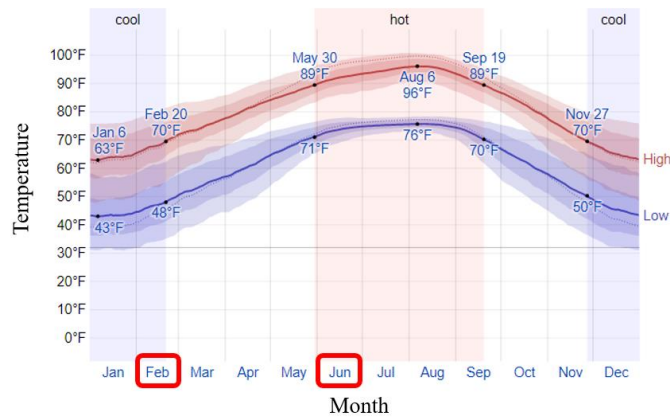
Figure 5.11. Annual Average Temperature in San Antonio, Texas (WeatherSpark Website)
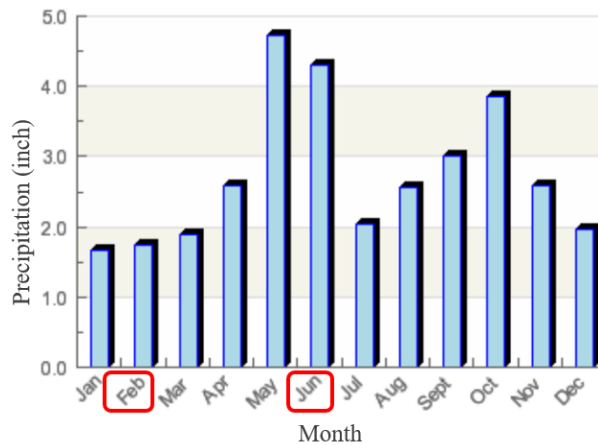
Figure 5.12. Average Monthly Precipitation in San Antonio, Texas (RSS Weather Website)

The site-specific back-calculated pavement layer modulus of all ten selected sites attributed to the summer and winter seasons are presented in Table 5.4. Additionally, to further clarify the seasonal variations of the back-calculated modulus values of pavement sections, the analysis results were contrasted and classified for the various roadway types, as indicated in Table 5.5. The results show that the summer-based layer modulus values are significantly lower than the winter-based values. This is primarily attributed to the viscoelastic behavior of the asphalt layers and the variations of stiffness properties of granular layers due to changes in the saturation state of the unbound granular layers due moisture infiltration or evapotranspiration during the service life of pavements, leading to softening of the surface layers due to elevated temperatures in summer seasons.

97

Table 5.4. Pavement Layer Modulus attributed to the Representative Roadways in the Eagle Ford Shale Network

District	County	Roadway	TRM	Pavement Layer Modulus in Summer Season (ksi)				Pavement Layer Modulus in Winter Season (ksi)			
				Overlay	AC	Base	Subgrade	Overlay	AC	Base	Subgrade
Laredo	Dimmit	US 83 (SB Lane)	Near 638	550	550	50	8	880	880	60	11.4
	La Salle	FM 468 (WB Lane)	440	-	450	22	6	-	628	25	9.4
San Antonio	McMullen	FM 624 (WB Lane)	500	-	358	20	6	-	416	22	7.1
	McMullen	FM 99 (SB Lane)	588	-	450	22	7	-	650	26	9.7
	Atascosa	SH 16 (SB Lane)	642	-	567	47	14	-	760	50	15.2
Corpus Christi	Live Oak	US 281 (NB Lane)	622	550	550	50	8	956	956	55	12.5
	Karnes	SH 72 (WB Lane)	536	429	429	234^a	22^b 8^c	688	688	201^a	27^b 10^c
	Karnes	SH 123 (SB Lane)	Near 552	-	550	40	7	-	705	45	8.2
Yoakum	Gonzales	US 183 (SB Lane)	Near 580	-	550	50	8	-	850	55	12
	Dewitt	SH 119 (EB Lane)	Near 544	-	540	38	7	-	717	40	8

a: Cement Treated Base, **b:** Cement Treated Subgrade, and **c:** Subgrade Soil

Table 5.5. Back-calculated Pavement Layer Modulus attributed to the Summer and Winter Seasons for Different Roadway Types

Roadway	Layer Modulus in Winter (ksi)			Layer Modulus in Summer (ksi)			Percent Difference (%)		
	AC	Base	Subgrade	AC	Base	Subgrade	AC	Base	Subgrade
FM	565	24	9	419	21	6	26	12	27
SH	718	45	12	522	42	10	27	7	14
US	895	57	12	550	50	8	39	12	33

5.5 Summary of the Major Points

This chapter presented the post-processed results of Non-Destructive Tests (NDT) and pavement condition surveys conducted at representative sites in the Eagle Ford Shale region. Evaluation of the GPR measurements validated by TxDOT databases and available historical information provided the site-specific pavement layer configurations and layer thicknesses. It was found that in the studied network, FM roadways, on average consisted of only 1.6 in. of treated surface layer, however, representative pavement sections of SH and especially US highways were found to be more robust, with an approximate average asphalt layer thicknesses of 4.8 in. and 6.3 in., respectively.

FWD testing was also conducted to determine the back-calculated layer moduli in the surveyed network. The research team devised a plan to perform FWD testing in two different seasons (summer of 2018 and winter of 2019), to account for the seasonal variations of the back-calculated modulus values of pavement sections. Analyzing the FWD data for summer and winter seasons indicated that the back-calculated layers modulus values in summer were substantially lower compared to winter time modulus values from nondestructive testing of pavement sections.

6. Development of a Mechanistic Damage Equivalency Factor

6.1 Introduction

As previously mentioned in this technical report, during the past decade, energy developing activities have created large volume of heavy truck traffic operations in the network. These energy-related activities have adversely affected the highway and bridge infrastructures. Damaged local and county roads have been a major source of inconvenience for the local residents. Some distresses in the highways of Eagle Ford Shale network are shown in Figure 6.1.

Figure 6.1. Distresses in Roadways of Eagle Ford Shale Region.

Additionally, premature failure of the local and country roads due to the passage of heavy truck traffic have greatly contributed to the increase in the number of accidents and fatalities in the region. In 2013, there were 3,430 traffic accident reports in the energy development areas that resulted in serious injuries or fatalities. The result was 236 fatalities in the 26-county Energy development areas that stretches from Laredo to Huntsville (TxDOT, 2014). Figure 6.2 shows an example of such crashes in Karnes County.

Figure 6.2. Crash in Karnes County, April 2013 (From San Antonio Express News).

Currently, TxDOT is seeking a robust methodology to assess the energy development impacts on the transportation facilities in the energy development areas. The quantification of the impacts on the highway network is the preface to develop uniform strategies to compensate the costs incurred to the users of the transportation systems in the affected network. For instance, operators of trucks that transport energy development related equipment and supplies often obtain a 2060 permit from the Texas Department of Motor Vehicles (DMV). The 2060 permit essentially allows the vehicles that weight in excess of the legal limit of 80,000 lbs. to operate on load zone roads that are designed for maximum gross weight of 58,420 lbs. Moreover, while a 2060 permit can cost as low as $255 per year, the costs associated with pavement repair are significantly higher. Therefore, there is a pressing need to properly quantify the damages imparted by the energy-related vehicles to protect the taxpayers' investment in the transportation system.

The primary step in the quantification of the pavement damage is to have an accurate account of the loading conditions in the network. Traditionally, once the traffic loads and the distributions are determined, the results are converted into the standard 18-kip single axle using the Equivalent Axle Load Factors (EALF). EALFs essentially allow for the quantification of the pavement damages per pass relative to a standard 18-kip single axle. The EALF values are primarily dependent on the type of pavement, pavement layer profile, and material properties of the pavement layers in the network. The traditional industry-standard EALFs are based on the AASHTO formulations with several simplifying assumptions for generalization across the nation. The major problem that pavement designers and other professionals face is that the analysis procedures rely on experimental information that was developed from field measurements in the late 1950s and early 1960s, with revisions later in 1993. Additionally, the majority of the road tests were conducted in regions with distinct climatic conditions, limited pavement profiles, and unrepresentative traffic

characteristics which ultimately jeopardizes the generalization of the EALFs for nationwide use. Therefore, the industry-standard EALF tables might be relevant for similar circumstances under which the tests were conducted; however, the pavement design engineers should proceed with caution if they intend to use the default EALF values in cases with major departure from the original assumptions under which the EALF tables were developed. This anomaly is more pronounced in overload corridors with taxing loading conditions. Considering the fact that each network has its own specific characteristics, this was the motivation for the research team to develop a mechanistic framework for the determination of site-specific EALF tables that is commensurate with the traffic characteristics such as loading magnitude, frequency, vehicle characteristics such as axle configurations and tire footprint, environmental conditions, pavement type, and layer configurations in this research project.

6.1.1 Objectives

The primary objective of this chapter is to develop a mechanistic approach to obtain the damage equivalency factors tailored towards the specific axle load and axle configuration of vehicles operating in the network, considering the environmental impacts and unique features of the transportation systems for the selected overweight corridors in the energy development areas. The Finite Element (FE) method was utilized in order to determine the pavement responses due to traffic loads for the purpose of developing damage factors. Truck traffic information as well as pavement layer properties obtained in preceding chapter were incorporated to the FE models to more accurately determine the site-specific Equivalent Axle Load Factors (EALFs).

6.2 Background

The EALF for flexible pavements, as established by AASHTO, is defined as follows:

$$EALF = \frac{W_{t18}}{W_{tx}} \tag{1}$$

where:

W_{tx} = Number of x-axle load repetitions after time t, and

W_{t18} = Number of 18-kip axle load repetitions after time t, calculated from Equation 2,

$$log\left(\frac{W_{tx}}{W_{t18}}\right) = 4.79 \log(18 + 1) - 4.79 \log(L_x + L_2) + log L_2 + \frac{G_t}{\beta_x} - \frac{G_t}{\beta_{18}} \tag{2}$$

where G_t and β_x are defined as:

$$G_t = log\left(\frac{4.2 - p_t}{4.2 - 1.5}\right) \tag{3}$$

$$\beta_x = 0.4 + \frac{0.081(L_x + L_2)^{3.23}}{(SN+1)^{5.19}L_2^{3.23}} \tag{4}$$

where:

L_x = Load in kips on one single axle, one set on tandem axles and one set of tridem axles,

L_2 = Axle code, 1 for single axle, 2 for tandem axle, and 3 for the ridem axle,

SN = Structural number,

p_t = Terminal Serviceability,

G_t = Function of terminal serviceability, and

β_{18} = Value of β_x when L_x is equal to 18-kip and L_2 is one.

As is evident in Equation 1, the EALF for each axle load group is a function of the structural number (SN), which in turn is related to stiffness properties of layers, drainage conditions, and the pavement layer thicknesses. For generalization purposes, Asphalt Institute (AI) assumed SN as 5 and terminal serviceability (p_t) as 2.5 for the development of EALF tables for nationwide use. The axle load equivalency tables essentially provide a means to characterize the damages imparted by i^{th}-axle load group relative to the standard 18-kips single axle on the pavements (Huang, 1993).

There are several sources of inaccuracies and systematic errors associated with such assumptions. The major shortcomings of using the current industry-standard load equivalency factors to quantify relative damages are as follows:

- The EALF tables were originally developed for specified SN and terminal serviceability (p_t) values based on equations proposed and later modified in the AASHTO road test. Considering the fact that many of the in-service pavements, particularly roadways in the energy developing areas have been subjected to heavy loads for several years and already show visible signs of distress and deterioration, the assumption of SN = 5 will result in underestimation of the damage in the network.
- The effect of terminal serviceability and structural number on the value of the EALF in the AASHTO equation is erratic and is not consistent with the theory. Super heavy wheel loads are expected to have significantly higher EALF than unity to indicate more damage compared to the standard 18-kip axle; however, the AASHTO equations predict less damage with lower SN values.
- SN is a function of the layer thicknesses, drainage conditions, and the stiffness properties of the layers. This basically indicates that EALF is not a single value and should be different based on the features of the pavement systems in the network. Considering the fact that the passage of an overweight truck over a thinly surfaced Farm-to-Market (FM) road will potentially induce more damage compared to the passage of the same truck over a well-designed and well-maintained State Highway (SH), using the same EALF for both cases will compromise the accuracy of damage analysis.

In addition to these limitations, issues such as general methodology for the calculations of EALF using AASHTO, coupled with the change in the material properties and loading conditions since the last modification of AASHTO equations, motivated the research team to explore a mechanistic framework for the determination of the axle load equivalency factors in this project.

6.3 Mechanistic Framework for Pavement Damage Quantification

Figure 6.3 provides the flowchart of the proposed procedure for the determination of the modified EALF values based on the parameters and properties directly derived from extensive field data collection efforts. Accurate and realistic characterization of the traffic information is an integral component of the damage quantification algorithms. Therefore, the research team deployed portable Weigh-In-Motion (WIM) devices to collect actual traffic data in ten representative sites during summer and winter months. The WIM data were further post-processed to obtain traffic distributions, classifications, and vehicle characteristics such as gross vehicle weights, axle weights, and axle configurations. The researchers further developed a procedure for routine measurements of tire pressure and tire footprint in the calibration process of portable WIM devices to have an accurate account of the loading conditions for further numerical analysis. The traffic loading information, and site-specific pavement layer thicknesses, as well as back-calculated layer moduli were incorporated in a finite element software to obtain pavement responses. Subsequently, critical pavement responses due to passage of overweight trucks, namely tensile strain at the bottom of Asphalt Concrete (AC) layer, compressive strain at the top of the subgrade layer, as well as the cumulative surface deflections under multiple load groups were determined. The pavement responses were further used in the damage quantification algorithm to calculate EALFs based on fatigue, rutting, and cumulative surface deflection criteria. Ultimately, the highest EALF value for each permutation was selected as the site-specific modified EALF value.
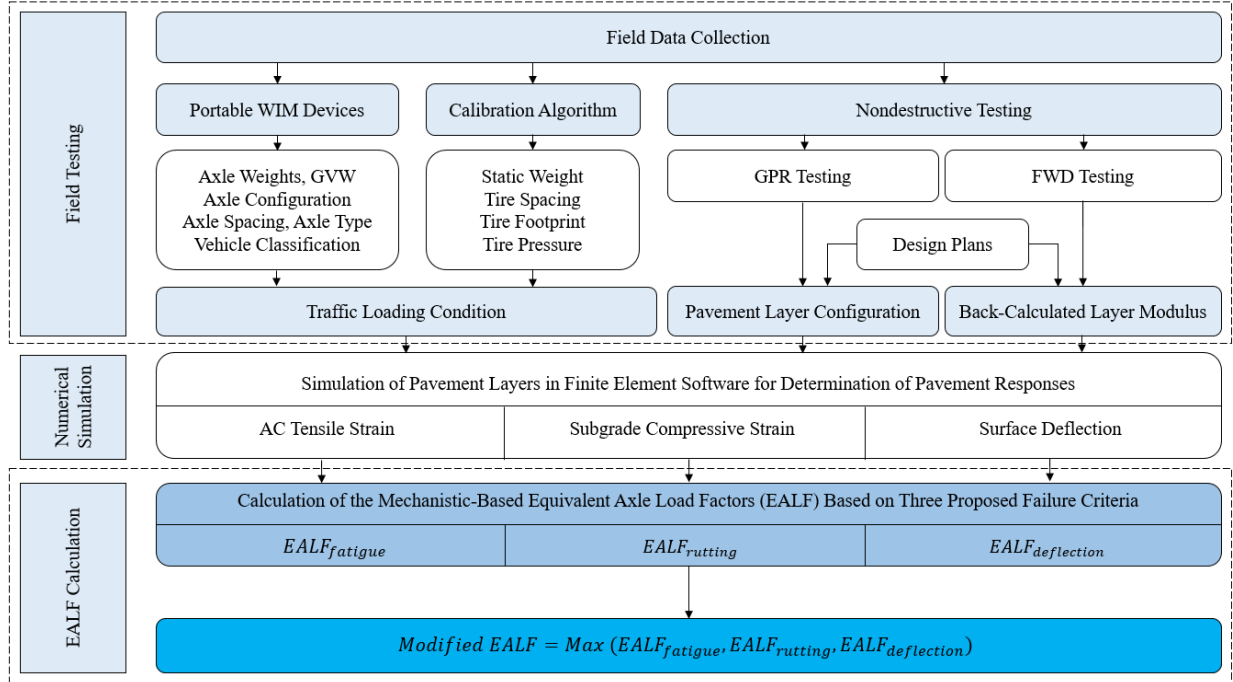
Figure 6.3. Proposed Mechanistic Approach Flowchart for the Determination of the Modified Equivalent Axle Load Factor (EALF).

Damage equivalency factors attributed to the various roadway types with similar characteristics, in terms of the functionality and structural pavement profile, were also classified to better represent the damages imparted by overload truck operations. In order to account for the influence of climate on the material properties of the pavement layers, the FWD testing and surface deflection measurements were conducted in both summer and winter months for all field test sections. The following sections provide detailed information on the field data collection, numerical simulations, and the rationale for the calculations of three axle load equivalency criteria in this research project.

6.4 Modified Equivalent Axle Load Factors

The following three different classifications of EALFs were used for accurate characterization of the damages imparted by OW truck operations in the network:

6.4.1 EALF based on Fatigue Criteria

In the AI approach, the tensile strain at the bottom of the asphalt layer was selected as the critical response that controls the fatigue performance of the flexible pavements, as shown in Equation 5:

$$N_f = 7.96 \times 10^{-2}(\varepsilon_t)^{3.29}(E_{AC})^{0.85} \tag{5}$$

where the N_f is the allowable number of load applications to fatigue failure, ε_t is the tensile strain at the bottom of the asphalt layer, E_{AC} is the modulus of the asphalt layer. The equivalent axle load

factor for axle load group x compared to standard 18-kip axle based on the fatigue criteria can be calculated from Equation 6 as:

$$EALF_{fatigue} = \left(\frac{W_{t18}}{W_{tx}}\right) = \left(\frac{\varepsilon_{t\,x}}{\varepsilon_{t\,18}}\right)^{3.29} \tag{6}$$

6.4.2 EALF based on Rutting Criteria

The AI rutting model assumes that the asphalt layer and the base layer will not experience any permanent deformation; therefore, all rutting is associated with subgrade permanent deformation (Bahia, 2000). Hence, the compressive strain ε_c at the top of the subgrade is assumed to be the controlling factor for the determination of the rutting performance of the flexible pavements. Equation 7 defines the rutting performance as:

$$N_f = 1.37 \times 10^{-9}(\varepsilon_c)^{4.47} \tag{7}$$

where N_f is the allowable number of load applications to rutting failure. The axle load factor based on the rutting criterion can be calculated from Equation 8 as:

$$EALF_{rutting} = \left(\frac{W_{t18}}{W_{tx}}\right) = \left(\frac{\varepsilon_{c\,x}}{\varepsilon_{c\,18}}\right)^{4.47} \tag{8}$$

6.4.3 EALF based on the Cumulative Surface Deflection Criteria

The AI rutting criterion assumed that the asphalt and base layer remains intact during the service life of the pavement, and all the deformation is due to subgrade rutting. This is often not true, as there will be rutting in the asphalt and base layers during the service life of flexible pavements. Therefore, it deems necessary to consider plastic deformations in individual layers, and the summation of all deformations manifested on the surface an additional measure to calculate the axle load equivalency factors. To achieve this objective, the cumulative deflection determined at the surface of the pavement from numerical simulations were used to calculate the deflection-based criteria. The cumulative plastic deformation was used to develop a new measure of EALF based on surface deflection criterion for different axle loads, as shown in Equations 9 through 11:

$$N = \left(\frac{1}{D}\right)^{3.8}, \tag{9}$$

Single Axles: $EALF_{deflection} = \left(\frac{W_{t18}}{W_{tx}}\right) = \left(\frac{D}{D_b}\right)^{3.8},$ (10)

Multiple Axles: $EALF_{deflection} = \left(\frac{W_{t18}}{W_{tx}}\right) = \left(\frac{D}{D_b}\right)^{3.8} + \Sigma\left(\frac{\Delta_i}{D_b}\right)^{3.8}$ (11)

where D is the surface deflection, $\frac{D}{D_b}$ is the ratio of pavement surface deflections caused by a single axle load to those calculated under the standard 18-kip axle (D_b). Furthermore, Δ_i represents the difference in magnitude between the maximum deflection calculated under each succeeding axle and the intermediate deflection between axles (Kawa et al., 1998).

Figure 6.4 illustrates the locations where critical responses are evaluated on a typical pavement structure: Surface deflection at Point A, tensile strain at bottom of the AC layer (Point B) and compressive strain at top of the subgrade (Point C) were obtained. Consequently, by making use of Equations 5 through 11, the research team calculated different measures of the EALF for specific pavement groups. Ultimately, the highest EALF value among the three criteria was selected as the modified axle load equivalency factor as shown in Equation 12:

$$Modified\ EALF = Max\ (EALF_{fatigue}, EALF_{rutting}, EALF_{deflection}) \tag{12}$$
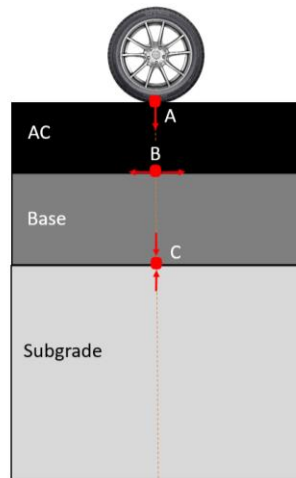
Figure 6.4. Locations of the Pavement Response Parameters.

6.5 Field Data Collection

Data collection procedure was adopted to obtain essential parameters required to develop mechanistic-based EALFs. The site-specific information were collected for ten representative sites strategically distributed throughout the overweight corridors of energy development areas of South Texas.

6.5.1 Deploying Portable WIM Devices

As discussed in previous chapters, the portable WIM devices were deployed for a period of at least two weeks and were left continuously recording traffic at each site. In addition, to obtain accurate and reliable WIM data, the research team implemented an elaborate calibration procedure pre and post installation of the WIM systems in the field. Axle weight, Gross Vehicle Weight (GVW), axle

configuration, axle type, and vehicle classifications were the most relevant traffic information that were collected by the portable WIM units. It should be noted that the performance of a pavement section is affected not only by the GVW values but also, more importantly, by vehicle axle weights. Hence, in this study, axle-loading conditions in different axle groups were fully evaluated. The traffic characteristics pertaining to the overweight trucks from the WIM data were further incorporated in the numerical simulations. Table 6.1 shows the overweight axle ranges, for different axle group types, as recorded by the WIM devices in this study. Texas permissible weight limits are also provided for comparison purposes in Table 6.1. Axle weights heavier than these values are primarily regarded as overweight. Another noteworthy results provided in Table 6.1 pertains to the large deviation of the maximum recorded GVW during this study and allowable maximum GVW in Texas. As indicated in this table, the highest gross vehicle weight was 364,000 lb. recorded in the summer data collection procedure in SH123.

Table 6.1. Overweight Loads Collected by WIM Devices

Axle Type	Axle Weight (lb.)		GVW (lb.)	
	Texas Maximum Permissible	Maximum Recorded	Texas Maximum Permissible	Maximum Recorded
Single Axle	20,000	42,000	80,000	364,000
Tandem Axle	34,000	64,000		
Tridem Axle	42,000	114,000		
Quad Axle	50,000	140,000		

Besides the OW axle passing in the network, some roadways such as SH123 were subjected to the movement of Super-Heavy Loads (SHLs). SHL hauling units are considerably heavier in weight compared to the standard trucks. SHL gross vehicle weights may range from few hundred thousand pounds to few million pounds (Nimeri, 2018). Typically, SHLs are defined and treated differently than the OW axles. As indicated in the following relationship, SHLs are heavier than OW loads, and essentially defined as the loads exceeding 250,000 lb:

Permissible Weight Limits (80,000 lb) < OW < SHL (GVW ≥ 250,000 lb) (13)

Based on the collected traffic data by WIM devices, it was observed that SHL trucks with GVW higher than 360 kips are passing in some studied sections of the highway network. Considering the fact that a single pass of a SHL vehicle could exert detrimental effects on the pavements as high as numerous passes of the reference vehicle, the research team paid special attention to properly quantify the damage factors for the SHL category.

6.5.2 Axle Configuration

As mentioned, WIM units are able to record different axle spacing corresponding to the vehicles passing over the installed piezoelectric sensors. Table 6.2 provides the average values of successive axle spacing for different axle types based on the field traffic information. It should be noted that the previous studies showed that when the center to center distance between each adjacent axle are more than 60 in., the pavement responses under one of the axles won't be affected by the adjacent axle load (Oh, et al., 2007). Such criteria for axle spacing was used to define the various axle groups for an OW vehicle in the finite element analysis. Therefore, the axles with more than 60 in. axle spacing were simulated as individual axles.

Table 6.2. Axle Spacing Values Used for Simulation Purposes

Axle Type	Axle Spacing (in.)
Tandem Axle	51.6
Tridem Axle	50
Quad Axle	50.4

6.5.3 Calculation of Tire Pressure and Tire Footprint

In recent years, tire pressure of the commercial vehicles operating in the transportation systems has increased significantly. In the road test of the AASHTO, tire inflation pressure varied from 75 to 80 psi. Nowadays, trucks usually use tires with pressure ranging from 85 to 115 psi and, in some cases; tire pressures can reach 130 to 145 psi (Filho, et al., 2016). According to a previous study by the Florida Department of Transportation (FDOT), tire pressures ranged between 80 and 125 psi (Greene, et al., 2010).

Considering the fact that the high tire pressure could extremely influence on the pavement responses such as stresses and strains, the research team was motivated to conduct some experimental investigations in the field to calculate the actual tire pressure, instead of assuming a typical value. Moreover, it should be noted that the tire pressure value is linked with the tire footprint area and axle weight and it can be calculated from Equation 14 as:

$$P = \frac{L}{A},$$
(14)

where P is the tire pressure, A is the tire footprint area and L is the specific axle weight divided by the number of tires in the axle.

Collaborating with TxDOT's Yoakum District Maintenance Division, the research team measured the tire footprint area for single and tandem axles for class 6 and 9 trucks using the print of painted

tires on the papers, as shown in Figure 6.5 and 6.6. In addition, axle weights were measured using the static scales, as shown in Figure 6.7.

Figure 6.5. Painting Tires for Tire Footprint Measurement.

(a)	(b)	(c)	(d)
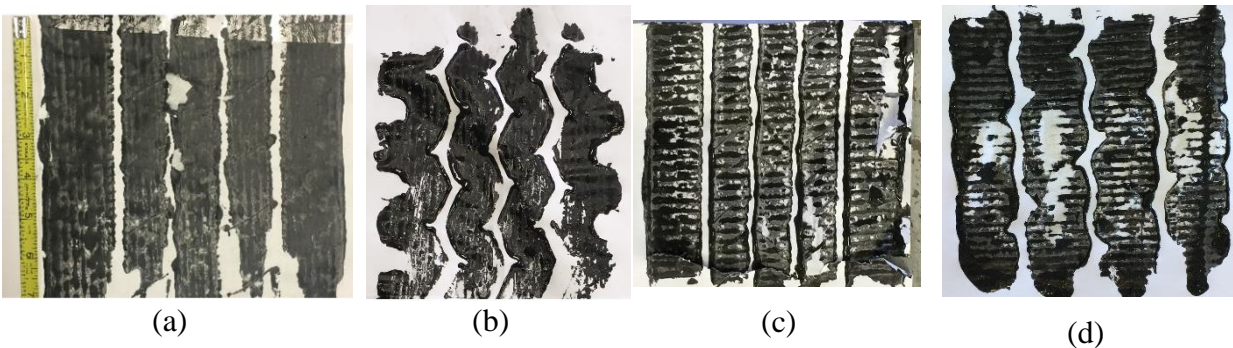
Figure 6.6. Different Tire Footprints for (a) Class 6, Front Axle, (b) Class 6, Rear Axle, (c) Class 9, Front Axle, (d) Class 9, Rear Axle.

(a)	**(b)**	**(c)**	**(d)**
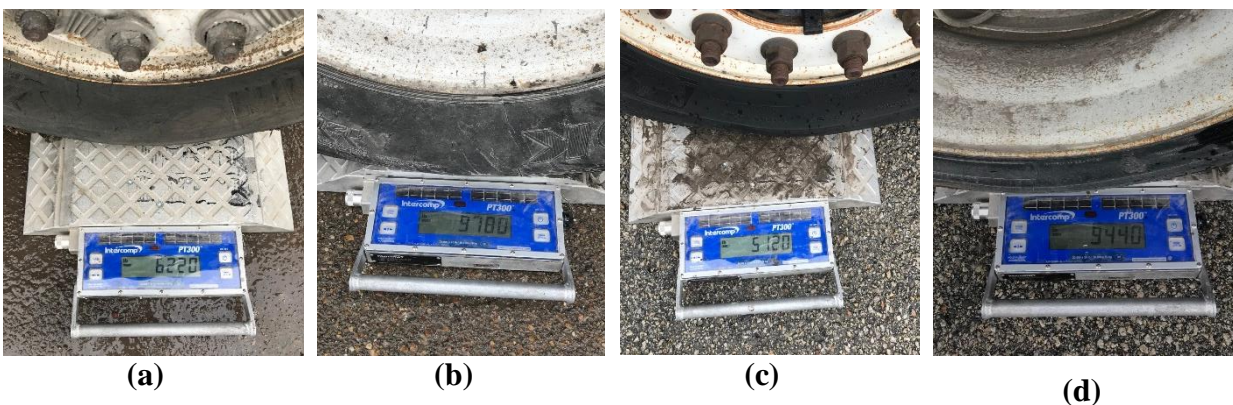
Figure 6.7. Axle Weight Measurement for (a) Class 6, Front Axle, (b) Class 6, Rear Axle, (c) Class 9, Front Axle, (d) Class 9, Rear Axle.

Table 6.3 summarizes the contact area, axle weight and the tire pressure values for different axle types. Based on the calculated values, 120 psi was selected as the most critical value for the tire pressure in the finite element analysis.

Table 6.3. Tire Pressure Calculation

Vehicle Classification	Axle Type	Contact Area (in²)	Weight per Axle Side (lb)	Tire Pressure (psi)
Class 6	Single Axle	51.8	6220	120
	Tandem Axle	42.2	9780	116
Class 9	Single Axle	44.4	5120	115
	Tandem Axle	42.8	9440	110

6.5.4 Nondestructive Testing

The research team deployed GPR and FWD to the field for determination of the site-specific material properties. Accurate material properties such layer thicknesses, layer configurations, and back-calculated layer modulus were incorporated into the FE models, as previously shown in Table 5.3 and 5.4.

6.6 Numerical Simulation of Truck Traffic on Pavements by Finite Element Method

The commercial finite element software ABAQUS was used to model the pavement structure and traffic loads for accurate determination of pavement responses when subjected to different truck loading configurations. The calculated responses were used in the pavement performance equations for the determination of the axle load equivalency factors. Model geometry, boundary condition, meshing as well as other detailed information regarding the finite element modeling are explained in the following sections.

6.6.1 Model Geometry

Different pavement layers consisting of surface layer, base and subgrade have been simulated in the ABAQUS program as is presented in Figure 6.8. Site-specific structural properties of the pavement layers such as the layer modulus and the layer configuration were assigned for each representative roadway in the finite element model. In order to optimize the computational efficiency of FE analysis and since the whole model is symmetric, only a quarter size of the model was simulated in the finite element program, as shown in Figure 6.9.

111
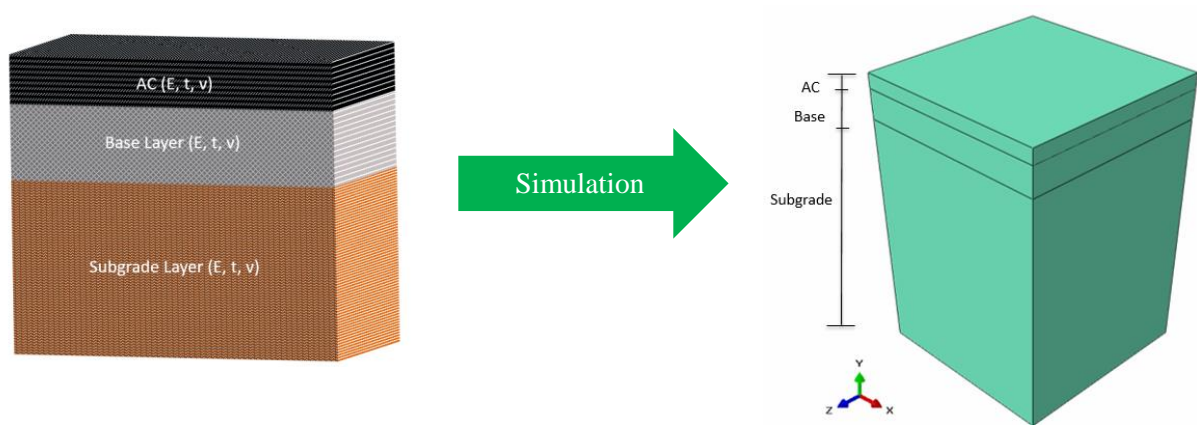
Figure 6.8. Pavement Layers Simulation in ABAQUS.
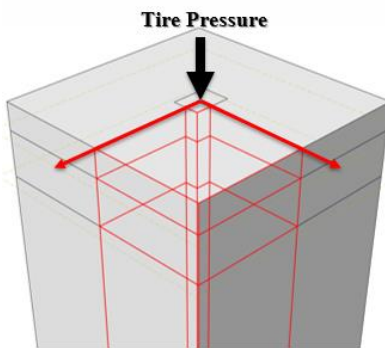
Figure 6.9. Simulated Quarter Model.

6.6.2 Model Dimension

Proper characterization of the dimensions and geometry of the pavements are of outmost importance to mitigate the systematic errors associated with boundary effect problems. The research team carried out a comprehensive sensitivity analysis to determine the adequate subgrade depth and model longitudinal and transverse widths for simulation purposes based on the specific pavement structure of the selected sites. To achieve this objective, the thickness of the subgrade was incrementally increased from 50 inches to 150 inches, the variations of the calculated responses were monitored accordingly. As shown in Figure 6.10, the sensitivity of the critical pavement responses are negligible when the simulated subgrade thickness exceeds 100 inches. Therefore, the research team selected 100 inches as representative thickness of subgrade layer for further numerical simulations
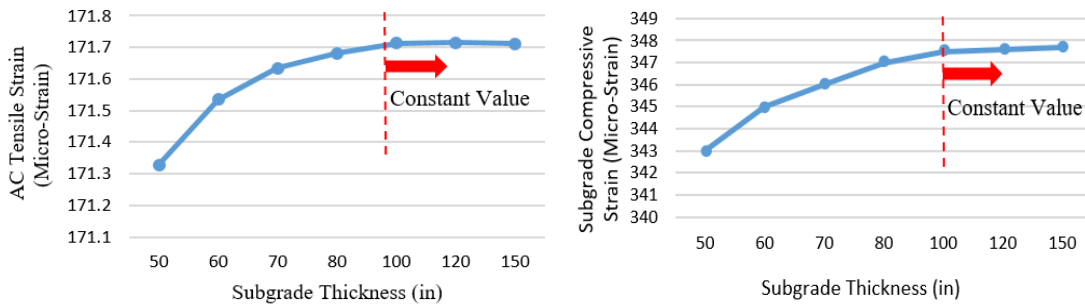
Figure 6.10. Pavement Responses for Different Subgrade Thicknesses.

6.6.3 Boundary Conditions

Boundary Conditions (BC) are essentially defined as the displacement or rotation constrains to avoid the movement of the selected degrees of freedom, or to prescribe the displacement or rotation for each selected degree of freedom (ABAQUS Manual, 2015). Since boundary conditions play a critical role in the FE modeling, attention should be paid to defining appropriate boundary conditions to assure a realistic model. Figure 6.11 shows different types of BCs defined in the simulation of pavement structure models. ENCASTRE boundary condition was used at the bottom of the subgrade layer to simulate the bedrock. ENCASTRE is a specific type of BCs that restrains the displacement and rotation in all directions. Moreover, two other BCs were defined in the FE models to restrict the displacement in the orthogonal direction to the indicated surfaces.
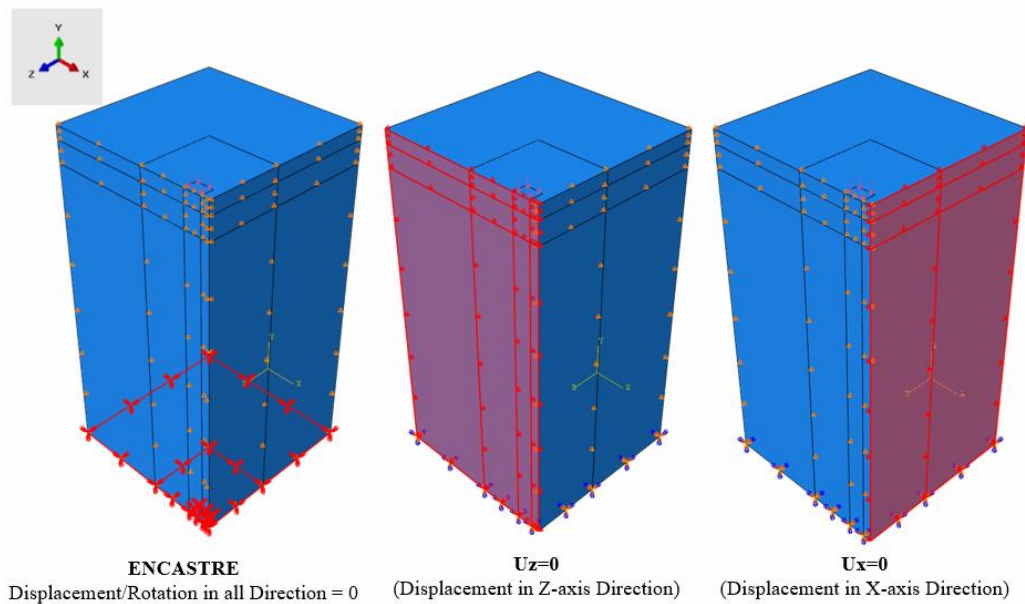
Figure 6.11. Boundary Conditions.

6.6.4 Meshing

Considering the fact that the most critical response points in the procedure of pavement performance analysis are located under the wheel path, the research team defined a finer mesh in this region for more accurate results. However, to expedite the computation time and reduce the output files size, a coarser mesh in the regions far from the loading areas were used. Therefore, as shown in Figure 6.12, three-dimensional continuum elements C3D8 (eight-node linear brick) with finer meshing size and C3D6 (six-node linear triangular prism) with coarser meshing size, assigned to the loading area elements and the other elements, respectively. In addition, a transition area was defined between fine and coarse mesh areas for gradual change of element size to ensure improved accuracy.
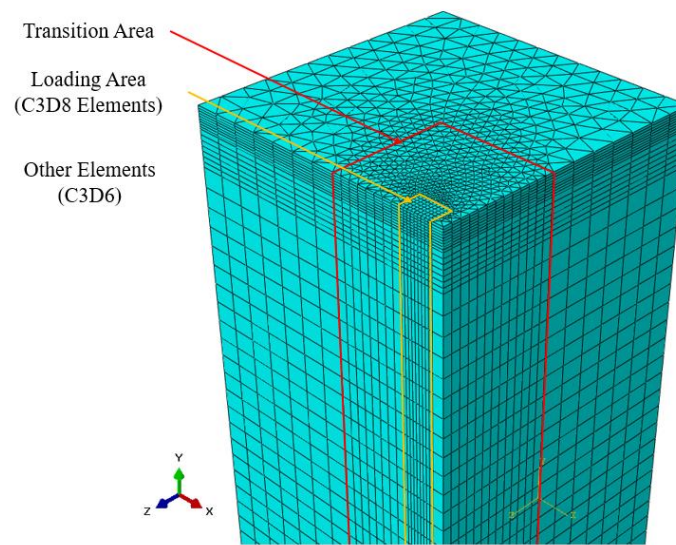
Figure 6.12. Meshing and Different Element Types.

6.6.5 Load Allocation

Using Equation 14, uniformly distributed tire pressure is assumed in the FE modeling for different groups of axle configurations and axle weights. Figure 6.13 illustrates the tire pressure exerted on the pavement structure in the ABAQUS program environment.

114
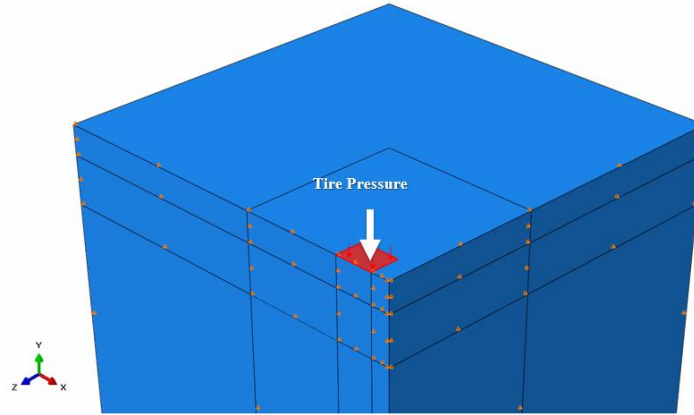
Figure 6.13. Assigning Load in FE Model.

6.6.6 FE Outputs

The research team analyzed the pavement structures associated with the distinct traffic characteristics and material properties for specific sites to obtain the dominant pavement responses on damage equivalency factors. The following three parameters were investigated using the FE model and analysis:

➢ Surface vertical deflection to determine *surface deflection-based EALF*
➢ Horizontal tensile strain at bottom of HMA layer to determine *fatigue failure-based EALF*
➢ Vertical compressive strain at the top of subgrade to determine *rutting failure-based EALF*

The above parameters were acquired by extracting the ABAQUS output results. Pavement response contours shown in Figure 6.14 are essentially instrumental in the calculation of the three parameters.

(a)   (b)   (c)
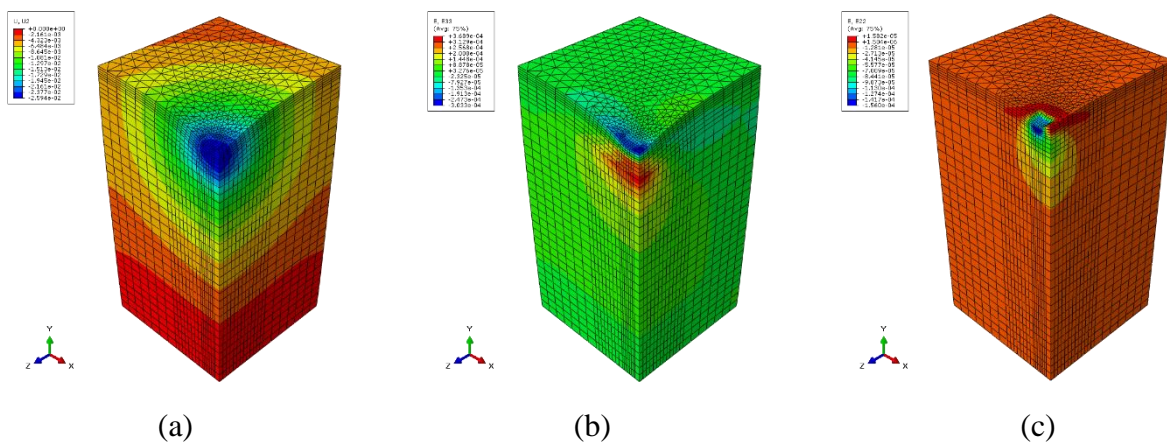
Figure 6.14. Pavement Responses Contours for (a) Surface Deflection, (b) Horizontal Tensile Strain and (c) Vertical Compressive Strain.

6.6.7 Sensitivity Analysis with Respect to the Critical Response Location

Three type of pavement responses were calculated at the critical locations within the pavement structure. Since the critical locations will be a function of the axle configuration and the pavement structure, the research team analyzed different locations of the pavement considering different axle types, and site-specific pavement layer properties, as shown in Figure 6.16. For instance, four locations were evaluated at the bottom of the HMA layer for the estimation of AC bottom-up fatigue cracking. Pavement responses (ε_t) were obtained for locations 1, 2, 3, and 4 for each axle type as shown in Figure 6.15. The highest value of the pavement response was incorporated in the algorithm for further calculations of the EALF values in this study. Similarly, the research team calculated the other pavement responses at all indicated points and obtained the maximum values corresponds to the critical locations. Generally, critical location is defined as the location where the maximum damage is most likely to occur under that specified point. Table 6.4 summarizes the results associated with the mentioned sensitivity analysis.

(Single Axle)

(Tandem Axle)   (Tridem Axle)   (Quad Axle)
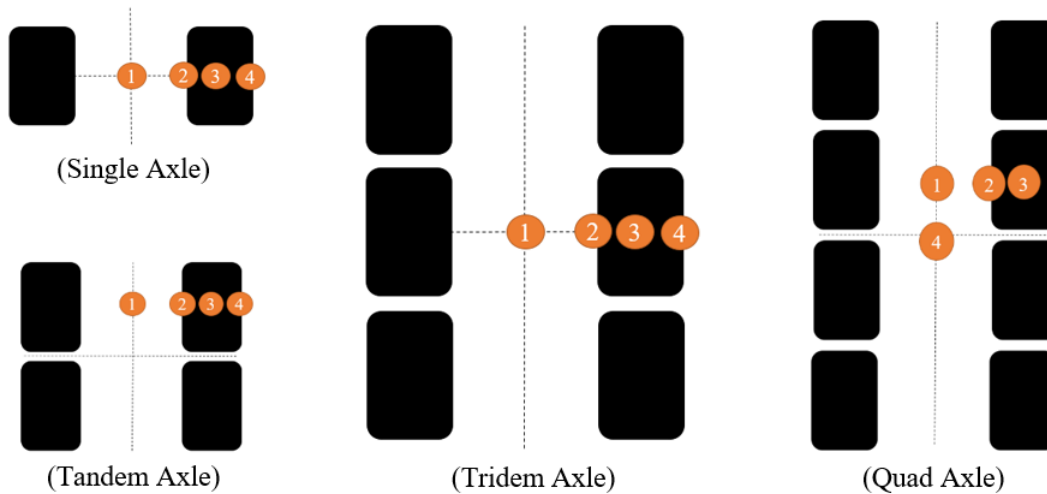
Figure 6.15. Sensitivity Analysis with respect to the Critical Response Location.

Table 6.4. Critical Locations of Pavement Responses

Pavement Responses	Critical Point for Different Axle Types			
	Single Axle	**Tandem Axle**	**Tridem Axle**	**Quad Axle**
Surface Deflection	2	2	2	2
AC Tensile Strain	2	3	3	3
Subgrade Compressive Strain	1	1	1	1

6.7 Modified EALF Values

Modified EALF values tailored towards the specific axle load and axle configuration of vehicles operating in 10 selected pavement sections in San Antonio, Corpus Christi, Yoakum and Laredo Districts were calculated. Using the approach described in section 6.3, the research team calculated different measures of the EALF based on three pavement responses derived from the FE analysis, and chose the highest value as a representative value of the modified EALF. Modified EALF values were also contrasted with traditional Asphalt Institute EALFs for comparison purposes in this research effort.

In order to evaluate the efficiency of finite element approach used for the determination of EALFs, a comparison analysis was conducted between ABAQUS finite element program and linear elastic programs such as FPS21, WinJULEA, BISAR and KENPAVE. Generally, the analysis confirms that the FE results were in a good agreement with other linear elastic programs, particularly with FPS21 and BISAR.

To further represent the calculated site-specific EALF values, damage factors attributed to the SH 123, as a heavily trafficked highway in Corpus Christi District are used as an example in this section. Comprehensive information on the modified EALF values for all ten selected sites are provided in the web-based module developed in this research project (link to the module: http://ctis.utep.edu/TXDOT-06965/).

6.7.1 Modified EALF value for SH123, Corpus Christi

Analysis of the GPR data validated by available TxDOT databases indicated that the State Highway 123 is consisted of 5.5 in. of asphalt (medium thickness) and 15 in. of granular base layer. This information was further used in the FE program for the calculations of the site-specific axle load equivalency factors. Since SH 123 was subjected to the movement of Over-Weight (OW) axles and Super Heavy Loads (SHLs), the research team have evaluated the effect of both categories on determination of the damage factors.

I.   **Over-Weight Axles**

EALF values in SH123 roadway for different axle types in OW range are shown in Figure 6.16. The post processed data for single axles showed that the rutting-based damage factors were mainly higher that the damage factors calculated based on fatigue and surface deflection criteria. Results of the multiple axles showed that EALF values attributed to the surface deflection criteria were significantly higher than the two other criteria proposed in this study. Consequently, rutting and surface deflection criteria lead to the most critical measures for quantification of the damage factors under passage of OW axles in SH123 highway.

In order to clarify the significance of the site-specific characterizations, modified EALF values (the highest EALFs) were compared with the traditional industry-standard values as depicted in Figure 6.16. The proposed mechanistic approach confirmed that the modified EALFs were significantly higher than the traditional damage equivalency factors, commonly used by the pavement design engineers. For instance, one passage of a 40 kips single axle load on SH123 can potentially induce 30 times the damage imparted by 18 kips reference axle. However, according to the industry-standard values, it equals to 21 passes of a reference axle. In other words, the use of traditional axle equivalency factors for SH123 can potentially under-estimate the damages by approximately 43%.
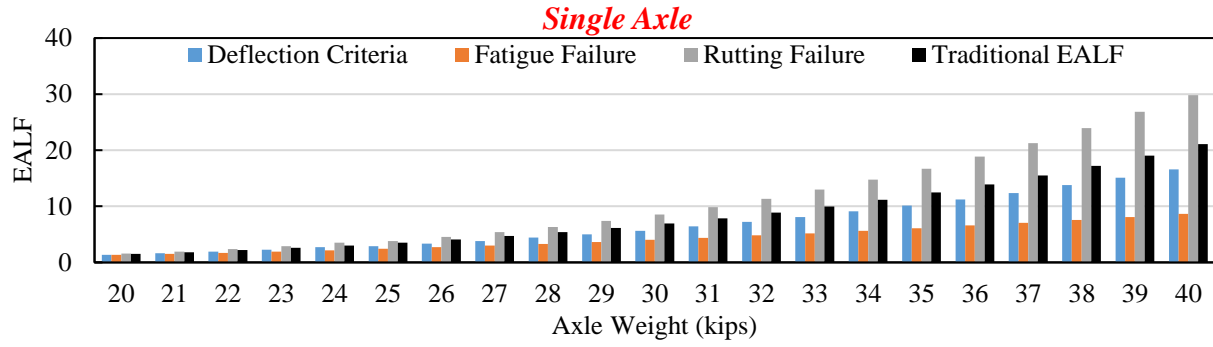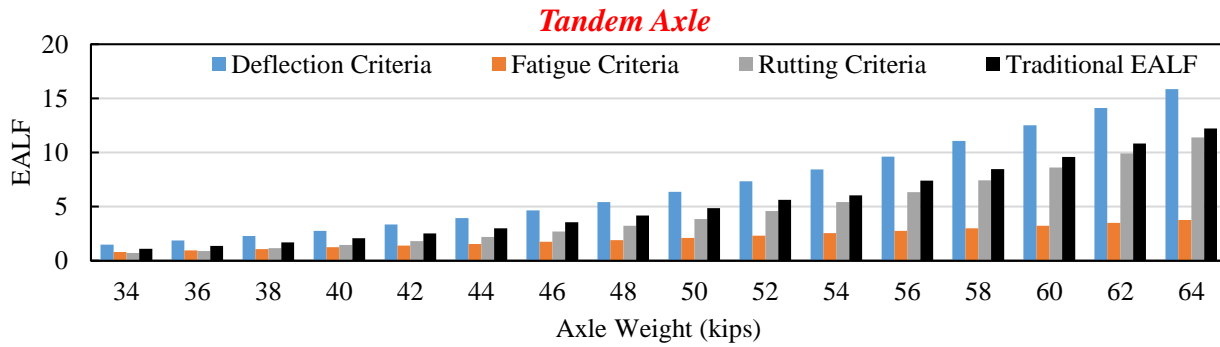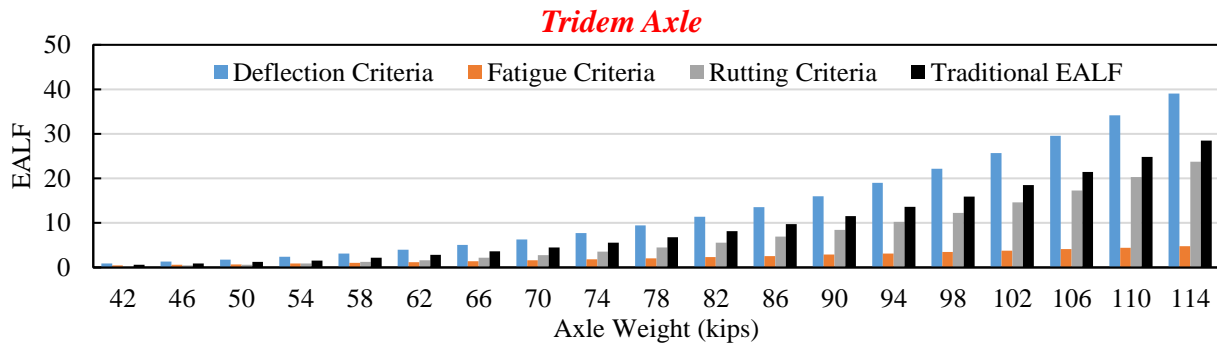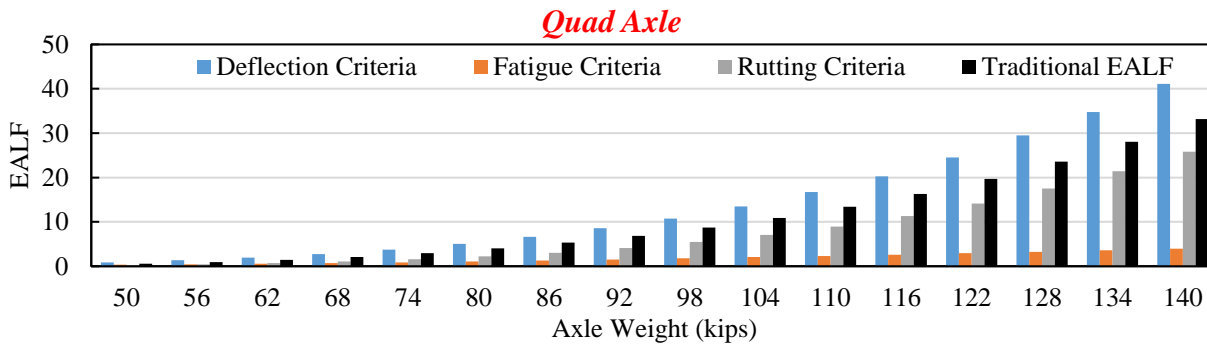
Figure 6.16. EALF Values in SH123-Corpus Christi for Different Axle Types a) Single Axle, b) Dual Axle, c) Tridem Axle, and d) Quad Axle.

II.   Super Heavy Loads (SHL)

Considering the fact that super heavy loads significantly contribute to loss of serviceability and pavement deteriorations, the research team also assessed the SHL impacts on the pavement performance and the corresponding damage factors. In order to better represent the detrimental effects of SHLs on the SH123 pavement sections, Load Equivalency Factors (LEFs) based on GVW have been calculated, which is defined as the damage per pass to a pavement by a specific GVW relative to the damage per pass of a reference vehicle (80 kips).

The most critical criteria for calculation of the load equivalency factors in SHLs was the surface deflection criteria, because SHLs typically consisted of several multiple axles and as mentioned, surface deflection-based equivalency factors are significantly higher than the two other criteria. Figure 6.17 shows the LEFs for different GVW values observed in the SHL category. Based on the analyzed results provided in the plots, it should be noted that the SHL trucks have high potential for significant damage on the pavement, due to more taxing stress paths. For instance, based on the mechanistic approach, one passage of a SHL with GVW of 364 kips on SH123 can potentially induce 125 times the damage imparted by an 80-kips reference vehicle. Another noteworthy observation was that the traditional method presented considerably lower values for LEFs. According to the traditional industry-standard values, one passage of a 364-kips SHL equals to 35 passes of a reference vehicle. In other words, the use of traditional axle equivalency factors for SHL trucks passing the SH123 can potentially underestimate the damages by approximately 257%. Consequently, the impacts of SHLs on the pavement are more pronounced, and traditional damage quantification approach is not capable of assessing the damages imparted on pavements by SHL operations.
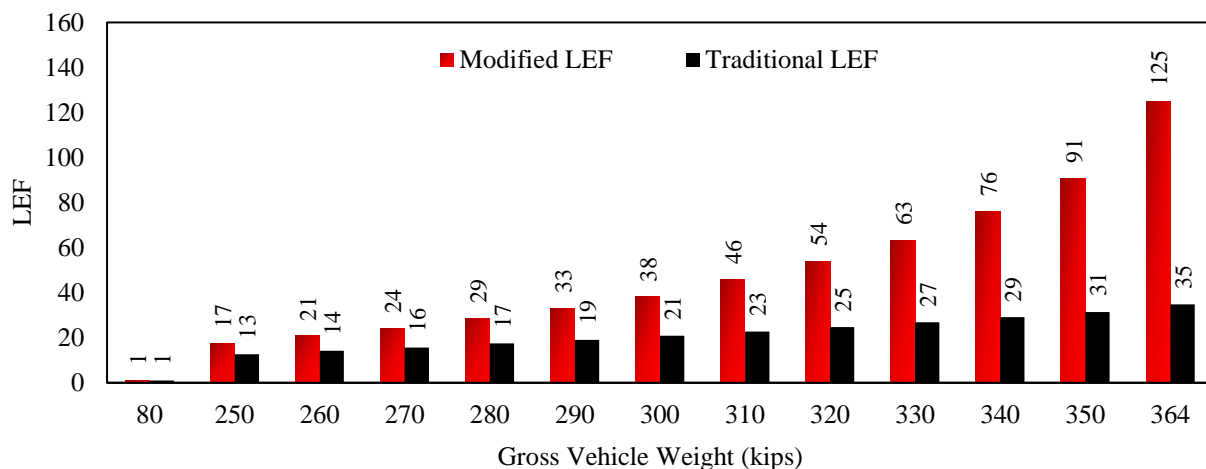
Figure 6.17. Super Heavy Load Equivalency Factors in SH123, Corpus Christi.

120

6.8 EALF Values Based on Three Proposed Criteria

Figure 6.18 to 6.20 present the results for the calculation of three different measures of axle load equivalency factors for different FM, SH, and US highways. The ascending nature of the EALF values in the Figure shows the influence of the axle load weights on the calculated damage equivalency factors. As evidenced in the plots, increasing axle load levels results in exponential increase in the axle load equivalency factors, which in turn translates into higher damages imparted on pavement facilities. Figures 6.18 to 6.20 also provide relative comparisons of different measures of axle load equivalency factors proposed in this study. Evidently, deflection based and rutting based EALF criteria showed the highest sensitivity to the increasing single-axle load weights. As evidenced in Figures 6.18 to 6.20, the deflection based and rutting based EALFs were substantially higher compared to the fatigue criteria. This observation was expected as the damages imparted by overweight vehicles are more relevant to distresses associated with load magnitude such as surface deformations rather than load repetitions as in fatigue-related distresses.

Similar EALF trends were observed for multiple axle load equivalency factors in this study. However, the analysis of tandem, tridem, and quad axles resulted in much higher axle load factors for all three classes of transportation facilities. The corresponding results associated with SH and US highways showed that the surface deflection criteria resulted in the highest EALF values among the three proposed criteria. As stated earlier in the methodology section, the highest value of the EALF among the three criteria is reported as the site-specific and loading group-specific axle load equivalency value for further post-processing and analysis of the remaining life of pavement structures. Table 6.5 provides a qualitative summary of the significance levels for three measures of damage factors proposed in this study. The qualitative significance levels were primarily attributed to the ratios of $\frac{EALF_{ij}}{EALF_{Max}}$, where EALFij is the average axle load equivalency factor for the ith axle group and jth damage factor criteria, and EALFMax is the highest value of the damage equivalency factor calculated for corresponding loading group and roadway type. The load-specific and site-specific damage factors $EALF_{ij}$ exceeding 90% of the maximum EALF value was qualitatively ranked as "significant", while variants with $\frac{EALF_{ij}}{EALF_{Max}}$ ratios below 0.7 were considered as "not significant" in ranking order presented in Table 6.5.
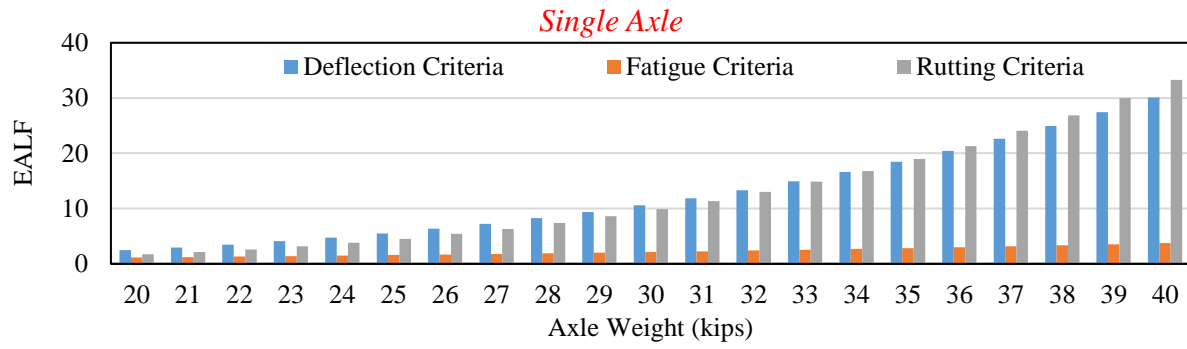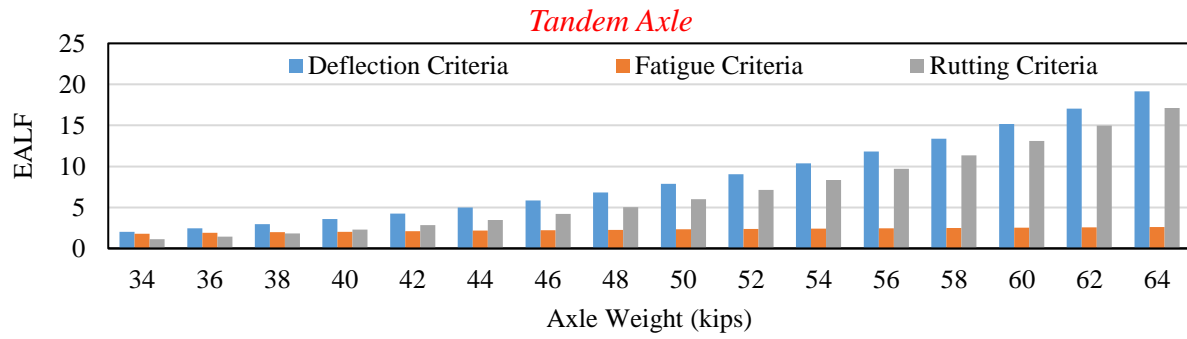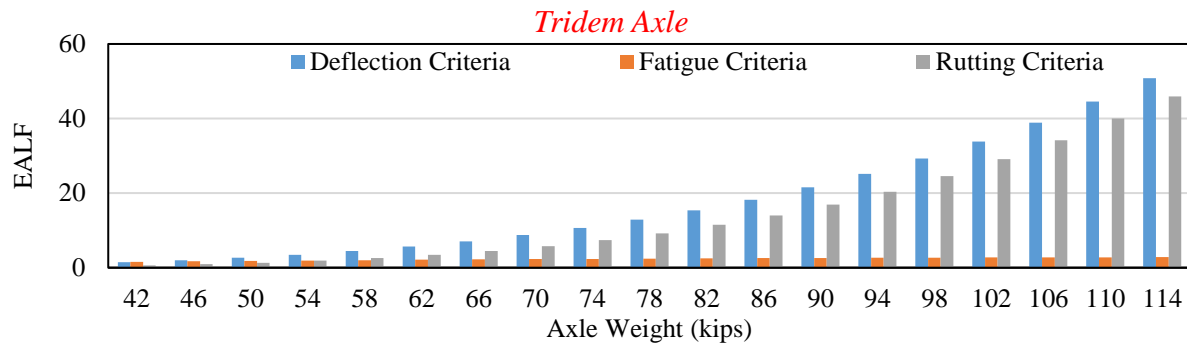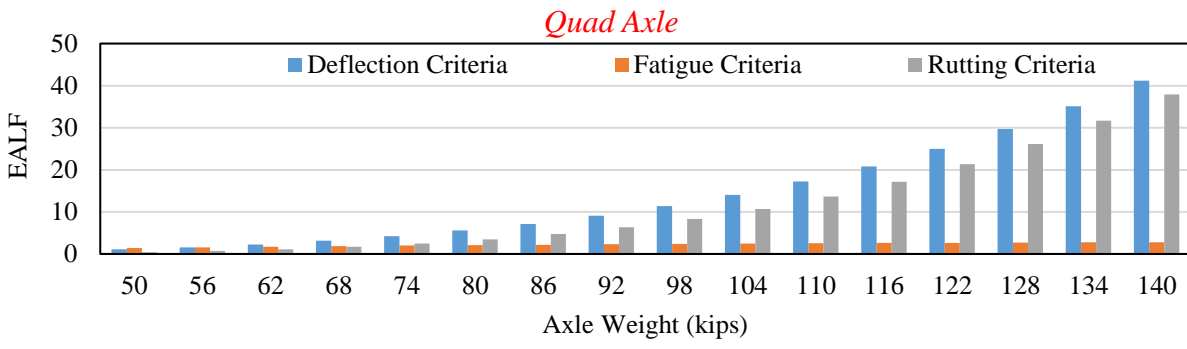
Figure 6.18. Mechanistic EALF values in FM Roadway for Different Axle Types a) Single Axle, b) Dual Axle, c) Tridem Axle, and d) Quad Axle.
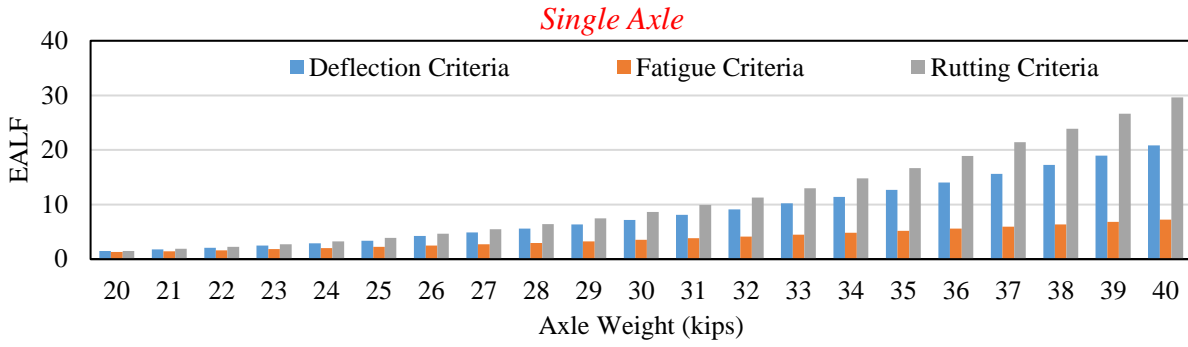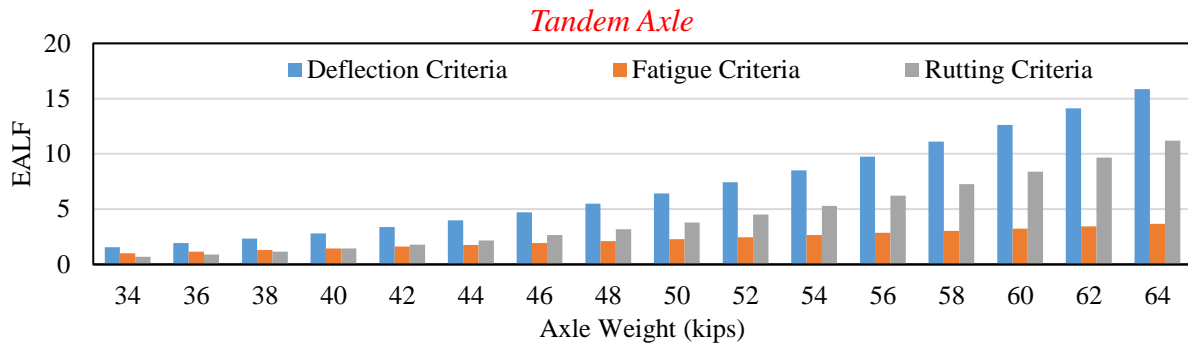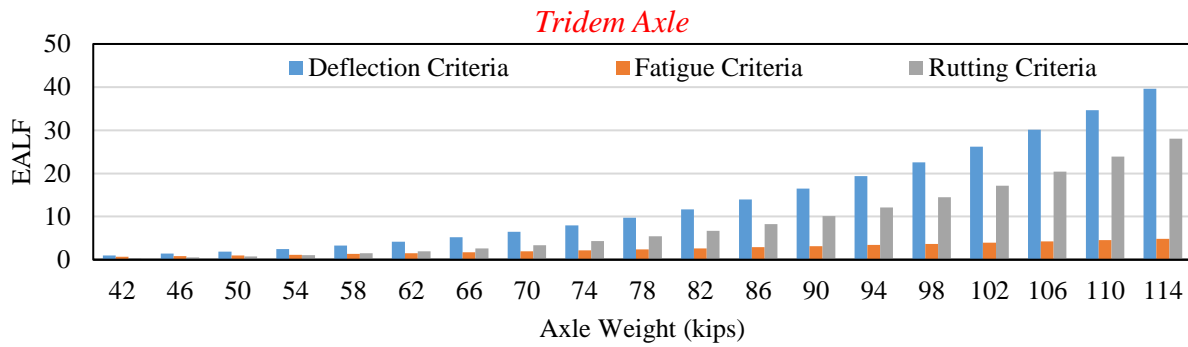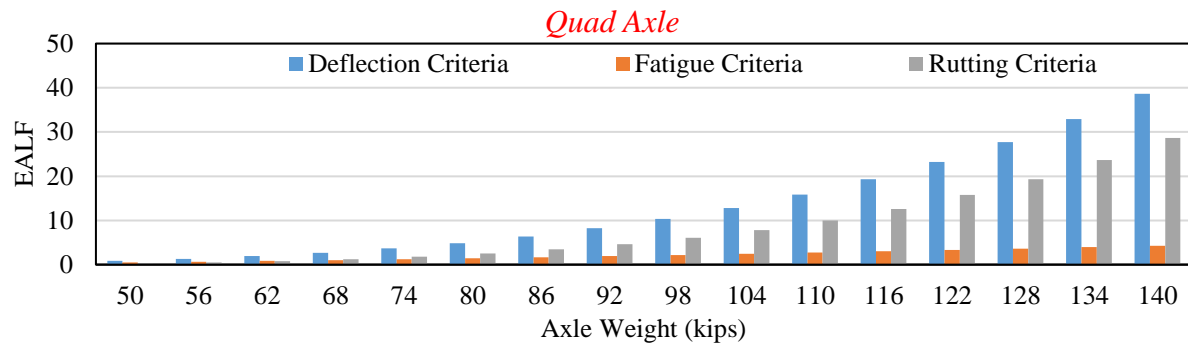
Figure 6.19. Mechanistic EALF values in State Highway for Different Axle Types a) Single Axle, b) Dual Axle, c) Tridem Axle, and d) Quad Axle.
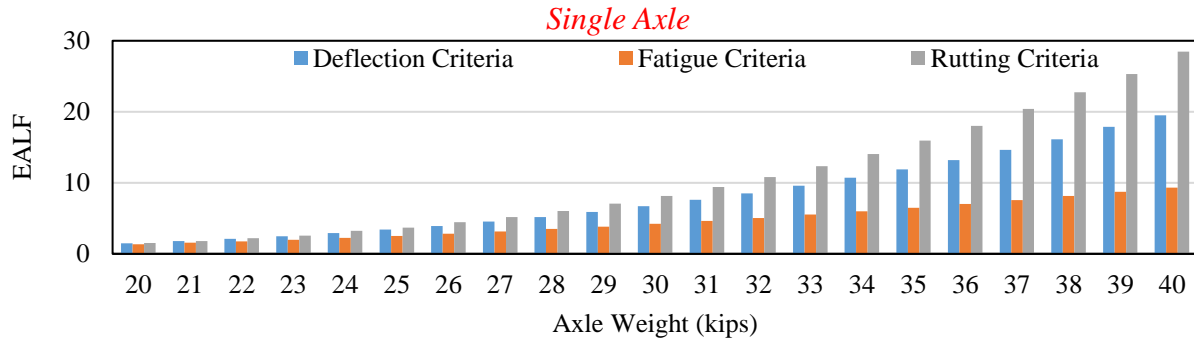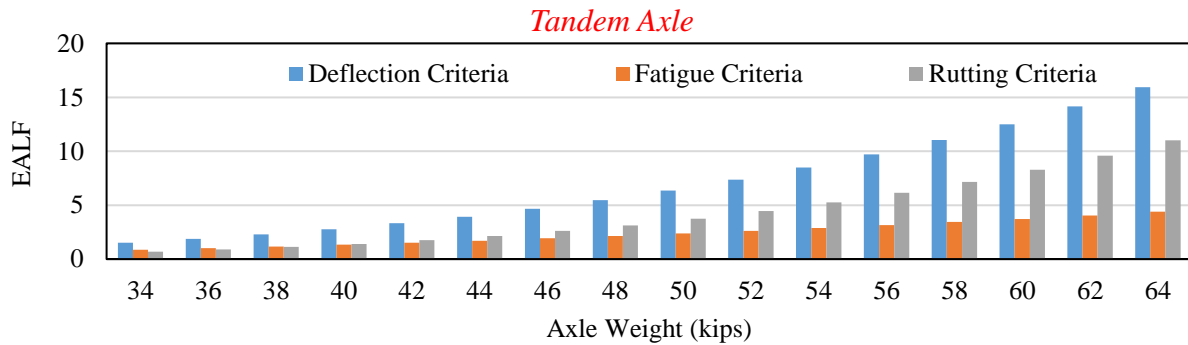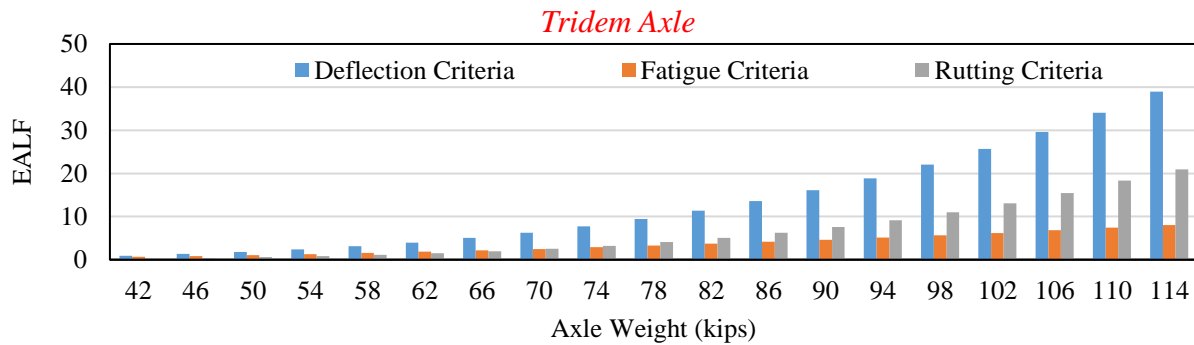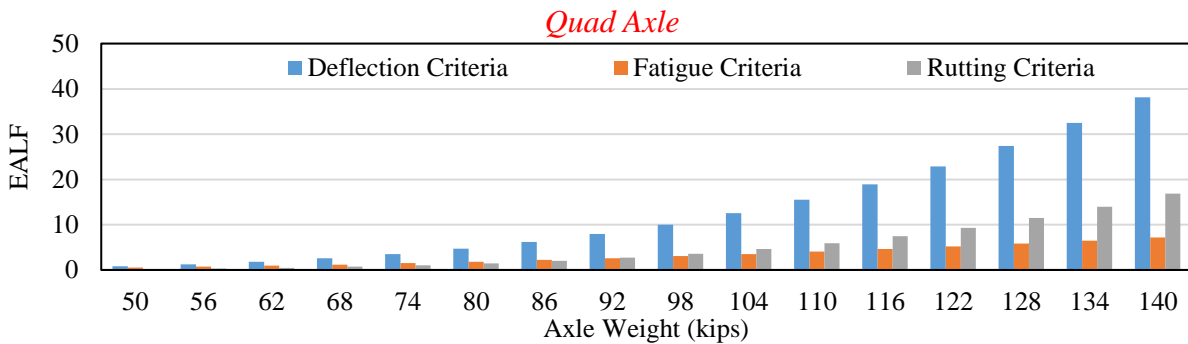
Figure 6.20. Mechanistic EALF values in US Highway for Different Axle Types a) Single Axle, b) Dual Axle, c) Tridem Axle, and d) Quad Axle.

124

Table 6.5. Influential Criteria in Determination of the Mechanistic EALF Values for Different Roadway Types and Different Axle Types

Roadway Type	Axle Type					
	Single Axle			Multiple Axles		
	Surface Deflection	Rutting	Fatigue	Surface Deflection	Rutting	Fatigue
FM						
SH						
US						

Significant: $\dfrac{EALF_{ij}}{EALF_{Max}} > 0.9$

Moderately Significant: $0.7 < \dfrac{EALF_{ij}}{EALF_{Max}} < 0.9$

Not Significant: $\dfrac{EALF_{ij}}{EALF_{Max}} < 0.7$

6.9 Modified EALF Values Based on Various Roadway Types

The modified EALF values attributed to the various roadway types (FM, SH, and US highways) in the network were contrasted with each other for comparison purposes in Figure 6.21. The results showed that in all axle types, FM roadways with less robust pavement profile had the highest damage factors among the three roadway types. Conversely, SH and especially US roadways with more robust layer configurations, with average asphalt thicknesses exceeding 5.5 inches in the surveyed network, had the lowest EALFs. This underscores the significance of the pavement profile on the mechanistic-based damage equivalency factors. Therefore, it is imperative to cluster and differentiate between different types of roadways, such as FM, SH, and US roadways, to realistically represent the damages imparted by overweight truck operations.

As illustrated in Figure 6.21, to clarify the significance of the site-specific damage factors, modified EALF values were also compared with the traditional Asphalt Institute EALFs, commonly used by the pavement design engineers. As evidenced in Figure 6.21, the traditional EALF values were substantially lower than the modified damage factors. Such underestimation of the axle load factors can potentially jeopardize the pavement design and rehabilitation plans in overweight corridors. Table 6.6 presents a summary of the differences between the site-specific and load-group specific EALF values. As evidenced in Table 6.6, the mechanistic EALF values substantially deviate from the traditional industry-standard axle load factors currently employed by the pavement design industry.
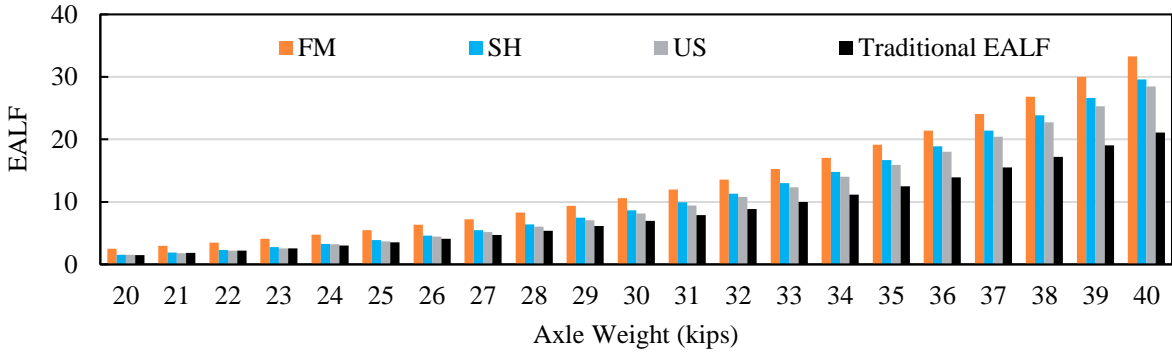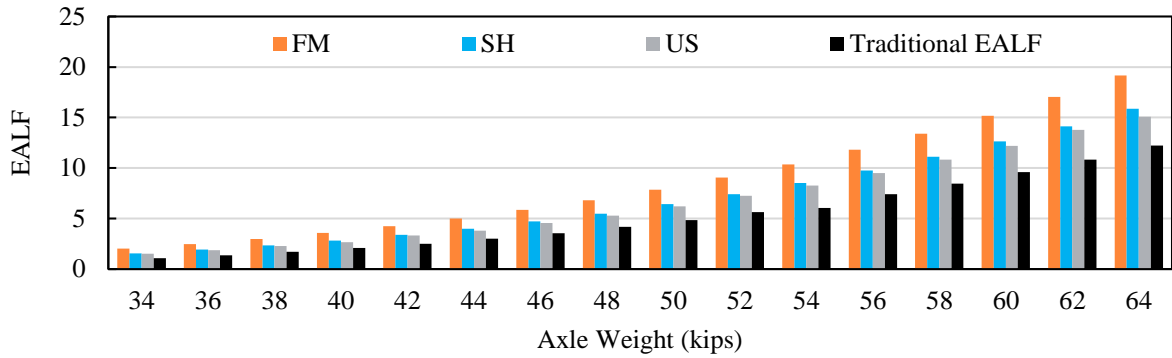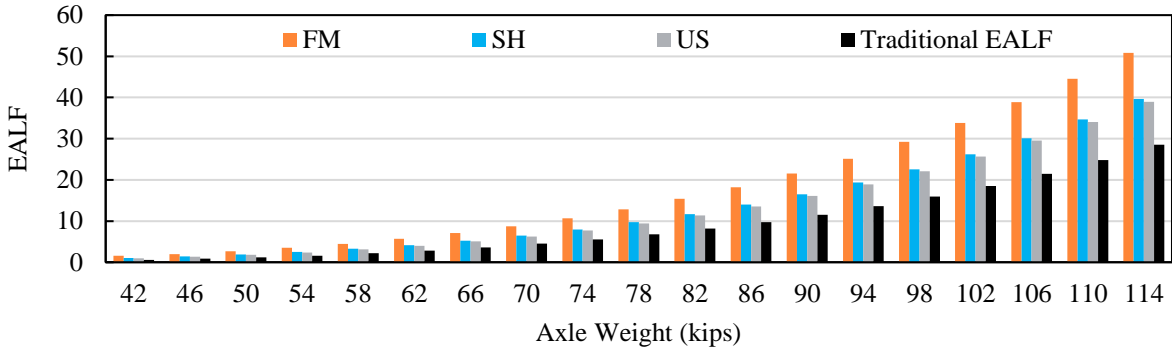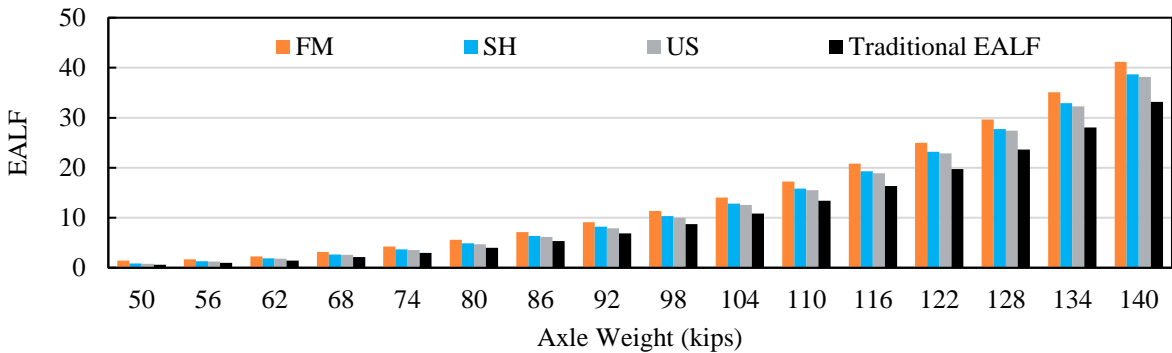
Figure 6.21. EALF Values for Different Roadways in the Network and Different Axle Types a) Single Axle, b) Dual Axle, c) Tridem Axle, and d) Quad Axle.

Table 6.6. Percent Difference between Traditional and Modified EALF Values

Roadway Type	Axle Type			
	Single	Tandem	Tridem	Quad
FM	57	55	78	24
SH	40	31	41	18
US	34	28	38	15

6.10 Influence of Climate on the Modified EALF Values

The research team conducted two series of field data collection in the summer and winter months to study the influence of environmental factors on the axle load equivalency factors. The two sets entail the installation of the portable WIM devices to account for the variations in traffic patterns in the network. Additionally, the authors conducted FWD testing of ten representative sites to account for the seasonal variations of the back-calculated modulus values of pavement sections. Evidently, due to the temperature dependency of the material properties in asphalt layers, and the stiffness softening of the base and subgrade soils due to moisture ingress in wet seasons, the structural capacity of multi-layer pavement structures is not monolithic throughout the year. Therefore, the responses under taxing loading conditions, and consequently, the damage factors are affected by the time of the year and seasonal variations of the layers material properties. This was the motivation to deploy portable WIM devices and conduct NDT field testing in the summer of 2018 and winter of 2019, to investigate the influence of environmental factors on the damage equivalency factors.

Figure 6.22 provides the axle load equivalency factors for the summer and winter seasons in FM roads for different axle groups in the surveyed network. The results are also contrasted with the traditional industry-standard EALFs values for comparison in Figures 6.22 (a) to 6.22 (d). As evidenced in these figures, the damage factors derived from the numerical simulations with June and July back-calculated material properties were substantially higher than the other counterparts. This is primarily attributed to the viscoelastic nature of the asphalt layer, and softening of the surface layers due to elevated temperatures in summer seasons. The variations in the material properties of the layers in summer and winter seasons essentially translate into various degrees of damages imparted by overweight vehicles. Consequently, the damage factors should also manifest such seasonal sensitivity for accurate assessment of distresses in the highway network. Another noteworthy observation was that the modified EALF values for both summer and winter seasons were substantially higher than the industry-standard damage factors. Such underestimation of the damage factors can potentially incur systematic errors for the design and life-cycle cost analysis of pavement sections.

Similar analyses were conducted on representative State Highway and US Highway sections in this study. Table 6.7 provides a summary of comparisons between the summer-based and winter-based EALF values, categorized based on the axle group and roadway type in this study. The differences between the two field trials, reported in percentages, underscores the significance of the variations in material properties and its contribution to the damage calculations in overload corridors. As indicated in Table 6.7, the difference between the summer-based and winter-based EALFs range from 5 percent to 25 percent. Such deviation is more pronounced for less robust pavement structures such as FM roads. However, the seasonal sensitivity of the damage factors is less significant for well-designed and well-maintained US Highways.
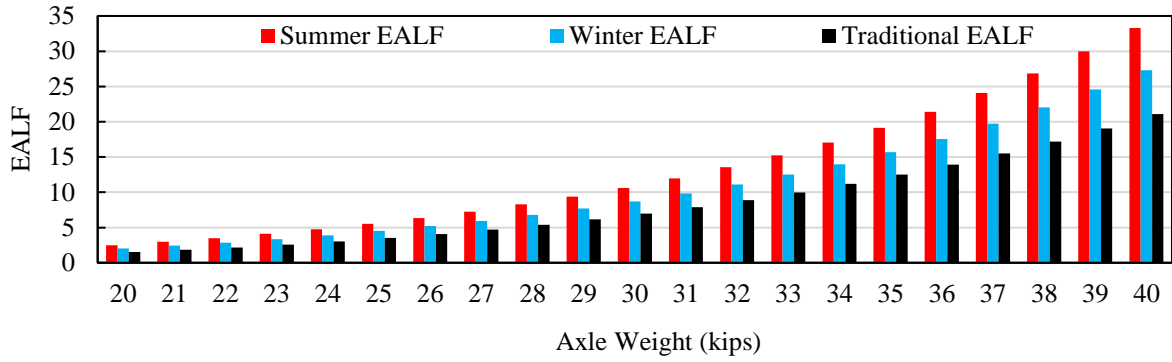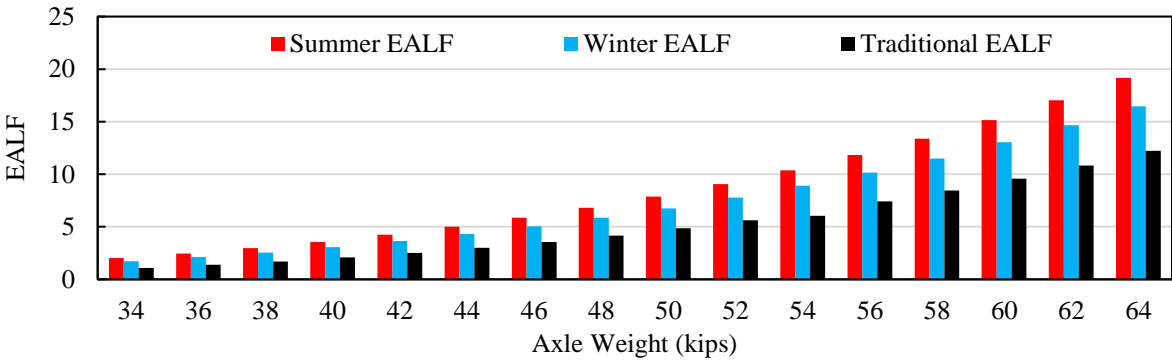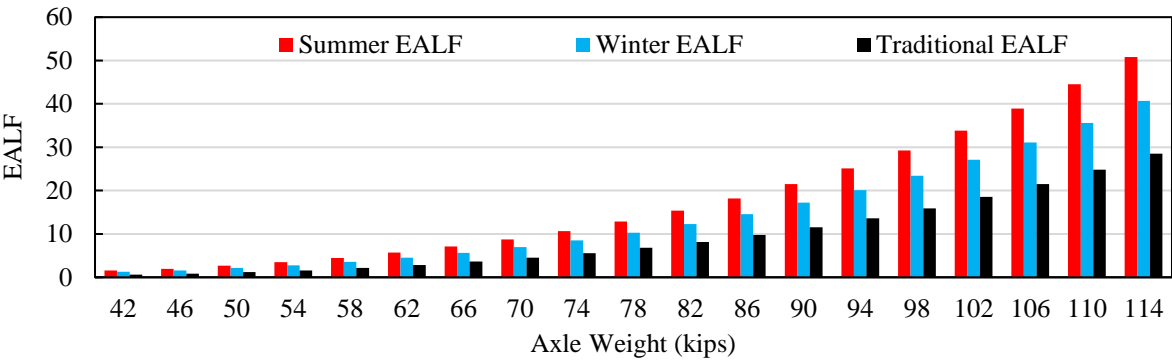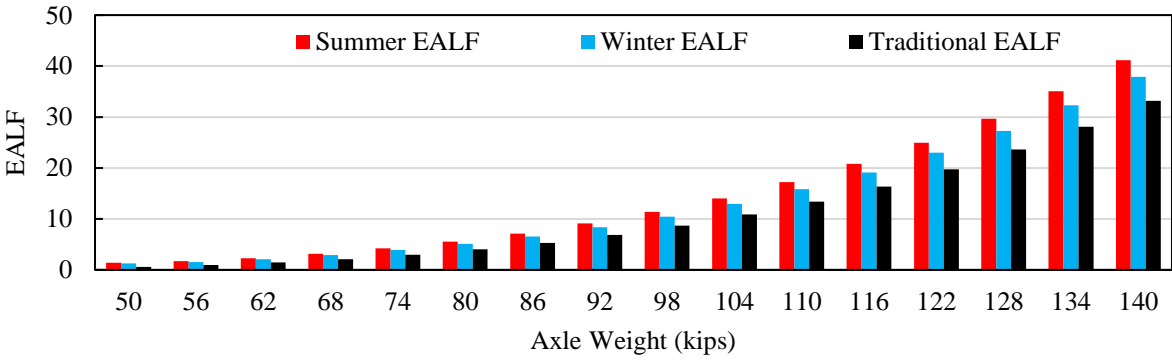
Figure 6.22. Modified EALF Values in FM Roadway for Different Seasons and Different Axle Types: a) Single Axle, b) Dual Axle, c) Tridem axle, and d) Quad Axle.

129

Table 6.7. Percent Differences between Summer and Winter-Based EALFs

Roadway Type	Percent Difference (%) for Various Axle Types			
	Single	Tandem	Tridem	Quad
FM	22	16	25	11
SH	12	8	14	5
US	11	8	13	5

6.11 Summary of the Major Points

The proposed mechanistic approach employs a theoretically sound approach to properly quantify pavement damages associated with the overweight vehicles operating in Texas energy developing zones. The major findings of this chapter are summarized as follows:

➢ The EALF values based on both surface deflection and rutting criteria increased considerably with the increase in the axle weights, and they resulted in the highest damage factors among the three proposed criteria. This behavior was expected, as the load magnitude, rather than the load repetition, is the primary cause for distresses by heavy truck operations in the overload network. Therefore, rutting and surface deflection criteria lead to higher damage factors in comparison with fatigue criteria.

➢ The numerical simulations of ten representative pavement sections in this study confirmed that the modified EALF values, obtained from the mechanistic approach, are significantly higher than the traditional Asphalt Institute values, commonly used by the pavement design engineers. In other words, conventional AI method underestimates the damage factors, since it is not capable of evaluating the EALF values tailored towards the site-specific characteristics.

➢ Proper evaluation of the pavement layer configurations and structural properties are primary components of the damage quantification algorithm, overlooking these parameters can potentially incur systematic errors for the pavement damage analysis. Therefore, it deems necessary to cluster similar highways, in terms of functionality and structural layer profile, to better represent the damages imparted by overload truck operations.

➢ The detrimental effect of traffic loads is higher for pavements with lower structural capacity. This is intuitively valid as heavy axle loads are more destructive to less robust pavement profiles such as FM roads than to US roadways. In the studied sections, FM roadways have the highest EALFs, followed by SH and ultimately US roadways.

➢ The numerical simulations of ten representative pavement sections in this study confirmed that the tridem and quad axles had lower damage factors per tonnage compared to single and tandem axles. This is mainly associated with the distribution of axle loads over multiple wheel arrangements, and therefore lower pressure exerted at the tire-pavement interface.

➢ Considering the fact that environmental factors such as temperature and moisture content significantly affect the pavement stiffness properties and the pavement responses, damage analysis protocol should carefully consider the seasonal climatic effect. In this study, the summer-based EALFs were noticeably higher than the winter-based values. Consequently, more significant pavement damage is anticipated when OW trucks operate at summer under hot and humid climates.

Accordingly, the proposed methodology has established a coherent framework for the determination of the damage equivalency factors for but not limited to the energy development regions in South Texas overload corridors. Since the developed approach is general in nature, it could be adopted in other TxDOT Districts in which the OW truck operations can potentially induce damage in transportation facilities.

7. Remaining Life Analysis

7.1 Introduction

Texas has experienced a boom in the production of energy-related activities such as natural gas and crude oil production since 2008 due to technological advances in the practice of hydraulic fracturing (fracking) of oil and gas-bearing rock formations (Newcomb et al., 2016). Despite the fact that the energy development activities have provided significant economic benefits to the state and the nation, these activities have also created large volumes of traffic operations in impacted zones that have adversely affected the quality of ride of transportation facilities in the overweight zones. A prime example of that is the unprecedented energy production activities in highly active oils fields such as Permian Basin and the Eagle Ford Shale region. The overweight truck operations pertaining to the energy development activities have substantially impacted Southern and South East Districts such as Corpus Christi, Laredo, Yoakum, and San Antonio Districts.

Figure 7.1 illustrates comparisons of projected traffic for ten representative pavement sections in this study. This plot provides comparative cumulative ESALs for pre-energy development in 2008, and the current projected ESALs for ten roadways in the surveyed network.
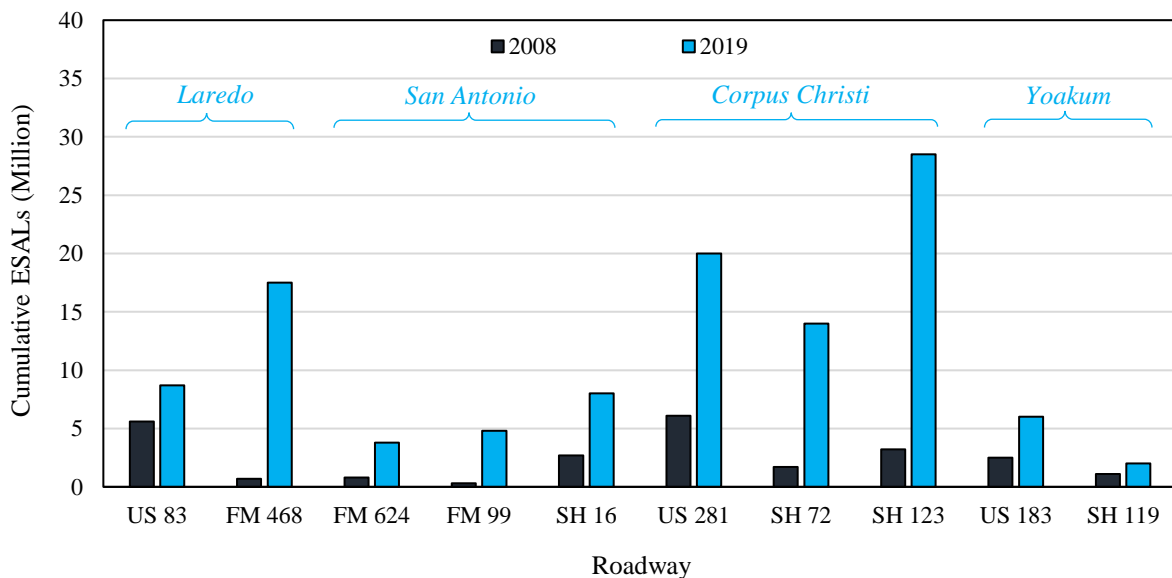
Figure 7.1.Cumulative 18-kip ESAL values (over 20-year design life) for Representative Roadways in the Eagle Ford Shale Region.

Based on the analysis of the deployed portable WIM devices in this project presented in the chapter 4, FM468 roadway in Laredo District, and US281 and SH123 highways in Corpus Christi District have undergone a considerable increase in truck traffic (2400%, 228%, and 790% increase, respectively) in the past decade.

The service life of the highway pavements are affected not only by the traffic volume (ESAL repetitions), but also by axle weights. Based on the post processing of the portable WIM traffic data, on average 32% of the truck traffic in FM468 exceed the Texas permissible axle weight load limits. SH 123 and US281 highways also had alarming overweight percentages of 36% and 45%, respectively.

In addition to damaging highways designed to carry legal loads of up to 80,000 lb. GVW, heavy trucks used by the energy companies are also travelling over Load-Zoned (LZ) roads, which are designed to accommodate vehicles that weight less than 58,420 lb. These roads are not designed to withstand such heavy loads; therefore, even a few passages of Over Weight (OW) trucks will cause permanent damage and consume the life of the pavement.

The loss of serviceability of the pavements is more evident in FM roads in the energy developing areas, since these rural roadways were never designed to carry such high truck traffic volumes and heavy loads. Based on the research team's distress surveys of the network, many of such roadways have suffered severe distresses.
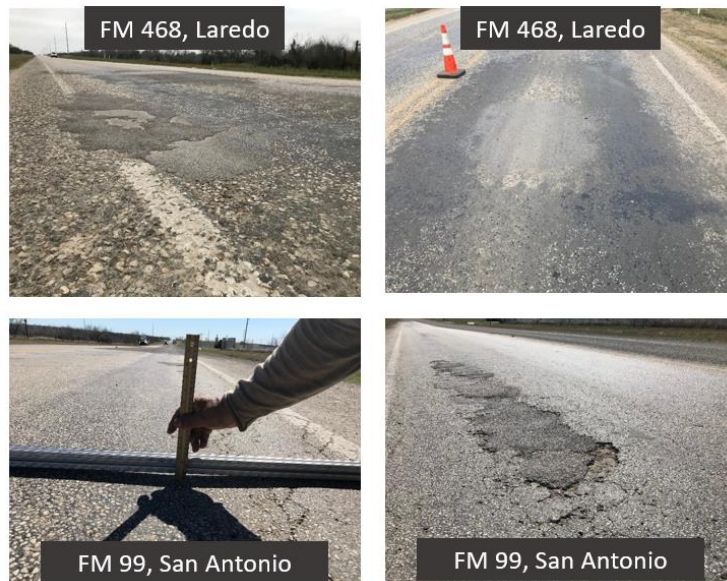
Figure 7.2 Pavement Condition of FM Roadways in the Eagle Ford Shale Region.

For instance, the pavement condition survey of FM468 in Laredo and FM99 in San Antonio Districts indicated that these FM roadways were in a severely distressed state exhibiting deep rutting, severe flushing, pothole formation, and with several patched areas, as shown in Figure 7.2. The maintenance and repair of Farm to Market roadways are a major concern for TxDOT. Routine maintenance costs on these FM roadways have increased from $500 to $1,500 per centerline mile to $35,000 to $45,000 per centerline mile due to the energy development activities (Epps and

Newcomb, 2016). Repair costs for state and local government roadways have been estimated at 2 billion dollars per year. Due to the unprecedented increase in energy production activities, the local government agencies and TxDOT were not able to ramp up their pavement preservation and maintenance efforts to meet the unexpected demand. Lack of funding resources coupled with unclear guidelines are among the many elements that contribute to the delay of the pavement maintenance and repair in several counties.

7.2 Objectives

The primary objective of this chapter is to provide our research team's methodology to mechanistically estimate the loss of service of life of pavements impacted by the heavy truck traffic in the Eagle Ford Shale region. Environmental impacts, pavement layer properties, and new traffic mix relevant to the energy development operations were considered in the analysis. Additionally, forensic studies were implemented to determine the expected new service life of the representative pavement sections.

7.3 Remaining Service Life Analysis Procedure

7.3.1 Expected New Service Life

Based on the field collected traffic data, GPR information, back-calculated modulus values, and a series of numerical simulations, the research team devised a methodology to estimate the remaining life of representative pavement sections. The Tx-ME under project 0-6622 adopted the incremental damage concept for the characterization of the performance of flexible pavement structures, using the axle load spectra. This will allow for the determination of incremental damage imparted by a specific vehicle class at a specific timeframe on a pavement section.

Figure 7.3 shows the analysis procedure followed for prediction of the Remaining Service Life (RSL) of the pavements due to energy development operations in the network. Initially, considering the pavement design plans, the layer properties obtained from the post-processing of the GPR and FWD data (Chapter 5), were incorporated into the TxME pavement design software. Information on the current traffic mix, axle configuration, vehicle class distribution, and the axle load spectra were obtained from the WIM data in the field. Additionally, to consider all the traffic load applications immediately after reconstruction and rehabilitation of the studied roadways, the current traffic mix was converted to an equivalent traffic mix corresponding to the year of roadway construction. To achieve this, the research team extracted historical traffic information and the growth rate values from the TxDOT's Traffic Count Database System (TCDS). Subsequently, the critical pavement responses for multiple axle load magnitudes and axle/tire configurations were calculated in this study. Based on the TxME's internal algorithms for the quantification of

pavement damages, the incremental increase in pavement damages were calculated. Service life of the pavement then equals to the period of time, when the cumulative monthly pavement distresses meet the performance criteria limits (e.g. 0.5 in. of total rut depth).

The results for the pre-energy developing traffic mix, and current traffic mix were in turn plotted for compassion purposes.
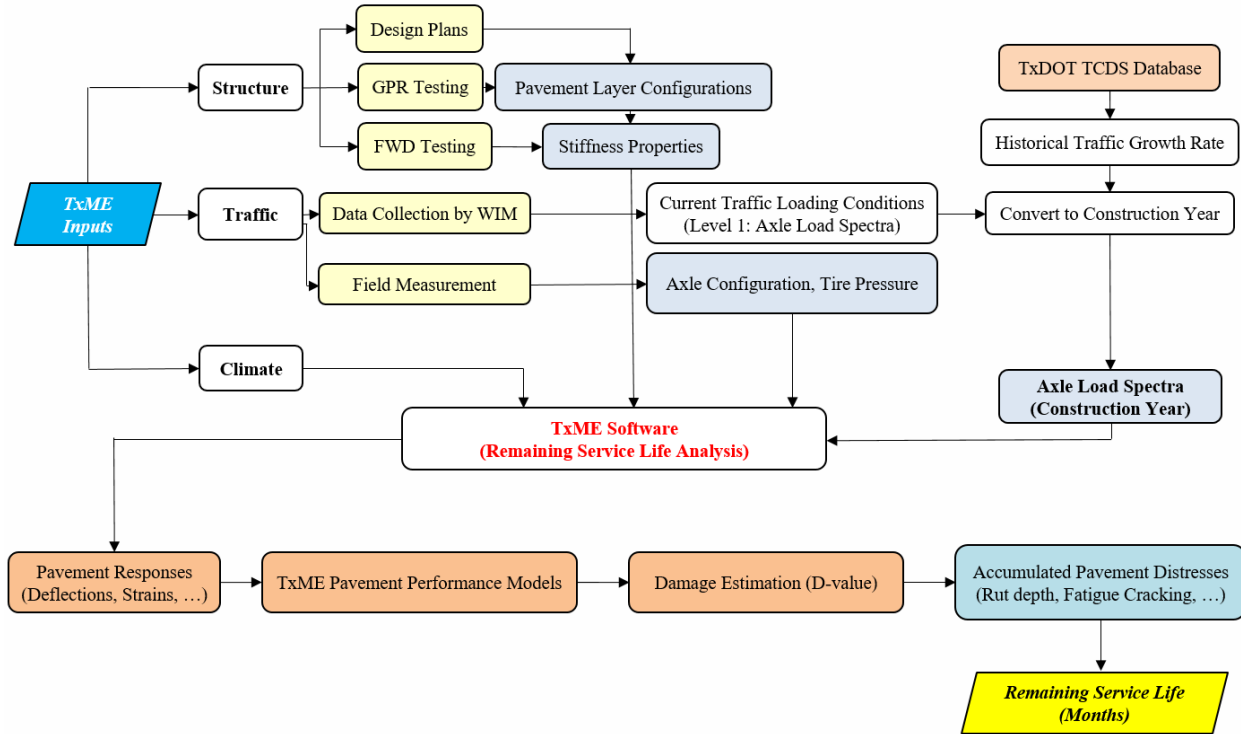
Figure 7.3. Flowchart for the Remaining Service Life Analysis Procedure.

The remaining life analysis results attributed to the heavily trafficked FM468 roadway in Laredo District are provided in Figure 7.4. Based on our communications with TxDOT's engineering personnel in Laredo District, the FM468 roadway was reconstructed in 2015, therefore the onset of the analysis (base year) was assumed from the date of reconstruction of this roadway. Figure 7.4 shows the rutting performance over a 20-year design period for FM468. Assuming that the rut depth limit is 0.5 in., the service life of FM468 based on the post energy development traffic characteristics is merely 53 months after major rehabilitation in 2015. This is in line with our field inspection and rut depth measurements in the vicinity of FM468 as shown in Figure 5. The pictures provided in Figure 7.5 show rut depth measurement under the straight edge within the wheel path exceeds 0.5 in. in the spring of 2019.
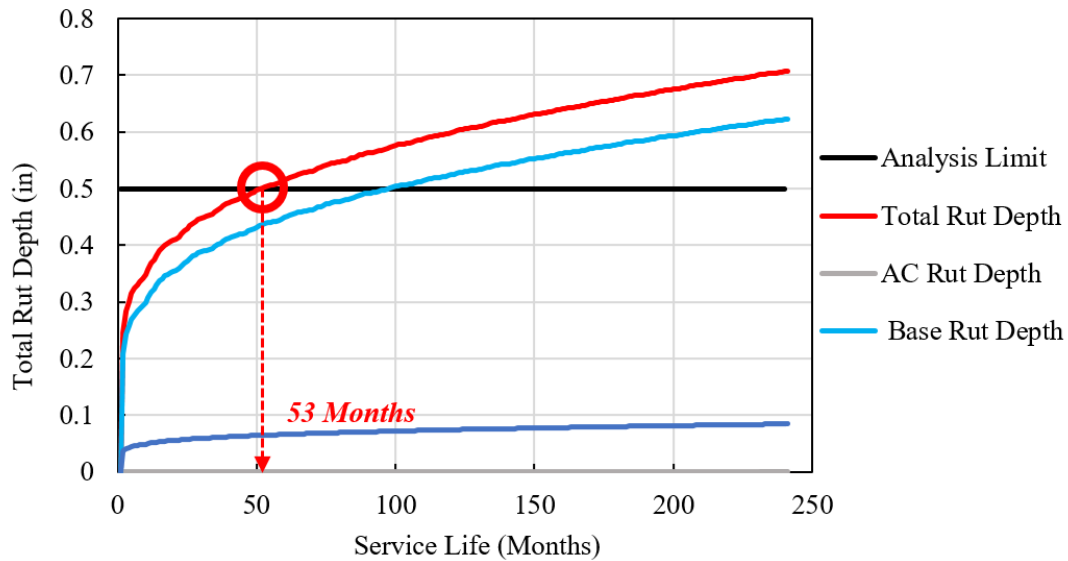
Figure 7.4. Rutting Remaining Service Life of the FM468 Roadway in Laredo.

Figure 7.5. Rutting Measurements in FM 468, Laredo District.

The research team conducted similar analyses for all other roadways evaluated in this study. Figure 7.6 shows the post-processed results obtained from TxME numerical simulations. The remaining life analysis results indicated that the three evaluated FM roadways (i.e. FM468, FM624, and FM99) have reached or surpassed the intended service life. The distresses were primarily associated with cumulative surface rutting due to overweight truck traffic in structurally deficient FM roadways. It was also found that, among State Highways, SH16 in San Antonio District, originally constructed in more than 30 years ago with several maintenance measures, has already surpassed the distress limits. This rationalizes recent reconstruction efforts in 2019 to improve the ride quality of SH16 in San Antonio District.
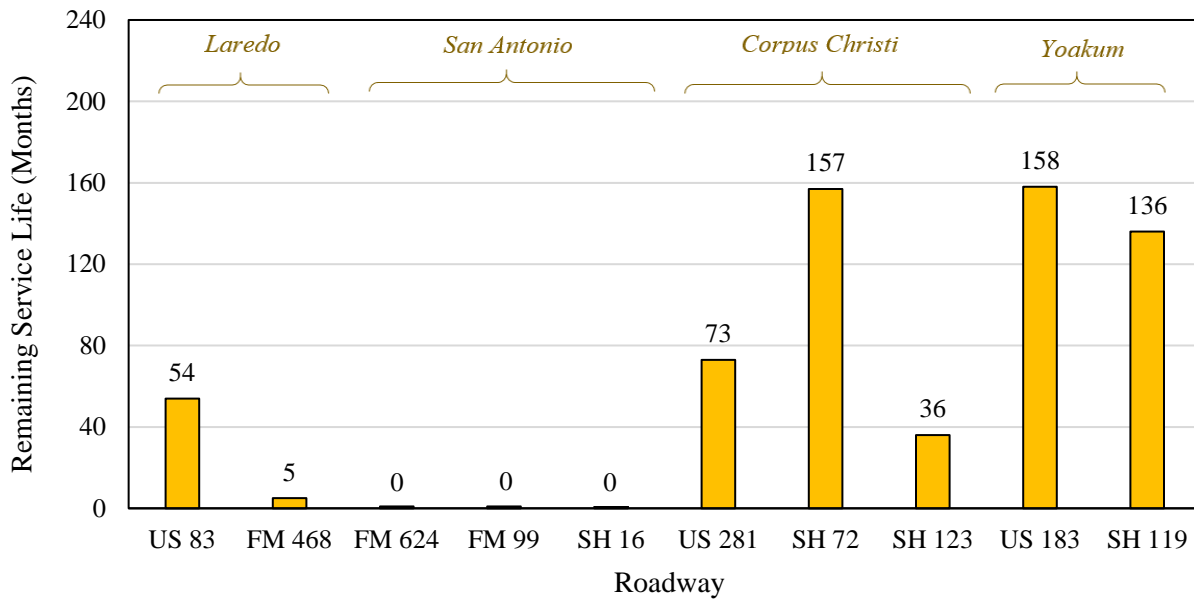
Figure 7.6. Remaining Service Life of the Representative Pavement Sections in the Network.

Based on the remaining life analysis of sections in Corpus Christi in the summer of 2019, State Highway 123 can accommodate another 3 years of current traffic mix with modest historical growth rate before it reaches the distress limits set forth in the TxME pavement design system.

7.3.2 Influence of Traffic Characterization Methodology on Service Life Predictions

Analysis of the remaining service life of the pavements due to changes in the traffic mix, and roadway utilizations provides valuable insight on the degree to which the energy developing activities impacted the quality of ride in overload corridors of East and Southeast Texas. Traditionally, the analysis of service life is primarily based on the Equivalent Single Axle Load (ESAL) concept, in which the traffic mix is converted to 18-kips standard single axle. This assumption can potentially induce systematic error for the calculation of the pavement damages, and distresses during the design life of the pavements. The ESAL concept also overlooks the influence of variations in the material properties throughout the year and with incurring damages during the service life of the pavements. To mitigate this anomaly, the new design guides, such as TxME, incorporate incremental damage concept, in combination with axle load spectra to realistically simulate the progression of the distresses with pavement age. Therefore, the site-specific traffic data, and back-calculate layer properties in different times of the year, are the primary elements for accurate characterization of service life of pavements. Hence, the most representative approach to incorporate the site-specific traffic information into the pavement service analysis, is the concept of the axle load spectra. In this approach, the performance of the pavement is tied to the traffic distributions of different vehicle classes. Currently, TxME pavement

137

design software allows the user to incorporate two levels of traffic data consisted of axle load spectra (Level 1) or ESALs (Level 2).

In order to highlight the influence of the method of traffic characterization for the analysis of the service life of pavements, the research team conducted a series of numerical analysis for comparisons. Initially, the site-specific axle load spectra database from portable WIM deployments, was used to as input in the TxME software. Field derived layers structural properties, and thicknesses were also incorporated in the simulations. A similar process, but with conversions of the traffic mix to traditional ESAL was also performed for comparison purposes.

Figure 7.7 shows the comparative analysis for US281, SH123, and FM468 roadways based on different traffic characterization methodologies. The results are reported as "number of months" remaining to surpass the pre-defined distress limits. For instance, the cumulative surface rutting of 0.5 inches was considered as the rutting limit in this study. As evidenced in this plot, simulations with site-specific axle load spectra resulted in significantly lower predictions of service life when compared to traditional ESAL concept in Level 2 traffic input. This is in line with our expectations, as the damage quantification based on ESAL concept overlooks the load groups, and time-dependency of the traffic distributions. For this reason, incorporation of ESALs into the Remaining Service Life (RSL) analysis can underestimate the imparted pavement damages by OW truck operations, leading to overestimation of the pavement remaining life.

Another method to assign traffic characteristics is by using the TxME default traffic distributions, as commonly used for pavement management purposes in practice. The post processed results illustrated in Figure 7.7 shows that by using the TxME default traffic distributions drastic variations are observed in the predicted service life compared to traditional ESAL concept and site-specific Axle Load Spectra databases. This underscores the significance of using site-specific traffic data rather than using the default software values for decision making purposes.

To further clarify the impact of various traffic inputs on the RSL analysis results, a case study for FM468 roadway is provided in the subsequent section of this chapter. Based on the series of numerical simulations using the TxME pavement design system, the remaining pavement service life was predicted as 48 months when the software default values were incorporated to simulate the traffic distributions in FM468. However, the site-specific axle load spectra resulted in approximately 5 months to reach the distress limit for this pavement section. Based on our field observations and distress monitoring of FM468, several segments of this roadway already exhibited 0.5 in. of rutting as shown in Figure 7.5. Comparisons between the numerical simulations and field distress records showed reasonable agreements between the RSL analysis using site-specific axle load spectra and field observations.
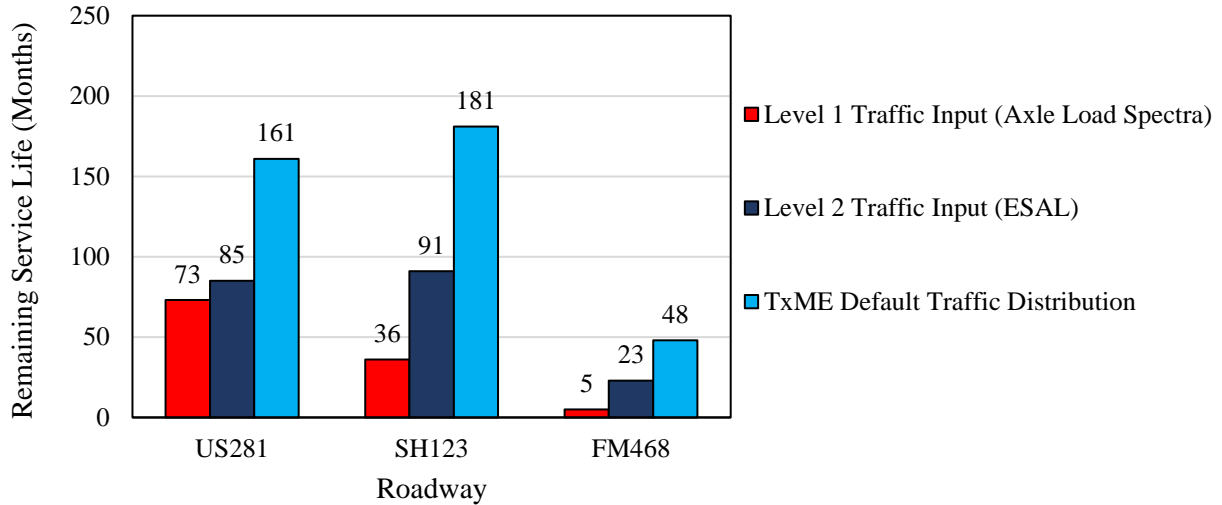
Figure 7.7. Comparative Results for RSL Analysis based on Different Traffic Inputs.

7.3.3 Reduction of the Pavement Service Life due to Energy Development Activities

In order to properly quantify the pavement-life reduction due to increased overweight traffic loads, it's imperative to have an accurate account of current and pre-energy development traffic loading conditions. Hence, our research team incorporated the estimated ESAL values, for both current, and pre-energy development traffic loading conditions, to characterize the traffic in numerical simulations in the TxME for further comparison purposes.

Figure 7.8 shows the proposed procedure for incorporation of the traffic information in this study. Initially, the research team calculated the cumulative 18-kip ESAL values that correspond to the current traffic condition from Equation 1 as:

$$ESAL_{current} = \sum_{i=1}^{m}(EALF)_i n_i \tag{1}$$

where:

$(EALF)_i$ = *Modified EALF Values* (Derived from Task 5),

n_i = *Projected Number of passes of ith-axle load group during the design period* (Derived from Task 3).

Subsequently, research team developed an algorithm to retrace the traffic to the onset of energy developing activities for each roadway. Based on the analysis of traffic growth in the region, the majority of representative pavement sections experienced drastic changes in truck operations between 2008 and 2012. Subsequently, the research team conducted an extensive search within the available databases, such as PMIS, TCDS, and LTPP to extract traffic information attributed

to the pre-energy development traffic conditions. Then, considering the traffic growth rate during the entire period, both ESALs (ESAL$_{Current}$, and ESAL$_{Pre\text{-}Energy\ Development}$) were converted to the equivalent 18-kip axles corresponding to the reconstruction/rehabilitation year, as shown in flowchart in Figure 7.8. Ultimately, the research team incorporated these ESAL values into the TxME and contrasted the corresponding service life results. The difference between these two results represents the service life reduction associated with the changes in traffic patterns for each pavement section in this study. Ultimately, the reduction of the service life based on the distress plots and preset distress limits were determined as schematically shown in Figure 7.9.

Table 7.1 provides summary of the remaining life analysis based on the approach described earlier in this section .This information, as well as the roadway reconstruction year are the key elements for further comparative analysis performed in this study.
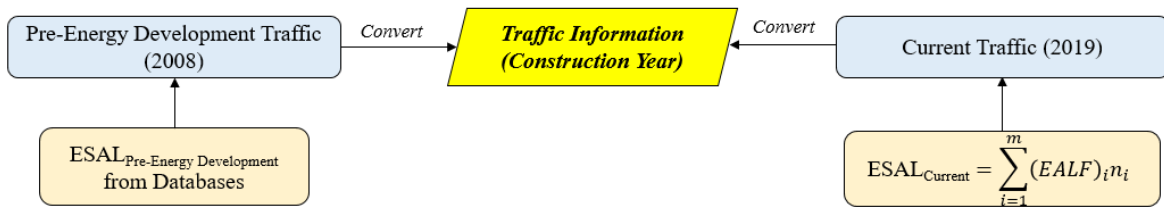
Figure 7.8. Flowchart Describing the Procedure for Backtracking the Current Traffic to Pre-Energy Development Traffic.
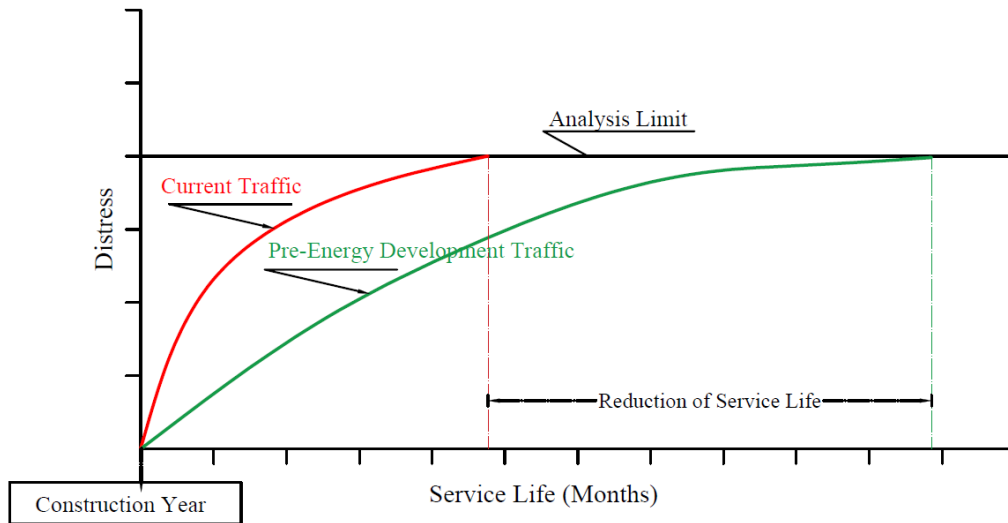
Figure 7.9. Schematic Diagram of the Service Life Reduction Analysis.

Table 7.1. Traffic Information attributed to the Current and Pre-Energy Development Conditions for Ten Representative Sites in the Network

District	Roadway	Traffic (2019)			Pre-Energy Development Traffic (e.g. 2008)		Reconstruction/ Rehabilitation (Year)
		20-Year ESAL (Million)	AADTT	ADT	20-Year ESAL (Million)	ADT	
Laredo	US 83	8.7	1636	6300	5.6	4100	2012
	FM 468	17.5	839	2150	0.7	460	2015
San Antonio	FM 624	3.8	289	875	0.8	530	2009
	FM 99	4.8	267	702	0.3	450	2006
	SH 16	8	1116	5072	2.7	3200	Under Reconstruction
Corpus Christi	US 281	20	1815	7000	6.1	5450	2014
	SH 72	14	1763	5700	1.7	2100	2017
	SH 123	28.5	1976	10400	3.2	5300	2012
Yoakum	US 183	6	1432	8420	2.5	4800	2013
	SH 119	2	659	2530	1.1	920	2013

Figure 7.10 shows an example of remaining life analysis for US281 highway in Corpus Christi District. The plot shows the rutting performance for US281 considering the pre-energy development and current traffic information based on the portable WIM data. Based on the internal distress algorithms in TxME, and pre-energy development traffic characteristics, it takes 254 months for US281 to develop 0.5 in. of surface rutting. However, if the 2019 traffic characteristics, determined by the portable WIM devices in the field were incorporated in the TxME, it takes 158 months to develop 0.5 in. of cumulative rut depth. In other words, changes in the traffic patterns attributed to the energy developing activities have consumed (254-158=96) months of the service life of US281 highway.
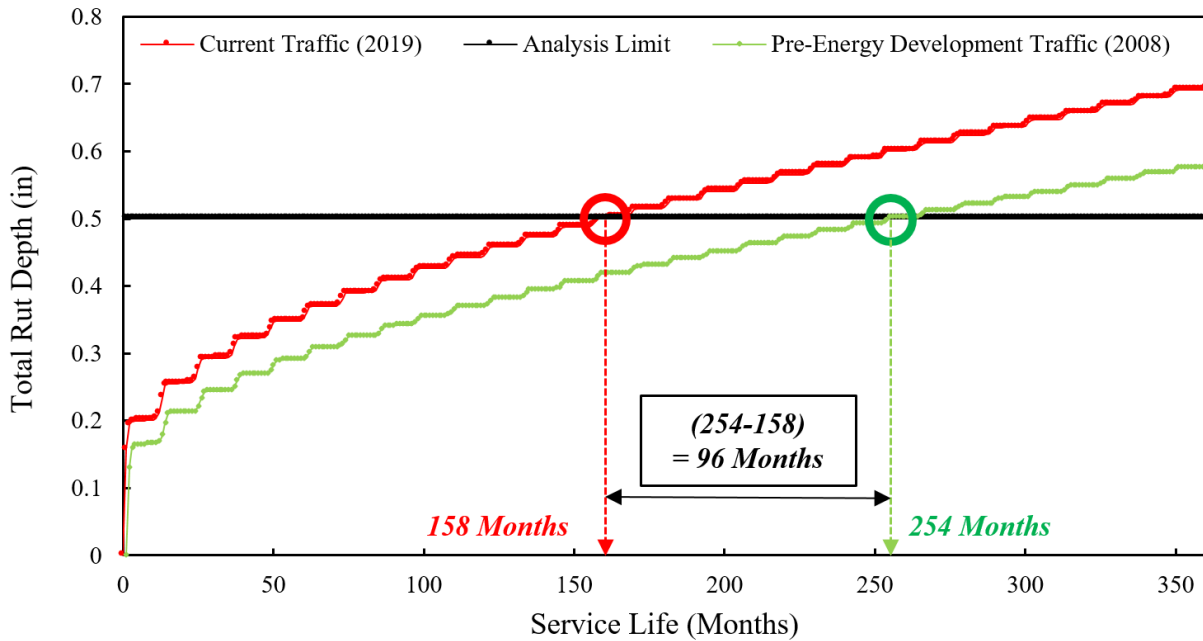
Figure 7.10. Reduction of Pavement Service Life for US281 Highway due Changes in Traffic Patterns.

Similar analysis was conducted for all ten representative roadways in the network. Figure 7.11 illustrates the post-processed results associated with the service life reduction of the studied overload corridors in South Texas Districts affected by the energy developing operations. As evidenced in Figure 7.11, pavement sections located in Corpus Christi and Laredo Districts, were greatly impacted by the change in traffic patterns since 2008. Specifically, FM468 roadway in Laredo District, followed by SH123 and ultimately US281 highways in Corpus Christi District have been subjected to the greatest pavement life reduction as 143, 114, and 96 months, respectively, due to the applications of unaccounted for vehicles active in the energy development operations. This is in line with our field visual observations and distress records of the sections. In addition to the influence of axle load magnitudes and traffic frequencies, pavement structural capacity was another major contributing factor in the pavement life consumption analysis in this study. FM roadways with less robust pavement profile were found to be more sensitive to the increasing traffic patterns, compared to SH and US highways.

Ultimately, Table 7.2 summarizes the post-processed results associated with the pavement-life analysis of the ten representative sites. This information can be instrumental for TxDOT engineers to adopt proper rehabilitation strategies to meet the future growth of traffic in affected corridors.
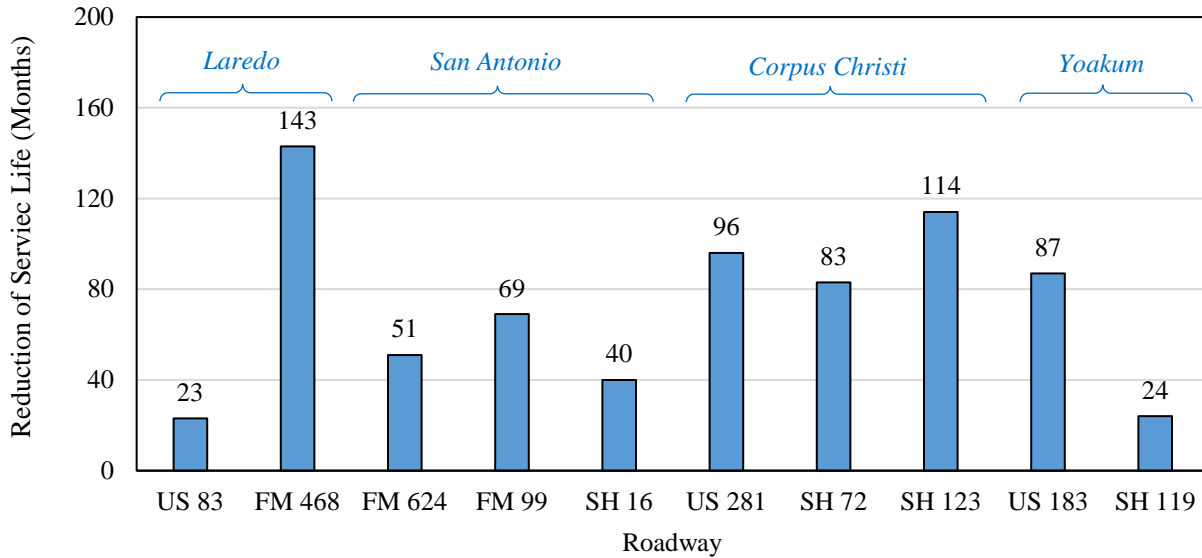
Figure 7.11. Service Life Reduction of Ten Studied Overload Corridors due to Energy Developing Activities in the Network.

Table 7.2. Service Life Analysis Results for the Representative Pavement Sections in the Eagle Ford Shale Network

District	County	Roadway	Remaining Service Life (Months)	Reduction of Service Life (Months)
Laredo	Dimmit	US 83	*54*	*23*
Laredo	La Salle	FM 468	*5*	*143*
San Antonio	McMullen	FM 624	*failed*	*51*
San Antonio	McMullen	FM 99	*failed*	*69*
San Antonio	Atascosa	SH 16	*failed*	*40*
Corpus Christi	Live Oak	US 281	*73*	*96*
Corpus Christi	Karnes	SH 72	*157*	*83*
Corpus Christi	Karnes	SH 123	*36*	*114*
Yoakum	Gonzales	US 183	*158*	*87*
Yoakum	Dewitt	SH 119	*136*	*24*

7.4 Summary of the Major Points

This chapter provided the framework for mechanistic characterization of the service life of the pavements affected by OW truck traffic in the Eagle Ford Shale network.

The major findings of this analysis are provided in the following:

- The numerical simulations using TxME for ten representative pavement sections in this study indicated that the three evaluated FM roadways (FM468, FM624, and FM99) have reached or exceeded the pre-defined distress limits in the TxME pavement design system. This was in line with our field visual observations and distress records of these pavement sections.
- Studied pavement section of State Highway 16 in San Antonio, originally constructed more than 30 years ago with several rehabilitations since then has already reached the intended service life. For this reason, the reconstruction of SH 16 is currently in process.
- The primary source of distresses in the evaluated pavement sections in this study was associated with cumulative surface rutting due to overweight truck traffic. This in line with our expectations, as the primary culprit for premature failure of the overload corridors pertains to the passage of overweight trucks in the network.
- A comparative analysis of various traffic characterization methodologies, i.e. axle load spectra and traditional ESAL concept, underscored the significance of using axle load spectra database in lieu of traditional conversion of traffic mix to standard axle for the prediction of the service life of pavements. The post-processed results showed that incorporating the site-specific axle load spectra in the remaining service life analysis protocols has the potential to realistically simulate the incremental progression of the distresses imparted during the service life of the pavements. Furthermore, the results of RSL analysis based on the field-derived axle load spectra were in good agreement with the field distress measurements of the representative pavement sections.
- Incorporation of ESALs, instead of axle load spectra, in RSL analysis, vastly overestimated the remaining service life of the pavements. This is primarily attributed to the fact that the damage quantification based on ESAL concept overlooks the load groups, and time-dependency of the traffic distributions, leading to underestimation of the imparted pavement damages by OW truck operations.
- Based on the analysis of service life provided earlier in this chapter, the changes in the traffic demands in the past decade adversely impacted the ride quality of pavement sections located in Corpus Christi and Laredo Districts.

8. Developed Web-Based Tool for Highway Network Assessment

8.1 Introduction

This chapter pertain to details regarding the development of an online module for the visualization of the modified axle load equivalency factors and the remaining life analysis of the studied sections. In addition to the comprehensive documentation of the surveyed data, traffic analysis, damage quantification procedure, and remaining service life analysis protocol, a web-based tool was developed to facilitate the users' access to the main findings of this research project. This chapter provides a brief description of the developed web-based tool and demonstrates how it allows TxDOT engineers to take advantage of the site-specific information in the ten representative sites in the overload corridors of the Eagle Ford Shale region. The information reported provides a perspective on the traffic distribution patterns of the overload truck operations as well as their impacts on the pavement systems in the network.

8.2 Developed Web-Based Tool for Highway Network Assessment

The research team developed an easy-to-use web-based tool that provides a visual representation of the truck traffic characteristics attributed to the selected overload corridors affected by oil/gas development in the Eagle Ford Shale Region. This visualization tool provides TxDOT engineers with different measures to quantify the impact OW vehicles have on the selected highways and their remaining service life due to current traffic loading conditions. The developed online module makes use of a database that comprises of site-specific traffic information and pavement damage equivalency factors associated with the summer and winter seasons. This information was the key element to assess the reduction of the pavement service life due to OW truck operations in the network. The web-based module allows users to export the site-specific axle load spectra information that can be easily imported into the TxME pavement design software. The online tool is accessible through any web browser using the following link:

http://ctis.utep.edu/TXDOT-06965/.

The developed module makes use of Google application programming interfaces (APIs) that allow communication and integration with Google Maps, offering a visual representation of the evaluated highway corridors located in the Eagle Ford Shale Region, as shown in Figure 8.1. Users can select a specific roadway for further data extraction, either by clicking on the corresponding GPS location pinned in Google Maps or by making a selection from the drop-down menus designed in the search criteria. Site-specific information, for each District, county, roadway, axle type, and vehicle class corresponding to two different seasons (i.e., summer and winter) can be

reported by the module. The information provided by the web-based tool is envisioned using three different tabs located in the Navigation menu as follows:

- Axle Load Distribution,
- Damage Factors,
- Reduction of Service Life.
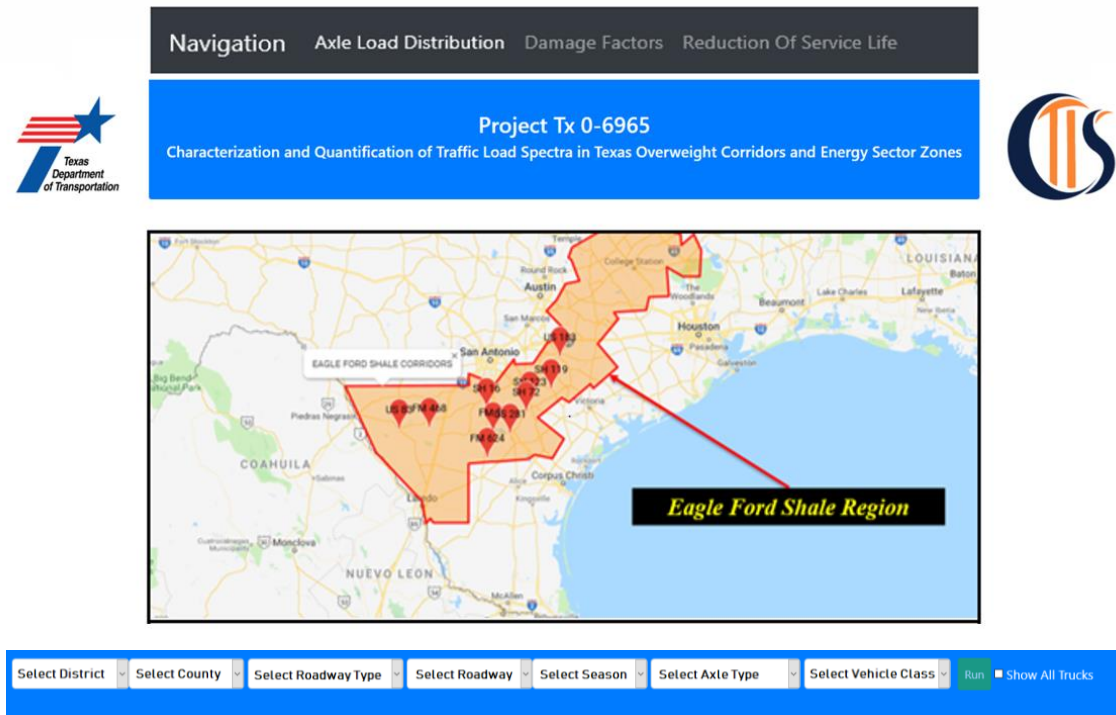
Figure 8.1. Developed Web-Based Tool.

Subsequent sections in this report demonstrate the main features of the developed web-based module and how they can be used as an effective and powerful tool for proper evaluation of the OW truck operations in the overload corridors in the network. A discussion on the efficient use of this web based module to extract site-specific information is also provided in the following sections of this chapter.

8.2.1 Axle Load Distribution

The axle load distribution of different vehicle classes is one of the key input information in the TxME pavement design software. This software allows users to incorporate the Level 1 traffic data, which is based on the concept of the axle load spectra. The Axle Load Distribution tab of the online module displays the information associated with the axle load distribution and the traffic

volume count acquired as part of the activities conducted in Task 3 of this project. The traffic-based information, after post-processing the WIM data, is provided graphically as follows:

➢ **Axle Load Distribution:** A sample of axle load distribution plot is shown in Figure 8.2. The provided data corresponds to one specific vehicle class passing through a particular roadway.
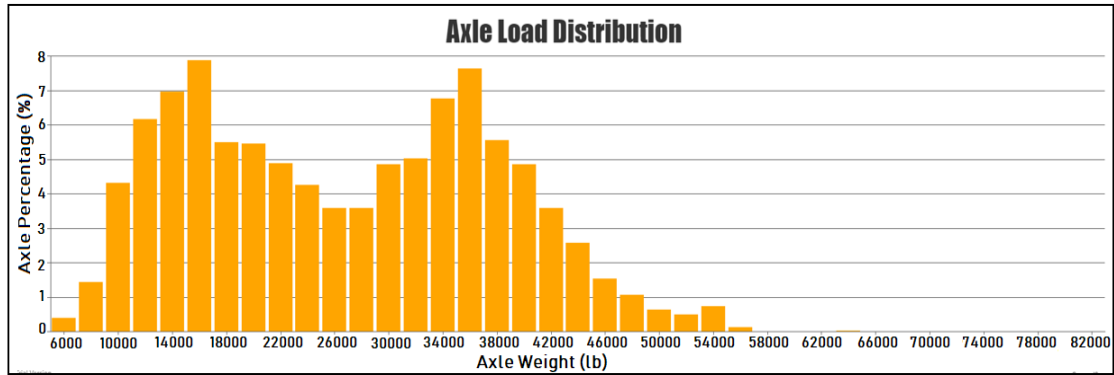
Figure 8.2. Axle Load Distribution Plot for one Specific Vehicle Class.

Additionally, generating a scatter plot, the module shows a graphical representation of the axle load distribution for all vehicle classes, as shown in Figure 8.3. To enable this feature, the "*Show All Trucks*" checkbox should be enabled.
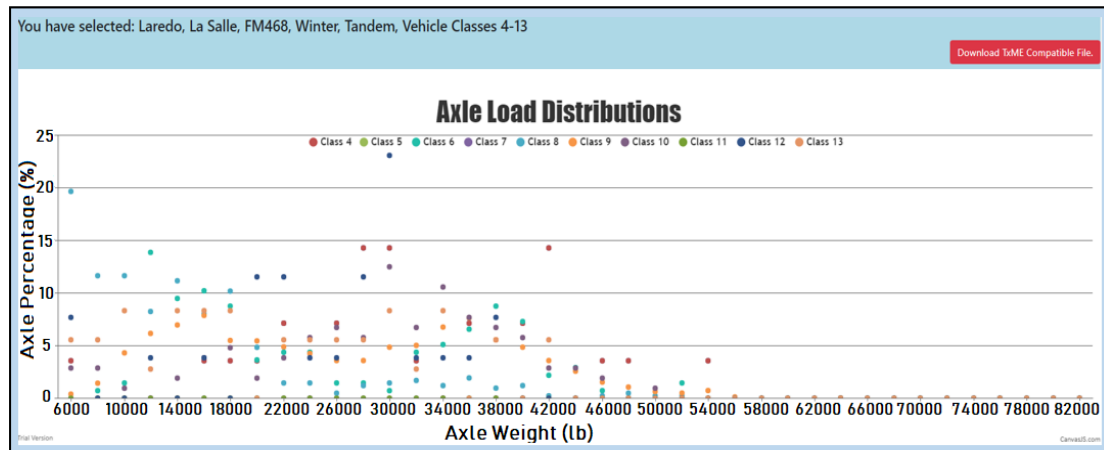
Figure 8.3. Scatter Plot of Axle Load Distributions for All Trucks.

➢ **TxME Compatible File:** One of the significant features of the developed online module is that the tool allows users to select a specific road section for generating ME-compatible traffic loading data. By clicking on the "*Download TxME Compatible File*" link (Figure 8.3), the module exports the axle load spectra information to an *ald* extension file, which is compatible with ME design software such as TxME, and AASHTOWare.

147

- ➢ **General Traffic Information**: General traffic information including two-way annual average daily truck traffic (AADTT), average daily traffic (ADT), percent trucks, and percent OW trucks are provided by the module to better describe the current truck traffic in the region. This information can be further incorporated into the pavement design analysis system.
- ➢ **Vehicle Class Distribution**: Another significant feature provided by the online module is vehicle class distribution. Figure 8.4 illustrates an example of the vehicle class distribution plot provided by the online module.
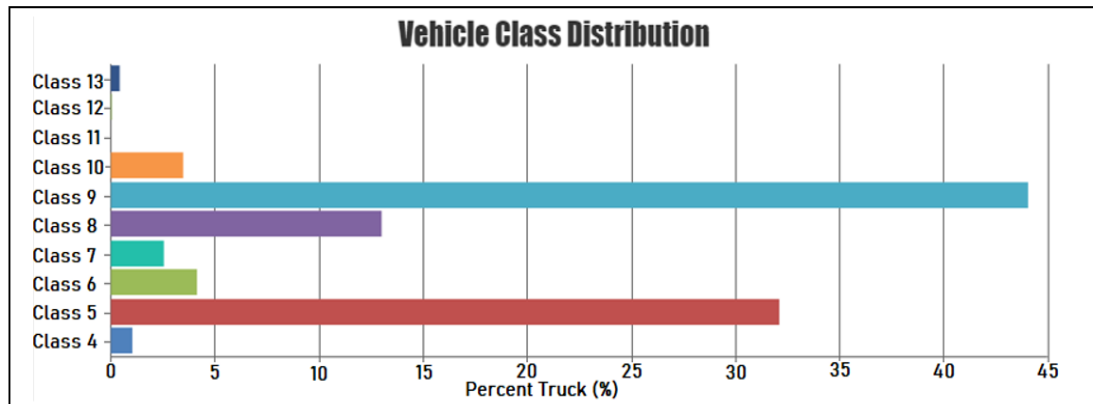
Figure 8.4. Vehicle Class Distribution Plot.

8.2.2 Damage Factors

Pavement damage equivalency factors are the integral components in pavement damage quantification, since they can effectively assess the equivalent damage imparted on pavement section by each individual OW axle load per pass to that of a standard 18-kip single axle. Hence, accurate calculation of these factors is of highest importance for proper determination of the serviceability loss due to energy development operations. The Damage Factors tab within the online module provides information associated with the pavement damage factors developed as part of the activities carried under Task 5. Modified Equivalent Axle Load Factors (EALFs) tailored towards the specific roadway, and specific axle load and axle configuration of vehicles operating in the network are provided in this tab.

Additionally, considering the environmental factors affecting the structural pavement properties, the module presents the damage equivalency factors for the summer and winter-based pavement layer moduli. As shown in Figure 8.5, the site-specific modified EALF values are also compared with the Asphalt Institute's values that are commonly used by pavement design engineers.
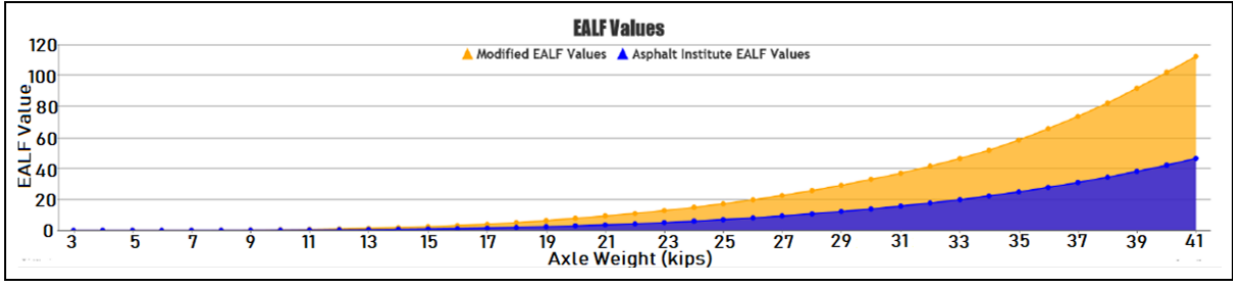
Figure 8.5. Equivalent Axle Load Factor (EALF) Plot.

8.2.3 Reduction of Service Life

Under the third tab "*Reduction of Service Life*" of the web-based tool, the reduction of the pavement service life due to the drastic change in overload truck operations in the network is provided. This feature considers the predicted service life associated with the current and pre-energy development traffic loading conditions, as described in Chapter 7.

Service Life of US281, Corpus Christi
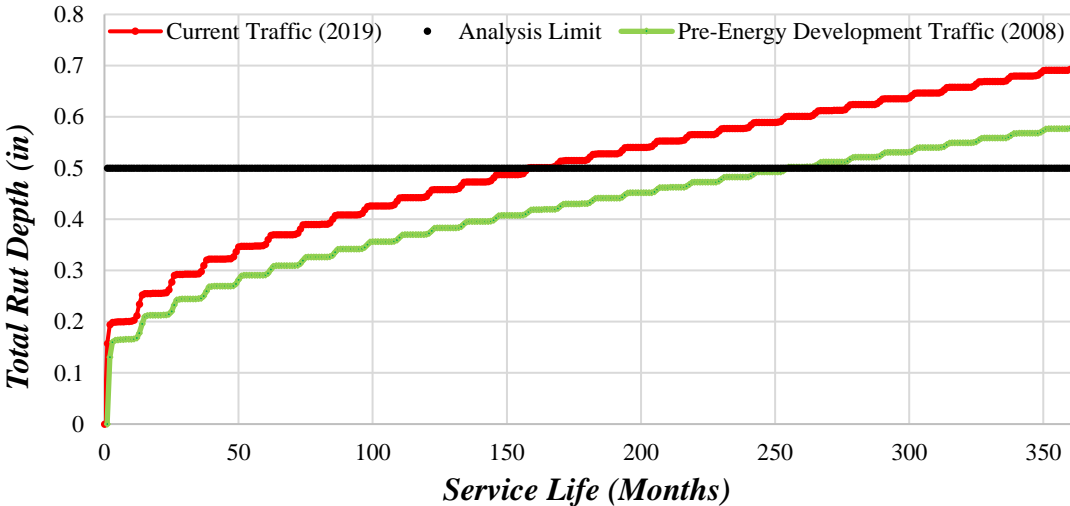
Service Life associated with the Pre-Energy Development Traffic	254 (Months)
Service Life associated with the Energy Developing Traffic	158 (Months)
Reduction of Service Life due to Energy Development Activities: 96 (Months)	

Figure 8.6. Reduction of Service Life of the US 281 Roadway.

By selecting a specific roadway from the drop-down menus designed in the search query, the module generates a PDF file that provides users the analysis results in a concise manner. Figure

8.6 shows an example of the output of the web-based module representing the service life reduction of US 281 roadway in Corpus Christi District.

8.3 Summary of the Major Points

The research team developed a web-based tool to better visualization of the major findings of this research effort. As indicated in Table 8.1, the online tool provides site-specific information considering the unique features of the ten selected sites in the overload corridors of the Eagle Ford Shale region. This information is connected with the main products developed as part of the activities performed under the listed tasks and reported in their corresponding chapters.

Table 8.1. Site Specific Information Available in the Developed Web-Based Tool

Designed Tab	Available Information	Comments
Axle Load Distribution	Axle Load Distribution for one Specific Vehicle Class	Main Products of Task 3 (Chapter 4)
	Axle Load Distributions for All Trucks	
	General Traffic Information: Two-Way AADTT, ADT, Percent Trucks, Percent OW Trucks	
	Vehicle Class Distribution	
	Seasonal Variation in Traffic Pattern	
	TxME/AASHTOWare Compatible File	
Damage Factors	Modified EALF values	Main Products of Task 5 (Chapter 6)
	Seasonal Variation in EALF values	
	Asphalt Institute EALF values	
Reduction of Service Life	Predicted Service Life (Considering the Pre-Energy Development Traffic)	Main Products of Task 6 (Chapter 7)
	Predicted Service Life (Considering the Energy Developing Traffic)	
	Reduction of Service Life	

9. Conclusions

This technical report summarizes two years of efforts to develop axle load spectra database of ten representative sites in the overload corridors of East and Southeast Texas, develop new methodology to calculate site-specific damage equivalency factors, perform remaining life analysis of the representative pavement sections, and to develop a web-based module for the visualization of the results of the project. The research team deployed portable WIM devices in the field, and developed a comprehensive calibration system with internal algorithms to monitor the survivability of the piezo-electric sensors for reliable traffic characterization in the field. Two sets of data were collected in the summer and winter times to analyze the seasonal variation of the overweight truck traffic in this study. Along with the traffic characterization efforts, the research team performed a series of non-destructive tests such as GPR and FWD to better understand the structural capacity of ten representative sites. The traffic distribution parameters and structural properties were in turn incorporated in a series of numerical simulations for the determination of the pavement responses subjected to taxing traffic conditions. Subsequently, the research team developed a novel approach for the calculation of the site-specific equivalent axle load factors in this study. The site specific damage factors for each load group were calculated using summer and winter seasons material properties to quantify the influence of seasonal variation of material properties on the damage accumulation in the overload corridors.

In another effort, the research team developed a novel framework for the determination of the remaining life of the pavement sections in this study. To achieve this objective, the research team developed an algorithm to backtrack the current traffic information to pre-energy developing era to quantify the energy developing impacts on highway facilities. Ultimately, the research team developed an online module with refined graphical user interface for the visualization of the traffic distributions, modified damage factors, comparison plots of modified EALFs with industry-standard axle load factors, and the results for the remaining life analysis of pavement sections. The online module also incorporated provisions for directly exporting the axle load spectra database for further analysis and post processing by Districts.

KEY FINDINGS

A summary of major findings of the project is provided in the following.

- Prior to the development of field experimental plans, the research team conducted an online survey among the Districts located in the overload corridors of East and Southeast Texas. 94% of the respondents indicated that their transportation infrastructure had been adversely affected by overweight vehicles due to energy development activities.

- Based on the analysis of the questionnaire regarding the types of pavement distresses,

TxDOT personnel 82.4% were attributed to rutting, 82.4% to potholes, and 76.5% to fatigue cracking in the overload zones.

- Based on the post processing of the portable WIM traffic data, on average 64% of the truck traffic in FM roads exceed the Texas permissible axle weight load limits. The State Highways and US Highways in this study also had alarming overweight percentages of 36% and 45%, respectively.

- Pavement sections in Corpus Christi and Laredo Districts were ranked highest in terms of percentages of overweight trucks in the network.

- Energy development activities in the Eagle Ford Shale adversely impacted FM roads more than the SH and US highways. This is in line with our visual field observations and forensic distress identification reports of FM roads in the energy developing areas.

- The research team developed a novel approach for the estimation of the site-specific damage factors with considerations of environmental factors on the material properties of layers, and the type of the pavement facility in this study. The developed mechanistic approach confirmed that the modified EALF values were substantially higher than traditional industry-standard axle load factors currently employed by the pavement design industry. This can result in underestimation of the potential damages imparted by overweight vehicle in overload zones.

- The EALF values based on surface deflection and rutting criteria were highly sensitive to the increasing axle load magnitude in numerical simulations. This behavior was anticipated, as the distresses associated with heavy truck operations are essentially attributed to the load magnitude rather than the load repetitions. Therefore, rutting and surface deflection criteria led to higher damage factors in comparison with fatigue criterion.

- Post-processing the FWD data for summer and winter seasons showed that the back-calculated layers modulus values in summer were significantly lower compared to winter time modulus values. This is primarily attributed to the viscoelastic behavior of the asphalt layer, and the stiffness softening of the granular base and subgrade layers due to moisture ingress in multi-layer pavement structure in wet seasons.

- Overlooking the influence of the type of roadway facility in damage quantification can potentially incur systematic errors for accurate assessment of the service life of the pavements in overload corridors. Therefore, it deems necessary to cluster similar highways, in terms of functionality and structural layer profile, to realistically represent the damages imparted by OW truck operations.

- The detrimental effect of OW loads was higher for pavements with lower structural capacity. This is in line with expectations due to the fact that heavy axle loads are more destructive to less robust pavement profiles such as FM roads than to US roadways. Based on the analysis provided in this research, FM roadways had the highest EALFs, followed by SH, and ultimately US highways.

- Accurate assessment of the damage factors should include seasonal variation of the material properties of pavement layers. This is primarily attributed to the viscoelastic behavior of the asphalt layers and the variations of stiffness properties of granular layers due freeze-thaw effects or changes in the saturation state of the unbound granular layers due moisture infiltration or evapotranspiration during the service life of pavements. Therefore, incremental assessment of the damages, rather than single value average damage factor, better represent the detrimental influence of overload vehicles in highway networks.

- Remaining service life analysis of the three studied FM roadways indicated that despite several remedial measures since 2008, almost all sections are approaching the predefined distress limits that defines the service life of the pavement sections. This is primarily attributed to the fact that these roadways with extremely thin surface treated layers were not designed to withstand current traffic loading conditions with large volumes of heavy truck traffic operations.

- Accurate account of traffic characteristics is the precursor for reliable assessment of damages imparted on pavements in overload corridors. Site-specific axle load spectra data, provides the primary Mechanistic-Empirical (ME) traffic data input for accurate and optimal pavement design and analysis. Incorporating the site-specific axle load spectra in the TxME rather than using agency default database in numerical simulations leading to remaining life analysis drastically improved the agreement between the simulations and field distress measurements.

10. References

Al-Qadi, I., Wang, H., Ouyang, Y., Grimmelsman, K., & Purdy, J. E. (2016). LTBP Program's Literature Review on Weigh-in-Motion System (No. FHWA-HRT-16-024). United States. Federal Highway Administration.

American Association of State Highway and Transportation Officials (AASHTO). (2008). Mechanistic-Empirical Pavement Design Guide, Interim Edition: A Manual of Practice. Washington, DC. Pavement Design Guide, Interim Edition: A Manual of Practice. Washington, DC.

Bahia, H. U. (2000). Layer coefficients for new and reprocessed asphaltic mixes. Wisconsin Department of Transportation, Division of Transportation Infrastructure Development, Bureau of Highway Construction, Technology Advancement Unit.

Bierling, D., Martin, M., See, A., Morgan, C., Bujanda, A., and Kelly, N. (2014). Energy Development Impacts on State Roadways: A Review of DOT Policies, Programs and Practices across Eight States Final Report. Transportation Policy Research Center.

Blincoe, L. J., Miller, T. R., Zaloshnja, E., and Lawrence, B. A. (2015). The economic and societal impact of motor vehicle crashes, 2010. Report No. DOT HS 812 013, National Highway Traffic Safety Administration, Washington, D.C.

Boulos Filho, P., Raymundo, H., Machado, S. T., Leite, A. R. C. A. P., & Sacomano, J. B. (2016). Configurations of tire pressure on the pavement for commercial vehicles: calculation of the 'n' number and the consequences on pavement performance. Independent Journal of Management & Production, 7(5), 584-605.

Buchanan, M. S. (2004). "Traffic load spectra development for the 2002 AASHTO Design Guide," Report No. FHWA/MS-DOT-RD-04-165, Mississippi State University, Jackson, MS.

Burnos, P., & Rys, D. (2017). The effect of flexible pavement mechanics on the accuracy of Axle load sensors in vehicle weigh-in-motion systems. Sensors, 17(9), 2053.

Cardinal Scales. (n.d.). Truck Scales. Retrieved November 14, 2017, from https://cardinalscale.com/product/product-category/Truck-Scales

Chandra, D., K. M. Chua, and R. L. Lytton (1989). "Effects of Temperature and Moisture on the Load Response of Granular Base Material in Thin Pavements." Transportation Research Record 1252, National Research Council, Washington, D.C., pp 33-41.

Chang, D. W., Kang, Y. V., Roesset, J. M., & Stokoe, K. (1992). Effect of depth to bedrock on deflection basins obtained with Dynaflect and falling weight deflectometer tests. Transportation Research Record, 8-8.

Charles Gurganus (2016). Project and Pavement Performance Associated with Energy Development and Production. Research Report RR-16-02. Texas A&M Transportation Institute. Texas Department of Transportation.

Chen, D. H., & Scullion, T. (2006). Using nondestructive testing technologies to assist in selecting the optimal pavement rehabilitation strategy. Journal of testing and evaluation, 35(2), 211-219.

Chen, F. H. (1988). Foundations on Expansive Soils. Elsevier, Amsterdam, the Netherlands.

Christison, J. T. (1986). Pavement response to heavy vehicles test program part 1-Load Equivalency factors. Transportation Research Record, 79-88.

Correspondence with TxDOT personnel (2018).

Correspondence with TxDOT personnel (2019).

David E. Newcomb, Fujie Zhou, and Jon A. Epps. (2016). Pavement Design Catalogue Development for Pavements in Energy Affected Areas of Texas. IR-15-01. Texas A&M Transportation Institute. Texas Department of Transportation.

Documentation, A. B. A. Q. U. S., & Manual, U. Version 6.14, Simulia, Dassault Systèmes. (2015). Google Scholar.

Epps, J. A., and Newcomb, D. E. (2016). Maintenance and Rehabilitation Strategies For Repair of Road Damage Associated with Energy Development and Production. Implementation Report IR-15-03. Retrieved October 20, 2017.

Epps, J. A., Newcomb, D., Ellis, D. and Stockton, B., "Impacts of Reduced Pavement Rehabilitation and Maintenance on Energy Development in Texas", Research Project 0-6581 Work Request No. 27, March 2013.

Ewing, B. T., Watson, M. C., McIntruff, T., and McIntruff, R. N. (2014). Economic Impact Permian Basin's Oil and Gas Industry, Texas Tech University College of Petroleum Engineering, Rawls College of Business, 1-80.

Faruk, A. N., Liu, W., Lee, S. I., Naik, B., Chen, D. H., & Walubita, L. F. (2016). Traffic volume and load data measurement using a portable weigh in motion system: A case study. International Journal of Pavement Research and Technology, 9(3), 202-213.

Federal Highway Administration (2014), "Traffic Monitoring Guide," Federal Highway Administration, Office of Highway Policy Information, U.S. Department of Transportation. https://www.fhwa.dot.gov/policyinformation/tmguide/tmg_2013/vehicle-types.cfm.

Federal Highway Administration, U. (2016). Traffic Volume Monitoring. Traffic Monitoring Guide.

Gordon, R. L., Reiss, R. A., Haenel, H., Case, E. R., French, R. L., Mohaddes, A., & Wolcott, R. (1996). TRAFFIC CONTROL SYSTEMS HANDBOOK-REVISED EDITION 1996(No. FHWA-SA-95-032).

Greene, J., Toros, U., Kim, S., Byron, T., & Choubane, B. (2010). Impact of wide-base single tires on pavement damage. Transportation Research Record, 2155(1), 82-90.

Haider, S. W., and Harichandran, R. S. (2007). "Relating Axle Load Spectra to Truck Gross Vehicle Weights and Volumes." Journal of Transportation Engineering, 133(12), 696-705.

Highway Research Board (1962), "The AASHO Road Test, Report 5, Pavement Research," Special Report 61E, Highway Research Board, National Academy of Sciences, Washington, D.C.

Hopman, R. C. (n.d.). Energy Sector, Powerpoint Presentation. TxDOT.

Hu, S., Zhou, F. and Scullion, T. (2011). Texas M-E Flexible Pavement Design System: Literature and Proposed Framework, Report No. FHWA/TX-12/0-6622-1, Texas Transportation Institute, College Station, TX.

Hu, S., Zhou, F., & Scullion, T. (2014). Development of Texas mechanistic-empirical flexible pavement design system (TxME) (No. FHWA/TX-14/0-6622-2). Texas A & M Transportation Institute.

Hu, S., Zhou, F., and Scullion, T. (2012). Texas M-E Flexible Pavement Design System: Literature Review and Proposed Framework, Report No. FHWA/TX-12/0-6622-1, Texas A&M Transportation Institute, College Station, TX.

Huang, Y. H. (1993). Pavement analysis and design (Second Edition). Pearson Education, Inc., Upper Saddle River, New Jersey.

Insurance Institute for Highway Safety, General Statistics. (2016). Retrieved October 05, 2017, from http://www.iihs.org/iihs/topics/t/general-statistics/fatalityfacts/state-by-state-overview.

Intercomp. (n.d.). LS630-WIM™ Portable Low-Speed Weigh-In-Motion Scale. Retrieved November 13, 2017, from https://www.intercompcompany.com/ls630-portable-low-speed-weigh-in-motion-scale-p-46.html

Intercomp. (n.d.). PT300DW™ Wheel Load Scales. Retrieved November 14, 2017, from https://www.intercompcompany.com/pt300dw-wheel-load-scales-p-10042.html

International Road Dynamics. (n.d.). Lineas Quartz WIM Sensor by Kistler for Weigh in Motion. Retrieved November 15, 2017, from https://www.irdinc.com/pcategory/wim-scales--sensors/lineas-quartz-wim-sensor-by-kistler.html

International Road Dynamics, Inc.(n.d.) PAT Bending Plate System® - Bending Plate WIM Scales. Retrieved November 13, 2017, from https://www.irdinc.com/pcategory/wim-scales--sensors/irdpat-bending-plate-system.html

International Road Dynamics. (n.d.). Piezoelectric RoadTrax BL. Retrieved November 15, 2017, from https://www.irdinc.com/pcategory/axle-sensors--accessories/piezoelectric-roadtrax-bl.html

Jiang, Y., Li, S., Nantung, T. E., and Chen, H. (2008). Analysis and Determination of Axle Load Spectra and Traffic Input for the Mechanistic-Empirical Pavement Design Guide, Publication FHWA/IN/JTRP-2008/07, Joint Transportation Research Program, Indiana Department of Transportation and Purdue University, West Lafayette, Indiana.

Jon A. Epps., and David E. Newcomb. (2016). Maintenance and Rehabilitation Strategies for Repair of Road Damage Associated with Energy Development and Production. IR-15-03. Texas A&M Transportation Institute. Texas Department of Transportation.

Kawa, I., Zhang, Z., & Hudson, W. R. (1998). Evaluation of the AASHTO 18-kip load equivalency concept (No. FHWA/TX-05/0-1713-1). Center for Transportation Research, Bureau of Engineering Research, University of Texas at Austin.

Klein, L. A. (2001). Sensor technologies and data requirements for ITS.

Kwon, T. M. (2012). "Development of a Weigh-Pad-Based Portable Weigh-In-Motion," Final Report MN/RC 2012-38, University of Minnesota Duluth, Duluth, MN.

Kwon, T. M. (2016). "Implementation and Evaluation of a Low-Cost Weigh-In-Motion System." Final Report MN/RC 2016-10, University of Minnesota Duluth, Duluth, MN.

Labarrere,J.(n.d.).BridgeWIM.RetrievedMay12,2019,fromhttp://www.iswim.org/index.php?nm=2&nsm=6&lg=en

Lawrence, K. (2001). Sensor Technologies and Data Requirements for ITS Applications. Artech House ITS Library, Boston, MA, USA.

Lydon, M., Taylor, S. E., Robinson, D., Mufti, A., & Brien, E. J. O. (2016). Recent developments in bridge weigh in motion (B-WIM). Journal of Civil Structural Health Monitoring, 6(1), 69-81.

Malla, R. B., Sen, A., and Garrick, N. W. (2008). "A special fiber optic sensor for measuring wheel loads of vehicles on highways." Sensors, 8(4), 2551-2568.

Marek , M. A. (2006, June 01). DCIS User Manual [PDF].

Mehta, Y., & Roque, R. (2003). Evaluation of FWD data for determination of layer moduli of pavements. Journal of Materials in Civil Engineering, 15(1), 25-31.

Mimbela, L. E. Y., & Klein, L. A. (2000). Summary of vehicle detection and surveillance technologies used in intelligent transportation systems.

NCHRP (2004), Guide for Mechanistic-Empirical Design of Pavement Structures, NCHRP Project 1-37A, National Cooperative Highway Research Program, Washington, D.C.

Nimeri, M., Nabizadeh, H., Hajj, E. Y., Siddharthan, R. V., & Elfass, S. (2018). Nucleus approach for pavement analysis under super-heavy load. In Advances in Materials and Pavement Prediction, CRC Press, 527-530.

Oh, J., Fernando, E., and Lytton, R. (2007). Evaluation of damage potential for pavements due to overweight truck traffic. Journal of Transportation Engineering, 133(5), 308-317.

Oh, J., Walubita, L. F., and Leidy, J. (2015). "Establishment of Statewide Axle Load Spectra Data using

Cluster Analysis." KSCE Journal of Civil Engineering, 19(7), 2083.

Olsen, L., and Media, A. S. (n.d.). Boom in oil and traffic deaths. Retrieved October 07, 2017, from http://www.houstonchronicle.com/local/boom-in-oil-traffic-deaths.

Pavement Management Information System: Rater's Manual, (2016), Texas Department of Transportation, 112 p.

Prozzi, J. A., and Hong, F. (2005). Evaluate Equipment, Methods, and Pavement Design Implications for Texas Conditions of the AASHTO 2002, Axle Load Spectra Traffic Methodology. Research Report FHWA/TX-05/0-4510, Center for Transportation Research, The University of Texas at Austin, Austin, TX.

Prozzi, J. A., Buddhavarapu, P., Kouchaki, S., Weissmann, J., Weissmann, A., Jiang, N., Savage, K., and Walton, C. M. (2017). Infrastructure-Friendly Vehicles to Support Texas Economic Competitiveness. Report No. FHWA/TX-16/0-6817-1, Center for Transportation Research, University of Texas at Austin, Austin, TX.

Prozzi, J. A., Murphy, M., Loftus-Otway, L., Banerjee, A., Kim, M., Wu, H., Prozzi, J.P., Hutchinson, R., Harrison, R., Walton, C.M., Weissmann, J., and Weissmann, A. (2012), Oversize/Overweight Vehicle Permit Fee Study, Report No. FHWA/TX-13/0-6736-2, Center for Transportation Research, University of Texas at Austin, Austin, TX.

Quiroga, C., Tsapakis, I., and Holik, W. (2016). Descriptive Statistics and Well County Maps. Implementation Reports.

Refai, H., Othman, A., and Tafish, H. (2014). "Portable Weigh-In-Motion for Pavement Design." Final Report No. FHWA-OK-14-07, The University of Oklahoma, Norman, OK.

Sayyady, F., Stone, J., List, G., Jadoun, F., Kim, Y., and Sajjadi, S. (2011). "Axle Load Distribution for Mechanistic-Empirical Pavement Design in North Carolina: Multidimensional Clustering Approach and Decision Tree Development." Transportation Research Record: Journal of the Transportation Research Board, (2256), 159-168.

Sridhar, B. K. (2008), "Characterization and Development of Axle Load Spectra to Enhance Pavement Design and Performance on the Basis of New Mechanistic-Empirical Design Guide in Louisiana", Louisiana State University, Baton Rouge, LA.

Stephen D. Sebesta (2014). Rehabilitation Recommendations for SH72 in Karnes County. TM-14-06. Texas A&M Transportation Institute. Texas Department of Transportation.

Swan, D., Tardif, R., Hajek, J., and Hein, D. (2008). "Development of Regional Traffic Data for the Mechanistic-Empirical Pavement Design Guide." Transportation Research Record: Journal of the Transportation Research Board, (2049), 54-62.

Tang, Y., Zhang, C., Gu, R., Li, P., & Yang, B. (2017). Vehicle detection and recognition for intelligent traffic surveillance system. Multimedia tools and applications, 76(4), 5817-5832.

Texas Permitting and Routing Optimization System Online Customer Interface User Guide.

Texas Transportation Researcher (1989). "Models Developed to Predict Climatic Effects on Low-Volume Roads." Vol. 25, No. 4, Texas Transportation Institute, Texas A&M University, College Station, TX, pp 5-6.

Turnstall, T., Oyakawa, J., Conti G,,Wells M., Hernandez,J ., Lee, Y., Loeffelhilz V,. Ravi N., Rodriguez J., Teng, F., Torres, C., Torrez, H., Wang, B., and Zhang, J. (2014). Economic Impact of the Eagle Ford Shale. Center for Community and Business Research, UTSA Institute for Economic Development, San Antonio, TX.

Turnstall, T., Oyakawa, J., Roberts, S., Eid, H., Abalos, R., Wang, T., Calderon, E., and Melara, K. (2013). Economic Impact of the Eagle Ford Shale. Center for Community and Business Research, UTSA Institute for Economic Development, San Antonio, TX.

Turnstall, T., Oyakawa, J., Roberts, S., Eid, H., Abalos, R., Wang, T., Calderon, E., and Melara, K. (2013).

Economic Impact of the Eagle Ford Shale. Center for Community and Business Research, UTSA Institute for Economic Development, San Antonio, TX.

Turochy, R. E., Timm, D. H., and Mai, D. (2015). Development of Alabama Traffic Factors for use in Mechanistic-Empirical Pavement Design, Report No. FHWA/ALDOT 930-793, Auburn University, Auburn, Alabama.

TxDOT. (2016). Transportation in the Energy Sector. Texas Department of Transportation.

TxDOT. (2017). Permian Road Safety Coalition Safety Forum. Texas Department of Transportation.

U. S. Energy Information Administration. (2017). Eagle Ford Region Drilling Productivity Report. Retrieved October 20, 2017, from https://www.eia.gov/petroleum/drilling/pdf/eagleford.pdf.

U. S. Energy Information Administration. (2017). Permian Region Drilling Productivity Report. Retrieved October 18, 2017, from https://www.eia.gov/petroleum/drilling/pdf/permian.pdf.

Walubita, L. F., Faruk, A. N., and Ntaimo, L. (2015). Intelligent Freight Monitoring: A Review of Potential Technologies. Texas A&M Transportation Institute Report 2015-8, College Station, TX.

Walubita, L. F., Prakoso, A., Aldo, A., Lee, S. I., & Djebou, C. (2019). Using WIM Systems and Tube Counters to Collect and Generate ME Traffic Data for Pavement Design and Analysis: Technical Report (No. FHWA/TX-18/0-6940-R1).

Wang, H., Zhao, J. and Wang, Z. (2015). "Impact of Overweight Traffic on Pavement Life using Weigh-in-Motion Data and Mechanistic-Empirical Pavement Analysis." 9th International Conference on Managing Pavement Assets, Washington, D.C.

Wilke, P. W. (2014). "Road Impacts from Shale Energy Development." 2014 Shale Energy Engineering Conference, C. L. Meehan, J. M. VanBriesen, F. Vahedifard, X. Yu, and C. Quiroga, eds., American Society of Civil Engineers, Pittsburgh, PA, 633–642.

Wu, D., Yuan, C. and Liu, H. (2017). "A Risk-based Optimization for Pavement Preventative Maintenance with Probabilistic LCCA: A Chinese Case," International Journal of Pavement Engineering, 11-25.

Xiao, D. X., and Wu, Z. (2016). "Using Systematic Indices to Relate Traffic Load Spectra to Pavement Performance." International Journal of Pavement Research and Technology, 9(4), 302-312.

Zhang, Z., and Machemehl, R. B. (2004). Pavement-related Databases in TxDOT. Center for Transportation Research, University of Texas at Austin, Austin, TX.

APPENDIX A. Visual Inspection of Selected Roadways in Eagle Ford Shale Region

- *Laredo District – Farm-to-Market (FM) 468*

The first visual inspection survey was conducted on Farm-to-Market (FM) 468 in LaSalle County of the Laredo District. Upon initial inspection, FM 468 appeared to be in a severely distressed state exhibiting multiple distress types. The first distress present on both K1 and K6 lanes was severe flushing on both right and left wheel paths throughout the entire section, as shown in Figure A.1. The flushing rated 3, according to TxDOT's 2018 PMIS Pavement Rater's Manual, begins in the intersection with FM 469 and continues past the Dimmit County line. The second documented distress was shallow to severe rutting throughout most of the inspected section. The rutting illustrated in Figure A.2, ranged from .25in to .50in in both wheel paths and covered approximately 70% of the wheel paths area. Moreover, an area with a large patch appearing to be milled out and replaced, as shown in Figure A.3, was also reported. However, the patch already seems to be disintegrating. Alligator cracking is also developing in the wheel paths covering an area of approximately 30%. In addition, raveling and potholes were also spotted in certain places of the inspected area. Heavily loaded vehicles coupled with a thin asphalt layer are believed to be the reasons for the many distresses present and the poor ride quality of FM 468.

Figure A.1. Severe Flushing in FM 468 - La Salle County

Figure A.2. Shallow Rutting in FM 468 - La Salle County

Figure A.3. Patches in FM 468 - La Salle County

- *Laredo District – US Highway 83*

US highway 83 displayed multiple distress types; raveling among the most significant. The raveling rated 2 was present throughout most of the inspected section, particularly in between the right and left wheel paths and towards the right shoulder. As illustrated in Figure A.4 and highlighted by the red oval one can identify areas where a significant amount of aggregate is missing. Shallow rutting was also reported in the inspected section ranging from .25in to .313in and covering approximately 40% of the wheel paths area. Additionally, as illustrated in Figure A.5, flushing rated 2 can be spotted in certain parts of the section along with alligator cracking.

Figure A.4. Raveling and Missing Aggregate in US 83 -Dimmit County

Figure A.5. Flushing and Shallow Rutting in US 83 -Dimmit County

- *San Antonio District – State Highway (SH) 16*

In State Highway (SH) 16 shallow and deep rutting conditions in both wheel paths were observed throughout the entire pavement section. The rutting ranged from .25in to .625in and covered approximately 90% of the wheel paths area. Severe flushing rated 3, was also present on both K1 and K6 lanes and both right and left wheel paths, as shown in Figure A.6. Additionally, the raveling rated 2, can be spotted primarily on the right wheel path and towards the right shoulder, illustrated in Figure A.7. As of 2019, work to reconstruct SH 16 between Tilden and Jourdanton is under progress.

Figure A.6. Distresses Present in SH 16-Atascosa County

Figure A.7. Raveling and Rutting in SH 16-Atascosa County

- *San Antonio District – Farm-to-Market (FM) 99*

FM 99 also appeared to be in a poor and distressed condition exhibiting shallow rutting, flushing, and pot hole formation. Shallow to severe rutting is present throughout the entire inspected section ranging from .25in to .50in. in both wheel paths and covering approximately 65% of the wheel paths area, as shown in Figure A.8. Flushing was also detected on both K1 and K6 lanes and rated at a level 2. Nonetheless, as illustrated in Figure A.9, the most significant distress was the severity of the potholes present in FM 99. Several large potholes were documented in the small inspection area however, while driving on the rest of FM 99 the inspectors encountered numerous potholes and failures. Heavily overloaded vehicles have adversely damaged much of FM 99 and have compromised its structural integrity.

162

Figure A.8. Rutting and Flushing in FM 99 - McMullen County

Figure A.9. Pothole Formation in FM 99 - McMullen County

- *San Antonio District – Farm-to-Market (FM) 624*

Similarly, FM 624 was also in a distressed condition exhibiting shallow to deep rutting, flushing, and pot hole formation. The research team documented shallow and deep rutting throughout most of the inspected section ranging from .25in to .625in in both wheel paths and covering approximately 60% of the wheel paths area as shown in Figure A.10. Moreover, severe flushing was also documented on both K1 and K6 lanes and rated at a level 3. As illustrated in Figure A.11, several large potholes were also identified and logged.

Figure A.10. Rutting and Flushing in FM 624 - McMullen County

Figure A.11. Pothole Formation in FM 624 - McMullen County

- *Corpus Christi District – US Highway 281*

US 281 also exhibited multiple distresses such as shallow rutting, alligator cracking, and longitudinal cracks. Shallow rutting was reported through most of the inspected section ranging from .25 in to .375 in. in both wheel paths and covering approximately 40% of the wheel paths area as illustrated in Figure A.12. Alligator cracking was also documented primarily on the right wheel path and covering approximately 30% of the wheel paths area. However, the most significant distress was the sealed and non-sealed longitudinal cracks present throughout the R1 lane and covering an approximate area of 30%. Additionally, the longitudinal cracking has led the right shoulder to separate and begin to sink in. Figures A.13 and A.14 respectively, show the severity of the longitudinal cracks present.

164

Figure A.12. Rutting in US 281 – Live Oak County

Figure A.13. Longitudinal Cracks in US 281 – Live Oak County

Figure A.14. Longitudinal Cracking in Right Shoulder in US 281 –Live Oak County

- *Corpus Christi District – State Highway (SH) 72*

Upon inspection, SH 72 appeared to be in a fair condition as illustrated in Figure A.15. Since its recent reconstruction in 2013-2014, the only observable distresses that have initiated are shallow rutting and moderate flushing. Moreover, if the current overweight traffic persists, SH 72 will soon start to develop more severe rutting.

Figure A.15. Pavement Conditions of SH 72 –Karnes County

- *Corpus Christi District – BU 181/SH 123*

Similarly, to the other highways, the pavement distresses documented in BU 181/SH 123 were also shallow rutting and flushing. The research team logged shallow rutting throughout most of the inspected section ranging from .25in to .375in primarily on the right wheel path and covering approximately 50% of the wheel paths area as shown in Figure A.16. Flushing was also spotted as

166

illustrated in Figure A.17 and rated at a level 2.

Figure A.16. Shallow Rutting in BU 181/SH 123 –Karnes County

Figure A.17. Flushing in BU 181/SH 123 –Karnes County

- *Yoakum District – SH 119*

SH 119 in the Yoakum District appeared to be in a structurally sound and fair condition as shown in Figure A.18. Since its recent lane widening, the only distress that has started to develop is shallow rutting. Despite drilling operations and pipe line construction, SH 119 has remained in an adequate condition.

Figure A.18. Pavement Conditions of SH 119 - Dewitt County

- *Yoakum District – US 183*

The final visual inspection survey was conducted on US highway 183, the major pavement distress documented was the seal and non-sealed longitudinal cracking throughout both K6 and K1 lanes, illustrated in Figure A.19 and A.20 respectively. The longitudinal cracks covered an approximate area of 95%. In addition, shallow rutting was also recorded ranging from .25in to .375in and covering approximately 30% of the wheel paths area.

Figure A.19. Pavement Conditions of US 183 - Gonzales County

Figure A.20. Longitudinal Cracks of US 183 - Gonzales County

APPENDIX B – PMIS Database Information

	FISCAL_YEAR	SIGNED_HIG	BEG_REF_MA	BEG_REF_M	RATING_CYC	PVMNT_TYP
+	2010	US0083 K	0636	0	P	10
+	2010	US0083 K	0636	0.5	P	10
+	2010	US0083 K	0636	1	P	10
+	2010	US0083 K	0636	1.5	P	10
+	2010	US0083 K	0638	0	P	10
+	2010	US0083 K	0638	0.5	P	10
+	2010	US0083 K	0638	1	P	10
+	2010	US0083 K	0638	1.5	P	10
+	2010	US0083 K	0640	0	P	10
+	2010	US0083 K	0640	0.5	P	10
+	2010	US0083 K	0640	1	P	10

**Figure B.1. PMIS Information of US 183, Laredo Pavement Type
(From PMIS Database, 2010).**

	FISCAL_YEAR	SIGNED_HIG	BEG_REF_MA	BEG_REF_M	RATING_CYC	PVMNT_TYP
+	2010	FM0468 K	0438	0	P	10
+	2010	FM0468 K	0438	0.5	P	10
+	2010	FM0468 K	0440	0	P	10
+	2010	FM0468 K	0440	0.5	P	10
+	2010	FM0468 K	0440	1	P	10
+	2010	FM0468 K	0440	1.5	P	10
+	2010	FM0468 K	0442	0	P	10
+	2010	FM0468 K	0442	0.5	P	10
+	2010	FM0468 K	0442	1	P	10

**Figure B.2. PMIS Information of FM 468, Laredo Pavement Type
(From PMIS Database, 2010).**

	FISCAL_YEAR	SIGNED_HIG	BEG_REF_MA	BEG_REF_M	RATING_CYC	PVMNT_TYP
+	2010	FM0624 K	0498	0	P	06
+	2010	FM0624 K	0498	0.5	P	06
+	2010	FM0624 K	0498	1	P	06
+	2010	FM0624 K	0498	1.5	P	06
+	2010	FM0624 K	0500	0	P	06
+	2010	FM0624 K	0500	0.5	P	06
+	2010	FM0624 K	0500	1	P	06
+	2010	FM0624 K	0500	1.5	P	06
+	2010	FM0624 K	0502	0	P	06
+	2010	FM0624 K	0502	0.5	P	06
+	2010	FM0624 K	0502	1	P	06
+	2010	FM0624 K	0502	1.5	P	06

**Figure B.3. PMIS Information of FM 624, San Antonio Pavement Type
(From PMIS Database, 2010).**

	FISCAL_YEAR	SIGNED_HIG	BEG_REF_M	BEG_REF_M	RATING_CYC	PVMNT_TYP
⊞	2010	FM0099 K	0586	0	P	10
⊞	2010	FM0099 K	0586	0.5	P	10
⊞	2010	FM0099 K	0586	1	P	10
⊞	2010	FM0099 K	0586	1.5	P	10
⊞	2010	FM0099 K	0588	0	P	10
⊞	2010	FM0099 K	0588	0.5	P	10
⊞	2010	FM0099 K	0588	1	P	10
⊞	2010	FM0099 K	0588	1.5	P	10
⊞	2010	FM0099 K	0590	0	P	10
⊞	2010	FM0099 K	0590	0.5	P	10
⊞	2010	FM0099 K	0590	1	P	10
⊞	2010	FM0099 K	0590	1.5	P	10

Figure B.4. PMIS Information of FM 99, San Antonio Pavement Type (From PMIS Database, 2010).

	FISCAL_YEAR	SIGNED_HIG	BEG_REF_M	BEG_REF_M	RATING_CYC	PVMNT_TYP
⊞	2010	SH0016 K	0640	0	P	10
⊞	2010	SH0016 K	0640	0.5	P	10
⊞	2010	SH0016 K	0640	1	P	10
⊞	2010	SH0016 K	0640	1.5	P	10
⊞	2010	SH0016 K	0642	0	P	10
⊞	2010	SH0016 K	0642	0.5	P	10
⊞	2010	SH0016 K	0642	1	P	10
⊞	2010	SH0016 K	0642	1.5	P	10
⊞	2010	SH0016 K	0644	0	P	10
⊞	2010	SH0016 K	0644	0.5	P	10
⊞	2010	SH0016 K	0644	1	P	10
⊞	2010	SH0016 K	0644	1.5	P	10

Figure B.5. PMIS Information of SH 16, San Antonio Pavement Type (From PMIS Database, 2010).

	FISCAL_YEAR	SIGNED_HIG	BEG_REF_M	BEG_REF_M	RATING_CYC	PVMNT_TYP
⊞	2010	US0281 R	0620	1.6	P	05
⊞	2010	US0281 R	0622	0	P	05
⊞	2010	US0281 R	0622	0	A	05
⊞	2010	US0281 R	0622	0.5	P	05
⊞	2010	US0281 R	0622	0.5	A	05
⊞	2010	US0281 R	0622	1	P	05
⊞	2010	US0281 R	0622	1	A	05
⊞	2010	US0281 R	0622	1.5	P	05
⊞	2010	US0281 R	0622	1.5	A	05
⊞	2010	US0281 R	0624	0	P	05
⊞	2010	US0281 R	0624	0.5	P	05

Figure B.6. PMIS Information of US 281, Corpus Christi Pavement Type (From PMIS Database, 2010).

FISCAL_YEAR	SIGNED_HIG	BEG_REF_M	BEG_REF_M	RATING_CYC	PVMNT_TYP
2010	SH0072 K	0534	0	P	06
2010	SH0072 K	0534	0	A	06
2010	SH0072 K	0534	0.5	P	06
2010	SH0072 K	0534	0.5	A	06
2010	SH0072 K	0534	1	P	06
2010	SH0072 K	0534	1	A	06
2010	SH0072 K	0534	1.5	P	06
2010	SH0072 K	0534	1.5	A	06
2010	SH0072 K	0536	0	P	05
2010	SH0072 K	0536	0.5	P	05
2010	SH0072 K	0536	1	P	05
2010	SH0072 K	0536	1.5	P	05
2010	SH0072 K	0538	0	P	06
2010	SH0072 K	0538	0.5	P	06

Figure B.7. PMIS Information of SH 72, Corpus Christi Pavement Type (From PMIS Database, 2010).

FISCAL_YEAR	SIGNED_HIG	BEG_REF_M	BEG_REF_M	RATING_CYC	PVMNT_TYP
2010	SH0080 K	0548	0	P	06
2010	SH0080 K	0548	0.5	P	06
2010	SH0080 K	0548	1	P	06
2010	SH0080 K	0548	1.5	P	10
2010	SH0080 K	0550	0	P	10
2010	SH0080 K	0550	0.5	P	05
2010	SH0080 K	0550	1	P	05
2010	SH0080 K	0550	1.2	P	05
2010	SH0080 K	0550	1.4	P	05
2010	SH0080 K	0552	0	P	05
2010	SH0080 K	0552	0.5	P	05

Figure B.8. PMIS Information of SH 123/80, Corpus Christi Pavement Type (From PMIS Database, 2010).

FISCAL_YEAR	SIGNED_HIG	BEG_REF_M	BEG_REF_M	RATING_CYC	PVMNT_TYP
2010	US0183 K	0580	0	P	05
2010	US0183 K	0580	0.5	P	05
2010	US0183 K	0580	1	P	05
2010	US0183 K	0580	1.5	P	05
2010	US0183 K	0582	0	P	05
2010	US0183 K	0582	0.5	P	05
2010	US0183 K	0582	1	P	05
2010	US0183 K	0582	1.5	P	05
2010	US0183 K	0584	0	P	05
2010	US0183 K	0584	0.5	P	05
2010	US0183 K	0584	1	P	05

Figure B.9. PMIS Information of US 183, Yoakum Pavement Type (From PMIS Database, 2010).

FISCAL_YEAR	SIGNED_HIG	BEG_REF_M	BEG_REF_M	RATING_CYC	PVMNT_TYP
2010	SH0119 K	0540	0.5	P	05
2010	SH0119 K	0540	1	P	05
2010	SH0119 K	0540	1.5	P	05
2010	SH0119 K	0542	0	P	05
2010	SH0119 K	0542	0.5	P	05
2010	SH0119 K	0542	1	P	05
2010	SH0119 K	0542	1.5	P	05
2010	SH0119 K	0544	0	P	05
2010	SH0119 K	0544	0.5	P	05
2010	SH0119 K	0544	1	P	05
2010	SH0119 K	0544	1.5	P	05
2010	SH0119 K	0546	0	P	05
2010	SH0119 K	0546	0.5	P	05
2010	SH0119 K	0546	1	P	05
2010	SH0119 K	0546	1.5	P	05

Figure B.10. PMIS Information of SH 119, Yoakum Pavement Type